# Identification and characterization of the *Arabidopsis thaliana PTI1* multigene family

**Rakesh David**

**June 2011**

**A thesis submitted for the degree of Doctor of Philosophy**

***of the Australian National University***

Australian
National
University

# Declaration

All the data presented in this thesis was obtained from my own experimental work undertaken under the supervision of Assoc. Prof. Josette Masle in the Division of Plant Sciences at the Research School of Biology, ANU college of Medicine, Biology and Environment, Canberra, Australia. This thesis has not been submitted for examination elsewhere.

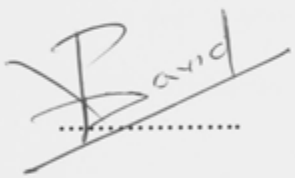

Rakesh David

June 2010

# Acknowledgements

I would like to thank my supervisor, Dr. Josette Masle for giving me the opportunity to undertake my PhD in her lab. Her enthusiasm for research and attention to experimental detail is something that never ceases to amaze me. Overall, it has been an enjoyable experience and I will never forget our "vibrant" discussions.

I would like to thank Ricarda Jost and Oliver Berkowitz for all their help and advice, frequent exchange of ideas, especially in the early years of my PhD. I would also like to thank my co-supervisor Dr. Peer Schenk (UQ) for accommodating me in his lab to carry out the pathogen related work of my study. I would also like to acknowledge Maryam Rafiqi for the help she provided with the transient tobacco infiltration protocol.

I also owe a great deal of gratitude to the staff at the Controlled Environment Facility, especially Sue Lyons.

To my colleagues, past and present, thank you for creating a great atmosphere to work in. The really long workdays spent in our windowless lab seemed so much more bearable with you guys around.

Agustin and Keith deserve special mention. Thanks guys, you have been excellent lab mates to work with. Agustin, will definitely miss the poker nights at your place. Keith, thanks a lot mate. You've been a real friend. We've have had a lot to discuss over our many many coffee runs to 'Degree' and I am surely going to miss that.

To the happy-hour(s) bar crew (you know who you are), thanks guys!

To my loving wife, Preethi, thank you for your unwavering support and love throughout the years. This PhD would simply not have been possibly without you. To my family back home; dad, mom and sis, thank you for your advice and support, both emotionally and financially over the years. You guys are inspiration to me.

***"As a child, I was an imaginary playmate" – Tom Robbins***

*Dedicated to my family*

## Table of contents


**Chapter 1: Introduction** ..... **1**

**1.1 Preamble** ..... **1**

**1.2 Common Signalling pathways in biotic and abiotic stress response** ..... **3**

1.2.1 Mitogen activated protein kinase (MPKs) ..... 4

1.2.1.1 The MAPK signalling module ..... 4

1.2.1.2 MAPK signal specificity ..... 4

1.2.2 Calcium-dependent protein kinases (CDPKs) ..... 7

1.2.2.1 CDPK activation ..... 7

1.2.2.2 Signal Specificity of CDPKs ..... 8

**1.3 Receptor-Like Cytoplasmic Kinases (RLCKs) - An emerging class of kinases in plant stress and developmental signalling** ..... **9**

1.3.1 Initial hypothesis of PTI1-like kinase involved in biotic and abiotic signalling cascades ..... 10

1.3.2 The tomato SlPTI1 - a downstream target of *Pseudomonas syringae* related SlPTO kinase ..... 11

1.3.3 Rice OsPti1a functions as a negative regulator of defence signalling ..... 12

1.3.4 ZmPti1a kinase plays a role in reproductive development by influencing pollen fitness ..... 15

**1.4 Projects Aims** ..... **18**

1.4.1 Rationale of the Study ..... 18

1.4.2 Chapter summary ..... 18

**1.5 References** ..... **20**

**Chapter 2 Identification of the Arabidopsis PTI1 gene family** ..... **24**

**2.1 Introduction** ..... **24**

**2.2 Materials and Methods** ..... **26**

2.2.1 Maintenance and cultivation of *Arabidopsis* plant material ..... 26

2.2.1.1 Seed sterilization and stratification of Arabidopsis seeds ..... 26

2.2.1.2 In vitro growth conditions ..... 26

2.2.1.3 Growth conditions of soil-grown plants ..... 28

2.2.1.4 Growth conditions of hydroponically grown plants ..... 28

2.2.2 Stress Conditions ..... 29

2.2.2.1 Pseudomonas syringae biotic stress challenge ..... 29

2.2.2.1.1 Maintenance of P. *syringae* pv. *tomato* cultures ..... 29

2.2.2.1.2 *P. syringae* pv. *tomato* inoculation ..... 30

2.2.2.2 PEG induced osmotic stress on plants grown hydroponically ..... 31

2.2.2.3 Mannitol induced osmotic stress of plants grown on agar based media ..... 32

2.2.3 Molecular techniques ..... 33

2.2.3.1 RNA isolation ..... 33

2.2.3.1.1 Precautionary measures ..... 33

2.2.3.1.2 Total RNA isolation ..... 33

2.2.3.2 cDNA synthesis ..... 34

2.2.3.3 Primer Design ..... 35

2.2.3.4 Quantitative Real-time RT-PCR (qRT-PCR) set up and analysis ..... 36

2.2.3.5 Analysis of qRT-PCR expression data ..... 37

**2.3 Results** ..... **39**

2.3.1 Identification of Amino acid signature pattern as a tool for finding potential *PTI1* orthologs in *Arabidopsis* thaliana ..... 39

2.3.2 Multiple sequence alignment of the functional Pti1 genes ..... 40

2.3.3 PTI1 Signature Pattern and Identification of *Arabidopsis PTI1*-like genes ..... 42

2.3.4 Prediction of putative *Arabidopsis PTI1* kinase genes ..... 46

2.3.5 *PTI1* phylogeny ..... 49

2.3.6 *PTI1* gene duplication in *Arabidopsis* ..... 51
2.3.7 *PTI1* gene regulation ..... 56
2.3.7.1 Promoter analysis ..... 56
2.3.7.2 PTI1-like gene expression profiling ..... 63
2.3.8 Isoform specific transcriptional regulation of *Arabidopsis PTI1*-like genes by biotic and abiotic stress ..... 65
2.3.8.1 Biotic stress ..... 67
2.3.8.2 Root mechanical stress ..... 67
2.3.8.3 Osmotic stress ..... 69
**2.4 Discussion ..... 76**
2.4.1 Expansion of the *PTI1* gene family in Arabiodopsis ..... 76
2.4.2 Differential expression for the 8 *PTI1* isoforms ..... 77
2.4.3 Concluding remarks ..... 80
**2.5 References ..... 81**
**2.6 Appendix ..... 85**

**Chapter 3 Functional analysis of PTI1 genes using reverse genetic approach ..... 91**
**3.1 Introduction ..... 91**
**3.2 Materials and Methods ..... 93**
3.2.1General plant growth conditions of *Arabidopsis* plant material ..... 93
3.2.1.1 In vitro growth conditions ..... 93
3.2.1.2 Growth conditions for tobacco plants ..... 93
3.2.2 Isolation of homozygous T-DNA insertion lines ..... 93
3.2.3 Generation of higher order mutants ..... 94
3.2.4 Quantitative analysis of root growth ..... 95
3.2.5 Germination assay ..... 95
3.2.6 Molecular Techniques ..... 96
3.2.6.1 Design of PTI1-8 constitutive silencing construct ..... 96
3.2.6.2 Constitutive and inducible RNAi silencing constructs for PTI1-8 silencing ..... 97
3.2.6.3 PTI1-8 GFP fusion constructs ..... 98
3.2.6.4 Standard PCR conditions ..... 99
3.2.6.5 Gel electrophoresis of DNA ..... 99
3.2.6.6 Vector manipulations ..... 100
3.2.6.7 CTAB DNA extractions ..... 100
3.2.6.8 Sequencing ..... 101
3.2.7 Plant Transformation Procedures ..... 101
3.2.7.1 Transient Expression Assay by leaf infiltration of Agrobacterium tumefaciens ..... 101
3.2.7.2 Arabidopsis transformation ..... 102
3.2.8 Selection of *Arabidopsis* transformants on nutrient media plates ..... 103
3.2.9 Dexamethasone Treatments ..... 104
3.2.9.1 Application of Dexamethasone by Leaf painting ..... 104
3.2.9.2 In vitro Application of Dexamethasone in culture media ..... 105
3.2.9.3 Application of Dexamethasone in Hydroponic media ..... 105
3.2.10 Staining ..... 106
3.2.10.1 Histological staining of GUS activity ..... 106
3.2.10.2 Propidium iodide staining ..... 107
3.2.11 Microscopy ..... 107
3.2.11.1 GFP imaging ..... 107
3.2.11.2 Confocal microscopy ..... 107
**3.3 Results ..... 109**
3.3.1 Identification of T-DNA insertion lines for individual *PTI1*-like genes in *Arabidopsis* ..... 109

3.3.2 Generation of *pti1*-like double mutant lines ..... 113
3.3.3 *pti1* single and double mutants show wild-type morphology under standard growing conditions ..... 113
3.3.4 *PTI1-8* expression is not, or only partially, down-regulated in available T-DNA insertional mutants ..... 115
3.3.5 Constitutive RNAi silencing of *PTI1-8* appears to be lethal ..... 118
3.3.6 Inducible silencing of *PTI1-8* yields viable plants with reduced *PTI1-8* transcript abundance ..... 123
3.3.7 Dexamethasone treatment induces high levels of *PTI1-8* silencing ..... 123
3.3.8 Evaluation of off-target silencing ..... 127
3.3.9 *PTI1-8* is a negative regulator of root elongation and meristem size ..... 130
3.3.10 *PTI1-8* functions in the root meristem and regulates the number of proliferating cells ..... 136
3.3.11 *PTI1-8* silencing induces earlier floral induction ..... 139
3.3.12 Transient expression studies demonstrate that PTI1-8 localises to the plasma membrane. ..... 142
3.3.12.1 In silico analysis of PTI1 protein structure ..... 142
3.3.12.2 Experimental evidence for PTI1-8 membrane targeting ..... 143
**3.4 Discussion ..... 152**
3.4.1 *PTI1-8* root developmental phenotype ..... 152
3.4.2 *PTI1-8* in context with root hormone signalling pathways ..... 153
3.4.3 Concluding remarks ..... 156
**3.5 References ..... 158**
**3.6 Appendix ..... 162**

**Chapter 4 Functional analysis of *pti1* mutants in response to biotic stress. 173**
**4.1 Introduction ..... 173**
**4.2 Materials and Methods ..... 176**
4.2.1 Plant material and growth conditions ..... 176
4.2.1.1 Plant growth conditions for DNA biomass assay ..... 176
4.2.2 DNA biomass assay ..... 178
4.2.3 CFU growth assay ..... 180
4.2.4 Gene expression analysis ..... 181
4.2.5 Yeast-two-hybrid assay ..... 182
**4.3 Results ..... 184**
4.3.1 Choice of *Arabidopsis pti1* mutants for pathogen challenge experiments ..... 184
4.3.2 *pti1-5* single and *pti1-5pti1-4* double mutants have enhanced resistance to the bacterial pathogen *Pst* DC3000 ..... 184
4.3.3 The *pti1-5* loss-of-function leads to impaired growth of virulent *Pst* DC3000 pathogen *in planta* ..... 185
4.3.4 Enhanced expression of defence genes in the *pti1-5* mutant after *Pst* DC3000 infection ..... 191
4.3.5 Evidence of direct protein-protein interaction between the PTI1-5 and OXI1 193
**4.4 Discussion ..... 198**
4.4.1 *PTI1-5* functions as a suppressor of plant basal resistance to *Pst* DC3000 ..... 198
4.4.2 Comparison with *PTI1* pathogen related genes in other species ..... 200
4.4.3 Signalling pathway for PTI1-5 ..... 202
4.4.4 Concluding remarks ..... 205
**4.5 References ..... 206**
**4.6 Appendix ..... 208**

**Chapter 5: Conclusions and future directions** ..... 211
**5.1 ROS, a common theme in *Arabidopsis* PTI1 signalling pathway?** ..... 211
**5.2 The negative regulatory role of the *Arabidopsis* PTI1 kinases in stress and developmental related responses** ..... 218
**5.3 Concluding Remarks** ..... 220
**5.4 References** ..... 221
**5.5 Appendix** ..... 223

## Abstract

Plants possess a complex network of signalling pathways to integrate environmental and developmental cues. Kinases play a central role in this process by linking inter- and intracellular signals to downstream adaptive responses. Pto-Interacting 1-like (*PTI1*) kinases represent a specific class of serine/threonine protein kinases involved in biotic stress signalling, that are also emerging as players in abiotic stress response or plant development. Little is known, however, about their precise functions. This study describes the identification and characterization of *PTI1*-like genes in *Arabidopsis thaliana*. A specific signature motif identified from previously characterised PTI1 kinases is used as a bait to retrieve 8 putative PTI1 sequences in *Arabidopsis*. Phylogenetic analysis reveals that these *PTI1* isoforms group into 4 pairs of paralogs that likely arose from a relatively recent duplication event. These genes are shown to vary in their expression patterns, during plant development and in response to both biotic and abiotic stresses, suggesting expression divergence as a possible driving force for the expansion of the family in Arabidopsis. Using indexed T-DNA insertion mutants and silencing lines, non-redundant biological functions are demonstrated for two *PTI1*-like genes. Silencing of *PTI1-8* promotes root elongation in young seedlings, through an increase in root meristem size, which identifies that isoform as a negative regulator of root development and cell production rates. Another *PTI1* isoform, PTI1-5, is shown to suppress plant basal resistance to the bacterial pathogen *Pseudomonas syringae* pathovar *tomato* (*Pst*) DC3000. *PTI1-5* loss-of-function leads to impaired growth of virulent *Pst* DC3000 pathogen in planta, as verified by two independent bacterial quantification methods. The oxidative signal-inducible 1 (*OXI1/AGC2-1*), known as an upstream component of ROS-dependent responses, is identified as a direct protein interacting partner of PTI1-5.

OXI1 is known to interact with 4 other PTI1-like kinases and circumstantial evidence from this thesis suggests its likely involvement with a sixth isoform, *PTI1-8*, in regulating root elongation. Based on these experimental data, a general model for *PTI1* signalling is proposed in which individual isoforms have evolved to transduce diverse upstream endogenous or exogenous cues through the *OXI1*-mediated ROS signalling pathway.

# List of Abbreviations

| | |
|---|---|
| Ade | Adenine |
| ARR | Type A response regulators |
| At | *Arabidopsis thaliana* |
| Avr | Avirulence |
| BiFC | Bimolecular fluorescence complementation |
| BLAST | Basic Local Alignment Search Tool |
| C4LK | Crinky 4 Line Kinase |
| cDNA | Complementary DNA |
| CDPK | Calcium Dependent Protein Kinase |
| Ct | Cycle threshold |
| CLD | Calmodulin Like Domain |
| CFU | Colony forming unit |
| Col-0 | Arabidopsis thaliana ecotype Columbia |
| CTAB | Cetyl-Trimethyl-Ammonium Bromide |
| DEX | Dexamethasone |
| DMSO | Dimethylsulfoxide |
| DNA | Deoxyribonucleic acid |
| dpi | Days post-infection |
| ET | Ethylene |
| ETI | Effector Triggered Immunity |
| FST | Flanking sequence tag |
| F1 | First filial generation |
| F2 | Second filial generation |
| EST | Expressed Sequence Tags |
| GA | Gibberellic Acid |
| GFP | Green fluoresecent protein |
| g/L | grams per litre |
| Gm | *Glyciene max* |
| GUS | Beta-glucuronidase |
| HD-ZP | Homeodomain Leucine Zipper |
| His | Histidine |
| hpi | Hours post-infection |
| hpRNA | Hairpin RNA |
| HR | Hypersensitive cell death response |
| HrpZ | Hypersensitive Reaction Pathogenicity Z |
| JA | Jasmonic Acid |
| KB | King's basal media |
| Leu | Leucine |
| LRRK | Leucine Rich Repeat Kinase |
| MAPK/M | Mitogen-activated protein kinase |
| MAP2K/MEK | Mitogen-activated protein kinase kinase |
| MAP3K/MEKK | Mitogen-activated protein kinase kinase kinase |
| MES | 2-(N-Morpholino)ethanesulfonic Acid |
| MPC | Magnetic Particle Concentrate |
| MS | Murashige and Skoog Basal salt mixture |
| MYA | Million years agao |
| mM | millimolar |

| | |
|---|---|
| Mpa | Mega pascal |
| mL/L | millilitre per litre |
| mL | millilitre |
| µg/mL | micrograms per millilitre |
| M | Molar |
| NADPH oxidase | Nicotinamide Adenine Dinucleotide Phosphate-oxidase |
| NB-LRR | Nucleotide binding-leucine rich repeats |
| Nt | *Nicotiana tobacum* |
| Os | *Oryzae sativa* |
| OXI1 | Oxidative signal inducible 1 |
| PAMP | Pathogen associated molecular patterns |
| PCR | Polymerase Chain Reaction |
| PEG | Polyethylene glycol |
| PERLK | Plant External Response Like Kinase |
| Pst | Pseudomonas syringae pv. Tomato |
| PTI1 | Pto-interacting 1 |
| PTI | PAMP-triggered immunity |
| qRT-PCR | Real-time Quantitative reverse transcriptase PCR |
| R | Resistance |
| RCF | Relative Centrifuge Force |
| RNA | Ribonucleic acid |
| RNAi | RNA interference |
| ROS | Reactive oxygen species |
| RLCK | Receptor like cytoplasmic kinase |
| RSRE | Rapid Stress Response Element |
| Sl | *Solanum lycopersicum* |
| SA | Salicylic Acid |
| Ta | Triticum aestivum |
| T-DNA | Transfer DNA |
| TF | Transcription factor |
| Trp | Tryptophan |
| UTR | Untranslated region |
| v/v | volume / volume |
| w/v | weight / volume |
| WT | Wildtype |
| WS-2 | Arabidopsis thaliana ecotype Wassilevskija |
| Y2H | Yeast-two-hybrid |
| YEP | Yeast extract powder |
| Zm | *Zea mays* |
| µE $m^{-2}s^{-1}$ cent | microeinstein per second and square meter |

# Chapter 1

## Introduction

# Chapter 1: Introduction

## 1.1 Preamble

Throughout their life cycle, plants are exposed to a wide range of environmental conditions that change dynamically over time and often in an unpredictable manner. As a result, they have evolved considerable plasticity in their response, to coordinate external environmental stimuli with internal developmental cues and regulate growth (Gilroy and Trewavas, 2001) (Figure 1.1). Key to this plasticity is the cell's robust sensing mechanisms which involve cell surface associated proteins perceiving and relaying the signal to the nucleus, causing changes in transcriptional activity and ultimately leading to adaptive reprogramming of the cell (Schenk and Snaar-Jagalska, 1999). The best-characterised signal relay is the reversible transfer of a phosphate (PO4) group by protein kinases. The importance of the phosphorylation signal transduction mechanism is highlighted by numerous studies that show it is essential in regulating growth, differentiation and responses to stress in all organisms (Shiu and Bleecker, 2001). Over the last two decades, rapid progress in whole-genome sequencing has revealed that land plants in general contain a much larger number of kinases than most other eukaryotes (Champion *et al.*, 2004). For example, the model plant species *Arabidopsis* (*Arabidopsis thaliana*) encodes an estimated 1,027 protein kinases in comparison to Human (*Homo sapiens*) and nematode (*C. elegans*) that have 518 and 400 kinases, respectively (Krupa *et al.*, 2004). Plants may have a large number of kinases to compensate for their sessile nature and the fixed positions of the cells within cell walls. Due to these constraints, plants may need to integrate a much wider range of signals than animals. Therefore, the expansion of the kinase family could be an evolutionary strategy to modulate these signals through

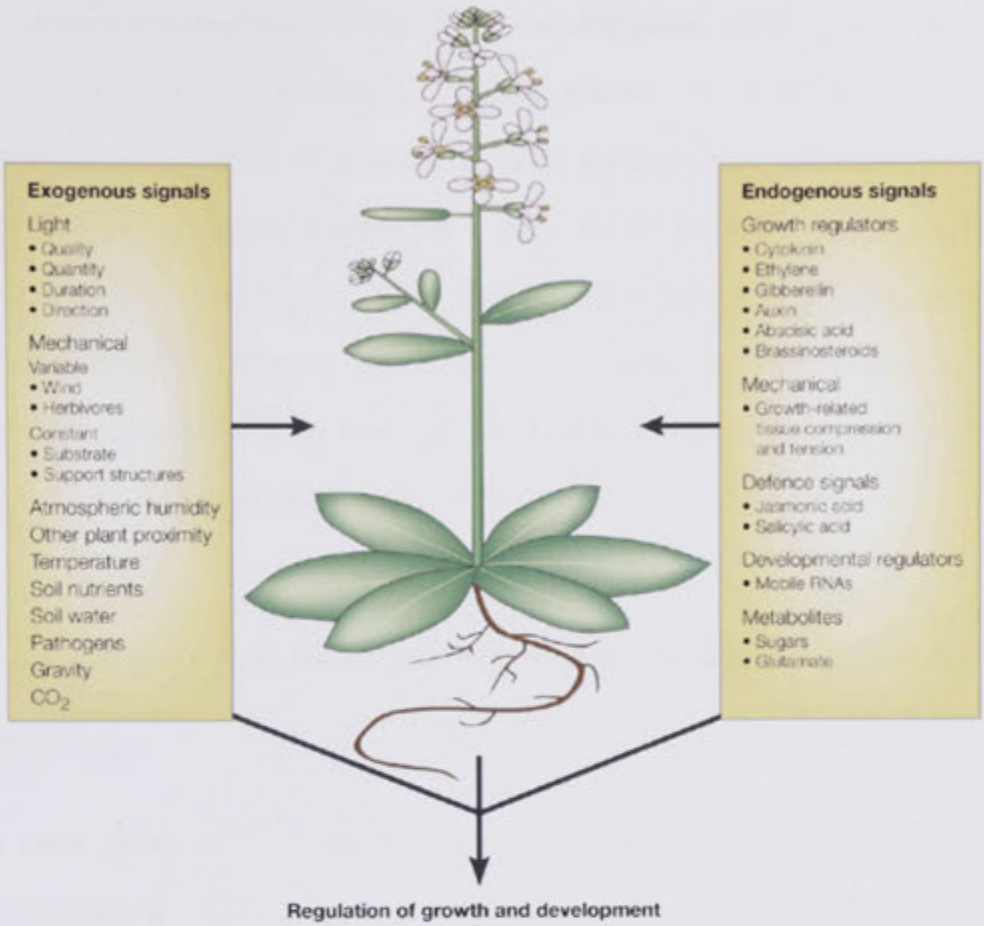


**Figure 1.1:** Plants integrate a wide range of exogenous and endogenous signals via signal transduction pathways to mount appropriate adaptive responses (diagram from Gilroy and Trewavas, 2001).

specific phosphorylation cascades. While impressive advances have been made in the characterization of many of these kinase-encoding genes, especially in the model species *Arabidopsis*, there remains a large number for which no functional information is available. This thesis focuses on a sub-group of kinases known as SIPTO kinase Interactor 1 (*PTI1*)-like genes that belong to the RLCK family (Receptor Like Cytoplasmic Kinase). *PTI1*-like genes have been characterised in other plant species, however this has been limited to a few individual genes and functional information is still scant and limited to one or two isoforms, with no study so far of the family as a whole, in any species.

## 1.2 Common Signalling pathways in biotic and abiotic stress response

In nature, plants encounter two broad types of stresses, biotic stresses induced by pathogens or attacks by insects and herbivores, and abiotic stresses that arise from unfavourable environmental conditions (Lichtenthaler, 1998). While in the pre-genome era research mainly focussed on physiological responses to these stresses (Mittler, 2006), in the last two decades, with the advent of molecular biology techniques and rapid progress in sequencing, there has been intense interest in studying the genetic determinants of plants responses to stress. Techniques such as RT-PCR differential display, large-scale mutant analyses and more recently cDNA microarray technology, have helped identify a number of genes with functions relating to stress perception, stress signalling and downstream adaptive responses (Hirayama and Shinozaki, 2010; Nishimura and Dangl, 2010). It is now becoming apparent that the gene regulatory networks of biotic and abiotic stresses share

numerous components, with intra-cellular kinases emerging as a common 'player' (Chinnusamy *et al.*, 2004; Fujita *et al.*, 2006) (Figure 1.2). In plants, the two major classes of stress-activated kinases that have been shown to transduce upstream signals into downstream cellular responses are the MAPK and CDPK families (Jonak *et al.*, 2002; Ludwig *et al.*, 2004; Rodriguez *et al.*, 2010).

### 1.2.1 Mitogen activated protein kinase (MPKs)

#### *1.2.1.1 The MAPK signalling module*

MAP kinases are ubiquitous proteins that have been shown to regulate numerous processes in plants, such as stress and hormone responses as well as developmental programs (Mishra *et al.*, 2006). Their role is mediated by reversible phosphorylation of three kinase modules that act in a hierarchical manner: MAP3Ks (MAPKKKs/MEKKs), MAP2K (MEKs/MKKs) and MAPKs (MPKs) (Figure 1.3). The *Arabidopsis* genome contains 60 putative MAP3Ks, 10 MAP2Ks and 20 MAPKs that can be distinguished from one another by specific amino acid signature patterns (Rodriguez *et al.*, 2010). Bioinformatics studies indicate that in *Arabidopsis*, approximately 60% of the MPK genes are associated with chromosomal regions that are likely to have evolved from large-scale duplication events (Champion *et al.*, 2004).

#### *1.2.1.2 MAPK signal specificity*

Biochemical and genetic analysis suggests that the MPK cascades converge and diverge at different levels and in doing so, maintain specificity for different

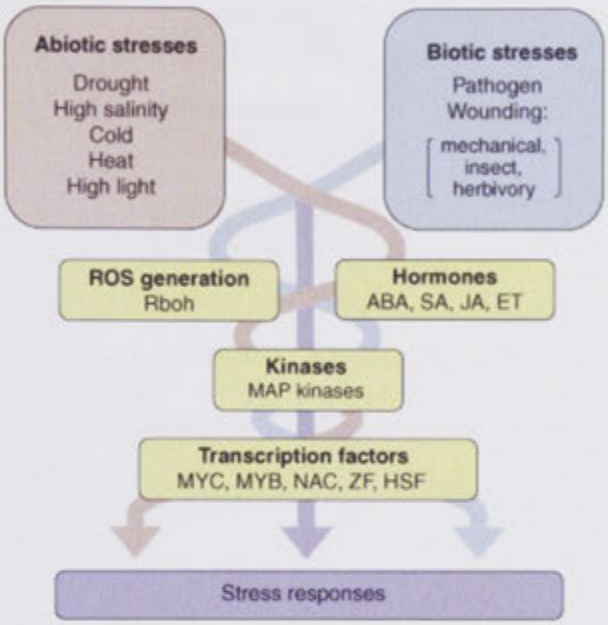


**Figure 1.2:** Abiotic and biotic stresses signalling pathways display a number of convergence points with kinases such as MAPKs playing a central and acting as nodes mediating cross-talks between stresses (diagram from Fujita *et al.*, 2006).

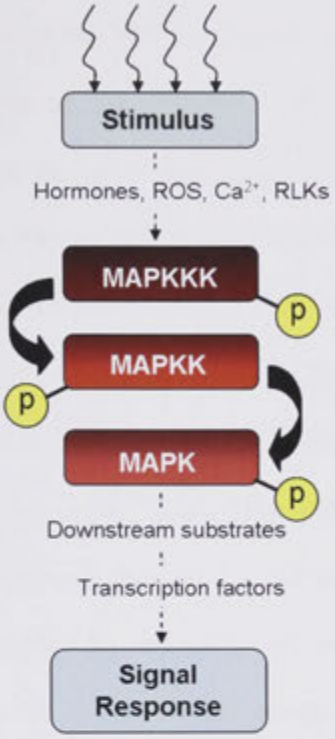


**Figure 1.3: Schematic representation of MAPK signalling cascade**. Activation of a MAPKKK by upstream hormones or secondary messengers leads to the sequential phosphorylation of MAPKK and MAPK. Activated MAPK may in turn phosphorylate downstream substrates or transcription factors thus inducing changes in gene expression (Adapted from Rodriguez *et al*., 2010).

signalling pathways (Jonak *et al.*, 2002). A number of regulatory mechanisms have been proposed. Depending on the stimulus, cell surface receptors can activate distinct MAPK signalling cascades leading to different cellular outcomes. For example, the MAP kinase module [MEKK1, MKK4/MKK5 and MPK3/MPK6] has been shown to function downstream of FLS2, a cell surface receptor that is essential for the bacterial flagellin recognition (Asai *et al.*, 2002). Similarly, another MAPK module consisting of MEKK1, MKK2 and MPK4/MPK6 is implicated in responses to cold and salt stresses (Teige *et al.*, 2004). Thus, different biotic and abiotic signals can be perceived and integrated through the action of specific MAPK modules. Moreover, the presence of MEKK1 and MPK6 in both modules suggests that vastly different upstream stimuli can also converge through overlapping components of the MPK signalling cascade (Zhang *et al.*, 2006), indicating that signal specificity can also be achieved by variation in MPK combinations within the modules.

Subcellular localisation can also contribute to signal specificity by preferentially targeting individual MAPK components to different cellular components. Protein phosphatases that regulate the phosphorylation status of kinases and scaffolding proteins that act as chaperones between MAPK components are additional mechanisms that have been proposed to maintain signal specificity (Rodriguez *et al.*, 2010).

## 1.2.2 Calcium-dependent protein kinases (CDPKs)

### *1.2.2.1 CDPK activation*

$Ca^{2+}$ ions play an important role in plant development and stress related responses (Scrase-Field and Knight, 2003; DeFalco *et al.*, 2010). CDPKs, in addition to related

kinases (CCaMKs and CRKs), are implicated in the transduction of $Ca^{2+}$ signals *via* their phosphorylation activity (Hrabak *et al.*, 2003). CDPK proteins are characterised by an N-terminal serine/threonine catalytic domain and four conserved $Ca^{2+}$ binding EF-hand motifs that make up the C-terminal calmodulin-like domain (CLD). Binding of $Ca^{2+}$ to the CLD, results in a conformational change of the protein, leading to autophosphorylation and activation of downstream signal relay. A junction domain between the kinase and CLD domains functions as an auto-inhibitor keeping the protein in an 'off' state in the absence of $Ca^{2+}$ induction (Harper and Harmon, 2005).

### *1.2.2.2 Signal Specificity of CDPKs*

Sequencing projects have revealed that CDPKs constitute a large multi-gene family in both eudicots and monocots. The *Arabidopsis* genome contains 34 *CDPK*-like genes that vary in their spatio-temporal expression patterns, reflecting the diverse role of $Ca^{2+}$ as a signalling molecule in plant development (Hrabak *et al.*, 2003). In addition, a number of *CDPK*s in *Arabidopsis* and other species have been shown to be specifically expressed in response to stress-related stimuli and hormone signals suggesting that these kinases might also mediate cross-talks between different stresses (Ludwig *et al.*, 2004). This is supported by biochemical studies showing inducible phosphorylation of CDPKs in response to biotic and abiotic stress (Witte *et al.*, 2010). As all CDPKs are thought to be activated by $Ca^{2+}$, a question is: what determines the specificity of CDPK signalling? One hypothesis that has been offered is that different stimuli may trigger different patterns of change in $Ca^{2+}$ ion concentrations within the cell and therefore calcium signatures may encode stress-specific information leading to different cellular outcomes (DeFalco *et al.*, 2010). Depending on the calcium signature, different CDPKs may become activated, or

alternatively the enzymatic activity of a single CDPK may vary in strength and duration and thus affect the phosphorylation of downstream substrates (Ludwig *et al.*, 2004). The latter mechanism seems to hold for the tobacco NtCDPK2 that is activated by both osmotic stress and pathogen elicitors (Romeis *et al.*, 2001). Interestingly, expression of a deregulated version of NtCDPK2 such that the kinase is constitutively active, has been shown to compromise stress-induced activation of two tobacco MAPKs, SIPK and WIPK (Ludwig *et al.*, 2005). Moreover, the inhibition of these two MAPKs by the deregulated NtCDPK2 is dependent on the production of the phytohormone ethylene. Application of pharmacological inhibitors of ethylene synthesis or production in leaves expressing the NtCDPK2 variant completely restored kinase activation of SIPK and WIPK (Ludwig *et al.*, 2005). These results point to a possible cross-talk between CDPK and MAPK signalling cascades mediated by ethylene and suggest an additional level of complexity in the signalling network of biotic and abiotic stresses in plants (Wurzinger *et al.*, 2011). As with MAPKs, variation in subcellular targeting of different CDPKs to the plasma membrane, cytoplasm, nucleus and peroxisome (Dammann *et al.*, 2003) may be another possible mechanism to maintain signal specificity for different pathways.

## 1.3 Receptor-Like Cytoplasmic Kinases (RLCKs) – An emerging class of kinases in plant stress and developmental signalling

RLCKs in plants constitute a large family of approximately 150 and 380 members in *Arabidopsis* and rice (*Oryzae sativa*), respectively (Shiu and Bleecker, 2003). They belong to the monophyletic superfamily known as Receptor-like kinases (RLKs)

(Shiu and Bleecker, 2001) based on the similarity of the catalytic domains but they do not have an extracellular nor transmembrane domain. Although functional information relating to individual RLCKs is limited, a few studies of individual isoforms have demonstrated a role of these kinases in stress responses (*SlPTO*, *PBS1*, *BIK1*, *CRCK1*) (Tang *et al.*, 1996; Swiderski and Innes, 2001; Yang *et al.*, 2004; Veronese *et al.*, 2006) and development (*CDG1*) (Muto *et al.*, 2004). An RLCK subfamily known as the PTI1 kinases represents an emerging class of regulators involved in diverse signalling processes. Individual isoforms from various plant species have been implicated in biotic, abiotic and developmental pathways (Zhou *et al.*, 1995; Herrmann *et al.*, 2006; Zou *et al.*, 2006; Takahashi *et al.*, 2007). A wheat PTI1-like kinase of particular interest to our lab was identified in roots during drought signalling, (Masle J, Unpublished data). The precise function of these PTI1 kinases in these different signalling pathways still needs to be elucidated, however. A serine threonine kinase belonging to the AGC (cAMP-dependent protein kinase A, cGMP-dependent protein kinase G and phospholipid dependent protein kinase C) family, known as oxidative signal-inducible 1 (OXI1/AGC2-1, hereafter referred to as OXI1), has been identified as an interacting partner of several PTI1-like kinases (Anthony et al., 2006; Forzani et al., 2011), but the physiological context for each of these interaction is still not known. A brief review summarising the roles of individual *PTI1* isoforms is given below.

### 1.3.1 Initial hypothesis of PTI1-like kinases involved in biotic and abiotic signalling cascades

My interest in *PTI1* genes stemmed from a separate project in the lab on root mechanical impedance, using wheat (*Triticum aestivum*) as a model system (Masle J,

Unpublished data). Root mechanical impedance is a condition inherently associated with soil drying and compaction that inhibits root elongation and triggers a systemic signalling to leaf meristems and stomata (Masle and Passioura, 1987; Cairns *et al.*, 2004). In the context of investigating the molecular pathways involved, gene expression studies were conducted to identify genes differentially expressed in response to mechanical stress. One of the ESTs induced by mechanical stress was found to share a strong homology with the tomato defence-related gene *SlPTI1* (Zhou *et al.*, 1995). The induction of a pathogen-related gene by an abiotic, physical stress was a very interesting finding which suggests an involvement of *PTI1*-like genes in both biotic and abiotic stress response pathways. The identification during the course of this thesis, of a maize *PTI1*-like gene, *ZmPTI1/ZmPTI1C*, induced by cold, mannitol and salt provided circumstantial evidence in support of that hypothesis (Zou *et al.*, 2006).

### 1.3.2 The tomato SlPTI1 - a downstream target of *Pseudomonas syringae* related SlPTO kinase

The tomato SlPTI1 (*Solanum lycopersicum*) was the first *PTI1* isoform to be identified, from its direct interaction with the SlPTO kinase in a yeast two-hybrid screen (Zhou *et al.*, 1995). *SlPTO* was the first resistance (R) gene found in plants and was isolated through map-based cloning in tomato (Martin *et al.*, 1993). Following infection with the bacterial pathogen *Pseudomonas syringae* pathovar *tomato* (*Pst*), the SlPTO kinase directly interacts with either of two pathogen secreted avirulence (Avr) effector proteins, AvrPTO or AvrPTOB. This interaction, together with SlPRF, a nucleotide-binding leucine rich repeat (NB-LRR) protein, results in the race-specific resistance against *P. syringae* pv *tomato* (Xiao *et al.*,

2003; Mucyn *et al.*, 2006). The SlPTO interactor, SlPTI1 was also shown to encode a functional serine/threonine protein kinase capable of autophosphorylation *in vitro*. Cross-phosphorylation assays demonstrated that SlPTI1 was also specifically phosphorylated by SlPTO, suggesting that the protein was likely to function downstream of SlPTO (Zhou *et al.*, 1995; Sessa *et al.*, 2000). The function of *SlPTI1* in *SlPTO*-mediated immunity is still not known, and unconfirmed reports indicate that *SlPTI1* loss-of-function mutants are indistinguishable from wild-type (WT), possibly due to redundancy with another *SlPTI1* paralog in tomato (Unpublished data, (Oh and Martin, 2011). Heterologous expression of *SlPTI1* in tobacco provided indirect evidence for the role of *SlPTI1* in pathogen response to *P. syringae* pv *tabaci* (AvrPto). Leaves of transgenic tobacco plants overexpressing *SlPTI1* showed enhanced Hypersensitive Response (HR) as manifested by rapid and localised cell death at the site of pathogen infection (Figure 1.4). The wild-type plants on the other hand, showed delayed HR against the pathogen. This suggested that *SlPTI1* functions as a positive regulator of *R* protein-mediated defence signalling in tobacco (Zhou *et al.*, 1995). The subsequent isolation of a soybean *PTI1*-like gene, *GmPTI1* whose expression was found to be induced by salicylic acid (SA) treatment (Tian *et al.*, 2004) further supported the role of PTI1-like kinases in plant defence responses.

### 1.3.3 Rice OsPti1a functions as a negative regulator of defence signalling

A rice *PTI1*-like gene, (*OsPTI1A*) with 87% similarity (amino-acid) with the tomato *SlPTI1* was recently identified in a T-DNA mutant screen for enhanced resistance to rice blast disease (Takahashi *et al.*, 2007). The *Ospti1a* mutant is characterised by spontaneous necrotic lesions and induction of defence related HR pathway

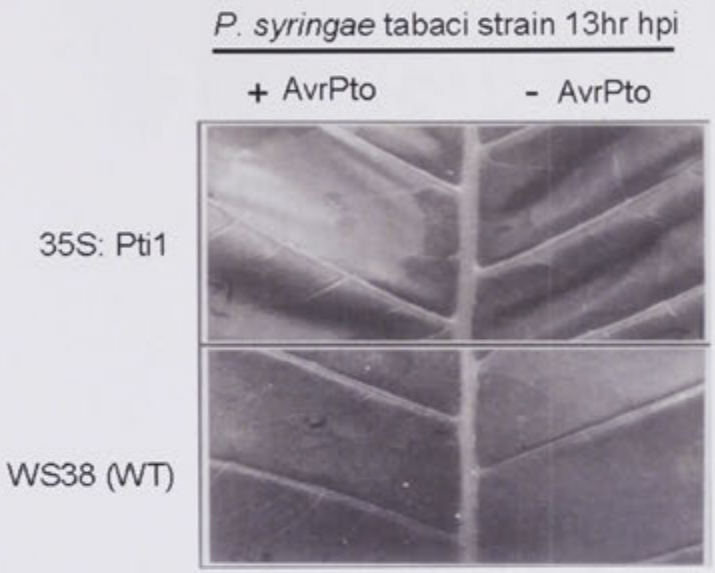


**Figure 1.4:** The tomato *SIPTI1* enhances the tobacco hypersensitive response to *Pseudomonas. syringae* pv. *tabaci* strain expressing the Avirulence effector AvrPT0. (Adapted from Zhou *et al.*, 1995).

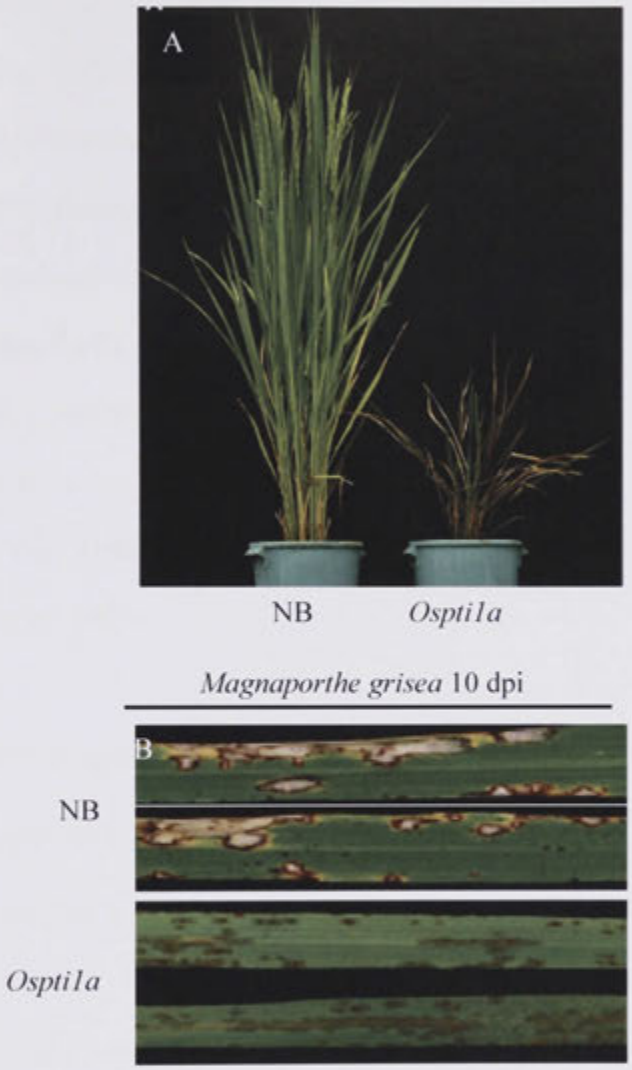


**Figure 1.5:** (A) Wild-type rice *Nipponbarre* (NB) and *Ospti1a* mutant (B) Increased resistance of *Ospti1a* mutant against the compatible race of the rice blast fungus *Magnaporthe grisea*. Adapted from Takahashi *et al.*, (2007).

suggesting that the gene negatively regulates defence signalling in rice (Figure 1.5). Consistent with this hypothesis, the mutant showed an increased resistance to the compatible race of rice blast fungus, *Magnaporthe grise*a. Conversely, plants overexpressing *OsPTI1A* were more susceptible to the compatible race of bacterial pathogen, *Xanthomonas oryzae* pv *oryzae* (Takahashi *et al*., 2007). A negative role of *OsPTI1A* in disease resistance is in stark contrast with the positive role of its *SlPTI1* tomato homolog which caused enhanced HR when overexpressed in tobacco plants challenged with *P. syringae* pv. *tabaci* expressing *AvrPTO* (Zhou *et al*., 1995). Interestingly however, complementation of the *Ospti1a* mutant with the *SlPTI1* cDNA suppressed the mutant phenotype. This indicates that the HR pathway in which these PTI1 proteins function may have evolved differently in tomato and rice (Takahashi *et al*., 2007).

### 1.3.4 ZmPti1a kinase plays a role in reproductive development by influencing pollen fitness

The *ZmPTI1A* gene is one four highly conserved PTI1-like genes present in maize (*ZmPTI1-A*, *-B*, *-C*, *-D*) that shares significant homology with the tomato *SlPTI1* isoform (75% amino acid similarity) (Herrmann *et al*., 2006). Maize transgenic lines stably transformed with the ZmPTI1A:GFP fusion construct revealed fluorescence to be targeted to the pollen plasma membrane and specifically localised to regions of callose deposition (Herrmann *et al*., 2006) (Figure 1.6 A,B). The polysaccharide callose in the form of (1,3)-β-glucan is ubiquitously found in many higher plants and is involved in a wide range of plant processes including plant development and response to abiotic and biotic stresses (Chen and Kim, 2009). The function of

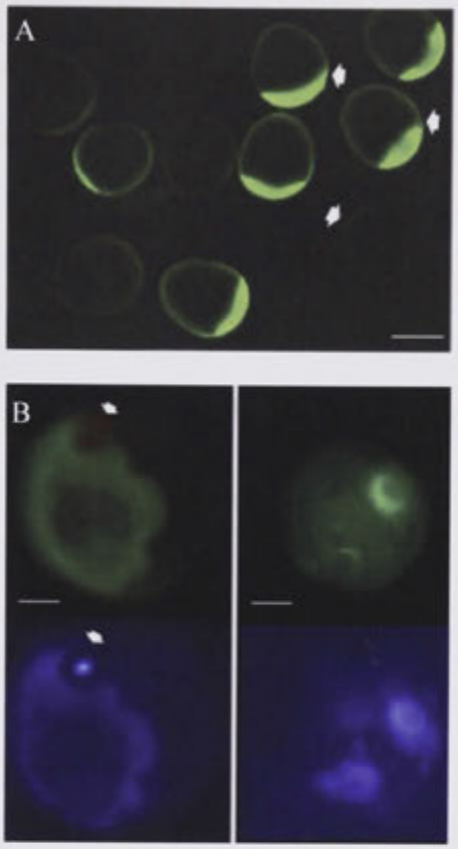


**Figure 1.6: Expression of ZmPTI1A:GFP fusion in maize pollen.** (A) ZmPTI1A:GFP expression targeted to the pollen plasma membrane. (B) A closer inspection revealed ZmPTI1A:GFP to co-localise with callose deposition, shown here in aniline blue staining (Figure from Hermann *et al.*, 2006).

*ZmPTI1A* in pollen development was investigated further by specific knockdown using a targeted RNA interference (RNAi) approach. Selfing of hemizygous transgenic plants as well as reciprocal crosses with WT showed that the RNAi transgene was not transmitted in the expected Mendelian ratio as demonstrated by aberrant segregation ratio in the progeny. The cause of this abnormal segregation was demonstrated to be a reduced ability of the transgenic pollen to fertilize the ovules. Interestingly however, homozygous *Zmpti1-a* pollen did not show any visible phenotypic defects when germinated *in vitro* and the relative amounts of callose were also unaltered. This implies that while ZmPTI1A kinase activity is not vital for pollen viability it still provides a competitive advantage to the pollen by influencing overall fitness (Herrmann *et al*., 2006).

## 1.4 Projects Aims

### 1.4.1 Rationale of the Study

A few *PTI1*-like genes have been characterised in a few plant species (Zhou *et al.*, 1995; Tian *et al.*, 2004; Anthony *et al.*, 2006; Herrmann *et al.*, 2006; Takahashi *et al.*, 2007); functional information is still scant, however, and limited to one or two specific isoforms, with no study so far of the family as a whole, in any species. The aim of this study was to identify and characterise the *Arabidopsis PTI1* gene family and in doing so offer insights into the general mechanism of PTI1 signal transduction pathway.

### 1.4.2 Chapter summary

The first step was to determine the size of the family in *Arabidopsis* (Chapter 2). I initially focussed on identifying a PTI1-specific amino-acid signature pattern and then used this conserved motif to retrieve 8 putative *PTI1* genes from the *Arabidopsis* genome. These 8 *PTI1*-like genes were then examined for conserved sequence patterns, and the phylogenetic relationship with previously characterised *PTI1* genes from other species was analysed. I discuss the likely role of chromosomal duplication events specific to the *Arabidopsis* lineage in the expansion of the *PTI1* family. I next examine the transcriptional activity of the 8 *PTI1*-like genes to see if duplication from an ancestral gene was followed by divergence in expression patterns. Results show some overlap but also variation in the expression of individual Arabidopsis *PTI1*-like genes, during development and in response to stress.

Characterisation of these genes was taken a step further, using a reverse genetics approach. T-DNA insertion lines for the different *PTI1* isoforms were isolated and analysed for developmental phenotypes. I provide evidence that one of the *Arabidopsis PTI1* isoforms performs a non-redundant function in root development. Using RNAi silencing, I show that this isoform is a negative regulator of early root elongation, affecting the size of the root apical meristem (**Chapter 3**).

I next asked whether some of the *Arabidopsis PTI1* isoforms may be functional homologues of the tomato and rice *PTI1* genes in their role in plant disease resistance. One PTI1 isoform, *PTI1-5*, is shown to confer enhanced basal resistance to the *Pseudomonas syringae* pathovar *tomato* DC3000 (*Pst* DC3000). Preliminary data that identify *OXI1* as a *PTI1-5* signalling partner in the *Pst* DC3000 defence pathway are also presented **(Chapter 4)**.

In the final chapter, I summarise the findings of the study and present a hypothetical model for a general *PTI1* signal transduction pathway in *Arabidopsis* **(Chapter 5)**.

## 1.5 Reference:


**Anthony RG, Khan S, Costa J, Pais MS, Bogre L** (2006) The *Arabidopsis* protein kinase PTI1-2 is activated by convergent phosphatidic acid and oxidative stress signaling pathways downstream of PDK1 and OXI1. J Biol Chem **281**: 37536-3746

**Asai T, Tena G, Plotnikova J, Willmann MR, Chiu WL, Gomez-Gomez L, Boller T, Ausubel FM, Sheen J** (2002) MAP kinase signalling cascade in *Arabidopsis* innate immunity. Nature **415:** 977-983

**Cairns JE, Audebert A, Townend J, Price AH, Mullins CE** (2004) Effect of soil mechanical impedance on root growth of two rice varieties under field drought stress. Plant and Soil **267:** 309-318

**Champion A, Kreis M, Mockaitis K, Picaud A, Henry Y** (2004) *Arabidopsis* kinome: after the casting. Funct Integr Genomics **4:** 163-187

**Chen XY, Kim JY** (2009) Callose synthesis in higher plants. Plant Signal Behav **4:** 489-492

**Chinnusamy V, Schumaker K, Zhu JK** (2004) Molecular genetic perspectives on cross-talk and specificity in abiotic stress signalling in plants. J Ex Bot **55:** 225-236

**Dammann C, Ichida A, Hong B, Romanowsky SM, Hrabak EM, Harmon AC, Pickard BG, Harper JF** (2003) Subcellular targeting of nine calcium-dependent protein kinase isoforms from *Arabidopsis*. Plant Physiol **132:** 1840-1848

**DeFalco TA, Bender KW, Snedden WA** (2010) Breaking the code: $Ca^{2+}$ sensors in plant signalling. Biochem J **425:** 27-40

**Forzani C, Carreri A, de la Fuente van Bentem S, Lecourieux D, Lecourieux F, Hirt H** (2011) The *Arabidopsis* protein kinase PTI1-4 is a common target of the oxidative signal-inducible1 (OXI1) and MAP kinases. Febs J **278**: 1126-1136

**Fujita M, Fujita Y, Noutoshi Y, Takahashi F, Narusaka Y, Yamaguchi-Shinozaki K, Shinozaki K** (2006) Crosstalk between abiotic and biotic stress responses: a current view from the points of convergence in the stress signaling networks. Current Opinion in Plant Biology **9:** 436-442

**Gilroy S, Trewavas A** (2001) Signal processing and transduction in plant cells: the end of the beginning? Nat Rev Mol Cell Biol **2:** 307-314

**Harper JF, Harmon A** (2005) Plants, symbiosis and parasites: a calcium signalling connection. Nat Rev Mol Cell Biol **6:** 555-566

**Herrmann MM, Pinto S, Kluth J, Wienand U, Lorbiecke R** (2006) The PTI1-like kinase ZmPti1a from maize (Zea mays L.) co-localizes with callose at the plasma membrane of pollen and facilitates a competitive advantage to the male gametophyte. BMC Plant Biol **6:** 22

**Hirayama T, Shinozaki K** (2010) Research on plant abiotic stress responses in the post-genome era: past, present and future. Plant J **61:** 1041-1052

**Hrabak EM, Chan CW, Gribskov M, Harper JF, Choi JH, Halford N, Kudla J, Luan S, Nimmo HG, Sussman MR, Thomas M, Walker-Simmons K, Zhu JK, Harmon AC** (2003) The *Arabidopsis* CDPK-SnRK superfamily of protein kinases. Plant Physiol **132:** 666-680

**Jonak C, Okresz L, Bogre L, Hirt H** (2002) Complexity, cross talk and integration of plant MAP kinase signalling. Current Opinion in Plant Biology **5:** 415-424

**Krupa A, Abhinandan KR, Srinivasan N** (2004) KinG: a database of protein kinases in genomes. Nucleic Acids Res **32:** D153-155

**Lichtenthaler HK** (1998) The stress concept in plants: an introduction. Ann N Y Acad Sci **851:** 187-198

**Ludwig AA, Romeis T, Jones JD** (2004) CDPK-mediated signalling pathways: specificity and cross-talk. J Exp Bot **55:** 181-188

**Ludwig AA, Saitoh H, Felix G, Freymark G, Miersch O, Wasternack C, Boller T, Jones JD, Romeis T** (2005) Ethylene-mediated cross-talk between calcium-dependent protein kinase and MAPK signaling controls stress responses in plants. Proc Natl Acad Sci U S A **102:** 10736-10741

**Martin GB, Brommonschenkel SH, Chunwongse J, Frary A, Ganal MW, Spivey R, Wu T, Earle ED, Tanksley SD** (1993) Map-based cloning of a protein kinase gene conferring disease resistance in tomato. Science **262:** 1432-1436

**Masle J, Passioura JB** (1987) The effect of soil strength on the growth of young wheat plants. Australian Journal of Plant Physiology **14:** 643-656

**Mishra NS, Tuteja R, Tuteja N** (2006) Signaling through MAP kinase networks in plants. Arch Biochem Biophys **452:** 55-68

**Mittler R** (2006) Abiotic stress, the field environment and stress combination. Trends in Plant Science **11:** 15-19

**Mucyn TS, Clemente A, Andriotis VME, Balmuth AL, Oldroyd GED, Staskawicz BJ, Rathjen JP** (2006) The tomato NBARC-LRR protein Prf interacts with Pto kinase *in vivo* to regulate specific plant immunity. Plant Cell **18:** 2792-2806

**Muto H, Yabe N, Asami T, Hasunuma K, Yamamoto KT** (2004) Overexpression of constitutive differential growth 1 gene, which encodes a RLCKVII-subfamily protein kinase, causes abnormal differential and elongation growth after organ differentiation in *Arabidopsis*. Plant Physiol **136:** 3124-3133

**Nishimura MT, Dangl JL** (2010) *Arabidopsis* and the plant immune system. Plant J **61:** 1053-1066

**Oh CS, Martin GB** (2011) Effector-triggered immunity mediated by the Pto kinase. Trends Plant Sci **16:** 132-140

**Rodriguez MC, Petersen M, Mundy J** (2010) Mitogen-activated protein kinase signaling in plants. Annu Rev Plant Biol **61:** 621-649

**Romeis T, Ludwig AA, Martin R, Jones JD** (2001) Calcium-dependent protein kinases play an essential role in a plant defence response. Embo J **20:** 5556-5567

**Schenk PW, Snaar-Jagalska BE** (1999) Signal perception and transduction: the role of protein kinases. Biochim Biophys Acta **1449:** 1-24

**Scrase-Field SAMG, Knight MR** (2003) Calcium: just a chemical switch? Current Opinion in Plant Biology **6:** 500-506

**Sessa G, D'Ascenzo M, Martin GB** (2000) The major site of the pti1 kinase phosphorylated by the pto kinase is located in the activation domain and is required for pto-pti1 physical interaction. Eur J Biochem **267:** 171-178

**Shiu SH, Bleecker AB** (2001) Plant receptor-like kinase gene family: diversity, function, and signaling. Sci STKE **2001:** re22

**Shiu SH, Bleecker AB** (2001) Receptor-like kinases from *Arabidopsis* form a monophyletic gene family related to animal receptor kinases. Proc Natl Acad Sci U S A **98:** 10763-10768

**Shiu SH, Bleecker AB** (2003) Expansion of the receptor-like kinase/Pelle gene family and receptor-like proteins in *Arabidopsis*. Plant Physiol **132:** 530-543

**Swiderski MR, Innes RW** (2001) The *Arabidopsis* PBS1 resistance gene encodes a member of a novel protein kinase subfamily. Plant J **26:** 101-112

**Takahashi A, Agrawal GK, Yamazaki M, Onosato K, Miyao A, Kawasaki T, Shimamoto K, Hirochika H** (2007) Rice Pti1a negatively regulates RAR1-dependent defense responses. Plant Cell **19:** 2940-2951

**Tang X, Frederick RD, Zhou J, Halterman DA, Jia Y, Martin GB** (1996) Initiation of Plant Disease Resistance by Physical Interaction of AvrPto and Pto Kinase. Science **274:** 2060-2063

**Teige M, Scheikl E, Eulgem T, Doczi R, Ichimura K, Shinozaki K, Dangl JL, Hirt H** (2004) The MKK2 pathway mediates cold and salt stress signaling in *Arabidopsis*. Mol Cell **15:** 141-152

**Tian AG, Luo GZ, Wang YJ, Zhang JS, Gai JY, Chen SY** (2004) Isolation and characterization of a Pti1 homologue from soybean. J Exp Bot **55:** 535-537

**Veronese P, Nakagami H, Bluhm B, Abuqamar S, Chen X, Salmeron J, Dietrich RA, Hirt H, Mengiste T** (2006) The membrane-anchored BOTRYTIS-INDUCED KINASE1 plays distinct roles in *Arabidopsis* resistance to necrotrophic and biotrophic pathogens. Plant Cell **18:** 257-273

**Witte CP, Keinath N, Dubiella U, Demouliere R, Seal A, Romeis T** (2010) Tobacco calcium-dependent protein kinases are differentially phosphorylated *in vivo* as part of a kinase cascade that regulates stress response. J Biol Chem **285:** 9740-9748

**Wurzinger B, Mair A, Pfister B, Teige M** (2011) Cross-talk of calcium-dependent protein kinase and MAP kinase signalling. Plant Sig Behav **6:** 8-12

**Xiao F, Lu M, Li J, Zhao T, Yi SY, Thara VK, Tang X, Zhou JM** (2003) Pto mutants differentially activate Prf-dependent, avrPto-independent resistance and gene-for-gene resistance. Plant Physiol **131:** 1239-1249

**Yang T, Chaudhuri S, Yang L, Chen Y, Poovaiah BW** (2004) Calcium/calmodulin up-regulates a cytoplasmic receptor-like kinase in plants. J Biol Chem **279:** 42552-42559

**Zhang T, Liu Y, Yang T, Zhang L, Xu S, Xue L, An L** (2006) Diverse signals converge at MAPK cascades in plant. Plant Physiology and Biochemistry **44:** 274-283

**Zhou J, Loh YT, Bressen RA, Martin GB** (1995) The tomato gene Pti1 Encodes a serine/threonine kinase that is phophorylated by Pto and is invloved in hypersensitive response. Cell **83:** 925-935

**Zou HW, Wu ZY, Yang Q, Zhang XH, Cao MQ, Jia WS, Huang CL, Xiao X** (2006) Gene expression analyses of ZmPti1, encoding a maize Pti-like kinase, suggest a role in stress signalling. Plant Science **171:** 99-105

# Chapter 2

## Identification of the *Arabidopsis* *PTI1* gene family

# Chapter 2

## 2.1 Introduction

The functional study of an uncharacterised gene family requires knowledge of gene annotation to first define the limits of the family size. This is particularly relevant when dealing with kinases as they comprise one of the largest families in eukaryotes and in *Arabidopsis*, represent 4.3% of the total genes (Champion *et al.*, 2004). Phylogenetic analysis of PTI1 kinases in rice, maize and *Arabidopsis* indicate the presence of 5 to 10 *PTI1*-like genes in the *Arabidopsis* genome (Anthony *et al.*, 2006; Herrmann *et al.*, 2006; Takahashi *et al.*, 2007). The PlantsP database (http://plantsp.genomics.purdue.edu/htmL/index.htmL), which classifies plant protein kinases based on their primary sequence, lists an even greater number. Thirteen genes, annotated *PTI1*-like are grouped together with the *SlPTI1* tomato gene in the RLCK8 subfamily. A complete search of the whole database reveals numerous other genes annotated as putative *PTI1*-like genes within related families such as RLCK6 and RLCK7 as well as other seemingly unrelated kinase families such as such as LRRK3 (Leucine Rich Repeat Kinase), C4LK (Crinky 4 Like Kinase), PERLK (Plant External Response Like Kinase). Intriguingly, in the same database, *SlPTI1* is only one of the characterised *PTI1* genes to be present.

Overall, there is therefore convergent information indicating the presence in *Arabidopsis* of a large *PTI1* family. Its size, however, and composition are quite uncertain. The published phylogenetic information and PlantsP classification are based on homology searches, using as a query, the primary full-length amino acid sequence. Thus, depending on the stringency and the parameters used in the search,

the number of genes that can putatively be annotated as *PTI1*-like can vary considerably. Homology BLAST based searches are designed to find optimal local alignments between two sequences (Altschul *et al.*, 1997) and therefore proteins that contain domain-to-domain similarity may be overrepresented in the search results. This may especially be the case of PTI1-like kinases, as all characterised orthologs described in the literature so far, possess a catalytic domain that on average covers 80% of the total protein sequence (Zhou *et al.*, 1995; Tian *et al.*, 2004; Herrmann *et al.*, 2006; Takahashi *et al.*, 2007). The presence of a single catalytic domain that is generally conserved among serine/threonine plant kinases thus increases the chances of selecting false-positives.

In this chapter, I present an alternative method for defining the *Arabidopsis PTI1* gene family. The underlying principle is the detection of a short conserved amino-acid pattern found in characterised members of the gene family which can then be used as a bait to search for putative orthologs. Through this approach, I identify 8 *Arabidopsis* genes as putative *PTI1* genes, based on the presence of a consensus signature pattern common with the known *PTI1* genes from tomato, rice, maize and soybean (Zhou *et al.*, 1995; Tian *et al.*, 2004; Herrmann *et al.*, 2006; Takahashi *et al.*, 2007). I then use the whole set of sequences for a phylogenetic analysis of evolutionary relationships of the *PTI1* family. An *in silico* analysis of promoters reveals conserved putative regulatory elements among the *Arabidopsis PTI1*-like genes. Experimental data on constitutive gene expression in various plant tissues and response to biotic and abiotic stress shows that all eight *PTI1* isoforms are expressed and suggests some functional specificity among them.

## 2.2 Materials and Methods

### 2.2.1 Maintenance and cultivation of *Arabidopsis* plant material

#### *2.2.1.1 Seed sterilization and stratification of Arabidopsis seeds*

*Arabidopsis* seeds that were cultivated on tissue culture media or in soil were surface sterilised in a laminar flow. A 10% v/v sodium hypochlorite solution containing 2 µL TritonX100 was first prepared. The seed sterilisation solution was prepared by mixing 1 part of the 10% sodium hypochlorite with 9 parts 100% Ethanol. Seeds were immersed in 1 mL of this solution and mixed for 5 minutes. Seeds were spun down momentarily in a bench top microcentrifuge (18,000 g) and the sterilisation solution was removed. Seeds were rinsed once in 100% ethanol and spun down as before. Ethanol solution was removed as much as possible and seeds were allowed to air dry by leaving the lid of the microcentrifuge tube open in the laminar flow overnight. For *in vitro* growth, surface sterilised seeds were plated on Hoagland's plant nutrient media and plates were wrapped in Al-foil and placed at $4^0$ C for 72 hours for stratification. For soil grown plants, surface sterilised seeds were resuspended in sterile water in microcentrifuge tubes and placed at $4^0$ C for 72 hours for stratification.

#### *2.2.1.2 In vitro growth conditions*

Hoaglands agar medium was made up of the following: 1x modified Hoaglands solution (Hoaglands and Arnon, 1950) (Table 2.1), 1% w/v sucrose, 1.2% w/v Agar (Type M, Sigma), 0.05% w/v MES, pH adjusted to 5.8, with KOH. The nutrient solution was prepared in MilliQ treated water and autoclaved before use. 25 mL of the autoclaved Hoagland's agar medium was poured in standard bacterial petri

dishes. Upon solidification, surface sterilized seeds were sown on the medium and the plates were wrapped with micropore surgical tape (3M) to prevent media contamination and to permit gas-exchange. Plates were oriented vertically and placed in growth cabinets (Conviron, Controlled Environments, Pembina, ND) fitted with white fluorescent tubes and incandescent bulbs providing 120 μE $m^{-2}s^{-1}$ cent at $21^0$ C and 60% relative humidity. A short-day cycle of 10 hours was chosen to promote vegetative growth.

Table 2.1 Concentration of nutrients in Hoagland's solution

| | Molecular weight (g/mol) | Final Concentration (mM) |
|---|---|---|
| **Macronutrients** | | |
| $KNO_3$ | 101.1 | 2 |
| $Ca[NO_3]_2. 4H_2O$ | 236.15 | 5 |
| $MgSO_4. 7H_20$ | 246.47 | 2 |
| $KH_2PO_4$ | 136.1 | 2 |
| **Micronutrients** | | |
| Fe-EDTA | 367.1 | 0.09 |
| $H_3BO_3$ | 61.83 | 46 |
| $MnCl_2. 4H_20$ | 197.91 | 9.1 |
| $ZnSO_4. 7H_20$ | 287.56 | 0.77 |
| $CuSO_4$ | 159.60 | 0.32 |
| $(NH_4)6Mo_7O_{24}. 4H_20$ | 1235.8 | 0.11 |

### *2.2.1.3 Growth conditions of soil-grown plants*

For the cultivation of *Arabidopsis* plants in soil, seed raising mix (Denbco, Victoria, Australia) was used supplemented with the slow release fertiliser, Osmocote® (Scotts, Australia) (5 g/L). Cold-treated seeds immersed in sterile water were pipetted directly onto the surface of pre-moistened soil or alternatively seedlings growing on nutrient media plates (~8 days) were transferred using forceps to 400 mL soil pots and placed in growth chambers. 8 seedlings are transferred initially and subsequently thinned leaving the 4 most uniform plants for each pot. Plastic domes were placed on top of the growth trays for the first 3 days to maintain high humidity and allow seedlings to be established in the soil. The growth conditions in the chamber are as described in the previous section. These conditions had to be modified for plants to be used for *Pseudomonas syringae* bacterial infection. Due to the inherent variability of bacterial growth *in planta*, a large number of soil grown plants were needed to be grown so as to ensure reproducibility. Plants were therefore grown in 20 cell punnet trays (100 mL each cell) with density of 2 plants per cell. In addition, humidity domes placed on top of the punnet trays were retained for entire duration of the experiment, as maintenance of high humidity is known to be an important factor in promoting *P. syringae* growth *in planta*. All soil-grown plants were watered from the bottom up by adding water to the flats.

### *2.2.1.4 Growth conditions of hydroponically grown plants*

Plants that were to be challenged with PEG induced osmotic stress were grown in hydroponic boxes with a removable lid. The hydroponic set-up was developed in the lab for an independent project (Schulze and Masle, Unpublished data) but was found to be ideal for the purpose of growing plants to be challenged with PEG induced

osmotic stress. Dislodged caps of 1.5 mL centrifuge tubes were filled with Hoagland's agar medium (without sucrose, 0.8% agar) and upon solidification the caps were placed in bored holes on the lid of the hydroponic box. The box was filled with 1/3 Hoagland's nutrient solution (Hoaglands and Arnon, 1950) (without sucrose) prepared fresh from a 1X stock. The level of nutrient solution in each box was adjusted such that it reached the level of the agar filled caps. Seeds were sown on the surface of Hoagland's agar media filled centrifuge caps and the hydroponic boxes were transferred to plant growth chamber rooms. The growth conditions were as described in section 2.2.1.2. To prevent drying, the boxes were covered with humidifier domes for 10 days till the seedling were established in the growing medium. The plants were grown for 16 days before the PEG induced osmotic stress was carried out. Two days prior to stress imposition, the nutrient solution was replenished with freshly prepared 1/3 Hoaglands solution. A representative box showing hydroponically grown plants just prior to stress treatment is shown in Appendix 2.6.1.

## 2.2.2 Stress Conditions

### *2.2.2.1 Pseudomonas syringae biotic stress challenge*

#### 2.2.2.1.1 Maintenance of P. *syringae* pv. *tomato* cultures

*Pseudomonas syringae* pv. *tomato* (*Pst*) strain DC3000 virulent strain was used for all biotic challenges in this study. The *Pst* isolates were obtained from Dr. Peer Schenk's lab (University of Queensland, Australia). The bacteria was streaked onto selective King's medium-B (KB) (King *et al.*, 1954) (10 g/L proteose peptone, 1.5 g/L anhydrous $K_2HPO_4$, 1.5 g/L $MgSO_4$. 7H20, 10 mL/L glycerol, 1.5% bacto Agar, pH=7) containing rifampicin (100 µg/mL) and kanamycin (50 µg/mL) from -80$^0$ C

glycerol stocks. Streaked plates were incubated at $28^0$ C for 48 hours before storing at $4^0$ C.

#### 2.2.2.1.2 *P. syringae* pv. *tomato* inoculation

Prior to plant inoculation, *Pst* DC3000 was re-streaked onto a fresh KB plate containing rifampicin (100 µg/mL) and kanamycin (50 µg/mL). A single colony was transferred to a 5 mL liquid KB pre-culture and incubated at $28^0$ C for 48 hours. 50 µL of the preculture was transferred to 100 mL KB culture with appropriate antibiotics and incubated at $28^0$ C for 16-20 hours until the reaching an optical density $OD_{600}$ = 0.1. 40 mL of the liquid culture was centrifuged at 1500 g and bacterial cells were pelleted. The cells were washed once with 10 mM $MgCl_2$ and spun down as before. The cells were resuspended in 10 mM $MgCl_2$ and the concentration of the bacterial suspension was adjusted so as to give a final $OD_{600}$ of 0.05 which corresponds to approximately to $2.5x10^7$ colonyforming units/mL. Lower inoculum density were tested, however $OD_{600}$ of 0.05 was chosen since it gave the most consistent results in terms of disease symptoms following infection (Appendix 2.6.3).

The syringe infiltration technique was based on the protocol described in the "The *Arabidopsis* Book" (chapter-*Arabidopsis* thaliana-*Pseudomonas syringae* interaction) (Katagiri *et al*., 2002). Plants were grown in growth chambers under short-day conditions, which promote development of bigger leaves and therefore provide a larger surface area for bacterial infiltration. Five week-old plants that were in the vegetative phase were used for inoculation. Prior to infiltration the leaves were marked at the base of petiole so as identify them the following day for harvest. The

*Pst* DC3000 bacteria suspension was pressure infiltrated on the abaxial side of the leaf using a needleless 1 mL syringe. Only a part of the leaf was infiltrated and care was taken to avoid the main vasculature, as damage is known to affect the viability of the leaf. Control plants were inoculated with 10 mM $MgCl_2$. Following inoculation the humidity domes were placed on the plant growth flats till the time of harvest. Twenty-four hours following infection, mock and bacterial infiltrated leaves were harvested for total RNA isolation.

### *2.2.2.2 PEG induced osmotic stress on plants grown hydroponically*

Osmotic stress treatments of hydroponically cultivated plants were initiated 16 days after sowing and 3 hours after dark/light transition. Each hydroponic box accommodates growth of ~ 60 plants and two replicate boxes each were used for osmotic stress and control treatment (Appendix 2.6.1). Non-permeating high molecular weight polyethylene glycol (Molecular Weight = 8000) (PEG8000) was employed as the osmotica to lower the water potential ($\psi_w$) of the media. Since PEG does not behave like an ideal solute, the concentration used in this experiment was based on a previously determined PEG calibration curve (Masle, unpublished data) where $\psi_w$ values were derived empirically. Earlier reports have suggested that typically unstressed plants are exposed to $\psi_w$ values of approximately -0.2 MPa (van der Weele *et al.*, 2000; Verslues *et al.*, 2006). In addition, the PEG8000 concentration range was initially tested on wildtype young seedlings in a root elongation bioassay. The results showed an expected reduction in primary root elongation as a classic response to lowering the $\psi_w$ of plant growth media (Appendix 2.6.2A). Based on these preliminary tests, for the purpose of this experiment, PEG8000 was used at a concentration of 140 g/L (17.5 mM) which would

approximately lower the $\psi_w$ of the media to -0.8225. Two days prior to stress treatment, the nutrient solution for all hydroponic boxes was replenished. PEG8000 (140 g/L) was dissolved in freshly prepared 1/3 Hoagland's nutrient solution. The hydroponic boxes were carefully transferred from the growth room to the laboratory where the osmotic stress treatment was performed and subsequently returned to the growth room. For the application of osmotic stress, the lid of the hydroponic box, which also supports the plants, was carefully lifted to minimise disturbances. The nutrient solution was then tipped out and replaced with PEG supplemented media. For control plants, the nutrient solution was replaced with identical media. For RNA isolation shoot samples were taken in 3 biological replicates (n= 6-8 seedlings) 1, 3 and 24 hours after the onset of the PEG treatment.

#### *2.2.2.3 Mannitol induced osmotic stress of plants grown on agar based media*

Seeds were plated on Hoagland's nutrient agar medium as described in section 2.2.1.2. The plates were transferred to growth cabinets and oriented vertically in racks. Osmotic stress treatments of plants were initiated 6 days after germination. Seedlings were transferred using forceps to Hoagland's plates supplemented with or without 200 mM mannitol. In both PEG and mannitol induced osmotic stress treatments, the solute concentration in the growth media was adjusted to cause a similar decrease in water potential (-0.8 MPa). In addition, a mannitol bioassay which monitored root elongation in wild-type seedlings, showed an expected reduction in root growth with an increase in solute concentration (Appendix 2.6.2B). RNA was isolated from whole seedlings taken in 3 biological replicates (n=8 seedlings) and sampled 1 and 7 hours after treatment.

## 2.2.3 Molecular techniques

### *2.2.3.1 RNA isolation*

#### 2.2.3.1.1 Precautionary measures

To avoid contamination of RNAse enzymes, the lab bench and materials were wiped with RNAse *AWAY*™ (Invitrogen) prior the RNA isolation procedure. In addition MilliQ water used during the protocol was made RNase free by treating with 0.2% (v/v) diethylpyrocarbonate (DEPC, Sigma-Aldrich) and leaving overnight on the lab bench. The DEPC was inactivated the following day by autoclaving.

#### 2.2.3.1.2 Total RNA isolation

For both endogenous and stress induced tissue samples, approximately 100 mg of liquid nitrogen frozen samples were ground to fine powder in chilled 1.5 mL centrifuge tubes using micropestles™ (Eppendorf). For root tip samples, substantially less starting material (~30 mg) was used for RNA isolation. For each ground sample, 0.4 mL of TRIzol® (Invitrogen) was added and homogenised by vortexing for 1 minute. 0.12 mL of chloroform was added and incubated at room temperature for 2 minutes. Samples were centrifuged for 15 minutes at $4^0$ C (18,000 g). The upper aqueous phase containing the RNA was transferred to a new microcentrifuge tube and RNA was precipitated using isopropanol (0.7 x volume of aqueous phase). In the case of root tip samples, 1 µL (20 µg) of RNA carrier, glycogen (Sigma-Aldrich) was added to improve the yield of total RNA isolated. Samples were incubated at $-20^0$ C for 4 hours and subsequently centrifuged for 30 minutes at $4^0$ C (18,000 g). The supernatant was removed and the pellet washed once with cold 75% ethanol and centrifuged as before. The supernatant was decanted and RNA pellet was air dried in the laminar flow for 15 minutes before dissolving in 22

μL of DEPC-treated water by incubating at $60^0$ C for 5 minutes. The RNA concentration ($A_{260}$) and quality ($A_{260}/A_{280}$ ratio) was measured using the NanoDrop® ND-1000 Spectrophotometer. Samples were snap-frozen with liquid nitrogen and stored at $-80^0$ C.

### *2.2.3.2 cDNA synthesis*

Prior to cDNA synthesis, Dynabeads® (Invitogen) coated with Oligo$(dT)_{25}$ was used to isolate poly A+ RNA from TRIzol® (Invitrogen) extracted total RNA. The basis of the protocol relies on base pairing between the poly $A^+$ residues at the 3' end of most eukaryotic mRNA and Oligo(dT)25 bound to the Dynabeads. The mRNA can then be separated from other RNA species using the magnetic particle concentrate (MPC) (Dynal MPC™, Invitrogen), which binds to the Dyanbeads. The isolated mRNA can be directly used for downstream cDNA synthesis. The protocol, which has been published ensures high quality mRNA with no genomic DNA contamination, a problem commonly associated with TRIzol extracted RNA (Jost et al., 2007; Berkowitz et al., 2008).

For all samples, 2 μg of total RNA was used for mRNA isolation, with the exception of root-tips for which less than 1 μg of total RNA was used. Dynabeads were resuspended in 15μL binding buffer (20 mM Tris-HCL at pH 7.5, 1 M LiCl, and 2 mM EDTA) in 0.2 mL PCR tubes. 2 μg of total RNA was added to the bead suspension and incubated for 15 minutes at room temperature. Tubes were placed in the MPC and liquid supernatant was removed. The tubes were removed from the MPC and the mRNA bound beads were washed twice with wash buffer (10 mM Tris-HCL at pH 7.5, 0.15 M LiCl, and 1 mM EDTA). The wash buffer was separated

and removed from the beads each time using the MPC. The beads were resuspended in 10 µL of elution buffer (10 mM Tris-HCL at pH 7.5) and incubated at $85^0$ C for two minutes which allows separation of the mRNA from the Oligo$(dT)_{25}$ bound to the Dynabeads. First strand cDNA synthesis was carried out on the eluted mRNA using M-MLV reverse transcriptase (Promega). Eluted mRNA was combined with 1 µL oligo$(dT)_{18}$ (50 µM) primer and 1 µL dNTPs (10 mM each dNTP) and incubated at $65^0$ C for five minutes. The tubes were placed immediately on ice and 10 µL of the reverse transcription master mix (4 µL 5x RT buffer, 40 U RNasin ribonuclease inhibitor, 100 U M-MLV reverse transcriptase, all from Promega) was added. The first strand cDNA synthesis was performed at $42^0$ C for 60 minutes and heat inactivated at $70^0$ C for 10 minutes. cDNA was stored in $-20^0$ C.

### *2.2.3.3 Primer Design*

Primers for qRT-PCR transcript measurements were initially searched for annealing specificity to the gene of interest on the AtRTPrimer database which is the repository for genome wide gene specific primer pairs for *Arabidopsis* (Han and Kim, 2006). The primers retrieved from the database were further optimised using the Vector NTI™ 10 (Invitrogen) software with following considerations:

- Product size in the range of 80-200 bp
- Primer annealing temperature approximately $60^0$ C
- GC content approximately 50%
- If possible one of the two primers were designed to cross exon-exon borders to avoid amplification from genomic DNA or alternatively, primers were designed on either side of an intron so contaminating genomic DNA could be

detected.

Primers were checked for specificity using BLASTN (TAIR BLAST 2.2.8) search on the TAIR website (http://www.*Arabidopsis*.org/Blast/index.jsp). All primers were ordered from Invitrogen, Australia Pty Ltd and stocks (100 µM) were stored at -20$^0$ C. All primers used in this chapter are mentioned in Appendix 2.6.4.

### *2.2.3.4 Quantitative Real-time RT-PCR (qRT-PCR) set up and analysis*

qRT-PCR transcript measurements were carried out using the ABI PRISM® 7900HT Sequence Detection System (Applied Biosystems) according to the manufacturers instructions. Each qRT-PCR reaction contained: 2.5 µL of cDNA template (1:10 dilution), 2.5 µL of forward and reverse primer mix (1.2 µM each), and SYBR Green PCR Master Mix). Two different SYBR Green Master mixes were used during the course of this study: 2006-mid 2009 – Power SYBR® Green supplied by Applied Biosystems, mid 2009-2011 – FastStart Universal SYBR® Green supplied by Roche Applied Science.

Each sample was tested with primers for the gene of interest and at least two reference genes. A minimum of 3 biological replicates (sample variability) and 2 technical replicates (process variability) were included in each qRT-PCR run. Typical cycling conditions were as follows:

- 50$^0$ C for 2 min (initial activation of Taq DNA polymerase)
- 95$^0$ C for 10 minutes (denaturation)
- 40 cycles of: 95$^0$ C for 15 sec (denaturation), 60$^0$ C for 1 min (primer annealing and elongation)

- $95^0$ C for 15 sec, $60^0$ C for 15 sec, $95^0$ C for 15 sec (Final Extension and Melt curve analysis.

### *2.2.3.5 Analysis of qRT-PCR expression data*

Data analysis was carried out using the software Sequence Detection System (SDS) (Version 2.2, Applied Biosystems). For each reaction, melt-curve analysis was performed to verify only a single product was being amplified. PCR amplification efficiencies were calculated using the LinRegPCR program (Ramakers *et al.*, 2003). Newly designed primers were tested on cDNA samples and were only used for further analysis if the PCR efficiencies were $\geq 1.8$.

Two previously validated internal reference gene primers, PDF2 (At1g13320) and APT1 (At1g27450) (Czechowski *et al.*, 2005; Jost *et al.*, 2007) were used for normalization of genes of interest expression by calculating Ct values (Pfaffl, 2001):

$\Delta Ct$ = Ct (gene of interest) – Ct (reference gene).

Fold change for gene of interest versus internal reference was expressed by using the formula: $2^{-\Delta Ct}$ (Reference gene = 1).

In cases where expression levels for the gene of interest are to be calculated relative to a reference samples (such as WT or unstressed control plants) the comparative $\Delta\Delta Ct$ method was used (Livak and Schmittgen, 2001):

$\Delta\Delta Ct$ = Ct (sample) – Ct (reference sample)

Fold change for gene of interest in sample versus reference sample was expressed by using the formula: $2^{-\Delta\Delta Ct}$ (Reference sample = 1).

## 2.3 Results

### 2.3.1 Identification of Amino acid signature pattern as a tool for finding potential *PTI1* orthologs in *Arabidopsis* thaliana

In order to identify putative *PTI1* functional orthologs in *Arabidopsis*, a method that relied on the use of a conserved motif was adopted in this study (Jonassen *et al.*, 1995). The practical use of a consensus signature pattern as a diagnostic tool to identify a family of proteins is well documented and is best illustrated by the PROSITE database (Bairoch, 1993). Here, groups of functionally related proteins are distinguished based on short stretches of amino acids that are positionally conserved and are stored as motif or signature patterns. They are presumed to arise as a result strong evolutionary pressure to retain these residues for the specific protein functions and are indicative of common ancestry (Bairoch, 1993).

In order to identify a unique signature pattern, PTI1 orthologs from tomato (SlPTI1) (Zhou *et al.*, 1995), rice (OsPTI1A) (Takahashi *et al.*, 2007), maize (ZmPTI1A, ZmPTI1C) (Herrmann *et al.*, 2006) and soybean (GmPTI1) (Tian *et al.*, 2004) that have been previously characterised in the literature were used to identify a unique signature pattern. Only orthologs that have been shown to be involved in either biotic or abiotic stress response or developmental related pathways were included in the analysis. In using these genes only, the aim was to ensure maximum stringency in the selection to retrieve *Arabidopsis* kinases with relevant functions.

### 2.3.2 Multiple sequence alignment of the functional Pti1 genes

As an initial step, a multiple amino-acid sequence alignment of the five characterised PTI1 kinases was carried out (Figure 2.1) using the ClustalW program available at the EMBOSS site (http://www.ebi.ac.uk/Tools/msa/clustalw2/). A very high level of conservation was observed in the regions spanning the catalytic domain common to the five genes. The kinase domain starts approximately 70 amino acids after the first methionine in all four genes. This catalytic region contains the 11 typical sub-domains found in most kinases (Hanks *et al.*, 1988). Embedded within these sub-domains are 14 kinases invariant residues, only 12 of which are conserved in the *PTI1*-like genes (Figure 2.1). The conserved glutamate residue in sub-domain III is substituted by glutamine and the glycine residue in subdomain VII is substituted by either an aspartate (Asp) or asparagine (Asn) residue. The glutamate to glutamine substitution is a conserved substitution of two polar residues with similar chemical structure, whereas the glycine to Asp/Asn is a non-conserved substitution. These substitutions do not, however, appear to affect the kinase activity of the protein (Zhou *et al.*, 1995; Herrmann *et al.*, 2006; Takahashi *et al.*, 2007).

Two residues (enclosed in red boxes in Figure 2.1) are known to play an important role in the phosphorylation activity of PTI1 kinases. The lysine 96 (K96) has been shown to be a critical residue for SlPTI1 and OsPTI1A auto-phosphorylation activity and in the tomato SlPTI1 protein the threonine 233 (T233) has been shown to be a main target for phosphorylation by SlPTO kinase (Zhou *et al.*, 1995; Takahashi *et al.*, 2007). Both residues are conserved in all 5 PTI1-like sequences analysed (Figure 2.1). These results provide a basis for the identification of a unique PTI1 specific signature pattern.

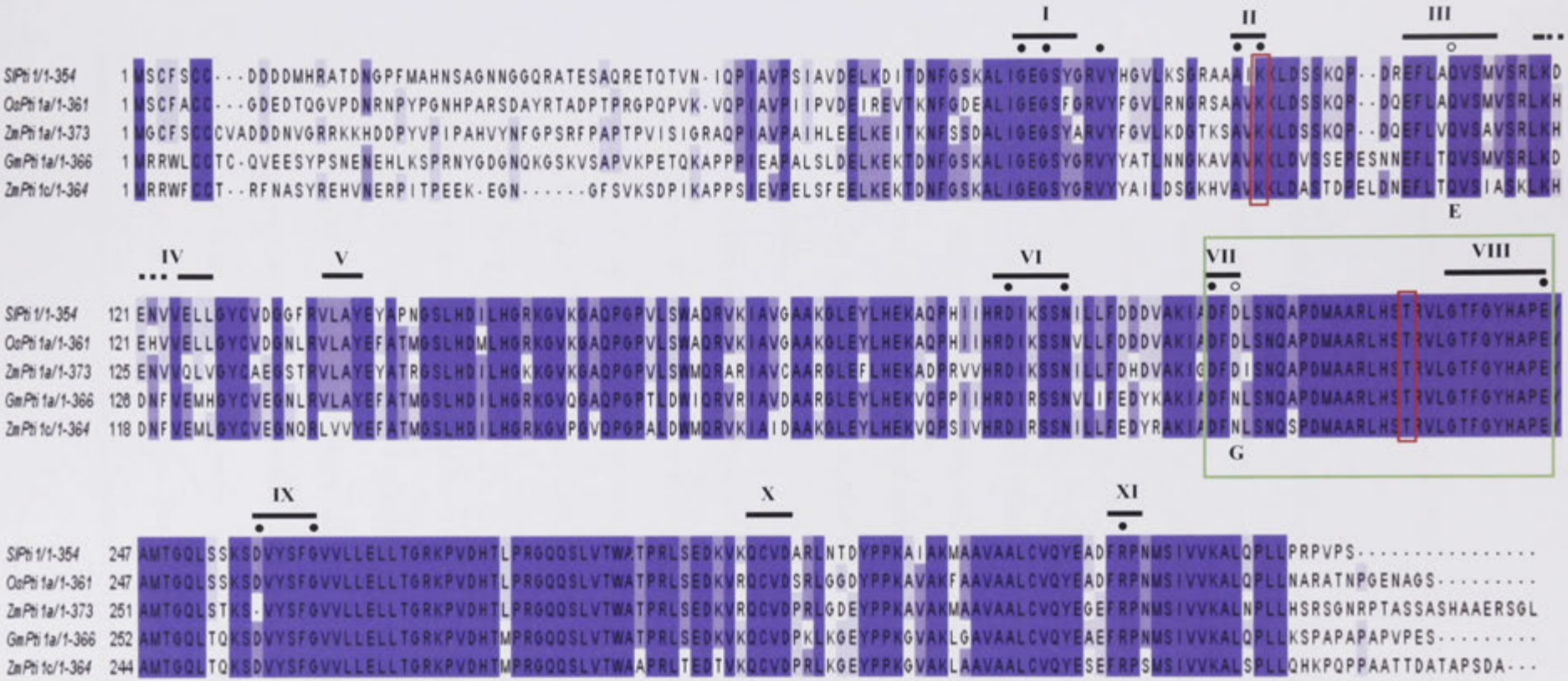


**Figure 2.1: Alignment of the characterised PTI1 kinases from Tomato (SlPTI1), Rice (OsPTI1A), Maize (ZmPTI1A,C) and Soybean (GmPTI1).** Different shades of blue denote amino acids shared between 3 (light), 4 (medium) or on all 5 (dark) PTI1 sequences. The 11 subdomains typical of all kinases are marked I – XI. Conserved residues found in most of the kinases are marked with closed circles. Conserved residues found in most kinases but substituted in PTI1 genes are marked with open circles. Residues important for PTI1 kinase function Red box: Lysine residue (K) target for SlPTI1 and OsPTI1A autophosphorylation; Threonine (T) residue in SlPTI1 and OsPTI1A is a phosphorylation target for other kinases. Amino acid stretch used for signature pattern identification green box.

### 2.3.3 PTI1 Signature Pattern and Identification of *Arabidopsis PTI1*-like genes

The multiple sequence alignment in Figure 2.1 shows a relatively high level of amino acid conservation in the catalytic domain particularly in the region between subdomains VII and X. In all kinases, the region between motifs DFG and APE is known as the 'activation segment' as it is known to alter the protein folding conformation upon phosphorylation and in effect has the capacity to switch the kinase between active and inactive states (Huse and Kuriyan, 2002). The activation segment is also known to contain highly conserved residues that are common to several kinases from different organisms (Johnson *et al.*, 1996). This site was chosen as a good candidate region for the identification of a sequence pattern unique to *PTI1*-like genes, based on two criteria:

1. The activation segment in the PTI1 kinases is of particular interest, since it shows a modification in the classical motif D-F-G replaced with D-F-(D/N).
2. The segment also contains the conserved threonine residue, which has been identified as the phosphorylation target site for SlPTI1 and OsPTI1A kinases (Sessa *et al.*, 2000; Takahashi *et al.*, 2007).

The unaligned sequences between the DFD and APE motifs of the tomato, rice, soybean and maize PTI1 proteins were submitted to a web based program called PRATT (http://au.expasy.org/) (Jonassen, 1997). This program searches for conserved patterns among a given number of unaligned input sequences. The 'percentage matching' parameter was set at 100 such that any pattern identified would be present in all input sequences. The results from the PRATT program identified 1 conserved pattern given below in the PROSITE syntax:

D-F-[DN]-[LI]-S-[DN]-Q-[AS]-P-D-X-A-A-R-L-H-S-T-R-V-L-G-T-F-G-Y-H-A-P-E

This consensus pattern was used to search for putative *Arabidopsis PTI1*-like genes using the online tool ScanProsite (http://au.expasy.org/) which allows conserved patterns to be used as queries (de Castro *et al.*, 2006). This search gave a total of 17 hits in the *Arabidopsis* protein sequence database (Table 2.1). Since the ScanPrositeS searches against several protein databases (Swiss-Prot, TrEMBL, PDB), a number of hits were redundant entries for the same gene. There were also 3 unknown sequences which were based on predictions only. These sequences were BLAST-searched (TAIR BLAST 2.2.8) against the *Arabidopsis* genomic database to identify the gene IDs. In total, 8 *Arabidopsis* genes were retrieved through the pattern search (Table 2.2) and are located on *Arabidopsis* chromosomes I, II and III (Figure 2.2). These putative orthologs include 4 *Arabidopsis* kinases previously named *PTI1-1*, *PTI1-2*, *PTI1-3* and *PTI1-4* from a yeast-two-hybrid (Y2H) analysis (indicated by asterisk in Table 2.2) (Anthony *et al.*, 2006; Forzani *et al.*, 2011). The 4 other genes were named *PTI1-5* to *PTI1-8* to be consistent with gene nomenclature in the literature.

Table 2.2: *Arabidopsis* genes retrieved from ScanProsite search using the *PTI1* signature motif.

| UniProt/SwissProt ID | Gene Locus | PRATT Pattern match % | Top BLAST hit for non-annotated sequences | Designated gene name in this study |
|---|---|---|---|---|
| O80719 | At2g47060* | 100% | - | *PTI1-4* |
| O80719-2 | At2g47060* | 100% | - | *PTI1-4* |
| O80719-3 | At2g47060* | 100% | - | *PTI1-4* |
| B9DFG5 | At3g59350* | 100% | - | *PTI1-3* |
| B9DHY7 | At3g59350* | 100% | - | *PTI1-3* |
| O49339 | At2g30740* | 100% | - | *PTI1-2* |
| Q8H1G6 | At1g06700* | 100% | - | *PTI1-1* |
| Q93Y19 | At1g48210 | 100% | - | *PTI1-7* |
| Q940H1 | At3g59350* | 100% | - | *PTI1-3* |
| Q94K67 | At1g06700* | 100% | - | *PTI1-1* |
| Q9LNH4 | Predicted protein | 100% | At1g48210 | *PTI1-7* |
| Q9LUT0 | At3g17410 | 100% | - | *PTI1-8* |
| Q9LX36 | At3g59350* | 100% | - | *PTI1-3* |
| Q9M1Q2 | At3g62220 | 100% | - | *PTI1-5* |
| Q9M9X8 | Predicted protein | 100% | At1g06700 | *PTI1-1* |
| Q9SHK8 | Predicted protein | 100% | At1g06700 | *PTI1-1* |
| Q9ZW72 | At2g43230 | 100% | - | *PTI1-6* |

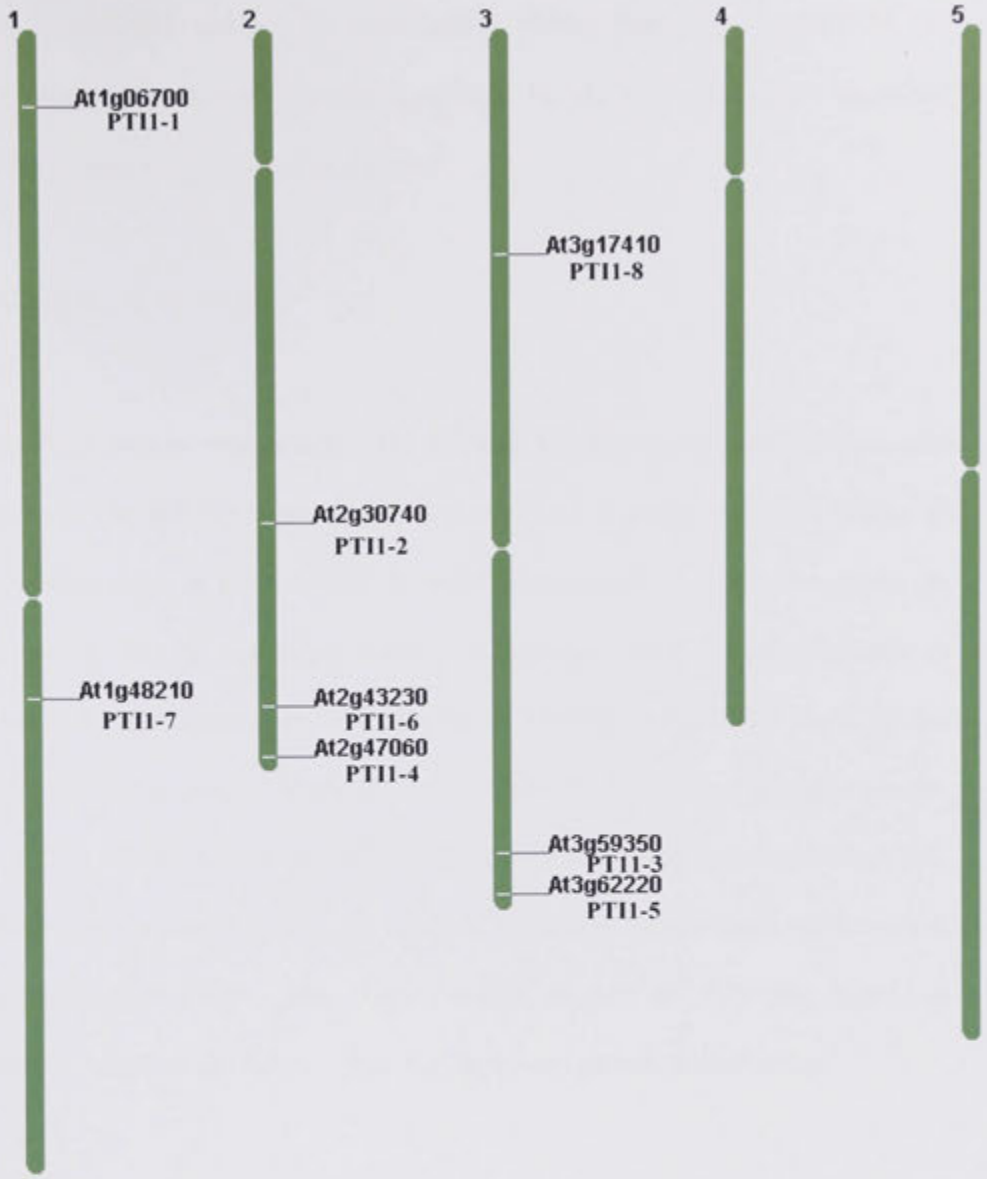


**Figure 2.2:** Chromosomal location of the *Arabidosis PTI1* genes using the 'MAP tool' available at the TAIR site (http://www.arabidopsis.org/jsp/ChromosomeMap/tool.jsp).

In order to ascertain whether an even smaller pattern than that identified by the PRATT program could still provide specificity for the *PTI1*-like genes identified above, the pattern was modified as follows:

F-[DN]-[LI]-S-x(8,12)-H-S-T

The modified pattern was smaller and allowed for more ambiguous amino acid substitutions. The x(8,12) syntax indicates that at least 8 and at most 12 residues of any type may occur at this position. In addition, the pattern only concentrates on regions surrounding the residues known to be important for PTI-1 function such as those surrounding the invariant Gly substituted Asp/Asn in the DFD motif, or the conserved threonine residue in the STR motif which constitutes a phosphorylation site in SlPTI1 and OsPTI1A kinases. A database search using ScanProsite and this modified pattern as query yielded the same 17 hits as before, comprising the same 8 *Arabidopsis* genes (Table 2.1). These results suggest 8 *PTI1*-like genes in *Arabidopsis*, based on overall sequence similarity and pattern conservation.

### 2.3.4 Prediction of putative *Arabidopsis PTI1* kinase genes

In order to examine the overall level of sequence similarity of the 8 *PTI1*-like *Arabidopsis* genes identified above, the full-length amino acid sequences were retrieved at TAIR (www.*Arabidopsis*.org) and aligned using the multiple sequence alignment program ClustalW (Figure 2.3). A high level of sequence conservation is observed among the 8 *Arabidopsis* isoforms (Figure 2.3). A pair-wise sequence comparison showed that the similarity extends to both nucleotide and amino-acid levels (Figure 2.4). In addition, the 11 canonical sub-domains characteristic of

**Figure 2.3: Multiple sequence alignment of PTI1 kinases from *Arabidopsis* (PTI1-1 to PTI1-8).** Different shades of blue denote amino acids shared between 6 (medium) or on all 8 (dark) PTI1 sequences. The 11 subdomains typical of all kinases are marked I – XI. Conserved residues found in most of the kinases are marked with closed circles. Conserved residues found in most kinases but substituted in PTI1 genes are marked with open circles. Residues important for tomato SlPTI1 and OsPTI1A kinase function are boxed: lysine (K), residue as a target for auto-phosphorylation; and threonine (T), phosphorylation target of other kinases.

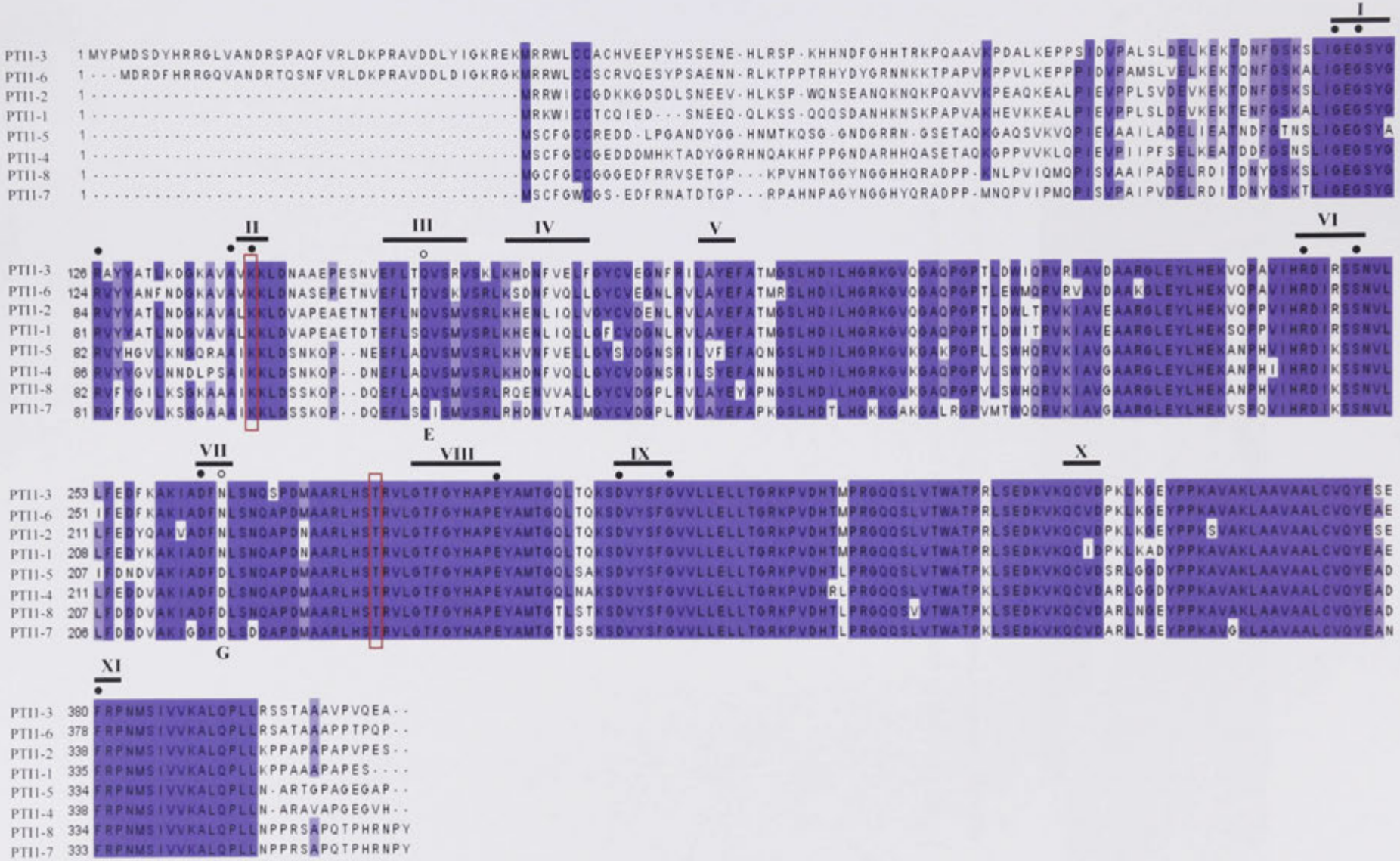
I
II
III
IV
V
VI
VII
VIII
IX
X
XI
E
G
PTI1-3
PTI1-6
PTI1-2
PTI1-1
PTI1-5
PTI1-4
PTI1-8
PTI1-7

| | PTI1-1 | PTI1-2 | PTI1-3 | PTI1-4 | PTI1-5 | PTI1-6 | PTI1-7 | PTI1-8 |
|---|---|---|---|---|---|---|---|---|
| PTI1-1 | | 84 | 66 | 61 | 66 | 69 | 65 | 65 |
| PTI1-2 | 88 | | 66 | 60 | 65 | 67 | 66 | 67 |
| PTI1-3 | 69 | 71 | | 59 | 59 | 81 | 61 | 62 |
| PTI1-4 | 69 | 68 | 62 | | 76 | 59 | 64 | 66 |
| PTI1-5 | 65 | 65 | 58 | 83 | | 61 | 69 | 72 |
| PTI1-6 | 71 | 69 | 83 | 62 | 58 | | 60 | 60 |
| PTI1-7 | 65 | 65 | 56 | 72 | 69 | 58 | | 86 |
| PTI1-8 | 66 | 68 | 59 | 76 | 73 | 61 | 87 | |

**Figure 2.4: Pairwise amino acid (purple) and nucleotide (green) sequence identity for the 8 PTI1 isoforms**. Highlighted in red are the highest conserved members for each gene (B).

kinases were present in all 8 proteins, supporting the TAIR database annotation of these genes as encoding putative kinases. As for the 5 characterised *PTI1*-like genes from other species, the catalytic domain in the 8 *Arabidopsis* putative PTI1 proteins starts approximately 70 amino acids after the first methionine except for PTI1-6 and PTI1-3 which have a longer N-terminal sequence of ~115 residues. The two same substitutions of invariant residues (subdomains III and VII, Figure 2.1) are also present (Figure 2.3). One of these substitutions, from Gly to Asp/Asn, was used as a criterion for identifying these genes. The second substitution, of a conserved glutamate residue in sub-domain III with a glutamine residue, was not. The lysine and threonine residues (sub-domains II and VIII respectively), known to be important for PTI1 kinase function, is present in all 8 *Arabidopsis* sequences. Overall, these results provide consistent data towards the annotation of the 8 retrieved *Arabidopsis* sequences as likely *PTI1* orthologs.

### 2.3.5 *PTI1* phylogeny

A phylogenetic analysis was carried out in order to investigate the evolutionary relationships among these 8 *Arabidopsis PTI1*-like kinases. The *Arabidopsis* amino acid sequences included in the analysis were chosen based on the results above, and were restricted to those containing the PTI1-specific signature pattern (F-[DN]-[LI]-Sx( 8,12)-H-S-T). Also included in the analysis were the published PTI1 kinases from tomato, rice, soybean and maize, as well as the putative wheat PTI1 kinase previously identified in our lab (Masle J, unpublished data).

The phylogenetic tree derived from the amino acid alignment using the MEGA3 program (http://www.megasoftware.net/mega4/mega.html) (Kumar *et al.*, 2004)

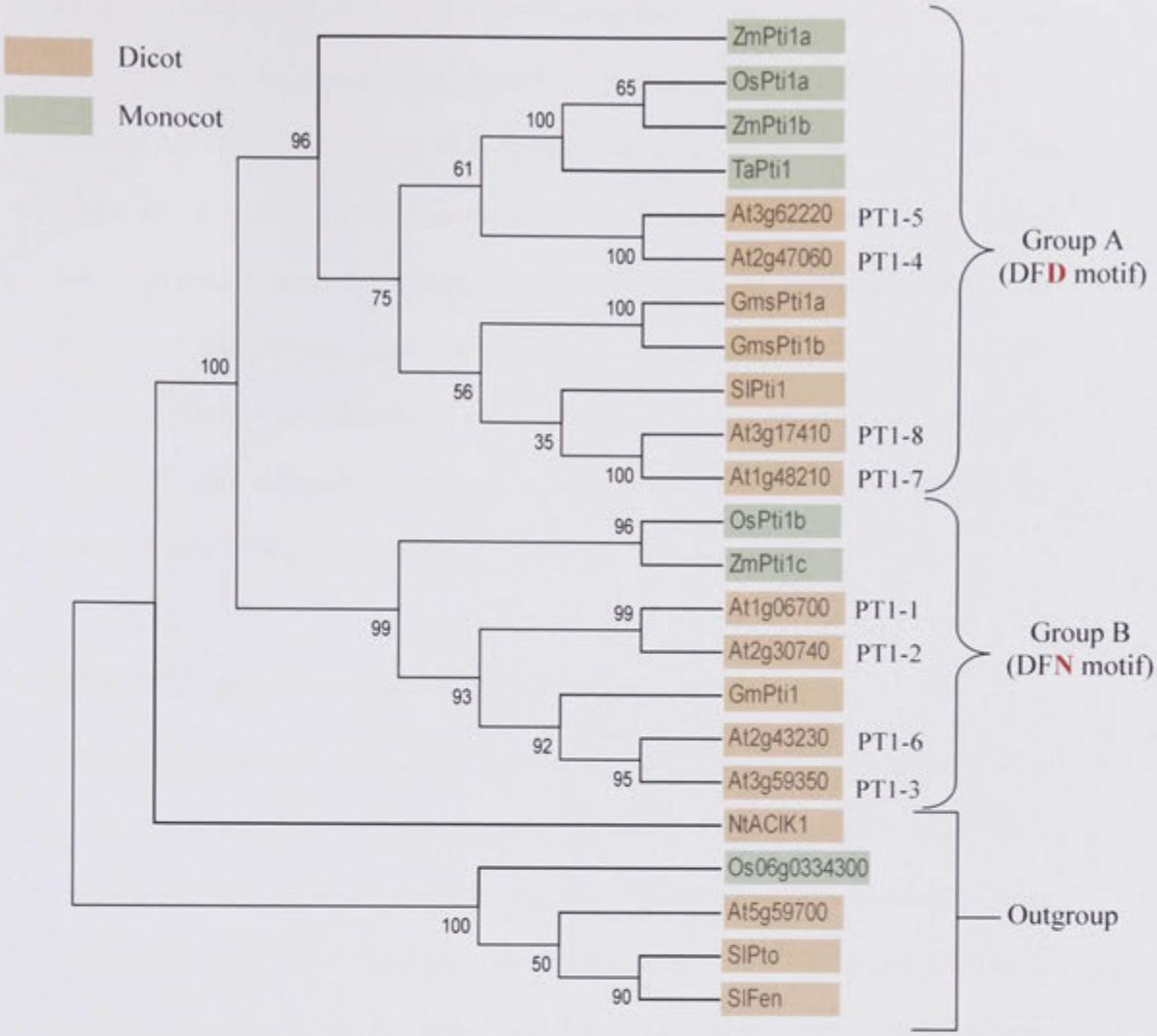


**Figure 2.5: Phylogenetic tree of the *PTI1* family**. The tree is based on PTI1-like sequences that were identified from the NCBI databases and also contained the signature pattern (F-[DN]-[LI]-S-x(8,12)-H-S-T). The isoforms are prefixed with a two letter abbreviation of the species botanical name: At - *Arabidopsis thaliana*, Sl - *Solanum lycopersicum*, Os – *Oryzae sativa*, Gm – *Glyciene max*, Nt – *Nicotiana tobacum*, Ta –*Triticum aestivum*, Zm – *Zea mays*. The sequences were aligned using CLUSTAW and tree constructed using the MEGA3 software (http://www.megasoftware.net/mega4/mega.html) (Kumar et al., 2004). Neighbour joining algorithm with 1000 bootstraps repetitions was used for the analysis.

shows the appearance of two major branches in the tree, suggesting that an ancestral *PTI1* gene may have undergone duplication giving rise to two different isoforms (Figure 2.5). The clustering of *PTI1* genes from monocots and eudicots in separate clades within each branch indicates that this duplication event occurred early, before the divergence of these two groups of species. Interestingly, the two major branches of the tree discriminate genes that have the invariant glycine residue of the DFG motif (subdomain VII) substituted either with aspartate (Group A) or with asparagine (Group B). This suggests that the aspartate and asparagine residues may have a key role in determining functional specificity among *PTI1*-like genes.

### 2.3.6 *PTI1* gene duplication in *Arabidopsis*

The phylogenetic tree presented in Figure 2.5 also shows that the *Arabidopsis PTI1* genes exist in pairs, suggesting single gene duplication events. The genes within each pair show a very similar exon-intron structure, indicating that the duplication from the ancestral gene was a relatively recent evolutionary event (Figure 2.6) (Boudet *et al.*, 2001). In order to test this hypothesis, I used the online bioinformatics resource Paralogons (http://wolfe.gen.tcd.ie/athal/dup) that enables the exploration of duplicated segments within the *Arabidopsis* genome (The-*Arabidopsis*-Genome-Initiative, 2000), that have been identified using genome scale computational analysis (Blanc *et al.*, 2003). These duplicated segments or blocks have been divided into two sets that correspond to two major polyploidy events that have occurred in the *Arabidopsis* lineage. The analysis of that database shows that the *Arabidopsis PTI1* gene pairs as apparent on the phylogenetic tree above, *PTI1-5*/*PTI1-4*, *PTI1-7*/*PTI1-8*, *PTI1-6*/*PTI1-3*, and *PTI1- 1*/*PTI1-2* (Figure 2.5), all map to genomic regions that reside within large chromosomal blocks (Figure 2.7A-C).

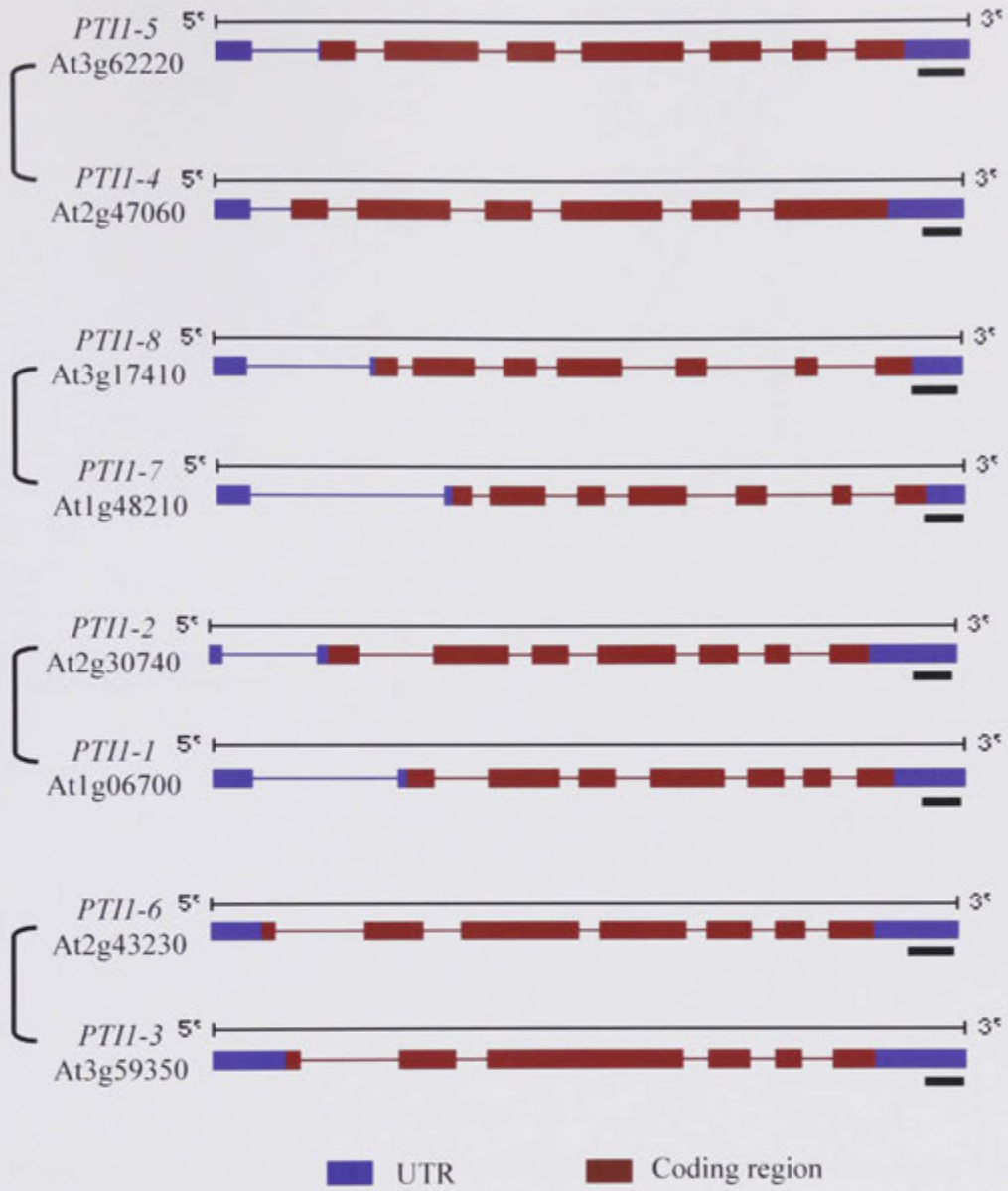


**Figure 2.6: Structure of Arabidopsis *PTI1*-like genes:** Exons and untranslated (UTR) regions are represented as brown and blue boxes, respectively. Introns are represented by lines connecting boxes. Square brackets indicate sequence grouping as seen in the *PTI1* phylogenetic tree Figure 2.4. Black scale bar -200 bp

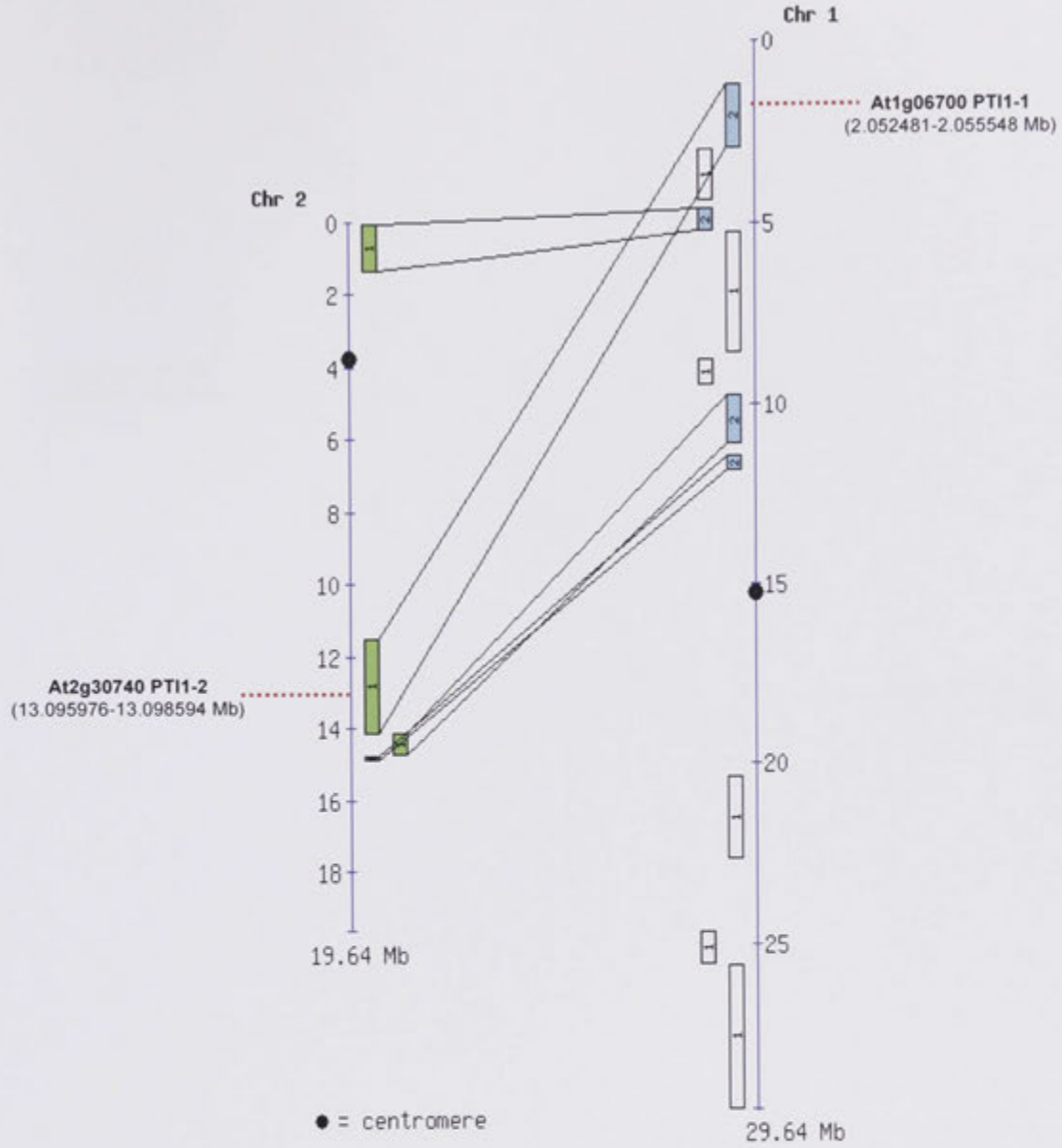


**Figure 2.7A: All segmental block duplications between chromosome 1 and 2 as determined by Paralogons.** Red dashed line shows the relative position of the *PTI1* genes located within the blocks

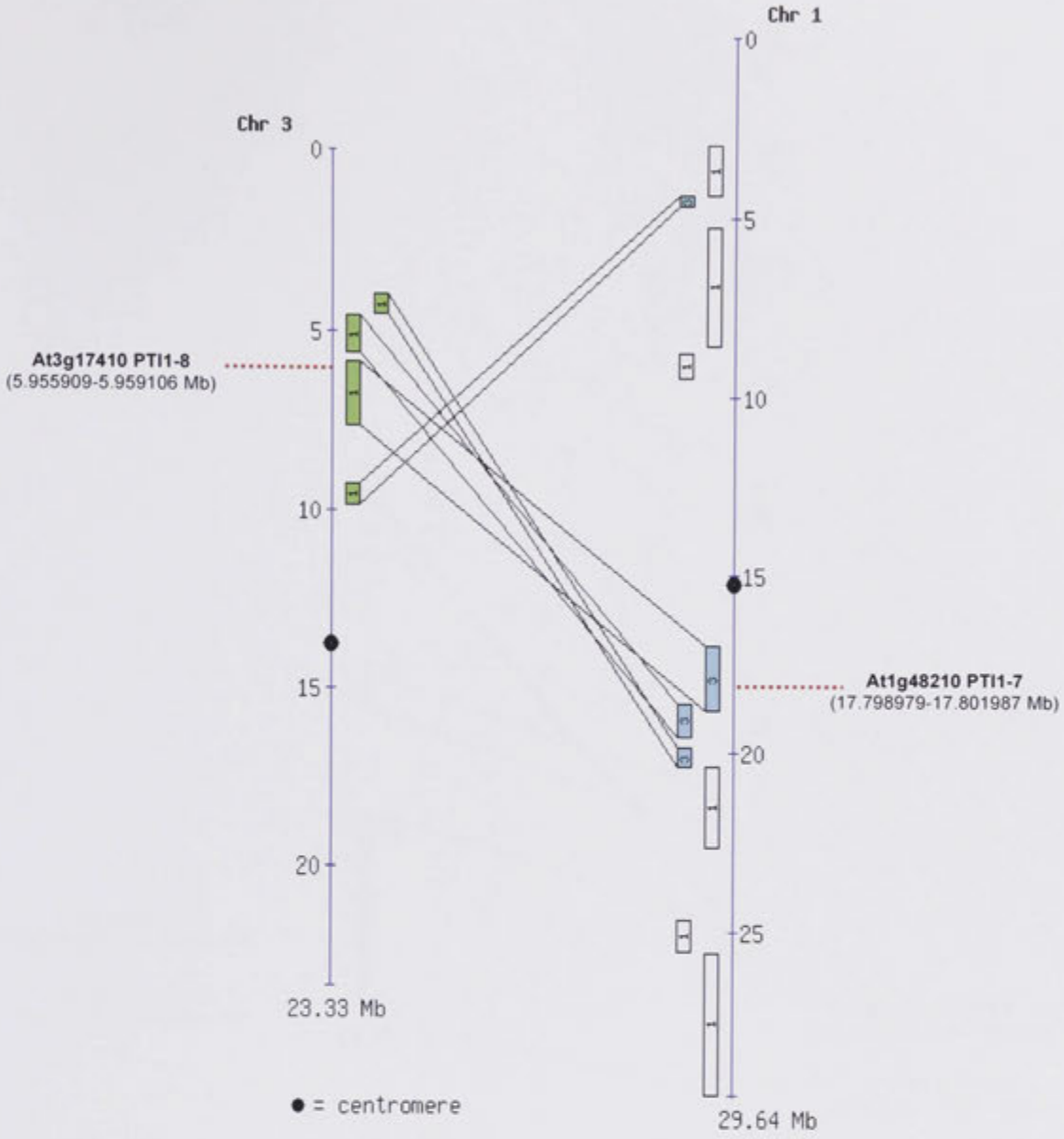


**Figure 2.7B: All segmental block duplications between chromosome 1 and 3 as determined by Paralogons.** Red dashed line shows the relative position of the *PTI1* genes located within the blocks.

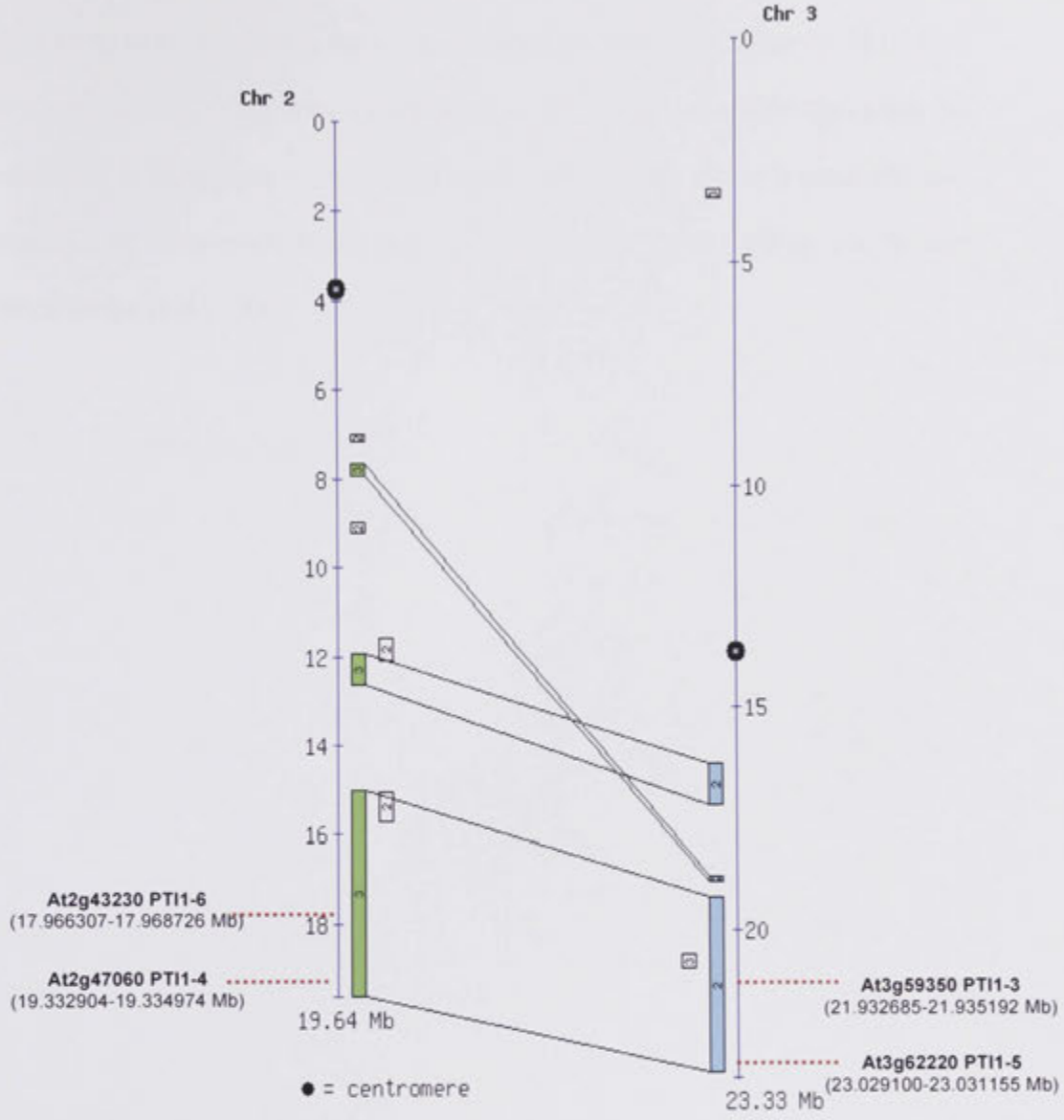


**Figure 2.7c: All segmental block duplications between chromosome 2 and 3 as determined by Paralogons.** Red dashed line shows the relative position of the *PTI1* genes located within the blocks.

The duplication events that gave rise to these duplicated chromosomal segments are estimated to have occurred in the more recent polyploidy event, about 25-26 million years ago (MYA). Therefore, the increase in the number of *PTI1*-like genes in *Arabidopsis* is most likely to be a recent evolutionary feature that took place after the divergence of other eudicot and monocot species (200 MYA) (Blanc and Wolfe, 2004; Schranz et al., 2006).

### 2.3.7 *PTI1* gene regulation

The evolutionary trend towards an increasing number of *PTI1* genes in *Arabidopsis*, and the high level of sequence conservation in the protein coding region of those genes suggest there may be functional redundancy among the various isoforms. Differential transcriptional regulation has been reported, however as an evolutionary strategy to maintain functional diversity among closely related genes (Haberer *et al.*, 2004). To further explore this possibility within the *Arabidopsis PTI1* family, *in silico* promoter analysis and qRT-PCR based expression profiling were carried out on the 8 putative *PTI1* genes.

#### *2.3.7.1 Promoter analysis*

In order to compare promoters, a 1000 bp sequence stretch upstream of the transcription start site was retrieved from the TAIR database for each of the 8 *Arabidopsis PTI1* genes. The ATHENA database (http://www.bioinformatics2.wsu.edu/cgibin/ Athena/cgi/home.pl) (O'Connor *et al.*, 2005) was mined using these upstream sequences for all known putative transcription factor (TF) binding sites. This analysis identified a diverse range of putative transcription factors binding sites in the different *Arabidopsis PTI1*-like

genes (Figure 2.8). These binding sites include canonical transcriptional motifs (GC-box and TATA-box) or more specialised motifs (DRE-core and W-box motifs) that are involved in the regulation of responses to environmental and pathogen stresses (Figure 2.9). Six of the eight promoters contained CpG islands (Figure 2.8, pale green box along the promoter sequences), which suggest that methylation may influence the transcriptional regulation of those genes (Reinders and Paszkowski, 2009).

One potential problem in using the ATHENA database is that it did not allow for the imposition of positional constraints in the *PTI1* upstream sequences as part of the query. The output generated thus lists all the putative TF binding sites that are found across the entire 1000 bp of upstream sequence of each *PTI1* gene considered in isolation. As a result, it has the potential to mask biologically significant motifs that may be evolutionarily conserved across members of the *PTI1* family. As an alternative approach to find conserved cis-elements, I scanned the putative *Arabidopsis PTI1* promoters for short stretches of statistically over-represented sequences. These sequences can then be used to query the PLACE (Plant Cis-acting Regulatory DNA Elements) database to look for conserved transcription factor binding motifs. The PLACE database (http://www.dna.affrc.go.jp/PLACE/) (Higo *et al.*, 1999) is a repository of all known plant cis-acting elements reported in the literature.

To this effect, the Promomer tool available on the BAR web site (http://www.bar.utoronto.ca/ntools/cgi-bin/BAR_Promomer.cgi) (Toufighi *et al.*, 2005) was first used for the identification of over-represented sequences in the *PTI1*

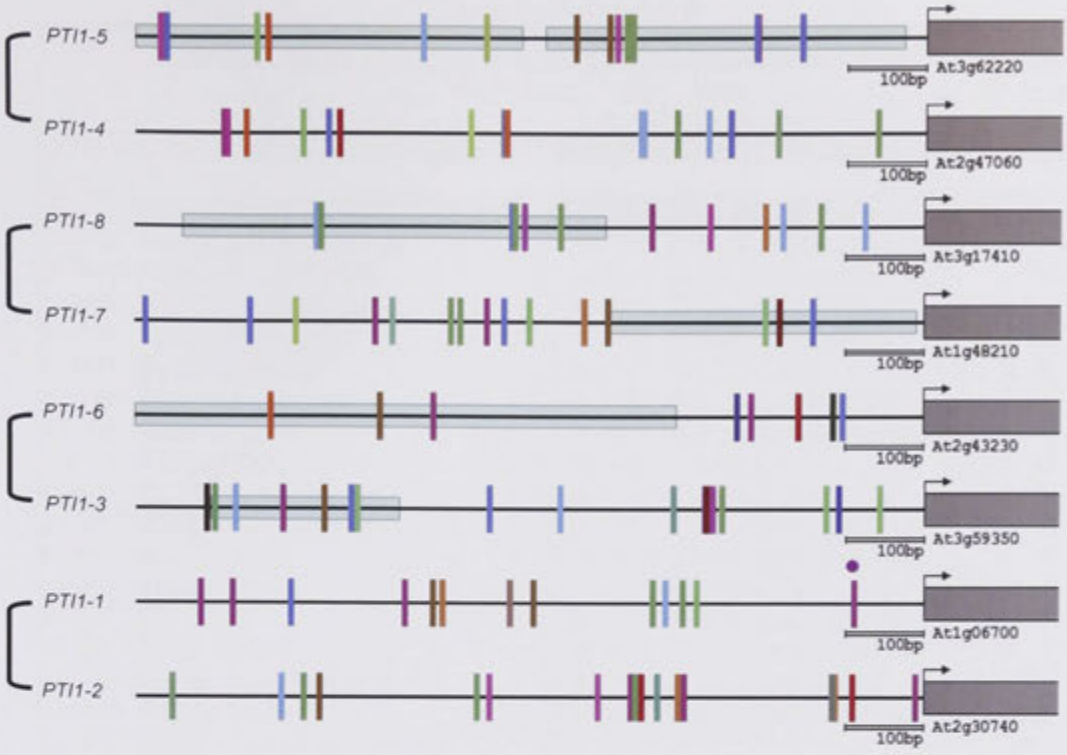


**Figure 2.8: Promoter elements in the eight *Arabidopsis PTI1* genes.** 'ATHENA' promoter analysis tool (http://www.bioinformatics2.wsu.edu/cgi-bin/Athena/cgi/home.pl) (O'Connor et al., 2005) was used to mine 1000 bp sequences upstream of the transcription start. The putative transcription factors binding sites are represented by bars of different colours, depending on TF type. The complete list of motifs, with matched color code is given in Figure 2.9. Grey box: coding sequence, arrow: transcription start site, pale green box: CpG islands. The brackets on the left indicate paralogous genes as shown in Figure 2.7.

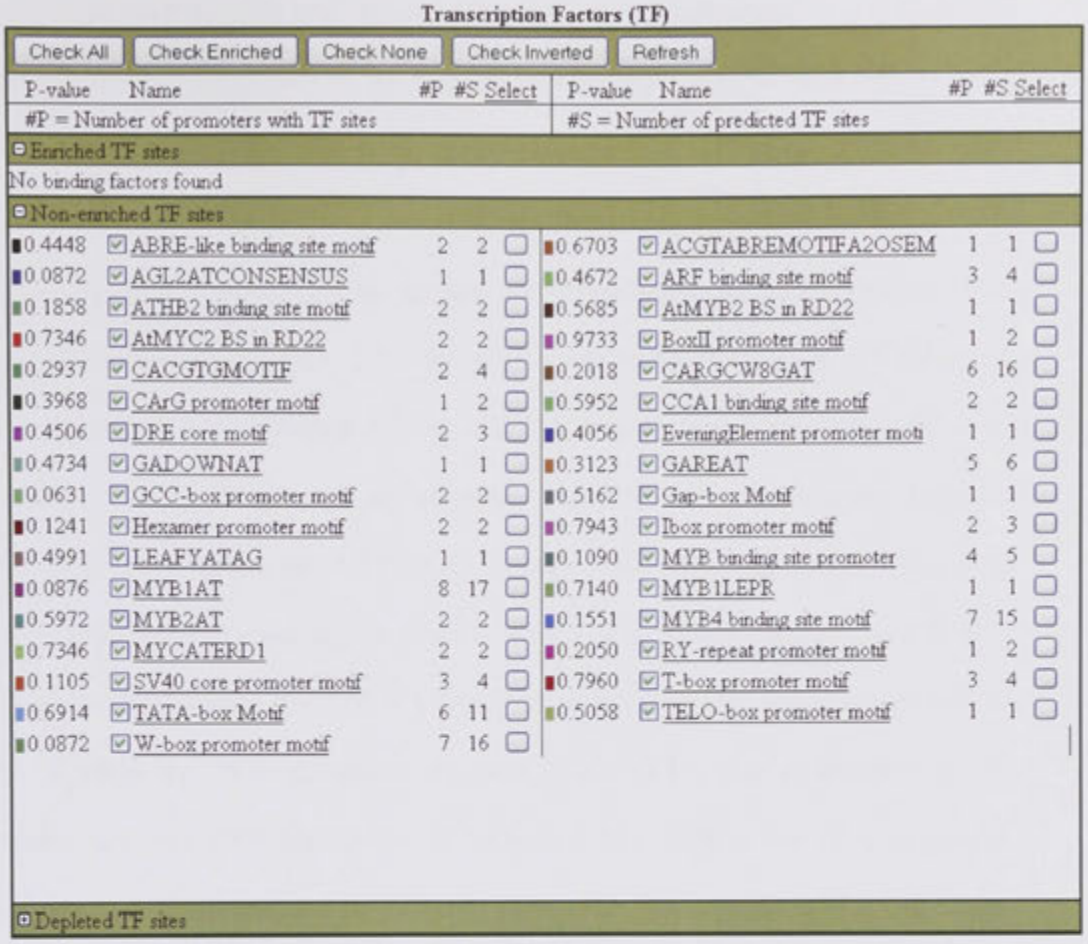


**Figure 2.9:** List of motifs identified as putative transcription factors binding sites in the upstream sequences of *PTI1*-like genes (see Figure 2.7) determined using the ATHENA promoter analysis tool (http://www.bioinformatics2.wsu.edu/cgi-in/Athena/cgi/home.pl) (O'Connor et al., 2005).

putative promoters. That tool also assigns a z-score to the elements as a quantitative estimate of their specificity to the target promoters compared to randomly selected promoters. Initially, the 1000 bp upstream sequences of each of the 8 *Arabidopsis PTI1* genes were submitted to Promomer, but this returned no significant hit. Next, sequences were submitted in two groups, corresponding to the two major clades of the phylogenetic tree (Figure 2.5). Group 'A' contained *PTI1-5*, *PTI1-4*, *PTI1-8* and *PTI1-7*. Group 'B' contained *PTI1-6*, *PTI1-3*, *PTI1-2*, and *PTI1-1*. Results from Promomer using Group 'A' set of genes identified two significantly enriched sequences, AGTCAAA and ATTTTGG. These correspond to the conserved binding sites of two types of transcription factors, WRKY and '(CA)n element', respectively (Figure 2.10) (Rushton *et al.*, 2010). Analysis of the Group 'B' set of genes showed one significantly over-represented sequence, TTCCTTTT, that corresponds to the conserved motif 'PYRIMIDINEBOX' (Figure 2.11). This is one of three motifs reported in the literature as necessary for gibberellin (GA) induction of genes in rice and barley, hence its name as the GA-responsive complex (GARC) (Lanahan *et al.*, 1992).

Together, these results indicate that, despite variability in the putative TF binding sites present in the promoter of the different *PTI1* genes, some aspects of their promoter regulation are evolutionarily conserved. Interestingly, this conservation does not seem to extend to the *PTI1* family as a whole but appears to be specific of the two main *PTI1* clades identified in the phylogenetic analysis, indicating functional specificity between members of these two branches.

A

| | n-mer | Bkg Ave | Set Ave | Z-score, Significance |
|---|---|---|---|---|
| 1. | AGTCAAA | 0.6 | 5.0 | 5.1, 0.001 |
| 2. | ATTTTGG | 0.8 | 4.0 | 3.5, 0.001 |

B

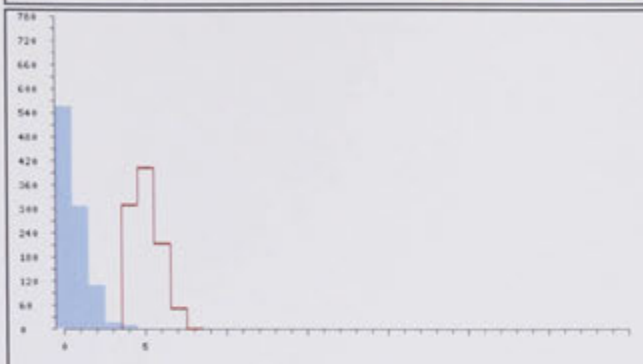

Sequence 1: AGTCAAA
Distribution in 1000 randomly generated promoter sets: Average 0.6
Distribution in 1000 bootstraps of your promoter set: Average 5.0
Z-score, Significance: 5.1, 0.001

X Axis: Number of occurences of motif in a set
Y Axis: Number of sets with given number of occurences of motif

Sequence 2: ATTTTGG
Distribution in 1000 randomly generated promoter sets: Average 0.8
Distribution in 1000 bootstraps of your promoter set: Average 4.0
Z-score, Significance: 3.5, 0.001

X Axis: Number of occurences of motif in a set
Y Axis: Number of sets with given number of occurences of motif

C

AGTCAAA

| Factor or Site Name | | Loc. | (Str.) | Signal Sequence |
|---|---|---|---|---|
| WBBOXPCWRKY1 | site | 1 | (-) | TTTGACY |
| WBOXATNPR1 | site | 2 | (-) | TTGAC |
| WBOXHVISO1 | site | 1 | (-) | TGACT |
| WBOXNTERF3 | site | 1 | (-) | TGACY |
| WRKY71OS | site | 2 | (-) | TGAC |

ATTTTGG

| Factor or Site Name | | Loc. | (Str.) | Signal Sequence |
|---|---|---|---|---|
| CANBNNAPA | site | 3 | (-) | CNAACAC |
| CANBNNAPA | site | 4 | (-) | CNAACAC |

**Figure 2.10: Promoter analysis of Group 'A' genes.** Two enriched n-mer sequences from the 'Group A' set of genes identified using the Promomer program (http://www.bar.utoronto.ca/ntools/cgi-bin/BAR_Promomer.cgi) (A). Distribution graph of the two n-mer sequences in the input 'Group A' set promoters (Red) compared to 1000 randomly generated background set of genomic promoters (Blue) (B). Results from the SignalScan Motif search at the PLACE database (http://www.dna.affrc.go.jp/PLACE/signalup.html) using the two enriched n-mer sequences (C).

A

| | n-mer | Bkg Ave | Set Ave | Z-score, Significance |
|---|---|---|---|---|
| 1. | TTCCTTTT | 0.4 | 4.0 | 5.2, 0.001 |

B

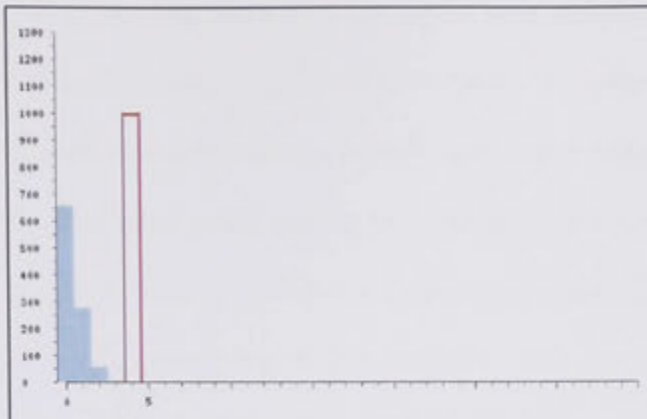

Sequence 1: TTCCTTTT
Distribution in 1000 randomly generated promoter sets: Average 0.4
Distribution in 1000 bootstraps of your promoter set: Average 4.0
Z-score, Significance: 5.2, 0.001

X Axis: Number of occurences of motif in a set
Y Axis: Number of sets with given number of occurences of motif

C

TTCCTTTT

| Factor or Site Name | | Loc. (Str.) | Signal Sequence |
|---|---|---|---|
| PYRIMIDINEBOXOSRAMY1A | site | 2 (+) | CCTTTT |

**Figure 2.11: Promoter analysis of 'Group B' genes.** Enriched n-mer sequence from the 'Group B' set of genes identified using the Promomer program (http://www.bar.utoronto.ca/ntools/cgi-bin/BAR_Promomer.cgi) (A). Distribution graph of the n-mer sequences in the input 'Group B' set of promoters (Red) compared to 1000 randomly generated background set of genomic promoters (Blue) (B). Results from the SignalScan Motif search at the PLACE database (http://www.dna.affrc.go.jp/PLACE/signalup.html) using the enriched n-mer sequences (C).

### *2.3.7.2 PTI1-like gene expression profiling*

It has been reported that random mutations in duplicated genes, both in their coding and non-coding sequences can direct their expression patterns to different tissues while still maintaining the same function as the ancestral gene, a phenomenon known as subfunctionalization. In certain cases, these mutations can also affect the role of the duplicated gene, leading to neofunctionalization (Force *et al.*, 1999; Gu *et al.*, 2003). In order to analyse the endogenous expression patterns of the *PTI1* genes as well as to determine if this correlates with the predicted TF binding sites, the transcript abundance of each of the 8 *PTI1*-like genes was measured in 5 independent total RNA pools extracted from roots and aerial tissues sampled at two developmental stages. Transcript abundance was quantified using real-time RT-PCR and is plotted in Figure 2.12 as relative gene expression normalised to a reference gene (*PDF2*, At1g13320). All 8 genes exhibit variable expression depending on plant organ/tissue and stage of development. *PTI1-6* was the only isoform showing organ specific expression with high transcript levels in the inflorescence. A comparison with the microarray data from the online Genevestigator expression database (https://www.genevestigator.ethz.ch/) (Zimmermann *et al.*, 2004) showed a similar expression pattern for *PTI1-6*.

The expression patterns of the 8 *PTI1*-like genes appear highly divergent both spatially and developmentally, even between genes with high sequence similarity likely to have arisen from more recent duplication events (*PTI1-5* and *PTI1-4*; *PTI1-6* and *PTI1-3*, *PTI1-8* and *PTI1-7* or *PTI1-2* and *PTI1-1*). Co-regulation between paralogous genes was also examined using the Expression Angler program (http://esc4037-shemp.csb.utoronto.ca/ntools/cgi-bin/ntools_expression_angler.cgi)

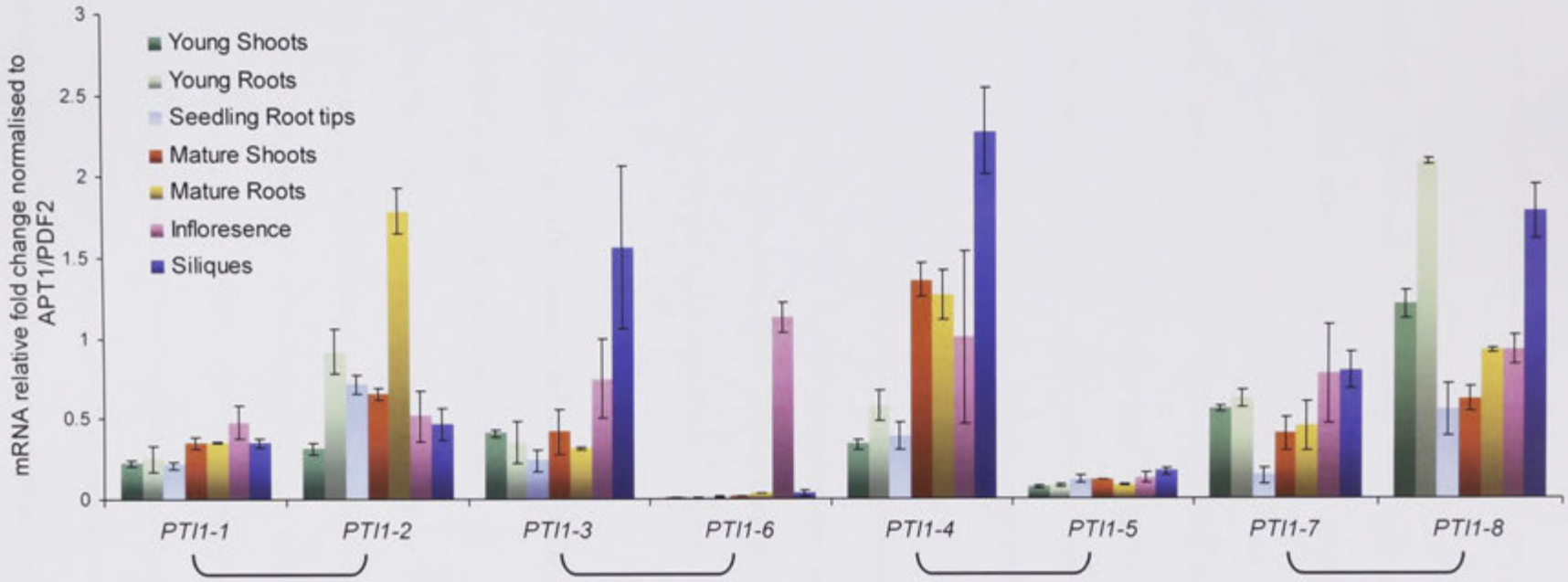


**Figure 2.12: Endogenous Expression profile of the *Arabidopsis PTI1* genes.** Transcript levels for each gene are represented as fold changes compared to the reference gene *PDF2* (At1g13320) set arbitrarily to 1. Young shoot, young root and root tip tissue samples harvested from 7 day old seedlings grown on vertical agar media plates. Mature shoots, mature roots, inflorescence and silique tissue samples harvested from 5-week old rosette plants. The brackets indicate paralogous genes as shown in Figure 2.6. Error bars represent SE of the mean of three biological replicates. For seedling tissue, each replicate is a pooled sample of approx 60 seedlings. For mature tissue, each biological replicate is a pooled sample of approx. 5-8 plants.

which allows for calculation of Pearson's coefficients of correlation between expression patterns of 2 genes across large data sets of published microarray data (Toufighi *et al.*, 2005). For each *PTI1*-like gene, normalised microarray data sets derived from the AtGenExpress developmental tissue series (63 samples) (Schmid *et al.*, 2005), were downloaded from the BAR (Botany Array Resource) website (http://esc4037-shemp.csb.utoronto.ca/welcome.htm). Data for the closely related gene pairs were then submitted to the Expression Angler program. This analysis showed that *PTI1* gene pairs with high sequence similarity did not show a corresponding high similarity of expression profiles across tissues (Figure 2.13), which is in agreement with the data obtained by qRT-PCR (Figure 2.12). For most of the *PTI1* gene pairs, the Pearson's r-value was well below 0.4. The highest correlation was between *PTI1-6* and *PTI1-3* expression patterns, but with an r-value of only 0.62. Together with my own experimental data, these results suggest that expression divergence between *PTI1* genes with high sequence homology may have been the cause for the retention of all duplicated genes in the genome's evolution.

### 2.3.8 Isoform specific transcriptional regulation of *Arabidopsis PTI1*-like genes by biotic and abiotic stress

Following from the literature, *PTI1*-like genes have previously been implicated in abiotic and biotic stress pathways (Zhou *et al.*, 1995; Zou *et al.*, 2006; Takahashi *et al.*, 2007). The presence of multiple *PTI1*-like genes in *Arabidopsis*, with high homology but differing spatial expression patterns suggested that individual or closely related isoforms may have evolved to specifically function in either biotic or abiotic stresses. To test this hypothesis, experiments were carried out to examine the sensitivity of *PTI1*- like gene expression to a range of stress treatments.

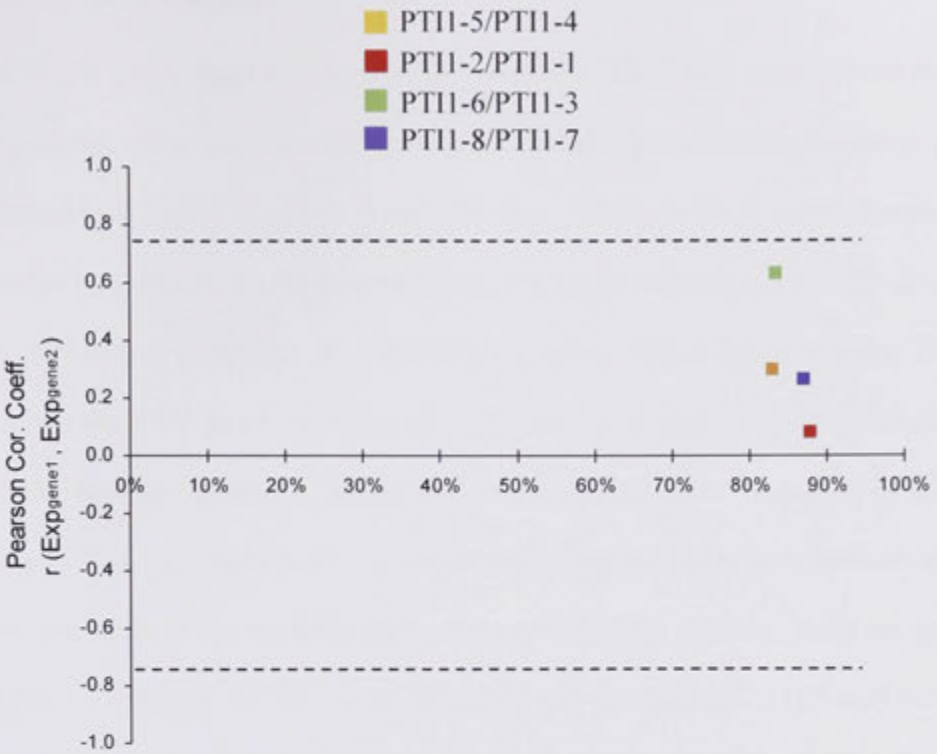


**Figure 2.13: Correlation coefficients between transcript abundance of putative paralogous *PTI1* genes (paired genes in phylogenetic tree, Fig 2.5) against amino acid sequence identity.** Y axis: Pearson correlation coefficient, r value for expression data calculated using Expression Angler tool (http://bar.utoronto.ca/ntools/cgi-bin/ntools_expression_angler.cgi) at BAR site (http://bar.utoronto.ca/). ($r \geq 0.75$ or $r \leq -0.75$ is cut-off threshold for significant correlation in expression between two genes as determined by the Expression Angler program) (Toufighi *et al.*, 2005)

Expression data from microarray -AtGenExpress Tissue Series (NASCArrays 149-153), 63 tissue samples (Schmid et al., 2005). X axis: Percentage of Amino-acid sequence identity. Information relating to individual experiments for the complete AtGenExpress data sets can be retrieved from the TAIR website (http://www.arabidopsis.org/portals/expression/microarray/ATGenExpress.jsp)

### *2.3.8.1 Biotic stress*

*PTI1*-like genes from tomato (*SlPTI1*) and rice (*OsPTI1A*) have previously been implicated, either directly or indirectly, in regulating plant defence responses against pathogens (Zhou *et al.*, 1995; Takahashi *et al.*, 2007). In *Arabidopsis*, however, no studies have been reported thus far, testing the direct involvement of *PTI1*-like genes in plant disease resistance. As a first step towards achieving this, expression levels of each of the *PTI1* genes were quantified in plants challenged with the virulent strain of the bacterial pathogen, *Pseudomonas syringae* pathovar *tomato* (*Pst*) DC3000 (Figure 2.14A). Rosette leaves of 5 week-old vegetative plants were infected with the virulent strain of the bacterial pathogen or with a mock solution, using the standard syringe infiltration technique (see Materials and Methods 2.2.2.1.2), and harvested 24h later for quantification of transcript levels. Three out of the 8 *PTI1*-like genes tested showed differential expression, being either repressed (*PTI1-4* and *PTI1-3*) or slightly induced (*PTI1-8*) (Figure 2.14-A1). Although significant, these responses were relatively small, despite successful infection as shown by the huge induction of the defence gene *PR1* (Figure 2.14-A2) (De Vos *et al.*, 2005) as well as the development of chlorotic lesions at the sites of infiltration within 2-3 days of treatment (Appendix 2.6.3).

### *2.3.8.2 Root mechanical stress*

For the purpose of this study, the effects of root mechanical stress on *PTI1*-like expression were analysed taking advantage of another project in the lab on the identification of mechano-sensitive genes in *Arabidopsis*. The experimental set-up and growth conditions were also the same as those shown in an earlier experiment in the lab to induce expression of a wheat *PTI1*-like gene. In the *Arabidopsis* study,

**Figure 2.14: Stress-induced expression analysis of Arabidopsis *PTI1* genes**

**Fig A**: Expression of *PTI1* genes in response to the bacterial pathogen *Pseudmonas syringae* DC3000 ($OD_{600}$ – 0.05). (left panel) Positive reporter gene, *PR1*, expression in response to *Pst* DC3000 challenge (right panel). Rosette leaves of 5 week-old soil grown Col-0 (WT) plants were infected with the bacterial pathogen using the standard syringe infiltration technique. Pathogen- and mock- treated leaves were harvested for qRT-PCR transcript measurements 24 hours post infection (hpi).

**Fig B: Expression of *PTI1* genes in response to Root Mechanical Stress (RMS)**. Four week-old Arabidopsis WT plants grown in pots were subjected to root mechanical stress for 1 hour (B1) and 3 hours (B2). At each time point, shoot (left panel) and root (right panel) tissue was harvested separately for qRT-PCR transcript measurements.

Error bars for all treatments indicate +SE of the means of three biological replicates (*Pst* DC3000 n > 12 rosette leaves/replicate; RMS n > 6 plants/replicate)

mRNA relative fold change was normalized to the reference gene *PDF2*

* and ** indicates statistically significant results between controls and treated values ( Students t-test, * $p \leq 0.05$, ** $p \leq 0.01$)

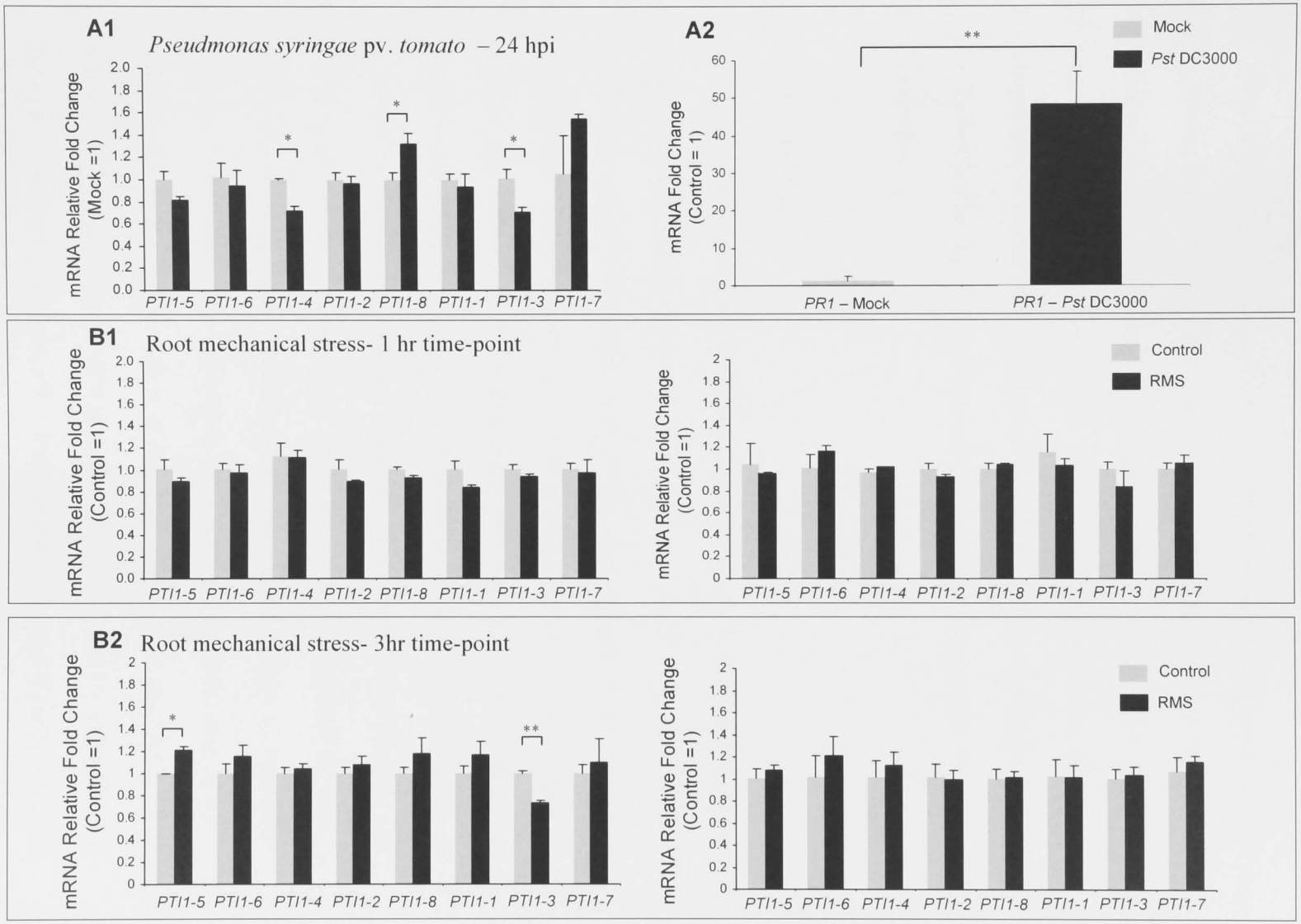
A1
Pseudmonas syringae pv. tomato – 24 hpi
mRNA Relative Fold Change (Mock =1)
PTI1-5 PTI1-6 PTI1-4 PTI1-2 PTI1-8 PTI1-1 PTI1-3 PTI1-7
A2
Mock
Pst DC3000
mRNA Fold Change (Control = 1)
PR1 – Mock
PR1 – Pst DC3000
B1
Root mechanical stress- 1 hr time-point
mRNA Relative Fold Change (Control =1)
Control
RMS
B2
Root mechanical stress- 3hr time-point

plants were subjected to a 2 MPa step change in soil strength through application of pressure, while soil water suction was maintained constant. Leaf and root tissues that were sampled for qRT-PCR analysis had shown a significant transcriptional reprogramming following that step change (Masle, unpublished). The same RNA pools, from tissues sampled 1h and 3h after application of the mechanical constraint were analysed for *PTI1* gene expression. *PTI1-3* showed a small but significant down-regulation in leaves at the 3hr time-point while *PTI1-5* was slightly induced (Figure 2.14-B2). The expression of the other isoforms appeared mostly insensitive to root impedance.

### *2.3.8.3 Osmotic stress*

In maize, Zou *et al* identified.a *PTI1* ortholog (*ZmPTI1*/*ZmPTI1C*) whose expression was up-regulated by mannitol-induced osmotic stress as well as by other abiotic stresses, including cold and salt (Zou *et al*., 2006). To investigate if one or more of the *Arabidopsis PTI1*-like genes responded in a similar manner, the expression of these genes was analysed in plants challenged with mannitol and also the non-permeating osmoticum polyethylene glycol MW-8000 (PEG8000) mimicking water stress. Mannitol was added into an agar based growth medium while PEG8000 was applied in hydroponic medium (Appendix 2.6.1) in order to better control the timing and uniformity of stress across seedlings. The solute concentrations of PEG-8000 and mannitol in the media were adjusted so as to cause a similar decrease in water potential of ~0.8 MPa (van der Weele *et al*., 2000; Verslues *et al*., 2006). These treatments revealed specific regulation of a few isoforms indicative of specialized functions of *PTI1* family members. *PTI1-3* transcription was significantly inhibited within the first hour of root exposure to PEG, while *PTI1-4* showed a small induction

at the 8h time point (Figure 2.15 A1-2). For both genes these responses were transient, whereas the osmotic/water stress reporter gene RD29 (Ishitani *et al.*, 1997) showed a large sustained induction over the 24h experimental period. The presence of mannitol in the root medium caused a 2-to-4 fold induction of *PTI1-4* (after 1h and 5h exposure, respectively), of similar magnitude to the response of the *RD29* gene (Figure 2.15 B1-2), while there was no detectable change in *PTI1-3* expression. The differential responses of *PTI1-3* and *PTI1-4* to PEG and mannitol may reflect differences in the experimental set-ups used for the two treatments (hydroponics for PEG treatment, growth agar for mannitol treatment), as well as the tissue types sampled (young rosettes for PEG, and whole seedlings for mannitol). One should note, however, that mannitol permeates cells and has direct metabolic effects, while the high molecular weight PEG8000 does not enter root cells and has a primary effect of increasing the external osmotic pressure.

Overall, these gene expression data gave several insights. One interesting aspect is the differential response seen within the *PTI1* gene family for each of the stresses tested, biotic or abiotic. The observed responses also indicate functional specificity within the family, with some genes like *PTI1-8* being transcriptionally regulated by *Pseudomonas* infection but not by the abiotic stresses tested in this study, and others such as *PTI1-4* and *PTI1-3* showing differential expression under *Pseudomonas* infection, mechanical and osmotic stress, with the rest of the *PTI1* isoforms being insensitive to all stresses applied.

**Figure 2.15: Stress-induced expression analysis of Arabidopsis *PTI1* genes**

**Fig A (1-3): Expression of *PTI1* genes in response to PEG8000-induced osmotic stress**. A hydroponic system was used for the cultivation of WT (Col-0) plants. Plants were grown in 1/3 Hoaglands liquid media for 16 days to allow the seedlings to be established before transferring subsets to control or PEG8000 (17.5 mM) supplemented media. Young rosette tissue was harvested for qRT-PCR analysis at 1 hour (A1), 3 hour (A2) and 24 hour (A3) time points following stress imposition. *RD29*, a well characterized water stress response gene, was used as positive reporter gene.

**Fig B (1-2): Expression of *PTI1* genes in response to mannitol-induced stress**. 5 day old wild-type plants growing on vertically oriented media plates were transferred to identical media plates supplemented with or without mannitol (200 mM), and whole seedlings were harvested for qRT-PCR analysis at 1 hour (B1) and 6 hour (B2) time points. *RD29*, a well characterized water stress response gene, was used as positive reporter gene.

Error bars for all treatments indicate +SE of the means of three biological replicates. (PEG n = 8 seedlings/replicate; Mannitol n = 8 seedlings/replicate)

mRNA relative fold change was normalized to the reference gene *PDF2* and *APT1*

* and ** indicates statistically significant results between controls and treated values ( Students t-test, * $p \leq 0.05$, ** $p \leq 0.01$)

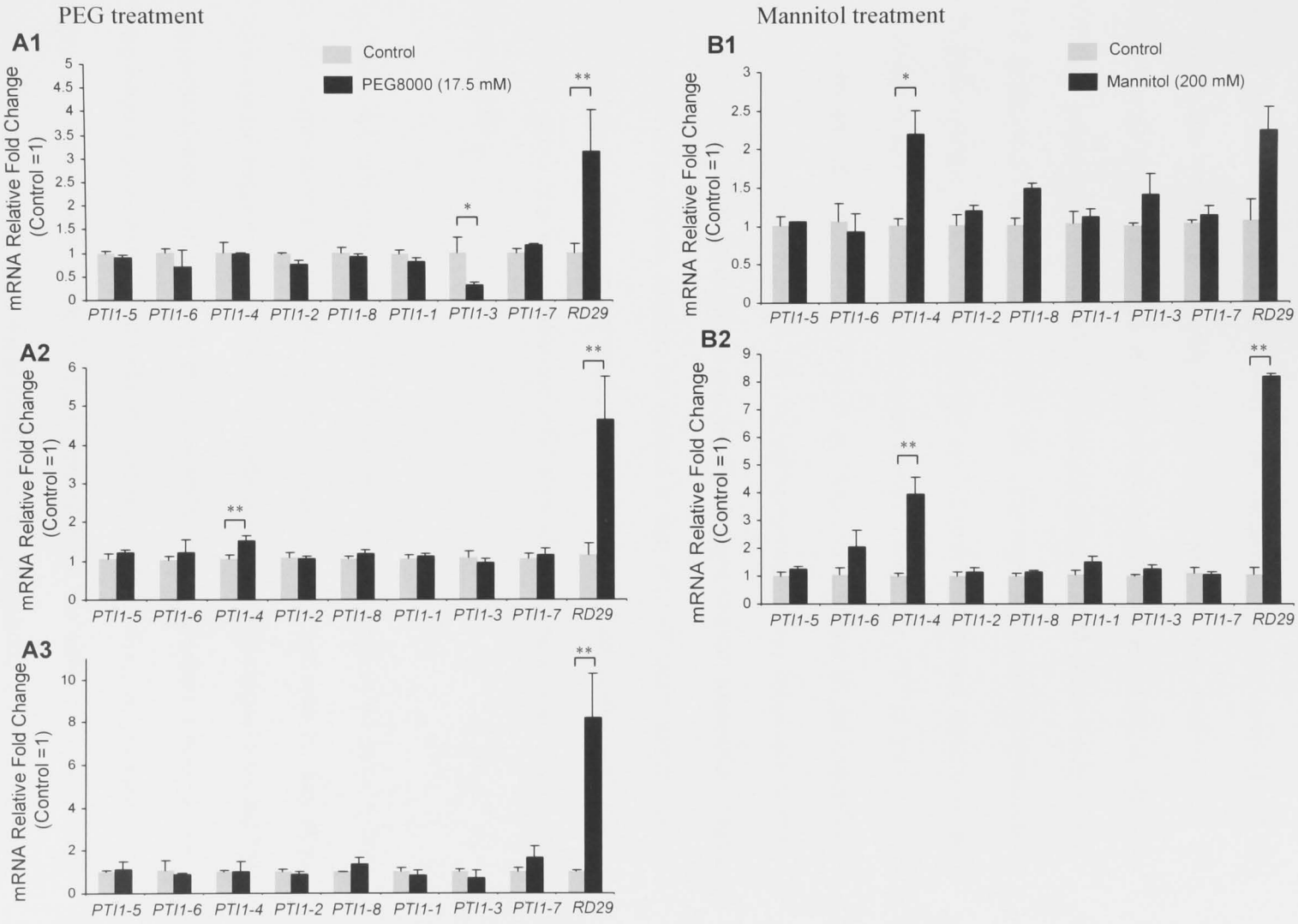
PEG treatment
Mannitol treatment
A1
B1
A2
B2
A3
Control
PEG8000 (17.5 mM)
Mannitol (200 mM)
mRNA Relative Fold Change (Control =1)
PTI1-5
PTI1-6
PTI1-4
PTI1-2
PTI1-8
PTI1-1
PTI1-3
PTI1-7
RD29
*
**

The differential expression of *PTI1* genes induced by stress in the experiments described above is in good agreement with the results of an *in silico* analysis of the publicly available microarray data sets. The meta-analysis tool available at the Genevestigator website (http://www.genevestigator.ethz.ch) was used to mine the AtGenExpress global stress data set for the expression profiles of the *Arabidopsis PTI1*- like genes under a wide range of stresses (Figure 2.16) (Zimmermann *et al.*, 2004; Kilian *et al.*, 2007). Overall, *PTI1*-like gene expression was relatively stable, with fold changes in transcript abundance between treated and tissues control clustering within 2 fold range for most genes, except for *PTI1-3* and *PTI1-4*. Consistent with the induction of *PTI1-4* by PEG and mannitol in the experiments carried out in this thesis (Figure 2.15), AtGenExpress microarray results show an up-regulation of this gene by mannitol and also by drought and salt treatments (Figure 2.16). These three abiotic stresses are related in that they all cause osmotic stress through increases of the growing media water potential (van der Weele *et al.*, 2000). Altogether, these data suggest that the *PTI1-4* protein may be involved in osmotic stress signalling.

The transcriptional regulation of *PTI1-3* by wounding (Figure 2.16) and its fast, transient response to root mechanical stress (Figure 2.14B), not seen for any other *PTI1*-like gene, suggests that this isoform might play a role in the signal transduction of mechanical stimuli. In a recently published microarray experiment, a large number of *Arabidopsis* genes were found to be touch-sensitive (Lee *et al.*, 2005). Inspection of this set of genes shows that *PTI1-3* is one of them. An interesting observation recorded by Chehab *et al.* (2009) was that 23% of the upregulated genes identified in that study contain in their promoters the consensus motif CGCGTT, therefore

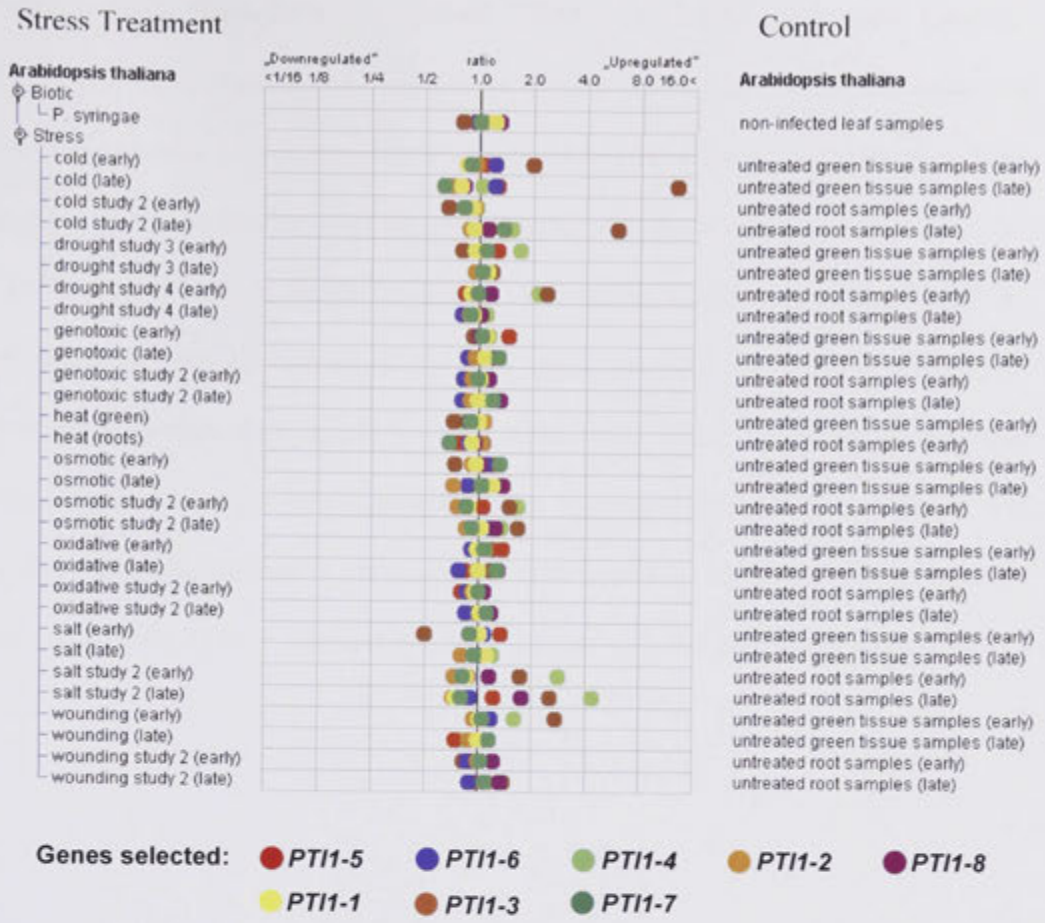


**Figure 2.16: Snapshot of Genevestigator results showing changes in expression of the 8 putative *Arabidopsis PTI1* genes in response to a range of stresses.** The AtGenexpress microarray stress dataset was mined for the analysis (Kilian et al., 2007). Cold stress ($4^0$C, NASCArrays -137,138 ), osmotic stress (Mannitol 300Mm, NASCArrays -139,137), salt (150Mm NaCl, NASCArrays -140,137), drought stress (15 min. dry air stream, NASCArrays -141,137), genotoxic (1.5 µg/mL bleomycin + 22 µg/mL mitomycin, NASCArrays -142,137), oxidative stress (10 µM methyl viologen, NASCArrays -143,137), wounding stress (pin punctured, NASCArrays -145,137), heat stress ($38^0$C, NASCArrays -143,137, NASCArrays -146,137), *Pesudomonas syringae* (half leaf syringe infiltration, pv. maculicola ES4326 virulent, TAIR ME00353) Information relating to individual experiments for the complete AtGenExpress data sets can be retrieved from the TAIR website (http://www.arabidopsis.org/portals/expression/microarray/ATGenExpress.jsp)

labelled Rapid Stress Response Element (RSRE). The RSRE was initially identified to be over represented in genes that were rapidly induced by mechanical wounding but the presence of the motif in many touch-sensitive genes suggests significant overlap at the molecular level between wound and touch responses (Walley *et al.*, 2007). Interestingly, a search for RSRE elements in promoter sequences (1000 bp upstream of START codon) of all *PTI1* genes revealed that *PTI1-3* is the only isoform to contain the consensus motif, immediately before the transcriptional start site (Figure 2.17). This result strengthens the hypothesis that *PTI1-3* may play a role in the signal transduction of mechanical stimuli generally, whether induced by touch, wound (Figure 2.16) or interactions of the root tip with soil particles (Figure 2.14B).


**Figure 2.17: *PTI1-3* putative promoter contains the RSRE element**

(C) Upstream putative promoter sequence for *PTI1-3* (green) with consensus sequence for the wound responsive Rapid Stress Response Element (RSRE) element (Red) (Chehab et al., 2009; Walley et al., 2007). *PTI1-3* 5'UTR (grey) and beginning of coding sequence (yellow).

## 2.4 Discussion

### 2.4.1 Expansion of the *PTI1* gene family in Arabiodopsis

By analysing amino acid sequences of characterised *PTI1* genes from rice, tomato, maize and soybean, a unique motif (F-[DN]-L-S-x(8,12)-H-S-T) was identified, which was then used as a signature pattern to identify 8 putative *PTI1* orthologs in *Arabidopsis* (Table 2.1) (Figure 2.3). This motif-based approach has proved to be particularly useful in classifying serine/threonine/tyrosine protein kinases which are defined by a single conserved catalytic domain. An example is the large MAP kinase superfamily in *Arabidopsis*, made up of three kinase modules and comprising approximately ninety genes which have been classified into various kinase subfamilies based on conserved signature motifs (Rodriguez *et al.*, 2010).

The presence in *Arabidopsis* of a large multigene *PTI1* family appears to reflect the evolutionary lineage of the *Arabidopsis* species which has undergone three rounds of tandem and/or segmental duplication events (α-, β-, γ- duplication) (Blanc *et al.*, 2003; Bowers *et al.*, 2003; Veitia, 2005). A case in point is the MAPK kinase family of which 60% of the genes are thought to have evolved from tandem or segmental chromosomal duplication events (Champion *et al.*, 2004). The 8 *PTI1*-like genes can be grouped into 4 highly conserved pairs (Figure 2.5), further suggesting that the expansion of the *Arabidopsis PTI1* family resulted from gene duplications. The mapping of gene pairs to regions that have likely emerged from large-scale inter-chromosomal segmental duplications (http://wolfe.gen.tcd.ie/athal/dup) (Figure 2.7) strengthens this interpretation (The-Arabidopsis-Genome-Initiative, 2000; Blanc et al., 2003). Computational analysis estimates that the duplication of these chromosomal blocks is a relatively recent polyploidy event, dated to 24-40 million

years ago (α- duplication) (Blanc *et al.*, 2003). This period coincides with the emergence of the first crucifers and suggests that an expanded *PTI1* family such as in *Arabidopsis* may be restricted to species within the *Brassicaceae* family only (Blanc and Wolfe, 2004). The presence of only three *PTI1*-like genes in Soybean which diverged from the *Brassicaceae* family an estimated 92 MYA is consistent with this hypothesis (Figure 2.5).

The phylogenetic analysis of the *Arabidopsis* putative *PTI1* gene family and characterised *PTI1* genes from other species provides further evolutionary clues. The topology of the phylogenetic tree (Figure 2.5) shows that the *PTI1* genes fall into two main branches suggesting duplication of an ancestral *PTI1* gene. This event is likely to have occurred early in the evolution of flowering plants given the presence of both moncot and eudicot *PTI1* genes within each group. Furthermore, the various *PTI1*-like genes from rice, *Arabidopsis* and maize are not clustered within one branch but spread across both branches. This suggests the existence of a strong selective pressure to retain the two *PTI1*-like genes representative of each branch and therefore the hypothesis that they may have non-redundant functions. Consistent with this hypothesis, the developmental and defence related phenotypes of the rice *Ospti1a* single mutant was identical to that of the double *Ospti1a*×*Ospti1b* mutant, thus suggesting a unique nonredundant function for the OsPTI1A protein (Takahashi *et al.*, 2007).

### 2.4.2 Differential expression for the 8 *PTI1* isoforms

One evolutionary strategy to retain highly similar paralogous genes is divergence based on specificity of expression patterns (Figures 2.12 and 2.13) which suggests

mutational changes in the regulatory sequences as a possible driving force for the diversification of the family (Haberer *et al.*, 2004). Supporting this hypothesis, gene expression data confirmed a diverse expression pattern for the 8 *PTI1* genes, in various plant organs and during different stages of development. Also consistent with this claim was the *in silico* promoter analysis which showed variable TF binding sites for the different *PTI1*-like genes (Figure 2.8), although, some level of conservation within the putative regulatory sequences was observed for *PTI1* genes in each of the major branches of the phylogenetic tree (Figures 2.10 & 2.11). The over-represented sequences relate to consensus TF binding sites for WRKY (*PTI1-5*, *PTI1-4*, *PTI1-8* and *PTI1-7*) and gibberellins-dependent transcriptional regulation (*PTI1-1*, *PTI1-2*, *PTI1-3* and *PTI1-6*). The WRKY family of transcriptional factors and the phytohormone gibberellin are both known to control a wide range of processes in plants relating to growth, development and stress responses (Jiang and Fu, 2007; Rushton *et al.*, 2010).

The *SlPTI1* (tomato), *OsPTI1A* (rice) and *ZmPTI1B* (maize) have all been linked, either directly or indirectly, to pathogen response (Zhou *et al.*, 1995; Herrmann *et al.*, 2006; Takahashi *et al.*, 2007). The maize *ZmPTI1C*, however, was shown to be up-regulated in response to osmotic, cold and salt stress (Zou *et al.*, 2006) and a wheat *PTI1*-like gene was previously identified in the lab from a root mechanical stress screen (Masle J, unpublished data). The results described in this chapter provide circumstantial evidence for an involvement of *PTI1* genes in a broad range of abiotic stresses, as well as in biotic stress, within the same species. This may be achieved in part through the expansion of the family and some specificity between isoforms, in endogenous expression patterns and responses to external cues. *PTI1-5*, for example

was specifically induced by mechanical stress, while *PTI1-8* was differentially expressed after infection by virulent pathogen, *Pseudomonas syringae* DC3000. Other isoforms such as *PTI1-4* and *PTI1-3* were differentially expressed under both biotic and abiotic stresses indicating that these kinases may function in a common stress signalling cascade, or constitute shared components of overlapping pathways. Secondary messengers such as reactive oxygen species (ROS), and $Ca^{2+}$ have been demonstrated to play key roles in both biotic and abiotic stress response through activation of kinase signal transduction pathways (Apel and Hirt, 2004; Mori and Schroeder, 2004; Torres and Dangl, 2005; Fujita *et al.*, 2006; Wong and Shimamoto, 2009). It remains to be elucidated if the 8 *Arabidopsis PTI1*-like kinases function in independent signalling pathways or overlap through integration of common upstream messengers.

While differential gene expression provides potential clues regarding environmental triggers for some *PTI1* genes such as *PTI1-4* and *PTI1-3*, it is striking that most isoforms showed no detectable response to stress treatments at the transcriptional level (Figure 2.14-15) and *in silco* analysis (Figure 2.16). The absence of differential expression, however, cannot be taken as evidence that these particular isoforms have no function in the responses to the stresses examined. *PTI1* genes encode kinases whose function is regulated by (auto-) phosphorylation (Zhou *et al.*, 1995; Herrmann *et al.*, 2006; Takahashi *et al.*, 2007). Therefore, the stress-specific response of these proteins may be limited to post-translational modifications such as a change in phosphorylation status (Takahashi *et al.*, 2007).

### 2.4.3 Concluding remarks

The data presented in this chapter identify 8 putative *PTI1* genes in *Arabidopsis* that are likely to have expanded through segmental chromosomal duplication. Endogenous as well as stress-induced expression analyses suggest some specialisation among paralogs, a hypothesis that is also supported by highly variable promoter sequence elements. In an effort to further characterise the *Arabidopsis PTI1*-like genes, I describe a reverse genetics approach in the following chapter to determine the specific physiological function of two *PTI1* isoforms.

## 2.5 Reference:


**Altschul SF, Madden TL, Schaffer AA, Zhang J, Zhang Z, Miller W, Lipman DJ** (1997) Gapped BLAST and PSI-BLAST: a new generation of protein database search programs. Nucleic Acids Res **25:** 3389-3402

**Anthony RG, Khan S, Costa J, Pais MS, Bogre L** (2006) The *f* protein kinase PTI1-2 is activated by convergent phosphatidic acid and oxidative stress signaling pathways downstream of PDK1 and OXI1. J Biol Chem **281**: 37536-3746

**Apel K, Hirt H** (2004) Reactive oxygen species: Metabolism, oxidative stress, and signal transduction. Ann Rev of Plant Biol **55:** 373-399

**Bairoch A** (1993) The PROSITE dictionary of sites and patterns in proteins, its current status. Nucleic Acids Res **21:** 3097-3103

**Berkowitz O, Jost R, Pollmann S, Masle J** (2008) Characterization of TCTP, the translationally controlled tumor protein, from *Arabidopsis* thaliana. Plant Cell **20:** 3430-3447

**Blanc G, Hokamp K, Wolfe KH** (2003) A recent polyploidy superimposed on older large-scale duplications in the *Arabidopsis* genome. Genome Res **13:** 137-144

**Blanc G, Wolfe KH** (2004) Widespread paleopolyploidy in model plant species inferred from age distributions of duplicate genes. Plant Cell **16:** 1667-1678

**Boudet N, Aubourg S, Toffano-Nioche C, Kreis M, Lecharny A** (2001) Evolution of intron/exon structure of DEAD helicase family genes in *Arabidopsis*, Caenorhabditis, and Drosophila. Genome Res **11:** 2101-2114

**Bowers JE, Chapman BA, Rong J, Paterson AH** (2003) Unravelling angiosperm genome evolution by phylogenetic analysis of chromosomal duplication events. Nature **422:** 433-438

**Champion A, Kreis M, Mockaitis K, Picaud A, Henry Y** (2004) *Arabidopsis* kinome: after the casting. Funct Integr Genomics **4:** 163-187

**Chehab EW, Eich E, Braam J** (2009) Thigmomorphogenesis: a complex plant response to mechano-stimulation. J Ex Bot **60:** 43-56

**Czechowski T, Stitt M, Altmann T, Udvardi MK, Scheible WR** (2005) Genome-wide identification and testing of superior reference genes for transcript normalization in *Arabidopsis*. Plant Physiol **139:** 5-17

**de Castro E, Sigrist CJ, Gattiker A, Bulliard V, Langendijk-Genevaux PS, Gasteiger E, Bairoch A, Hulo N** (2006) ScanProsite: detection of PROSITE signature matches and ProRule-associated functional and structural residues in proteins. Nucleic Acids Res **34:** W362-365

**De Vos M, Van Oosten VR, Van Poecke RM, Van Pelt JA, Pozo MJ, Mueller MJ, Buchala AJ, Metraux JP, Van Loon LC, Dicke M, Pieterse CM** (2005) Signal signature and transcriptome changes of *Arabidopsis* during pathogen and insect attack. Mol Plant Microbe Interact **18:** 923-937

**Force A, Lynch M, Pickett FB, Amores A, Yan YL, Postlethwait J** (1999) Preservation of duplicate genes by complementary, degenerative mutations. Genetics **151:** 1531-1545

**Forzani C, Carreri A, de la Fuente van Bentem S, Lecourieux D, Lecourieux F, Hirt H** (2011) The *Arabidopsis* protein kinase PTI1-4 is a common target of the oxidative signal-inducible1 (OXI1) and MAP kinases. Febs J **278**: 1126-1136

**Fujita M, Fujita Y, Noutoshi Y, Takahashi F, Narusaka Y, Yamaguchi-Shinozaki K, Shinozaki K** (2006) Crosstalk between abiotic and biotic stress responses: a current view from the points of convergence in the stress signaling networks. Curr Opin Plant Biol **9:** 436-442

**Gu Z, Steinmetz LM, Gu X, Scharfe C, Davis RW, Li WH** (2003) Role of duplicate genes in genetic robustness against null mutations. Nature **421:** 63-66

**Haberer G, Hindemitt T, Meyers BC, Mayer KF** (2004) Transcriptional similarities, dissimilarities, and conservation of cis-elements in duplicated genes of *Arabidopsis*. Plant Physiol **136:** 3009-3022

**Han S, Kim D** (2006) AtRTPrimer: database for *Arabidopsis* genome-wide homogeneous and specific RT-PCR primer-pairs. BMC Bioinform **7:** 179

**Hanks SK, Quinn AM, Hunter T** (1988) The protein kinase family: conserved features and deduced phylogeny of the catalytic domains. Science **241:** 42-52

**Herrmann MM, Pinto S, Kluth J, Wienand U, Lorbiecke R** (2006) The PTI1-like kinase ZmPti1a from maize (Zea mays L.) co-localizes with callose at the plasma membrane of pollen and facilitates a competitive advantage to the male gametophyte. BMC Plant Biol **6:** 22

**Higo K, Ugawa Y, Iwamoto M, Korenaga T** (1999) Plant cis-acting regulatory DNA elements (PLACE) database: 1999. Nucleic Acids Res **27:** 297-300

**Hoaglands DR, Arnon DA** (1950) The Water Culture Method of Growing Plants Without Soil. California Agricultural Experiment Station Bulletin: 1-39

**Huse M, Kuriyan J** (2002) The conformational plasticity of protein kinases. Cell **109:** 275-282

**Ishitani M, Xiong L, Stevenson B, Zhu JK** (1997) Genetic analysis of osmotic and cold stress signal transduction in *Arabidopsis*: interactions and convergence of abscisic acid-dependent and abscisic acid-independent pathways. Plant Cell **9:** 1935-1949

**Jiang C, Fu X** (2007) GA action: turning on de-DELLA repressing signaling. Curr Opin Plant Biol **10:** 461-465

**Johnson LN, Noble ME, Owen DJ** (1996) Active and inactive protein kinases: structural basis for regulation. Cell **85:** 149-158

**Jonassen I** (1997) Efficient discovery of conserved patterns using a pattern graph. Comput Appl Biosci **13:** 509-522

**Jonassen I, Collins JF, Higgins DG** (1995) Finding flexible patterns in unaligned protein sequences. Protein Sci **4:** 1587-1595

**Jost R, Berkowitz O, Masle J** (2007) Magnetic quantitative reverse transcription PCR: a high-throughput method for mRNA extraction and quantitative reverse transcription PCR. Biotechniques **43:** 206-211

**Katagiri F, Thilmony R, He SY** (2002) The *Arabidopsis* Thaliana-Pseudomonas Syringae Interaction. *In* The *Arabidopsis* Book, Vol 1, p doi: 10.1199/tab.0039

**Kilian J, Whitehead D, Horak J, Wanke D, Weinl S, Batistic O, D'Angelo C, Bornberg-Bauer E, Kudla J, Harter K** (2007) The AtGenExpress global stress expression data set: protocols, evaluation and model data analysis of UV-B light, drought and cold stress responses. Plant J **50:** 347-363

**King EO, Ward MK, Raney DE** (1954) Two simple media for the demonstration of pyocyanin and fluorescin. J Lab Clin Med **44:** 301-307

**Kumar S, Tamura K, Nei M** (2004) MEGA3: Integrated software for Molecular Evolutionary Genetics Analysis and sequence alignment. Brief Bioinform **5:** 150-163

**Lanahan MB, Ho TH, Rogers SW, Rogers JC** (1992) A gibberellin response complex in cereal alpha-amylase gene promoters. Plant Cell **4:** 203-211

**Lee D, Polisensky DH, Braam J** (2005) Genome-wide identification of touch- and darkness-regulated *Arabidopsis* genes: a focus on calmodulin-like and XTH genes. New Phytol **165:** 429-444

**Livak KJ, Schmittgen TD** (2001) Analysis of relative gene expression data using real-time quantitative PCR and the 2(-Delta Delta C(T)) Method. Methods **25:** 402-408

**Logemann E, Hahlbrock K** (2002) Crosstalk among stress responses in plants: Pathogen defense overrides UV protection through an inversely regulated ACE/ACE type of light-responsive gene promoter unit. Proc Natl Acad Sci U S A **99:** 2428-2432

**Ludwig AA, Romeis T, Jones JD** (2004) CDPK-mediated signalling pathways: specificity and cross-talk. J Exp Bot **55:** 181-188

**Ma SS, Bohnert HJ** (2007) Integration of *Arabidopsis* thaliana stress-related transcript profiles, promoter structures, and cell-specific expression. Genome Biol **8:** -

**Mori IC, Schroeder JI** (2004) Reactive oxygen species activation of plant $Ca^{2+}$ channels. A signaling mechanism in polar growth, hormone transduction, stress signaling, and hypothetically mechanotransduction. Plant Physiol **135:** 702-708

**O'Connor TR, Dyreson C, Wyrick JJ** (2005) Athena: a resource for rapid visualization and systematic analysis of *Arabidopsis* promoter sequences. Bioinform **21:** 4411-4413

**Pfaffl MW** (2001) A new mathematical model for relative quantification in real-time RT-PCR. Nucleic Acids Res **29:** e45

**Ramakers C, Ruijter JM, Deprez RH, Moorman AF** (2003) Assumption-free analysis of quantitative real-time polymerase chain reaction (PCR) data. Neurosci Lett **339:** 62-66

**Reinders J, Paszkowski J** (2009) Unlocking the *Arabidopsis* epigenome. Epigenetics **4:** 557-563

**Rodriguez MC, Petersen M, Mundy J** (2010) Mitogen-activated protein kinase signaling in plants. Annu Rev Plant Biol **61:** 621-649

**Rushton PJ, Somssich IE, Ringler P, Shen QJ** (2010) WRKY transcription factors. Trends Plant Sci **15:** 247-258

**Sappl PG, Heazlewood JL, Millar AH** (2004) Untangling multi-gene families in plants by integrating proteomics into functional genomics. Phytochem **65:** 1517-1530

**Schmid M, Davison TS, Henz SR, Pape UJ, Demar M, Vingron M, Scholkopf B, Weigel D, Lohmann JU** (2005) A gene expression map of *Arabidopsis* thaliana development. Nat Genet **37:** 501-506

**Schranz ME, Lysak MA, Mitchell-Olds T** (2006) The ABC's of comparative genomics in the Brassicaceae: building blocks of crucifer genomes. Trends Plant Sci **11:** 535-542

**Sessa G, D'Ascenzo M, Martin GB** (2000) The major site of the pti1 kinase phosphorylated by the pto kinase is located in the activation domain and is required for pto-pti1 physical interaction. Eur J Biochem **267:** 171-178

**Takahashi A, Agrawal GK, Yamazaki M, Onosato K, Miyao A, Kawasaki T, Shimamoto K, Hirochika H** (2007) Rice Pti1a negatively regulates RAR1-dependent defense responses. Plant Cell **19:** 2940-2951

**The-*Arabidopsis*-Genome-Initiative** (2000) Analysis of the genome sequence of the flowering plant *Arabidopsis* thaliana. Nature **408:** 796-815

**Tian AG, Luo GZ, Wang YJ, Zhang JS, Gai JY, Chen SY** (2004) Isolation and characterization of a Pti1 homologue from soybean. J Exp Bot **55:** 535-537

**Torres MA, Dangl JL** (2005) Functions of the respiratory burst oxidase in biotic interactions, abiotic stress and development. Curr Opin Plan Biol **8:** 397-403

**Toufighi K, Brady SM, Austin R, Ly E, Provart NJ** (2005) The Botany Array Resource: e-Northerns, Expression Angling, and promoter analyses. Plant J **43:** 153-163

**van der Weele CM, Spollen WG, Sharp RE, Baskin TI** (2000) Growth of *Arabidopsis* thaliana seedlings under water deficit studied by control of water potential in nutrient-agar media. J Exp Bot **51:** 1555-1562

**Veitia RA** (2005) Paralogs in polyploids: one for all and all for one? Plant Cell **17:** 4-11

**Verslues PE, Agarwal M, Katiyar-Agarwal S, Zhu JH, Zhu JK** (2006) Methods and concepts in quantifying resistance to drought, salt and freezing, abiotic stresses that affect plant water status. Plant J **45:** 523-539

**Walley JW, Coughlan S, Hudson ME, Covington MF, Kaspi R, Banu G, Harmer SL, Dehesh K** (2007) Mechanical stress induces biotic and abiotic stress responses via a novel cis-element. PLoS Genet **3:** 1800-1812

**Walley JW, Dehesh K** (2010) Molecular mechanisms regulating rapid stress signaling networks in *Arabidopsis*. J Integr Plant Biol **52:** 354-359

**Wong HL, Shimamoto K** (2009) Sending ROS on a bullet train. Sci Signal **2:** pe60

**Zhang T, Liu Y, Yang T, Zhang L, Xu S, Xue L, An L** (2006) Diverse signals converge at MAPK cascades in plant. Plant Physiol and Biochem **44:** 274-283

**Zhou J, Loh YT, Bressen RA, Martin GB** (1995) The tomato gene Pti1 Encodes a serine/threonine kinase that is phophorylated by Pto and is invloved in hypersensitive response. Cell **83:** 925-935

**Zimmermann P, Hirsch-Hoffmann M, Hennig L, Gruissem W** (2004) GENEVESTIGATOR. *Arabidopsis* microarray database and analysis toolbox. Plant Physiol **136:** 2621-2632

**Zou HW, Wu ZY, Yang Q, Zhang XH, Cao MQ, Jia WS, Huang CL, Xiao X** (2006) Gene expression analyses of ZmPti1, encoding a maize Pti-like kinase, suggest a role in stress signaling. Plant Sci **171:** 99-105

## 2.6 Appendix

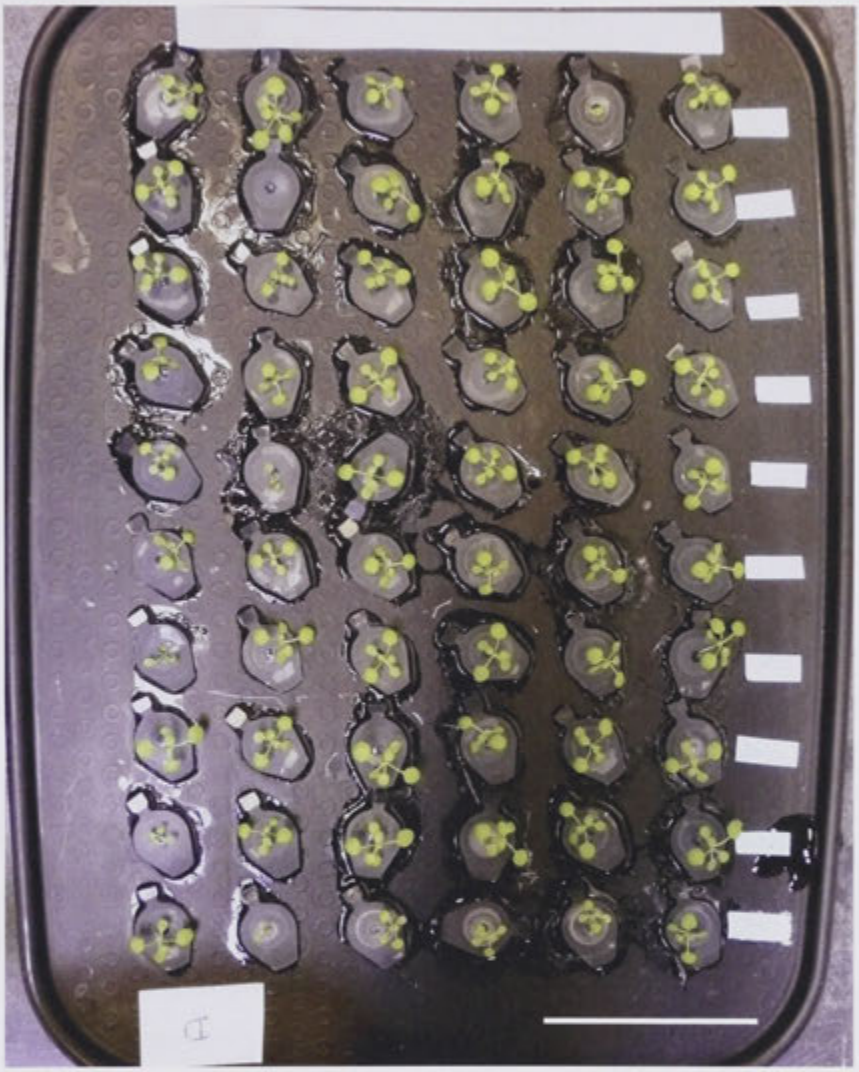

**Appendix 2.6.1: A representative hydroponic box with 2 week old Col-0 WT seedlings**. The hydroponic cultivation system was developed previously in lab (Schulze and Masle, unpublished). Plants were cultivated in Hoaglands liquid nutrient media (Hoaglands and Arnon, 1950). For imposition of osmotic stress, lids for the boxes were momentarily lifted the nutrient solution was then tipped out and replaced with PEG8000 (17.5 mM) supplemented media. Plants from two representative boxes were used for each of the treatments.

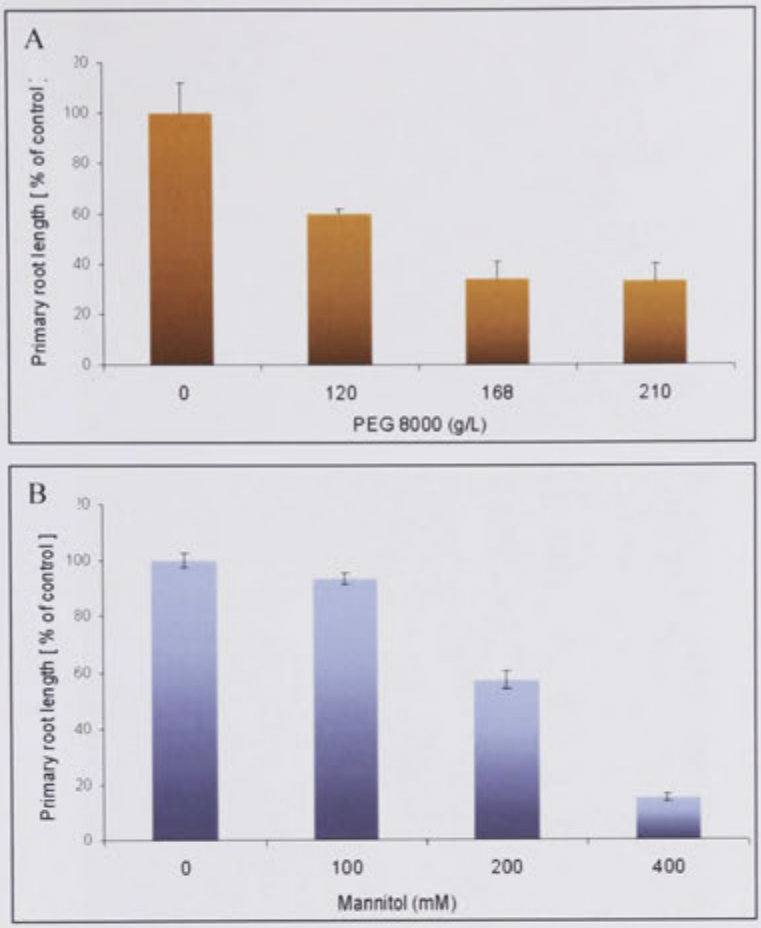


**Appendix 2.6.2(A,B): Relative primary root length of WT (Col-0) after 5 days of growth on PEG (MW 8000) or Mannitol supplemented media**. Col-0 seeds were germinated on control plates ([mannitol or PEG] =0), and transferred to fresh plates on day 5 supplemented with PEG or mannitol concentrations as indicated. Col-0 plants showed expected reduction in primary root growth with increasing concentrations of PEG or mannitol


**Appendix 2.6.3: Syringe infiltration of *Arabidopsis* leaves with virulent *Pseudomonas syringae* pv. *tomato* DC3000 bacteria**. Abaxial side of 5 week old rosette leaves were pressure infiltrated with needless syringe (A). Infiltrated area appears water soaked (B). Disease symptoms such as chlorosis were apparent 2-3 days post inoculation at the site of infiltration (C).

| Primer Name | Target | Sequence 5' → 3' | Purpose | Upper (U) /Lower (L) |
|---|---|---|---|---|
| AtPTOi_L | At3g62220 PTI1-5 | CAGGCTTTGCTCCCTTCACACCTT | qRT-PCR | L |
| AtPTOi_U | At3g62220 PTI1-5 | ATGGGAATTCGAGGATACTTGTCTTTGAGT | qRT-PCR | U |
| AtPTi1_L | At2g43230 PTI1-6 | AGATCGTCTACAGCTCTCGGTTTATCCAA | qRT-PCR | L |
| AtPTi1_U | At2g43230 PTI1-6 | TCGTCTCTCTGGTTTATTGCTCGTTGAT | qRT-PCR | U |
| AtPTi2_U | At2g47060 PTI1-4 | GCTTTGGGTGTTGTGGGGAGGAT | qRT-PCR | U |
| AtPTi2_L | At2g47060 PTI1-4 | GTGCAGTTTCAGAGGCTTGGTGGT | qRT-PCR | L |
| AtPTi3_U | At2g30740 PTI1-2 | AATGAAGAGGTGCATTTGAAAAGTCCAT | qRT-PCR | U |
| AtPTi3_L | At2g30740 PTI1-2 | CTCATCCACAGACAAGGGAGGAACTTC | qRT-PCR | L |
| AtPti5_U | At1g06700 PTI1-1 | AATAGAAGACTCAAATGAAGAGCAACAACTGA | qRT-PCR | U |
| AtPti5_L | At1g06700 PTI1-1 | ACAGGTGCTGGTTTTGAATTCTTATGATTT | qRT-PCR | L |
| AtPti6_U | At3g59350 PTI1-3 | TGAAAATGAACACCTCAGAAGCCCTAA | qRT-PCR | U |
| AtPti6_L | At3g59350 PTI1-3 | GCAGGCACATCAATAGATGGAGGCT | qRT-PCR | L |
| AtPti4newfor | At3g17410 PTI1-8 | GACGGGGACGTTGAGCACAAAGA | qRT-PCR | U |
| AtPti4newrev | At3g17410 PTI1-8 | AATTTAGGGGTTGCCCATGTCACGA | qRT-PCR | L |
| Pti7F | At1g48210 PTI1-7 | GAGGATTTTCGCAACGCTACTGACAC | qRT-PCR | U |
| Pti7R | At1g48210 PTI1-7 | ACTGGAATGGCTGGTACAGAAATAGGC | qRT-PCR | L |
| AtAPTnew-for | At1g27450 APT1 | GGTGAGCGTGCTATTATTATTGATGACCT | qRT-PCR (Internal Reference) | U |
| AtAPTnew-rev | At1g27450 APT1 | CTAGTTTCTCCTTTCCCTTAAGCTCTGGTA | qRT-PCR(Internal Reference) | R |

| Primer Name | Target | Sequence | Purpose | Upper/Lower |
|---|---|---|---|---|
| PDF2_qPCR_for | At1g13320 PDF2 | TAACGTGGCCAAAATGATGC | qRT-PCR | U |
| PDF2_qPCR_rev | At1g13320 PDF2 | GTTCTCCACAACCGCTTGGT | qRT-PCR | L |
| PR1-for | At2g14610 PR1 | GCAGCCTATGCTCGGAGCTAC | qRT-PCR | U |
| PR1-rev | At2g14610 PR1 | GCCAGACAAGTCACCGCTACC | qRT-PCR | L |
| RD29a-for | At5g52310 RD29a | GAGGCGGTGGAAGAGGAAGTGAAA | qRT-PCR | U |
| RD29a-rev | At5g52310 RD29a | ACCACCACCAAACCAGCCAGATG | qRT-PCR | L |

**Appendix 2.6.4: Real-time primers used in Chapter 2**

# Chapter 3

## Functional analysis of *PTI1* genes using reverse genetic approaches

# Chapter 3

## 3.1 Introduction

In the previous chapter, 8 *Arabidopsis PTI1*-like genes were identified on the basis of a conserved signature pattern found in PTI1 kinases previously described in the literature. These isoforms are highly similar in sequence (Figure 2.4) and chromosomal locations suggested that duplication played a significant role in the evolution of this gene family (Figure 2.7). This raises interesting questions of isoform specificity and of the extent to which redundancy plays a part in their function. Expression analysis of individual members in a range of tissues and under different stresses showed that at least at the transcript level, these genes are differentially regulated, hinting at possible functional divergence.

As the next logical step in characterising the *PTI1* gene family, a reverse genetics approach was adopted to provide initial clues on the biological functions of individual isoforms (Alonso *et al.*, 2003). This strategy, which relies on interfering with proper gene function, has successfully been employed in studying closely related genes. The study of the Class III homoedomain leucine zipper (*HD-ZP III*) family members provides an excellent example of this approach. Although the five *HD-ZIP III* genes in *Arabidopsis* are highly conserved at the sequence level, analysis of loss-of-function alleles of each member revealed distinct phenotypes during development (Prigge *et al.*, 2005). In contrast, other multigenic families, such as the type A response regulators (*ARRs*) do not show any apparent phenotype when individual gene members have been knocked out, however, by combining single T-DNA *arr* mutants through crosses, a cytokinin sensitive phenotype was eventually

revealed, thus proving overlapping functional redundancy of individual members within this family (To *et al*., 2004).

In an effort to further characterise the *Arabidopsis PTI1* gene family, I describe the use of T-DNA insertion or RNAi silencing to generate knockout or knockdown lines, respectively, of the various *PTI1* isoforms. Based on observations of the developmental phenotype of the different mutants, I demonstrate that one of the *PTI1*-like isoforms, *PTI1-8*, is a negative regulator of root growth. In addition, sequence analysis of *PTI1-8* revealed the presence of a membrane targeting motif not found in other members of the gene family. This *in silico* prediction was further supported by GFP fusion studies, which strongly suggested that PTI1-8 localises to the cell's plasma membrane.

## 3.2 Materials and Methods

### 3.2.1General plant growth conditions of *Arabidopsis* plant material

#### *3.2.1.1 In vitro growth conditions*

The *Arabidopsis* thaliana accessions (ecotype Columbia) Col-0 and/or (ecotype Wassilevskija) WS-2 were used in the experiments described in this chapter. Seed surface sterilization, cultivation in soil and tissue culture media and growth conditions were as described in Chapter 2 - Materials and methods.

#### *3.2.1.2 Growth conditions for Nicotiana benthamiana plants*

Ten to twelve Wild-type *Nicotiana benthamiana* seeds were sown directly on the surface of a soil mix in a germination tray. Once the seedlings were established (~7-10 days), individual plants were transplanted to larger pots and grown in a glasshouse at ~$23^0$ C for 4-5 weeks to obtain well-developed leaves suitable for the *Agrobacterium* infiltration assay.

### 3.2.2 Isolation of homozygous T-DNA insertion lines

For each *PTI1* isoform, FST information available from the SIGnal T-DNA express database (http://signal.salk.edu/cgi-bin/tdnaexpress) was used to BLAST search the *Arabidopsis* genome and ascertain the approximate position of T-DNA insertion. Priority was given to those lines where the insertion mapped to an exon, and preferably towards the 5' end of the gene so as to minimise the possibility of a hypomorphic allele. T-DNA insertion lines for five *PTI1* (*PTI1-5, PTI1-4, PTI1-1, PTI1-3, and PTI1-6*) genes were sourced from:

- SALK institute (http://signal.salk.edu/tabout.html) (Alonso *et al.*, 2003)

- INRA collection (FLAGdb, Functional analysis of the *Arabidopsis* genome database) (Samson *et al.*, 2002)
- SAIL, Syngenta *Arabidopsis* insertion library (Sessions *et al.*, 2002)

Segregating T2 seeds from the T-DNA lines listed in Table 3.2 were ordered and PCR-based genotyping of 10-15 individual plants was carried out to identify homozygous lines for the T-DNA insert. To that end, two sets of primers were used: a gene-specific primer pair that selectively amplifies the WT allele by hybridising to regions flanking the estimated insertion site; a second set including a T-DNA-specific primer and a gene-specific primer in order to amplify the gene allele carrying T-DNA. The PCR product amplified from the latter primer pair was sequenced to ascertain the precise position of the T-DNA insertion within the gene. Primers used for genotyping and semi-quantitative RT-PCR are given in Appendix 3.6.7.

### 3.2.3 Generation of higher order mutants

The various *pti1* homozygous T-DNA mutants were grown until flowering. Using fine tweezers, individual flowers that had well-developed stigma but immature stamens were emasculated. Pollen from independent stamens was dabbed onto each single stigma. Mature siliques containing F1 seeds were harvested. The F1 population heterozygous for both genes was allowed to self and F2 plants were sown. In order to have a 95% confidence level of identifying a double mutant in a segregating F2 population with an expected 9:3:3:1 segregation ratio, 48 seeds were sown (3 times the average sampling size). PCR based genotyping as described in the previous section was employed for screening the F2 plants. Approximately 10-12

plants that were null (-/-) for one of the 2 genes (probability 1:4 in F2) were first identified. The genotype at the second locus was examined in this sub-population of plants to isolate a double mutant (probability 1:4 in F2 sub-population).

### 3.2.4 Quantitative analysis of root growth

*pti1* T-DNA mutants and inducible silencing *PTI1-8* lines (Engineering of this construct is described in section 3.2.6.2) were grown on vertically oriented agar supplemented with Hoaglands solution (Hoaglands and Arnon, 1950). Plates were placed in growth cabinets (Conviron, Controlled Environments, Pembina, ND) fitted with white fluorescent tubes and incandescent bulbs providing 120 μE $m^{-2}s^{-1}$ cent at $21^0$ C and 60% relative humidity (short-day cycle: 10 hour light). For each genotype, 3 replicate plates containing 8-10 seedlings each were used for the analysis. The position of the advancing root tip was recorded under a standard dissection microscope at 24 hour intervals by marking the petri dish with a scalpel. Individual plates were scanned on a flatbed scanner (Epson) at (600 pixels $inch^{-1}$) and root measurements were determined from these images using ImageJ software by pixel to distance conversion.

### 3.2.5 Germination assay

Germination rates were calculated for two independent *PTI1-8* inducible silencing lines. Approximately 60 seeds per line were sown on plates supplemented with 1x Hoagland's solution and with 0 or 20 μM Dexamethasone for control treatment and inducible silencing, respectively (3 replicates per treatment). Seeds were stratified on the plates for 3 days in the dark at $4^0$ C and subsequently transferred to growth cabinets under short day conditions (10 hour photoperiod, $21^0$ C, light intensity 120

μE $m^{-2}s^{-1}$). All other conditions were as described previously in Chapter 2. Germination was scored at 8 hour intervals and until all seeds had germinated. Germination time was defined as the time the breaking of the seed coat by the emerging radicle was first seen.

### 3.2.6 Molecular Techniques

#### *3.2.6.1 Design of PTI1-8 constitutive silencing construct*

The Gateway compatible vector pHELLSGATE12 directs RNAi silencing using hairpin RNA (hpRNA) to specifically knockdown the gene of interest. The key factor that influences the successful silencing of a target gene is the sequence specificity of the encoding hpRNA. Two important considerations have been described by Helliwell and Waterhouse (2003), when choosing a target region to be cloned into the pHELLSGATE12 silencing vector:

1. Fragment sizes ranging from 300-600 bp were found to be optimal for maximum silencing.
2. In order avoid off-target silencing the chosen fragment should not contain blocks of 20 bp length that are identical to any unintended target gene in the *Arabidopsis* genome.

The multiple sequence alignment of the various *PTI1* genes in Chapter 2 showed a very high degree of amino acid conservation in the kinase domain, which was also reflected in the DNA sequence. Specifying a region for *PTI1-8* silencing in this conserved domain would increase the probability of off-target genes being knocked down. Since the kinase domain makes up 70% of the *PTI1-8* cDNA sequence, the remaining 380 bp at the 5' end, which include the 5' UTR, were analysed for

candidate regions that could be used as silencing targets. The dsCheck tool (Naito *et al.*, 2005) available online (http://dscheck.rnai.jp/) was used for identifying candidate regions. Further optimization was done manually to select a 267 bp region highly specific of *PTI1-8*. That fragment was then submitted to the siRNA scan tool (http://bioinfo2.noble.org/RNAiScan.htm) (Xu *et al.*, 2006) that searches for 20-nt off –target matches in the mRNA *Arabidopsis* database. Other than the intended target *PTI1-8*, the RNAi fragment contained no 20-nt sequences (direct and reverse complementary) that was identical to any gene in the database (Appendix 3.6.1).

### *3.2.6.2 Constitutive and inducible RNAi (inRNAi) silencing constructs for PTI1-8 silencing*

The 267 bp fragment of the *PTI1-8* (At3g17410) gene spans a region containing the end of the 5'UTR until the second exon. It was PCR amplified from a Col-0 seedling cDNA template. The fragment was restriction cloned into the Gateway entry vector pENTR1A (Invitrogen) using the restriction sites *Bam*H1 and *Eco*R1. This genomic fragment was then transferred to the constitutive silencing vector pHELLSGATE12 (Helliwell and Waterhouse, 2003) by Multisite Gateway® LR recombination reaction according to the manufacturer's instructions (Invitrogen).

The *PTI1-8* RNAi fragment introduced into the inducible silencing pOpOff2 vector construct (Wielopolska *et al.*, 2005) was cloned from the same pENTR1A vector previously used for the constitutive silencing. The pOpOFF2:PTI1-8 construct was transformed into Col-0 plants along side the pHELLSGATE12 construct as a control for assessing transformation efficiency and the phenotypes induced by *PTI1-8* silencing. T0 seeds were screened for kanamycin resistance in the absence of

dexamethasone in the culture media.

### *3.2.6.3 PTI1-8 GFP fusion constructs*

All *PTI1-8* reporter constructs were designed using Gateway™ compatible pMDC series vectors (Curtis and Grossniklaus, 2003). To account for the possibility of the translation fusion resulting in incorrect folding of the hybrid protein, two separate constructs with GFP cloned either at N-terminal (35S:GFPPTI1-8, pMDC44) or C-terminal (35S:PTI1-8GFP, pMDC84) ends of *PTI1-8* sequence were designed. In both these vectors, the *PTI1-8* fused to GFP is under the control of the 35S constitutive promoter. For the N-terminal fusion construct, the coding region of *PTI1-8* was PCR amplified from WT-Col0 cDNA and restriction cloned into pENTR1A vector using *Eco*RI and *Bam*HI sites. In the case of the C-terminal fusion, the *PTI1-8* coding region without the stop codon was PCR amplified and cloned into pENTR1A using the restriction sites *Bam*H1 and *Hind*III.

An additional reporter construct was also designed in which the genomic *PTI1-8* fragment was fused to GFP (genPTI1-8GFP, pMDC110) to analyse tissue specific expression pattern of *PTI1-8* in stably transformed *Arabidopsis* plants. Here, the genomic region from the end of the 5' upstream gene (At3g17400, *SKP2*-like) to the end of the *PTI1-8* coding region (without the stop codon) was PCR amplified from genomic DNA and cloned into pENTR1A using the restriction sites *Bam*H1 and *Not*1 and cloned into pENTR1A vector.

The 3 *PTI1-8* fragments for N-terminal, C-terminal and genomic fusions were transferred from pENTR1A vector to the respective plant binary pMDC vectors by

Gateway® LR recombination reaction according to the manufacturer's instruction (Invitrogen). *PTI1-8* sequence integrity and translational read through for the C-terminal fusion to GFP was verified through sequencing. The positive 35S:GFP control plasmid and *Arabidopsis* seeds stably transformed with this construct were kindly provided by Dr. Peter Waterhouse (University of Sydney, Australia).

### *3.2.6.4 Standard PCR conditions*

Standard PCR reactions (Table 3.1) were performed using GoTaq® Hot Start DNA polymerase (Promega). For *PTI1-8* RNAi and GFP reporter fusion constructs, highfidelity *Taq* DNA polymerase (iProof®, BIORAD) was used as per the manufacturer's instruction. A typical PCR reaction mix:

Table 3.1: Standard PCR reaction mix (20 µL total volume)

| Component | Volume |
|---|---|
| Template DNA (genomic or plasmid) | 0.1-20 ng |
| 5X Green GoTaq® Buffer | 4 µL |
| dNTP mix (2.5 mM each: dATP, dCTP, dGTP, dTTP) | 0.5 µL |
| Forward Primer (10 µM) | 0.5 µL |
| Reverse Primer (10 µM) | 0.5 µL |
| GoTaq® DNA Poymerase | 0.4 µL |
| MilliQ water (Autoclaved) | To 20 µL total volume |

### *3.2.6.5 Gel electrophoresis of DNA*

DNA fragments were separated by agarose (Fisher Biotec) gel electrophoresis in gels containing 1-3% (w/v) agarose in TAE buffer (40mM Tris-acetate, 20mM $Na_2EDTA$, pH 8.5). Agarose was dissolved in TAE buffer by heating in a microwave and 2.5 µL ethidium bromide (Sigma) (10 mg/mL) was added. Hyperladder II

(Bioline) 1 kb ladder was loaded alongside the samples for size quantification. Homemade loading buffer (70% glycerol, 30% $H_20$, bromophenol blue) was added to samples and agarose gels were run in a traditional electrophoresis set-up at typically 100V and imaged over a UV light source.

### *3.2.6.6 Vector manipulations*

Restriction digests were carried out as recommended by the manufacturer's instructions. For all construct designs, restriction enzymes used were ordered from Promega and typically 0.5 µL of restriction enzyme was used per 10 µL reaction. All digestions were carried out at the appropriate temperature for a minimum of three hours and reactions were stopped by freezing at -20$^0$ C. Plasmids were isolated from 5 ml overnight bacterial cultures using AxyPrep$^{TM}$ miniprep kit and when needed gel extraction of DNA fragments was isolated using AxyPrep$^{TM}$ gel extraction kit.

### *3.2.6.7 CTAB DNA extractions*

CTAB DNA extraction was used for isolating genomic DNA for PCR genotyping of the various pti1 single and double mutants. Leaf samples (approx 2-3 cm$^2$) were harvested from each plant and ground in a motar and pestle with 800 µL of 1.5X CTAB buffer (15 g/L cetyl-trimethyl-ammonium bromide [CTAB], 1 M Tris HCL pH 8.0, 0.5 M EDTA, 61.4 g/L NaCl). The ground sample was transferred to a 1.5 mL microcentrifuge tube and incubated at 65$^0$ C for 30 minutes, with mixing every 8 minutes. To each sample, 600 µL of 24:1 chloroform:isoamyl alcohol was added and gently shaken for 20 minutes. The samples were then centrifuged at 8000 rpm for 20 minutes. 450 µL of the supernatant was transferred to a fresh 1.5 mL microcentrifuge tube and 1 mL of precooled 95% ethanol was added for precipitation of the DNA.

The samples were inverted gently and incubated for 2 hours before spinning at 12000 rpm for 15 minutes. The ethanol was decanted and washed with 500 µL of fresh ethanol. The samples were spun again at 12000 rpm for 5 minutes. The ethanol was decanted and the pellet was air-dried in the laminar flow hood and then resuspended in 80 µL of sterile $H_2O$. DNA concentration ($A_{260}$) and quality ($A_{260}/A_{280}$ ratio) was measured using the NanoDrop® ND-1000 Spectrophotometer. Samples were stored at $-20^0$ C.

#### *3.2.6.8 Sequencing*

DNA cloned fragments or plasmids were sent with appropriate primers for sequencing to the Bimolecular Resource Facility (JCSMR, ANU, Canberra) or to the Australian Genome Research Facility (AGRF, Brisbane).

### 3.2.7 Plant Transformation Procedures

#### *3.2.7.1 Transient Expression Assay by leaf infiltration of Agrobacterium tumefaciens*

Wild-type *Nicotiana benthamiana* leaves were infiltrated for transient expression with *Agrobacterium* strains (GV3101) carrying the pMDC vector (PTI1-8 translationally fused GFP). Five mL YEP inoculate (10 g/L peptone, 10g/L yeast, 5 g/L NaCl) starter culture containing the appropriate antibiotics (pMDC binary vector: kanamycin, (Sigma) 50 µg/mL; pRENE35SGFP: Spectinomycin (Sigma) 100 µg/mL and GV3101:Rifampicin (Sigma), 15 µg/mL) with the *Agrobacterium* strain was incubated at $28^0$ C for 48 hours. 0.5 mL of this starter culture was used to inoculate 25 mL YEP supplemented with 20mM MES (pH 5.6) and 20 µM Acetosyringone

(Sigma), followed by an incubation period of 14-16 hours or until $OD_{600}$ reached ~1.2-1.5. Fifteen mL of this culture was centrifuged at 7000 rpm for 10 minutes (Beckman coulter JA20 rotor) and the supernatant decanted. The *Agrobacterium* pellet was resuspended in the infiltration buffer (1x MS salts [Duschefa Biochemie], pH 5.6; 10mM MES, pH 5.6; 3% sucrose and 200 μM Acetosyringone) and incubated at room temperature for 30-60 minutes. Approximately 15-30 minutes prior to infiltration, plants were watered so as to induce opening of stomata, which facilitates absorption of the *Agrobacterium* infiltrate. Infiltration was carried out on the abaxial surface of fully expanded leaves. For each construct, replicate infiltration for a single construct was carried out on 2-3 leaves. Samples were harvested from infiltrated *Nicotiana benthamiana* leaves 2 or 3 days post-infiltration and tissue was directly imaged by light microscopy in a wet mount using a few drops of water. For induction of plasmolysis, 0.8 M mannitol solution was syringe infiltrated into the sampled leaf sections and incubated for 15-20 minutes before imaging.

### *3.2.7.2 Arabidopsis transformation*

*Arabidopsis* plants were stably transformed with *PTI1-8* silencing (pHELLSGATE12:PTI1-8, pOpOff2:PTI1-8) and GFP fusion construct (genPTI1-8GFP) using the floral-dip mediated *Agrobacterium* transformation (Clough and Bent, 1998; Davis *et al.*, 2009). *Arabidopsis* wild-type Col-0 plants used for all transformations were grown as described above under long day conditions (16 hour photoperiod) day conditions. The primary bolts were clipped, reducing apical dominance and promoting the formation of axillary inflorescences.

A 50 mL volume of YEP media (10 g/L peptone, 10g/L yeast, 5 g/L NaCl) was inoculated with the *Agrobacterium* (AGL1) carrying the binary vectors and appropriate antibiotics. The liquid culture was grown for 2 days at $28^0$ C until cell optical density was saturated. The entire 50 mL culture was poured into 450 mL 'direct dip media' (1% w/v yeast extract, 1% w/v Bacto peptone, 0.5% w/v NaCl, 0.5% w/v sucrose, 0.05% w/v $MgSO_4$ in MilliQ water, pH adjusted to 7.0) as described by Davis *et al.* (2009). Just prior to floral dipping the surfactant Silwett L77 (Lehle seeds) was added to the media at a final concentration of 0.05% (v/v). Flowers were dipped in the solution for ~5 seconds before being placed flat on trays and covered with cling wrap to maintain high humidity. The following day the cling wrap was removed and plants were allowed to set seed under standard long day (16 hour photoperiod) conditions. For each construct, a minimum of two pots containing 4-6 Col-0 plants each was transformed as replicates. $T_0$ seeds were harvested from each pot separately. 10-20 T1 independent primary transformants selected through antibiotic resistance on MS media plates (3.2.8) were carried through to T3 generation to identify homozygous individuals. Due to time constraints, the phenotypic analysis of genPTI1-8GFP fusion construct was carried out on 5 independent primary T1 transgenics.

### 3.2.8 Selection of *Arabidopsis* transformants on nutrient media plates

All selection of transformants were on Murashige and Skoog (MS) (Duschefa Biochemie) plant nutrient media supplemented with either kanamycin (Sigma) (50 µg/mL) (*PTI1-8* silencing vectors: pHELLSGATE12, pOpOff) or hygromycin B (Sigma) (15 µg/mL) (PTI1-8 GFP reporter studies: pMDC32, pMDC110). The

protocol for identifying transformants was followed as described in Harrison *et al* (2006).

MS agar was made up of the following in milliQ water: 4.3 g/L MS salts, 20 g/L sucrose, 0.05% MES, 0.7% phytoagar, pH adjusted to 5.8 with KOH. Surface-sterilised seeds were pipetted onto MS agar supplemented with appropriate selectable markers. Seeds were stratified at $4^0$ C in the dark for 3 days and then transferred to growth chambers for 6 hours under continuous light (120 µE $m^{-2}s^{-1}$) to stimulate germination (other conditions were the same as described in Chapter 2). The media plates were then wrapped in aluminium foil and incubated for 2 days in the same growth chamber. The foil was then removed and plates kept for a further 24-48h under continuous light. Kanamycin resistant seedlings were identified by long hypocotyls and green cotyledons (susceptible seedlings: long hypocotyls and pale cotyledons). Hygromycin B resistant seedlings were identified as those with long hypocotyl and green cotyledons (susceptible seedlings will have short hypocotyl and green cotyledons). Resistant seedlings were left on selection plate for 1 week before being transplanted to soil.

### 3.2.9 Dexamethasone Treatments

#### *3.2.9.1 Application of Dexamethasone by Leaf painting*

Screening of the primary inRNAi *PTI1-8* transformants (pOpOff2) for the levels of *PTI1-8* silencing was carried out by 'painting' single rosette leaves of 4 week old plants. This has been demonstrated before to induce rapid-localized induction of the pOp6 promoter (Craft *et al.*, 2005) and can be visualized by the simultaneous activation of the GUS reporter gene. A 20 µM Dexamethasone solution (diluted from

a 20 mM stock in 100% ethanol containing 0.02% (v/v) Silwett L-77 (Lehle seeds) was prepared just prior to application. A fine paintbrush was dipped into the 20 μM Dexamethasone solution and brushed on both sides of the rosette leaves of 21 T1 transgenics and wild-type Col0 control. 24 hours after application the treated leaves were harvested; the distal end was used for RNA isolation and the proximal end for GUS staining.

### *3.2.9.2 In vitro Application of Dexamethasone in culture media*

To investigate the developmental effects of *PTI1-8* silencing in young seedlings, Dexamethasone was supplemented in the Hoagland media. A 20 μM Dexamethasone solution (from a 100 mM stock in dimethylsufoxide, DMSO) was added to the media just prior to pouring into petri dishes. For control seedlings, an equivalent volume of DMSO was added to the media (0.02% v/v). For each genotype, 3 replicate plates for + Dex and – Dex (DMSO) were prepared.

### *3.2.9.3 Application of Dexamethasone in Hydroponic media*

In order to maintain continuous levels of *PTI1-8* silencing throughout the life cycle of the plant, a hydroponic based cultivation system was employed. In a review of chemical inducible expression system, Moore *et al.* (2006) have noted that under greenhouse conditions, irrigating *Arabidopsis* soil-grown plants with a dexamethasone containing solution results in rapid uptake via the roots and transport to the shoots as evident from the GUS activity seen in the leaves 6 hours only after treatment. A similar result for dexamethasone uptake was also shown in another

study by (van Dijken *et al.*, 2004). In the experiments where continuous silencing of *PTI1-8* was required, a soil-based system was therefore avoided as DMSO has been shown to accumulate in the soil after repeated watering and to affect plant physiology. An hydroponic system was therefore an attractive alternative as the growing solution can be replaced thus avoiding accumulation of DMSO. The detailed set-up used is as described previously in Chapter 2 (Section 2.2.2.2) with the following modifications: the seeds were initially germinated on a small volume of Hoaglands agar media (Hoaglands and Arnon, 1950) supplemented with 20 μM Dexamethasone solution or equal volume of the solvent DMSO (0.02% v/v) for control plants. Similarly, an equal concentration of Dex and DMSO was added to the 1/3X Hoagland solution within the hydroponic container and this solution was replaced every 3 days from germination to maturity. Three hydroponic boxes with solution supplemented with Dex and one with solution supplemented with DMSO were used for the analysis, with 6-9 plants of each genotype.

### 3.2.10 Staining

#### *3.2.10.1 Histological staining of GUS activity*

The 21 independent T1 inRNAi *PTI1-8* lines were assayed for GUS activity following Dexamethasone treatment. The detached leaves were incubated in staining buffer (50mM $NaPO_4$ pH=7.0, 10mM EDTA, 0.1% Triton X-100, 10 mM potassium ferricyanide, 10 mM potassium ferrocyanide) containing 1 mg/mL X-Gluc in scintillation vials. The leaves were vacuum infiltrated for 30 minutes and then transferred to $37^0$ C overnight. The solution was then removed and leaves incubated in increasing concentrations of ethanol for 30 minutes each. The leaves were mounted on a slide in water and photographed using a digital camera (Lumix DMC-

FS15).

### *3.2.10.2 Propidium iodide staining*

Propidium iodide was used as a cell wall stain to delineate root structures of inRNAi *PTI1-8* line 6.3 seedlings. Seedlings growing on vertically oriented plates for 8 days were transferred to a 10 µM propidium iodide (Sigma-Aldrich) solution (dissolved in 1X Hoaglands solution) and incubated for 3-6 minutes, rinsed and mounted in 1X Hoaglands solution.

## 3.2.11 Microscopy

### *3.2.11.1 GFP imaging*

Visual detection of GFP fluorescence in infiltrated *Nicotiana benthamiana* leaf sections and *Arabidopsis* roots were performed using epifluorescent microscope (Zeiss Axioplan) and images were photographed using a SPOT CCD camera (SPOT FLEX 1.25 Megapixel). Images were then processed with ImageJ software.

### *3.2.11.2 Confocal microscopy*

Propidium iodide stained inRNAi *PTI1-8* roots were visualized using a Leica confocal microscope (Leica, TCS-SP2-UV) and the following settings: excitation wave-length nm; emission 550-800 nm; beam splitter: 488/543/633 nm triple dichroic; objective: HCPL APO CS 20.0x0.70 IMM/COR. Images were processed using ImageJ. GFP fluorescence for *PTI1-8* reporter constructs in transiently transformed *Nicotiana benthamiana* cells was observed using Zeiss confocal microscope (Carl Zeiss, LSM510) with an 488 nm excitation from an argon laser and

a 505-530 nm band pass filter for GFP detection. All images were processed using ImageJ software.

## 3.3 Results

### 3.3.1 Identification of T-DNA insertion lines for individual *PTI1*-like genes in *Arabidopsis*

A simple and relatively expeditious approach in assigning gene function is making use of the large collections of indexed T-DNA insertions available from seeds stock centres (O'Malley and Ecker, 2010). Accordingly, the public SIGnal T-DNA express database (http://signal.salk.edu/cgi-bin/tdnaexpress) was queried for T-DNA insertions in the 8 *PTI1*-like genes. The search revealed unambiguous exon-localised insertions in five out of eight *PTI1*-like genes (*PTI1-5*, *-6*, *-4*, *-1* and *-3*) in the T-DNA mutant populations from the SALK Institute. Although not available at the time the search was carried out, T-DNA insertion lines have since become available for two of the three remaining *PTI1* genes, *PTI1-2* and *PTI1-7*. As this was late in the project, these lines could not be studied further and were hence excluded from the subsequent phenotypic analysis.

Segregating T1 seeds for the 5 *PTI1* T-DNA lines listed in table 1 were ordered and lines homozygous for the T-DNA insert were identified by PCR-genotyping (see details in Materials and Methods) (Table 3.2). Sequencing of the flanking T-DNA regions for all 5 lines verified the exact position of the T-DNA within the coding region (Figure 3.1). Expression analysis by semi-quantitative RT-PCR showed the absence of gene transcript (Figure 3.2).

Table 3.2: Information on T-DNA mutants for five *Arabidopsis* PTI1 genes

| T-DNA ID (background ecotype) | Gene accession | Gene insertion position | Left border Insertion point in the genomic sequence and 20 bp gene sequence ( insert position indicated by ↓) |
|---|---|---|---|
| SALK 020728 (Col-0) | At3g62220 (*PTI1-5*) | 2nd exon | +501 bp gcacaaaaag↓gtgctcagag |
| FLAG325B10 (Ws-2) | At2g43230 (*PTI1-6*) | 1st exon | +177 bp tgatggatcgt↓gattttcat |
| SALK 065325 (Col-0) | At2g47060 (*PTI1-4*) | 4th exon | +1004 bp ggtcctgtc↓ttgtcgtggta |
| SALK 086563 (Col-0) | At1g06700 (*PTI1-1*) | 3rd exon | +1439 bp atggaaacc↓tccgcgtcctt |
| FLAG 543G06 (Ws-2) | At3g59350 (*PTI1-3*) | 3rd exon | +1240 bp ttgctactat↓gggatcttta |

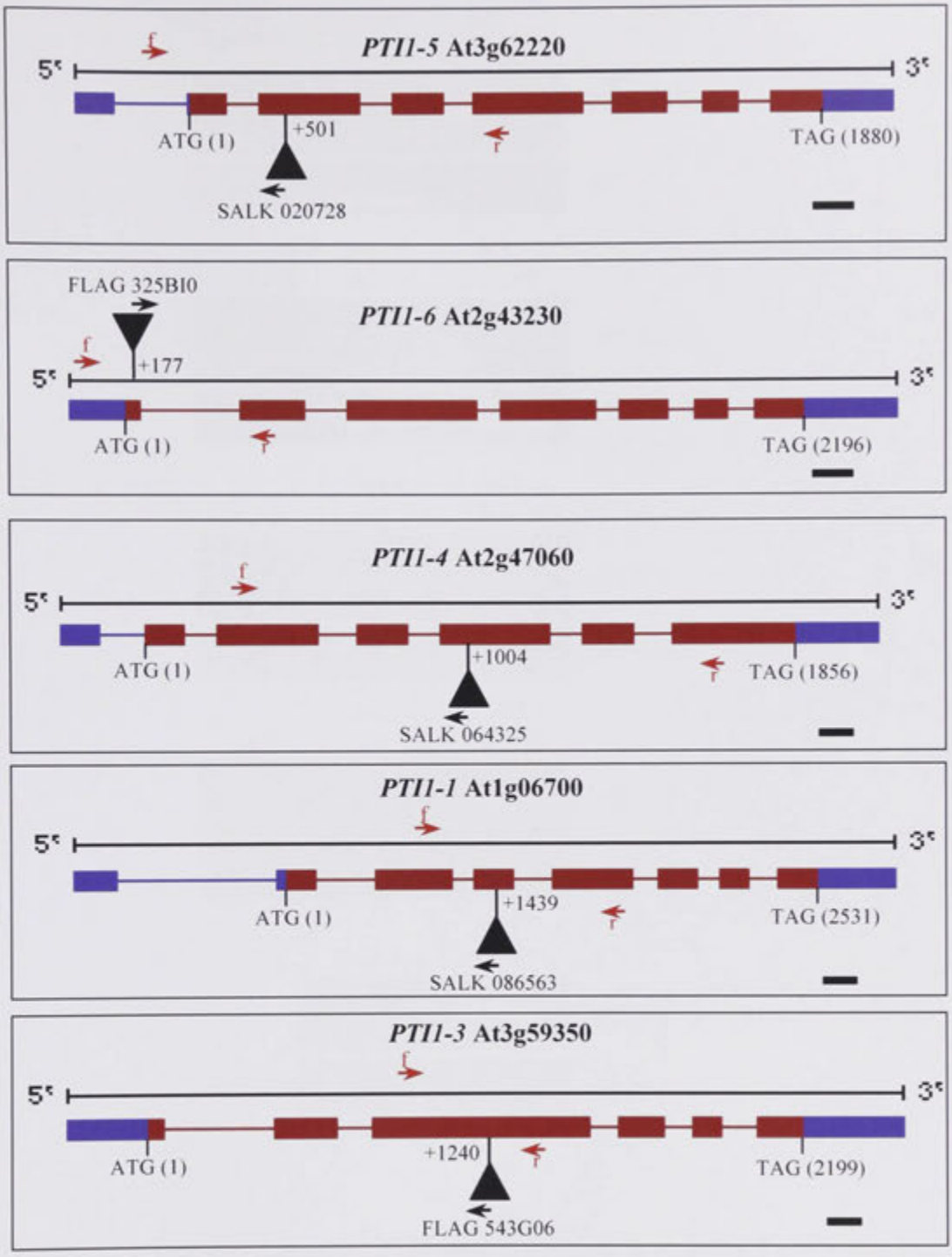


**Figure 3.1: T-DNA insertion sites in five *AtPTI1* genes:** Exons (Brown boxes) and UTR (blue boxes), Introns (Thin brown lines connecting boxes). T-DNA insertion lines (black triangles) isolated for 5 *PTI1* genes. Forward (f) and reverse (r) gene specific primers (red arrow) in combination with T-DNA specific primer (Black arrow) was used for genotyping of T-DNA alleles. Scale bars-100 bp.

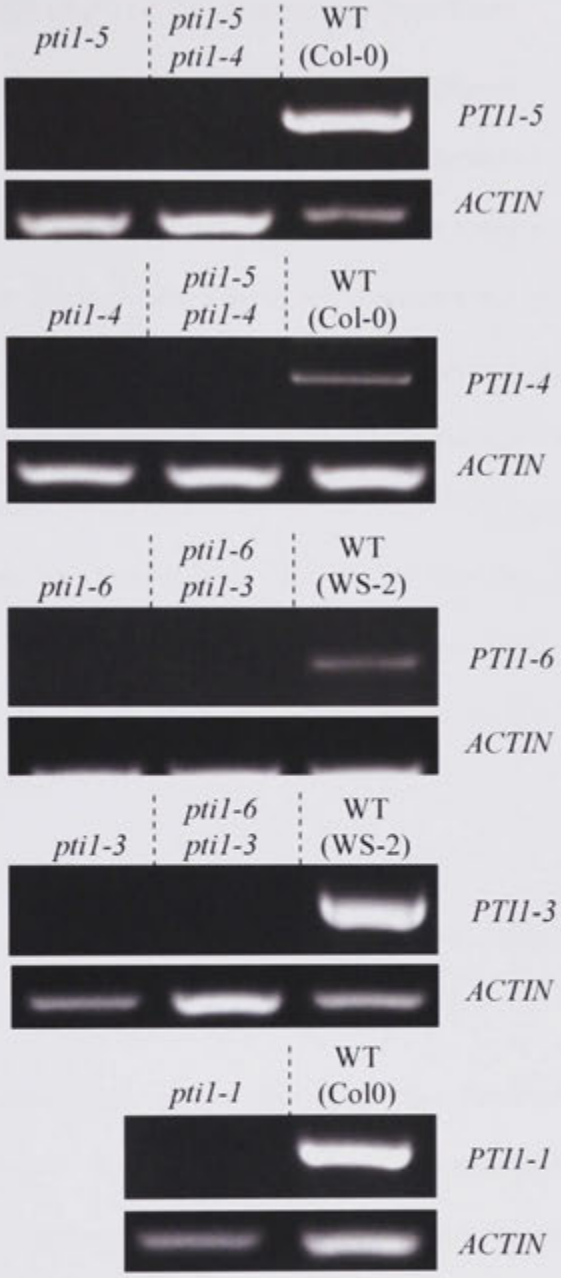


**Figure 3.2: Absence of residual PTI1 gene expression in *pti1*-like T-DNA mutants.** RT-PCR analysis using individual PTI1 and ACTIN primers (*ACT2*, At3g18780) (loading control) and total RNA extracts from wild-type (Col-0 or WS-2) and mutant seedlings as template. *PTI1-5* and *PTI1-4* were amplified for 31 cycles; *PTI1-6*, *PTI1-3* and *PTI1-1* were amplified for 35 cycles; the control *ACTIN* was amplified for 31 cycles.

### 3.3.2 Generation of *pti1*-like double mutant lines

In chapter 2, phylogenetic analysis showed the *Arabidopsis PTI1* genes to group into distinct pairs and comparison of chromosomal locations suggested segmental duplication as a likely evolutionary scenario for the formation of these gene pairs (Chapter 2, Figure 2.5 and 2.6). Therefore, to address the possibility of functional redundancy of closely related *PTI1* genes, the corresponding knockout mutants were crossed to generate double mutant lines (*pti1-5*/*pti1-4* and *pti1-6*/*pti1-3*) (Figure 3.3). This was not possible for *PTI1-8*/*PTI1-7* and *PTI1-2*/*PTI1-1* gene pairs as no T-DNA insertional mutant was available at the time for the first three of these genes. Confirmed single and double mutant lines were grown along with WT plants under uniform conditions to avoid confounding batch seed effects in subsequent physiological studies.

### 3.3.3 *pti1* single and double mutants show wild-type morphology under standard growing conditions

As an initial screening approach to identify putative functions of *PTI1*-like genes, single and double *pti1* mutant lines were grown on agar plates for comparison of growth and development of young seedlings, and in soil to assess overall developmental and morphological phenotypes at later stages.

Seeds for all *pti1* single and double mutant lines including the corresponding WT controls (Col-0 and WS-2) were stratified for 3 days at $4^0$ C in the dark and sown directly on 1.2% agar plates supplemented with Hoaglands nutrient solution (Hoaglands and Arnon, 1950) and 1% sucrose or on soil (seed raising mix) supplemented with slow release fertilizer and maintained well-watered through

A

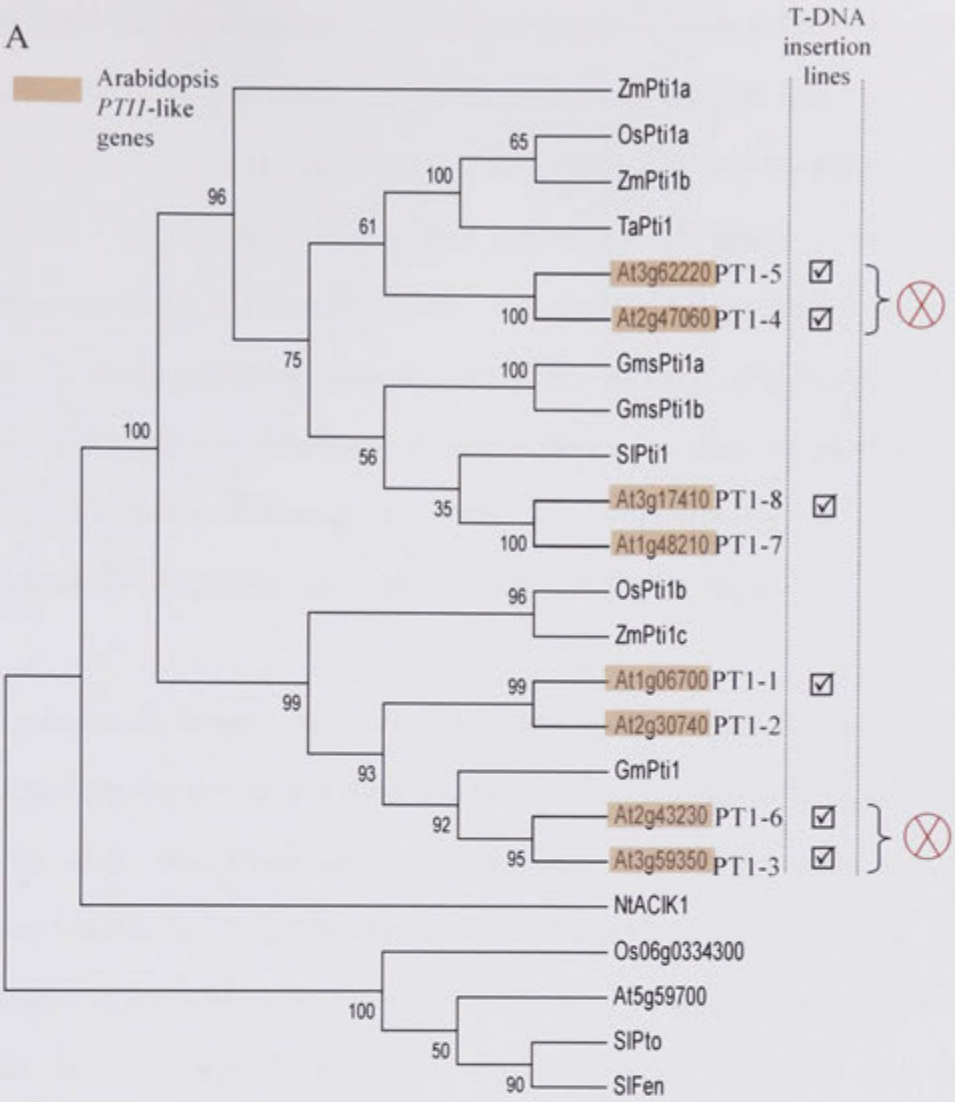


B

| | PTI1-1 | PTI1-2 | PTI1-3 | PTI1-4 | PTI1-5 | PTI1-6 | PTI1-7 | PTI1-8 |
|---|---|---|---|---|---|---|---|---|
| PTI1-1 | | 84 | 66 | 61 | 66 | 69 | 65 | 65 |
| PTI1-2 | 88 | | 66 | 60 | 65 | 67 | 66 | 67 |
| PTI1-3 | 69 | 71 | | 59 | 59 | 81 | 61 | 62 |
| PTI1-4 | 69 | 68 | 62 | | 76 | 59 | 64 | 66 |
| PTI1-5 | 65 | 65 | 58 | 83 | | 61 | 69 | 72 |
| PTI1-6 | 71 | 69 | 83 | 62 | 58 | | 60 | 60 |
| PTI1-7 | 65 | 65 | 56 | 72 | 69 | 58 | | 86 |
| PTI1-8 | 66 | 68 | 59 | 76 | 73 | 61 | 87 | |

**Figure 3.3 (A,B):** Summary of T-DNA insertion lines for Arabidopsis *PTI1* genes obtained from stock centres ☑ and double mutant lines generated ⊗ (A). Pairwise amino acid (purple) and nucleotide (green) sequence identity for the 8 *PTI1* isoforms. Highlighted in red are the highest conserved members for each gene (B).

capillarity feeding. Germination rates (where germination was defined as the time the radicle broke the seed coat) were similar for mutants and wild type seeds (data not shown), as were the elongation rates of the primary root over the following 7 days (Figure 3.4 A-C). At this early stage seedlings of all genotypes were visually indistinguishable, and showed no variation in either root length, root branching, root hairs or rosette size. Comparison of rosette phenotypes of 21 day-old plants grown in soil, under 'optimal' conditions, confirmed these early observations (Figure 3.4D, Appendix 3.6.2), indicating that *PTI1* loss-of-function was of no apparent consequence for *Arabidopsis* vegetative growth and development.

It is important, however, to note here that the majority of *PTI1*-like genes that have so far been characterized in other species have been implicated in stress responses (Zhou *et al.*, 1995; Herrmann *et al.*, 2006; Zou *et al.*, 2006; Takahashi *et al.*, 2007) (See Chapter 1, Introduction for details). One obvious hypothesis then, for the absence of detectable growth and developmental phenotypes in any of the the *pti1*-like mutants examined, is that the "optimal" growth conditions used in our experiments above may have masked *PTI1* function. In Chapter 4, I examine this possibility in more detail by assessing the phenotypic response of *pti1* mutants to the bacterial pathogen, *Pseudomonas syringae*.

### 3.3.4 *PTI1-8* expression is not, or only partially, down-regulated in available T-DNA insertional mutants

Interestingly, *PTI1-8* was the only isoform for which no exon-localised insertion was available across 6 different T-DNA populations. 11 FSTs were located within 500 bp up- or downstream of the *PTI1-8* coding region except for one, which mapped to the

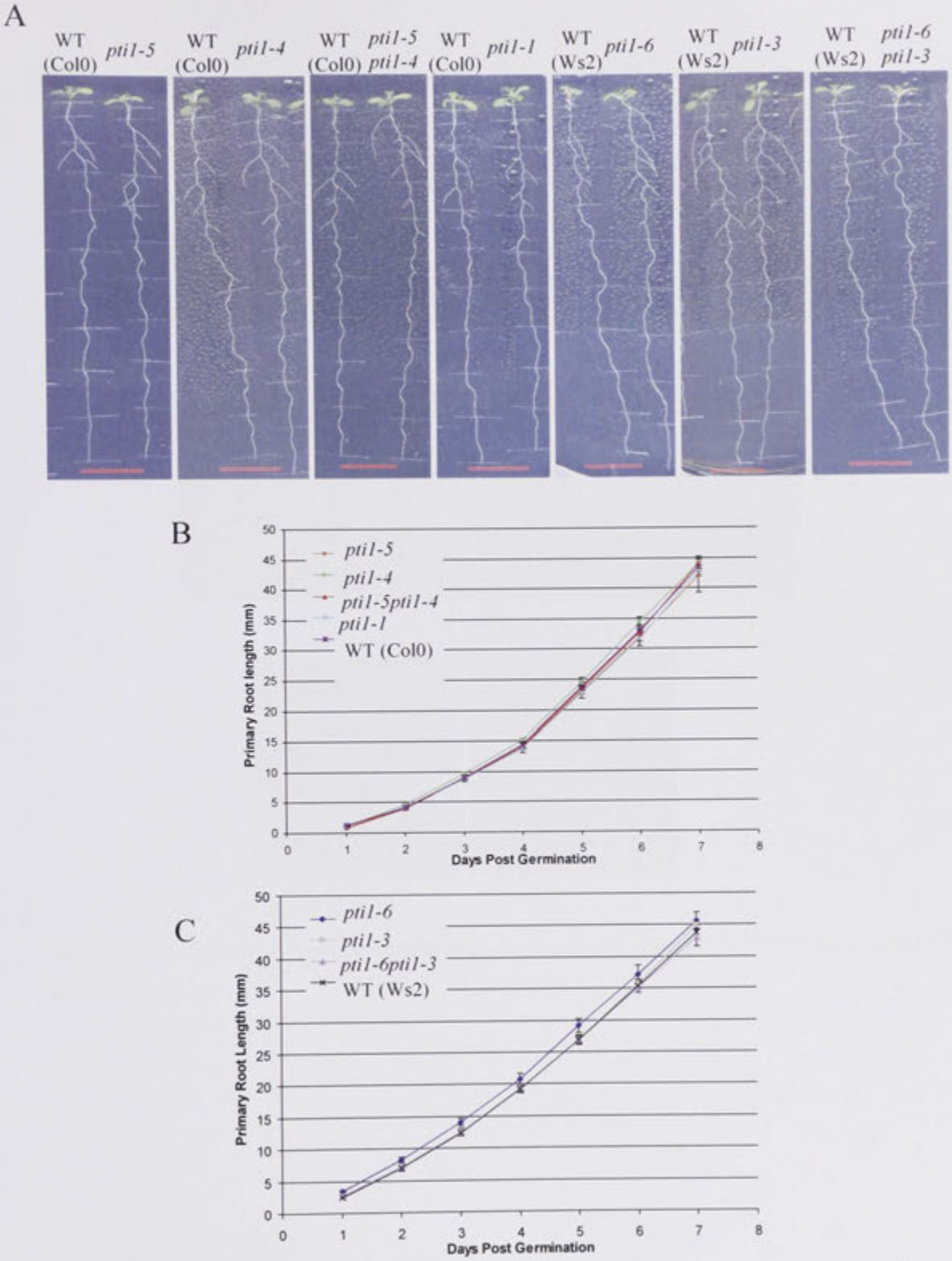


**Figure 3.4 (A-C) Representative images of 10 day old *pti1* mutant and corresponding WT seedlings grown on vertically oriented Hoagland media plates** (A). Primary root length of *pti1* mutants in the Col0 background (B) and Ws2 background (C) ecotypes. Error bars represent SE of the mean (n=30). Red scale bar = 1.5 cm

D


**Figure 3.4 (D) Representative images of 3 week old *pti1* mutant and WT plants grown in soil.** Scale bar = 2 cm

fourth intron (Figure 3.5A). Seeds of that line (SALK_094451.35.55.x) and of another one with the T-DNA insert predicted to be in the promoter-5'UTR region (SALK_013791) of the *PTI1-8* gene were ordered for further analysis (Figure 3.5B). PCR genotyping was carried out to identify individual plants homozygous for the insert. As the T-DNA insert in both insertional lines was predicted to map to non-coding regions of the *PTI1-8* gene, there was a possibility it may not disrupt the activity of the gene. To test this, *PTI1-8* transcript levels in homozygous plants of each line were compared to those in WT (Col-0) plants using quantitative real-time PCR (Figure 3.6). In SALK line (SALK_013791) where the T-DNA insertion was predicted to be in the promoter:5'UTR border, *PTI1-8* transcript levels were similar to the level in WT. In contrast, there was an approximately 40% reduction in *PTI1-8* expression levels in the other SALK line (094451.35.55.x) where the insertion mapped to the 4th intron. Although the intronic T-DNA would most likely be removed by splicing, the reduced *PTI1-8* expression level suggested some interference with the transcriptional efficiency, complicating the interpretation of functional studies of that line. I therefore decided to switch to an alternative approach and use RNA interference mediated gene silencing to down- regulate *PTI1-8* and study its function.

### 3.3.5 Constitutive RNAi silencing of *PTI1-8* appears to be lethal

The pHELLSGATE12 binary vector directs RNAi silencing in plants using hairpin RNA (hpRNA) to specifically knockdown a gene of interest (Helliwell and Waterhouse, 2003). In choosing an appropriate target region for *PTI1-8* silencing, sequence specificity of the encoding hpRNA was analysed using the dsCheck (http://dscheck.rnai.jp/) and siRNA scan tools

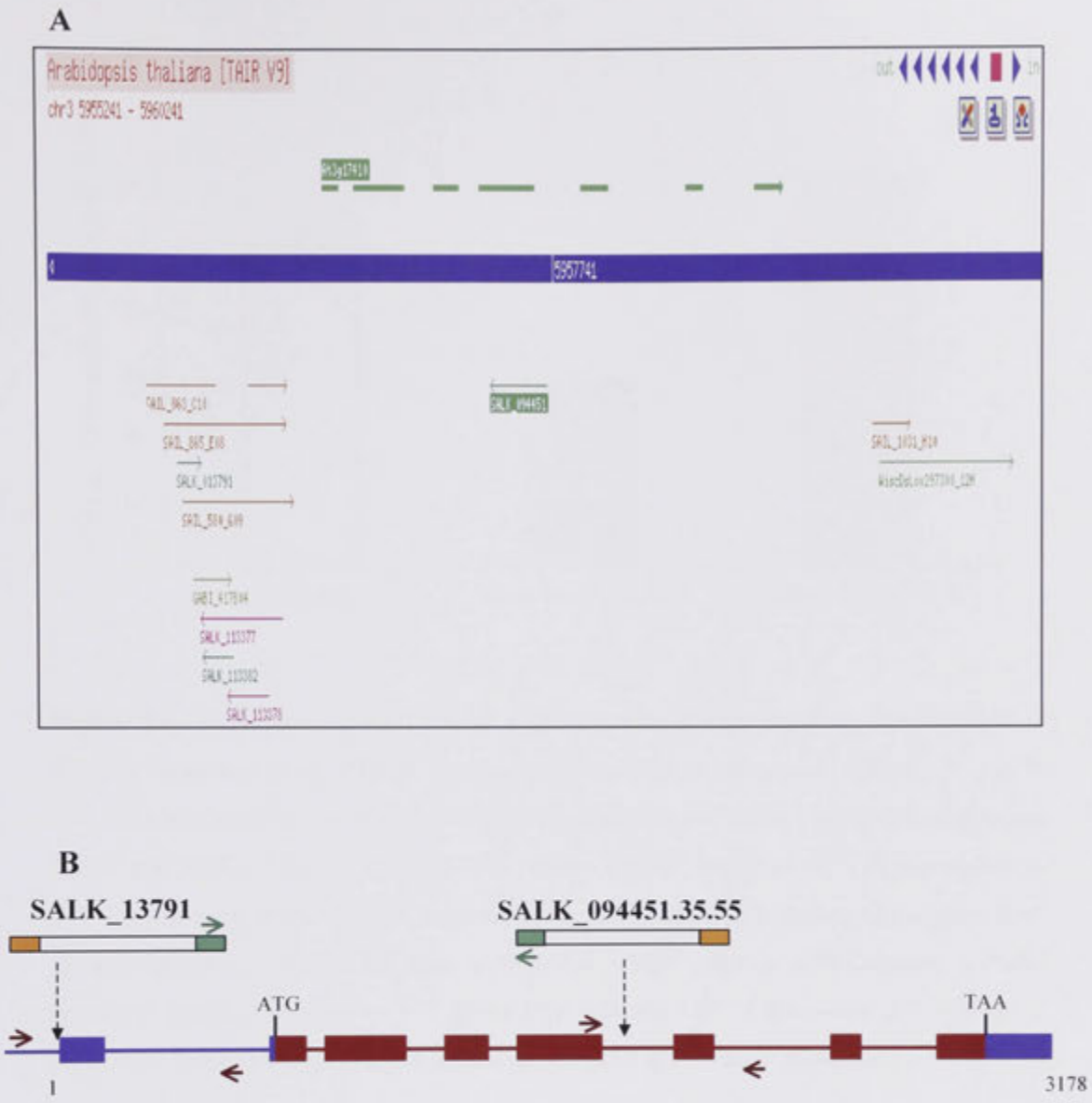


**Figure 3.5 (A,B). T-DNA insertion lines for *PTI1-8*.** Screen capture of the window provided by the T-DNA express tool available at the SIGnAL website, showing genomic locus of *PTI1-8* gene (At3g17410) (Exons are represented by dashed green lines). Arrows indicate the positions of the 11 FST's corresponding to T-DNA's insertions in non-coding or intronic regions of the gene (A) Genomic locus of *PTI1-8* and position of two SALK lines chosen for further analysis (B). Start and stops codons are labelled. Predicted location of T-DNA insertions are indicated with dashed arrows. PCR genotyping using T-DNA primers (Green arrow) and/or gene specific primers (Brown arrow).

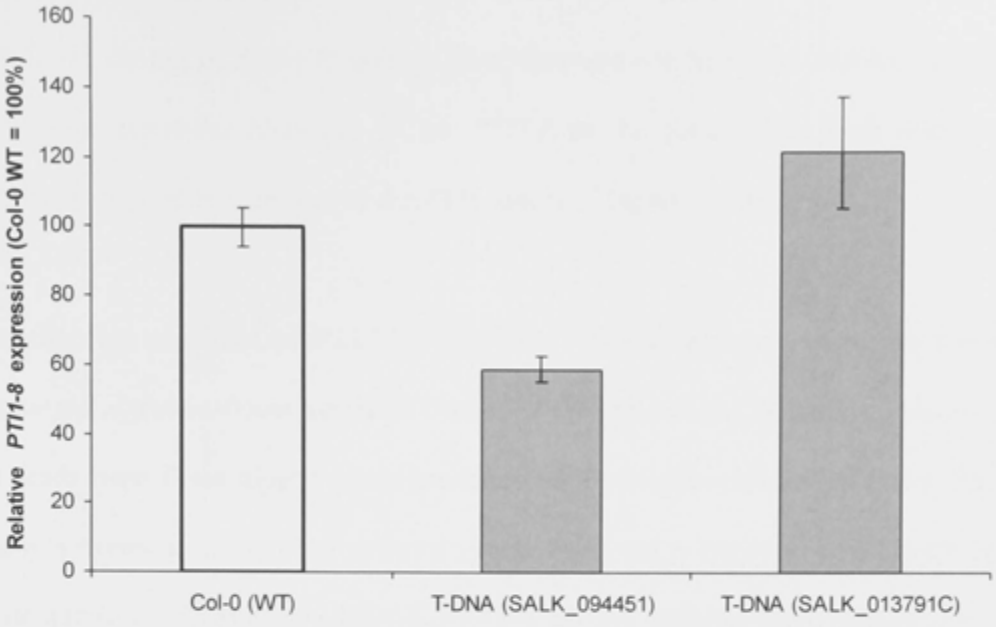


**Figure 3.6. Analysis by qRT-PCR of *PTI1-8* residual expression in the two SALK T-DNA insertion lines**. *PTI1-8* expression in mutants is expressed relative to that in WT (Col-0, white bar), after normalisation to expression of control house-keeping genes *PDF2* and *APT1*. Line SALK_013791C shows similar levels of *PTI1-8* expression to WT suggesting that the T-DNA inserted in the promoter/5'UTR region of the gene does not disrupt transcription of the gene. Line SALK_094451 shows 40% decrease in *PTI-8* transcript levels compared to WT. Error bars indicate ±SE of the mean of 3 biological replicates. Each replicate is a pooled sample of 8-10 seven day old seedlings.

(http://bioinfo2.noble.org/RNAiScan.htm) (Naito *et al.*, 2005; Xu *et al.*, 2006) which aids in the design of RNAi fragments (See Materials and Methods, section 3.2.6.1). This is of particular relevance to the *PTI1-8* as the gene shares high sequence similarity with other members of the *PTI1* family (Chapter 2, Figure 2.4).

The silencing construct, *pHELLPTI1-8* (Figure 3.7A,B) was transformed into Col-0 plants via *Agrobacterium*-mediated floral-dip transformation. Strikingly, however, T0 seeds from floral dipped plants produced no kanamycin resistant progeny. This inability to rescue any positive primary transformant was unexpected as the floral dip technique is a well-established protocol in the lab and transformation efficiencies in the range of 0.1% to 0.5 % are routinely observed. The sample size did not seem to be an issue as approximately 2000 seeds from 10 individual pots containing 4 plants each, were screened. Similar, negative results were obtained from a second round of transformation, on a batch of plants grown alongside others that were successfully transformed with another vector (pOpOff2, see below). The inability to recover primary transformants with constitutive expression of pHellsgate12 vector, together with the unavailability of *pt1i-8* T-DNA insertion mutants across several *Arabidopsis* insertional mutant collections indicated that *PTI1-8* loss of function may cause a gametophytic or early sporophytic lethal phenotype.

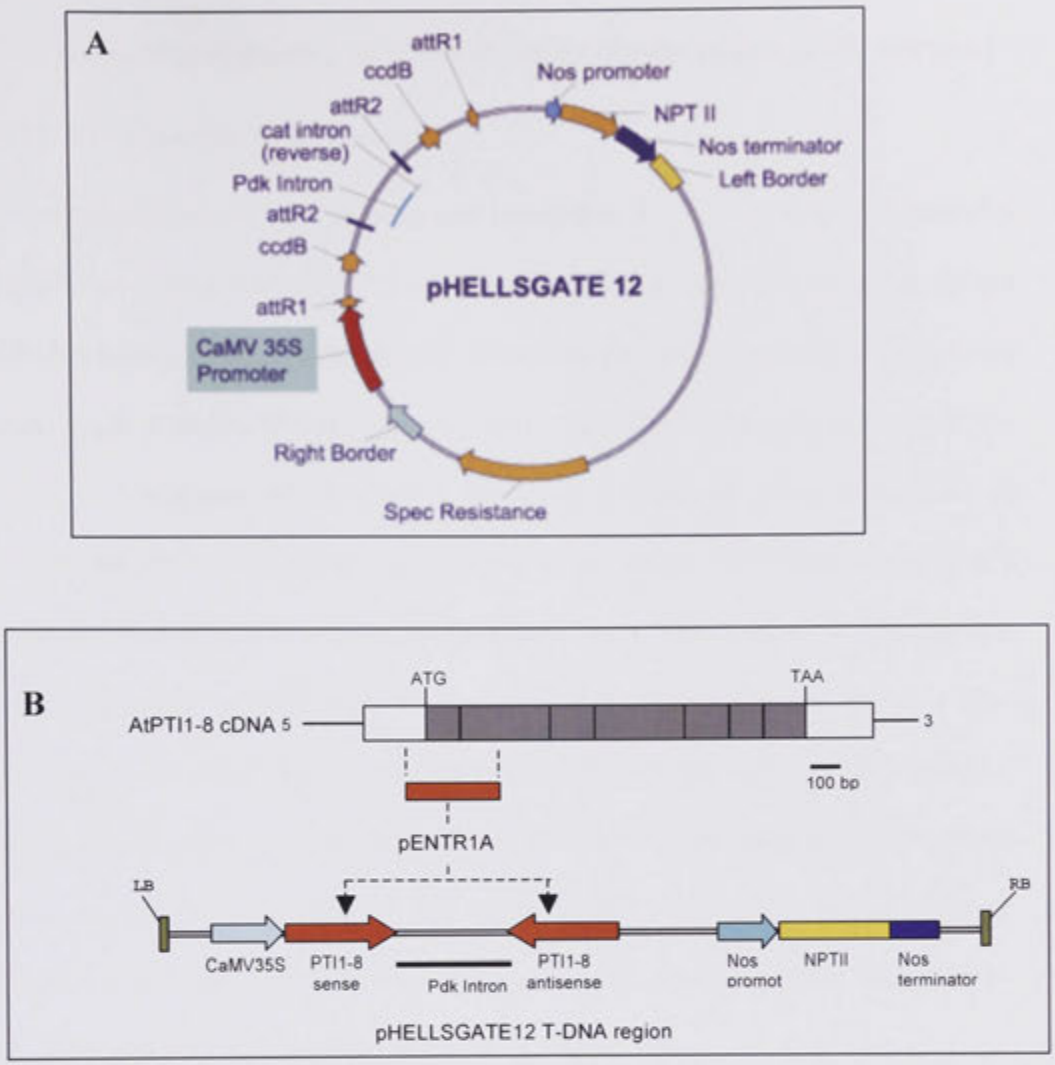


**Figure 3.7 (A,B): Cloning strategy for generating the PTI1-8 RNAi construct.** Schematic of pHELLSGATE12 vector (Helliwell and Waterhouse, 2003) (http://www.pi.csiro.au/RNAi/vectors.htm) Amplified *PTI1-8* RNAi fragment was first restriction cloned into the pENTR1A vector and inserted between the attR1 and attR2 sites and then recombined with the pHELLSGATE12 vector using the LR Gateway reaction (B). Transformation of the final RNAi construct into WT (Col-0) plants allowed for the production of hairpin RNA to mediate sequence specific degradation of the *PTI1-8* mRNA.

### 3.3.6 Inducible silencing of *PTI1-8* yields viable plants with reduced *PTI1-8* transcript abundance

In order to circumvent this problem and investigate *PTI1-8* function, an alternative approach was taken where the *PTI1-8* silencing construct would be under the control of an inducible promoter rather than a constitutive promoter, such as the Cauliflower mosaic virus (CaMV) 35S promoter in pHELLSGATE12. The pOpOff2 vector was chosen as it was successfully used to transiently knockdown genes in *Arabidopsis* (Reddy and Meyerowitz, 2005; Wielopolska *et al.*, 2005). This vector consists of a constitutively expressed synthetic transcription factor, LhG4 which in the presence of an exogenously supplied steroid hormone, dexamethasone (Dex), is able to bind to and activate the pOp6 promoter (Craft *et al.*, 2005). When activated this promoter drives the transcription of the pHELLSGATE12 hpRNA encoding silencing cassette and thus mediates silencing of the target gene. The *PTI1-8* RNAi fragment introduced into the pOpOff2 construct was cloned from the same entry vector previously used for the constitutive silencing (Figure 3.8).

Twenty-one pOpPTI1-8 transgenic plants were identified that were kanamycin resistant, out of approximately 2000 T0 seeds screened, as opposed to none from the progeny of plants transformed at the same time with the pHELLSGATE12 vector.

### 3.3.7 Dexamethasone treatment induces high levels of *PTI1-8* silencing

As the RNAi effect is dominant for the gene of interest, primary transformants can be used for initial evaluation of silencing levels and gross developmental phenotypes. The Dex-inducible silencing approach to down-regulate gene expression is a

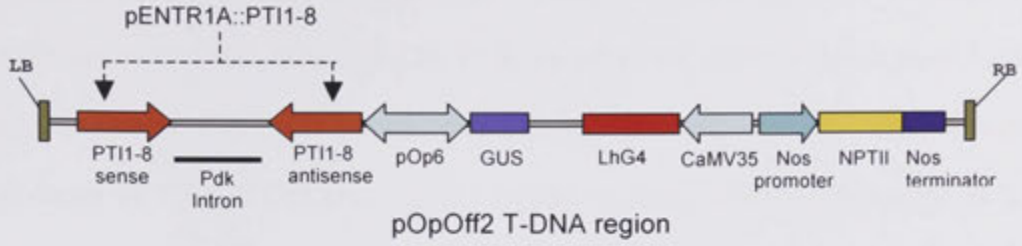


**Figure 3.8. Schematic diagram of the inducible silencing construct (pOpOff2:PTI1-8).** The pENTR1A:PTI1-8 vector used previously as a cloning intermediate for generating the constitutive silencing vector pHELLSGATE12:PTI1-8 (Fig 3.2) was used for Gateway cloning of the RNAi fragment into pOpOff2 vector (Wielopolska et al., 2005). Once this vector was transformed into Col-0, silencing of the *PTI1-8* target gene was achieved by application of the steroid hormone dexamethasone. In the presence of dexamethasone, the constitutively expressed transcription factor LhG4 binds to the inducible promoter pOp6, which in turn activates the transcription of the silencing cassette.

relatively new technique, emphasising the importance of testing its efficacy before proceeding to the isolation of single-insert homozygous lines for in-depth functional analysis. To that end, each of the 21 T1 independent transgenic plants rescued from antibiotic screening was treated with Dex to compare levels of Dex-induced silencing of *PTI1-8*. Dex was applied locally on selected mature leaves so as to minimise potential deleterious effects of *PTI1-8* silencing at the whole plant level. Leaves were painted with 20 μM Dex solution as described by Craft *et al* (2005) (details in Materials and Methods) and harvested 24 hours later. The distal end was used for RNA isolation and the proximal end for GUS staining. The pOpOff2 construct also contains the GUS reporter gene which is activated by the bi-directional pOp6 promoter that also drives the hpRNA silencing cassette. Previous reports have established that GUS activity does correlate quantitatively with silencing levels of the gene of interest (Craft *et al*., 2005; Wielopolska *et al*., 2005). Therefore GUS expression is seen as a visual marker for prescreening of primary of transformants.

All leaves except in one line, showed strong GUS staining, of variable intensity however (Figure 3.9A), indicating activation of the pOp6 promoter. *PTI1-8* transcript abundance varied from 100% to 5% of that in wild-type (Figure 3.9B). The reliability of inducible silencing constructs to consistently express the hpRNA over successive generations has not been demonstrated unequivocally (Moore *et al*., 2006). A subset of T1 plants covering the entire range of *PTI1-8* silencing levels depicted in Figure 3.9B was therefore chosen for propagation through two generations and selection of single-insert homozygous lines.

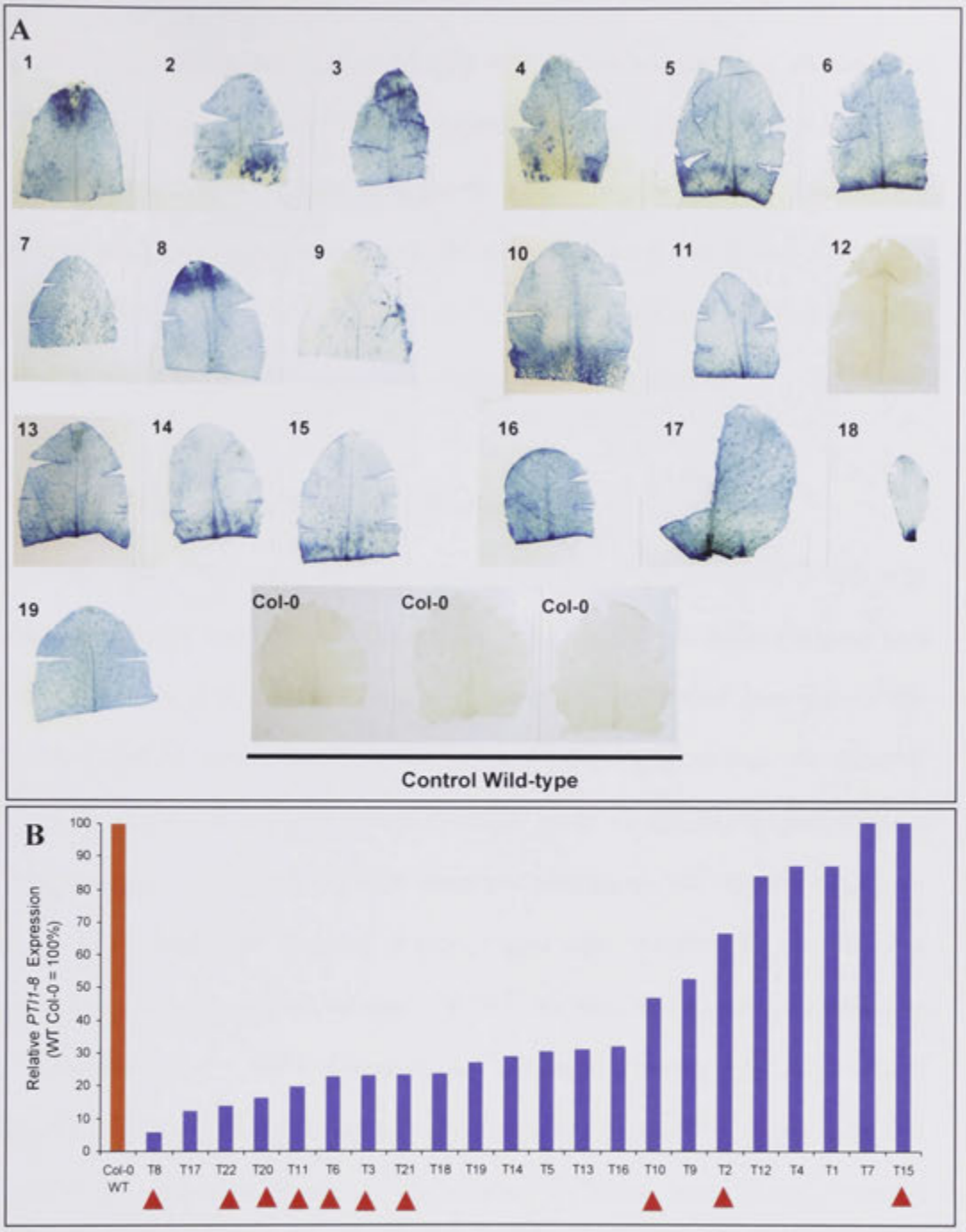


**Figure 3.9 (A,B): *PTI1-8* gene expression in inRNAi *PTI1-8* (pOpOff2) T1 transformants**. Rosette leaf of 4 week old T1 transgenic plant was painted with 20 µM Dexamethasone and 24 hours later were cut transversely into two halves. The proximal end of the leaf was used for GUS staining as a visual marker of the inducible construct activation (A). The distal end was used for qRT-PCR analysis of the levels of *PTI1-8* silencing. *PTI1-8* expression is expressed relative to that in an untransformed wild-type Col-0 plant (B). Red arrows indicate T1 transgenic plants chosen to carry through homozygosity for in-depth characterisation.

T3 seedlings were screened again by qRT-PCR to confirm effective silencing and identify highly silenced *PTI1-8* lines (inRNAi *PTI1-8*) (Figure 3.10). 5 day-old seedlings of individual T3 lines were transferred to Hoagland's media supplemented with 20 μM Dex or equal volumes of DMSO (Dex solvent) and harvested 48 hours later for RNA isolation. Two lines (6.3 and 3.1) that showed lowest *PTI1-8* transcript levels (<5% of that in wild-type), were selected for further analysis.

### 3.3.8 Evaluation of off-target silencing

In *Arabidopsis*, *PTI1*-like genes constitute a well-conserved gene family with high sequence identity both at the nucleotide and amino acid level. Although great care was taken in the design of the *PTI1-8* RNAi construct, unintended silencing of other family members cannot simply be excluded. *PTI1-8* silencing may also directly affect the expression levels of related *PTI1*-like genes, as may be expected within a large multigene family with possible functional redundancy and interactions (Briggs *et al.*, 2006). Maximum silencing of a target gene using the pOpOff2 construct has been reported to be achieved between 6 to 24 hours after dexamethasone application (Wielopolska *et al.*, 2005). Therefore, any off-target silencing of *PTI1-8* related genes was deemed to likely occur within the same time-frame. To examine these two possibilities, transcript levels of all putative *PTI1*-like genes were measured alongside *PTI1-8* mRNA in Dex-treated and untreated seedlings of line pOpOff 6.3 (one of the two lines showing highest inducible silencing among those screened in T3 generation). Five day-old seedlings grown on Hoagland's media were transferred to identical media except for the presenceor absence of 20 μM Dex, and harvested 18h later (Figure 3.11). Consistent with transcript levels measured earlier, *PTI1-8* expression in the inRNAi line was reduced by 85% compared to that in control plants


**Figure 3.10: *PTI1-8* silencing levels in T3 transformants measured by qRT-PCR.** Five day old seedlings were transferred to Hoagland's nutrient media plates supplemented with 20 µM Dex and harvested after 48 hours for *PTI1-8* transcript measurements. Two independent T3 lines, (6.3 and 3.10) with lowest *PTI1-8* transcript level (<5% of that in wild type) were selected for further analysis

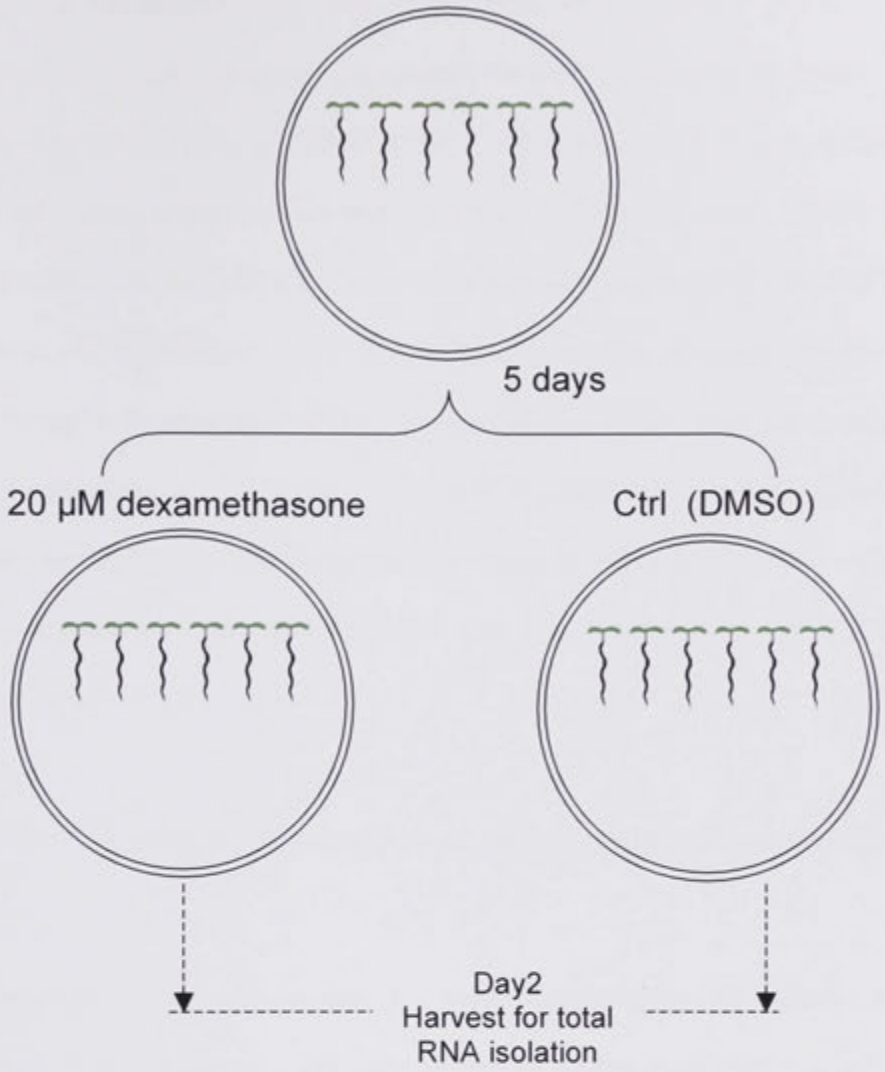


**Figure 3.11: Analysis of off-target silencing in *PTI1-8* inducible silencing lines**

T3 seeds of inRNAi *PTI1-8* line 6.3 were germinated and grown on Hoagland's media for 5 days and then transferred to medium containing 20 µM dexamethasone or 0.1% DMSO (solvent for Dex). After 2 days, seedlings from Dex supplemented and control plates were harvested for total RNA isolation and cDNA synthesis

(Figure 3.12), i.e. slightly less than in the previous experiment (95%) where measurements were taken at a later time point (48h after Dex treatment). Expression of 5 PTI1-like genes, *PTI1-4*, *PTI1-2*, *PTI1-1*, *PTI1-3* and *PTI1-7* was similar in pOpOff and corresponding control lines. For two isoforms, however, *PTI1-5* and *PTI1-6*, a mild but statistically significant, induction was observed in the pOpOff line compared to wild type (Figure 3.12). This indicates a possible compensatory role for these isoforms in the absence of *PTI1-8* or alternatively, *PTI1-8* may act directly to inhibit the expression of *PTI1-5* and *PTI1-6* in wild-type plants. Together, this result shows that the siRNA produced by the hpRNA fragment had high specificity towards mediating degradation of the *PTI1-8* mRNA and did not bind to related *PTI1*-like gene transcripts.

### 3.3.9 *PTI1-8* is a negative regulator of root elongation and meristem size

On the basis of the above results, lines 6.3 and 3.1, characterised by a similar high *PTI1-8* silencing level (Figure 3.10), were chosen for further functional studies. In a first experiment, seeds of these two lines and wild type Col-0 were germinated on vertical agar plates in the presence or absence of Dex in order to monitor root growth and investigate the role of *PTI1-8* on early seedling development. Within a week after germination, the primary root of both *inRNAi PTI1-8* lines was ~20% longer on Dex supplemented (+ Dex) plates compared to mock treated seedlings grown on no Dex (– Dex) plates (Figure 3.13 A and B). This difference could not be explained by differences in germination rates which were insensitive to Dex, in all lines (Appendix 3.6.3). The similar response observed in two independent transgenic lines suggested a causal relationship between decrease in *PTI1-8* transcript abundance and

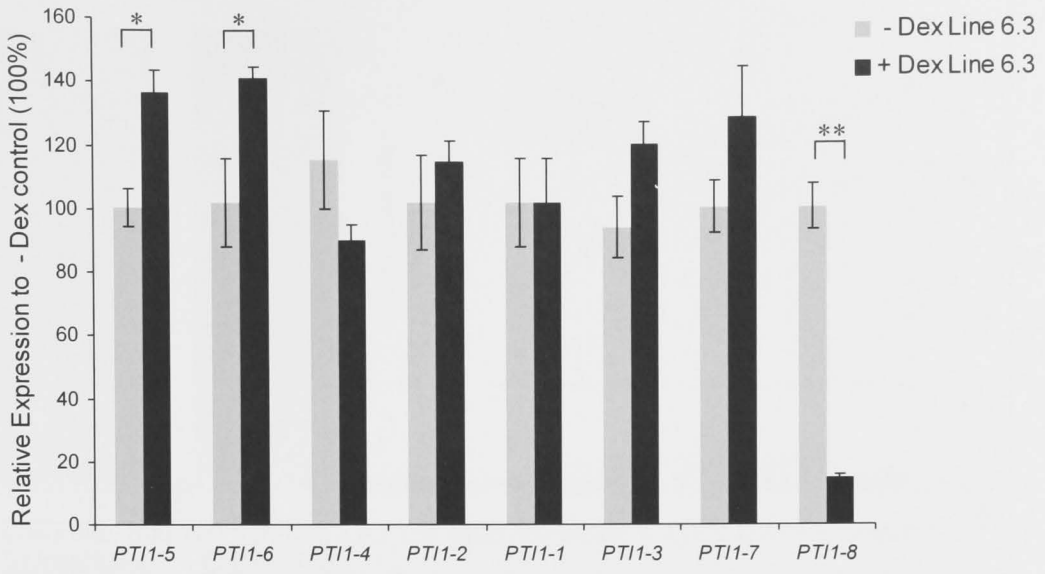


**Figure 3.12: qRT-PCR expression analysis of individual *PTI1*-like genes in Dex induced inRNAi *PTI1-8* silenced line 6.3**. Transcript levels of individual *PTI1* genes are expressed relative to expression in control seedlings (100%). Error bars represent ±SE of mean of three biological replicates. Each replicate is a pooled sample of approximately 10 whole seedlings. '*' and '**' indicates statistically significant between Dex treated and untreated seedlings (Students t-test, * $p \leq 0.05$, ** $p \leq 0.001$)

**Figure 3.13 (A-C): Enhanced root elongation rates of inRNAi *PTI1-8* silencing lines**. inRNAi *PTI1-8* silencing lines 6.3 (A) and 3.1 (B) and untransformed WT (Col-0) (C) were grown in presence (+ Dex, left-hand panels) or absence (- Dex, right-hand panels) of 20 µM dexamethasone. Representative images of two seedlings for each genotype are shown. After 8 days of growth on nutrient media, inRNAi lines growing on + Dex plates showed an increased primary root length compared to seedlings growing on – Dex plates. A time course of primary root growth for the growing period revealed a transient increase in elongation rate for Dex induced lines 6.3 (A) and 3.1 (B) between day 2 and day 3 after germination, while no change in elongation rate was observed for untransformed WT (C) seedlings. Scale bars = 2 cm

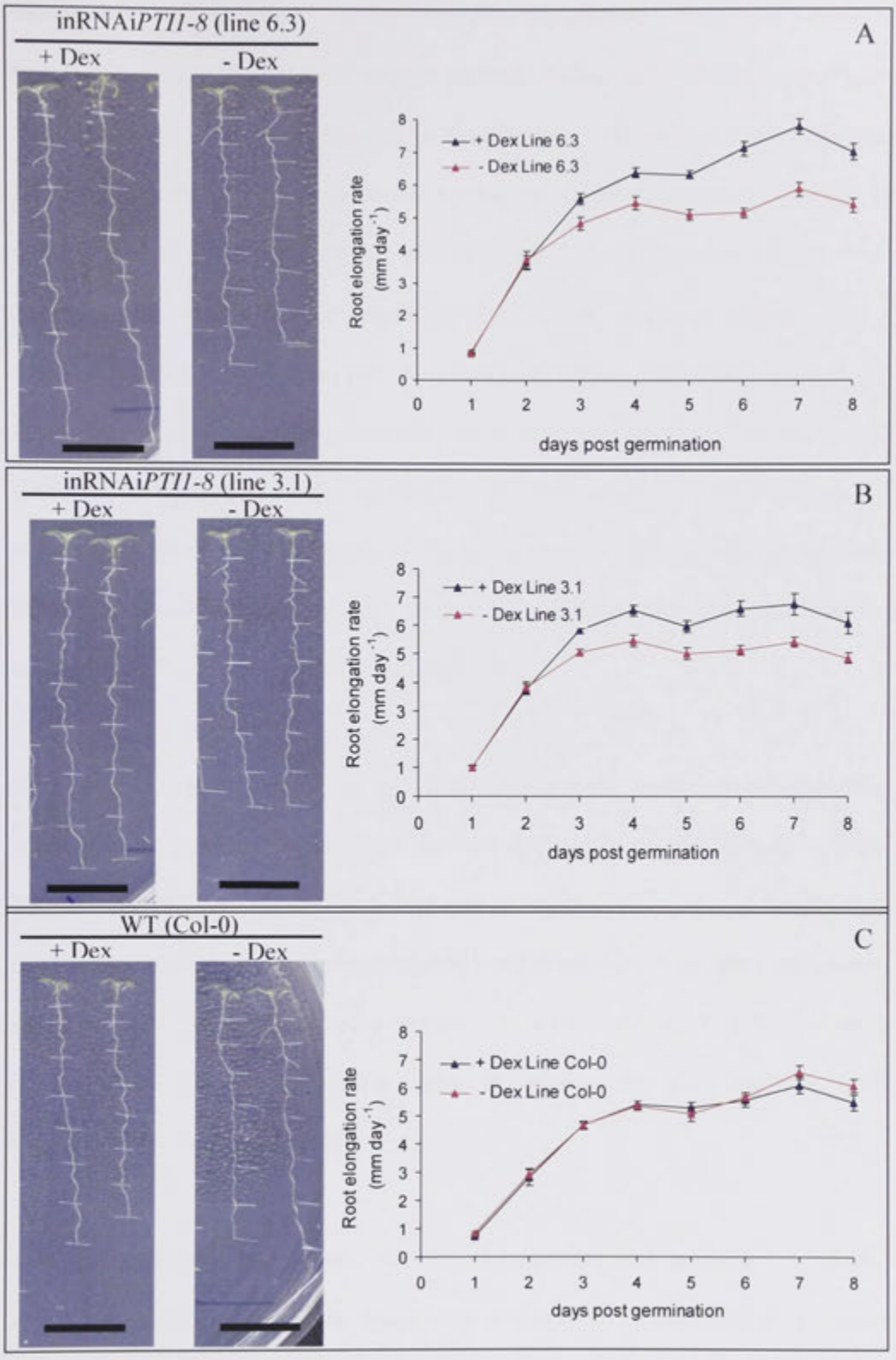
inRNAi*PTI1-8* (line 6.3)
A
+ Dex
- Dex
Root elongation rate (mm day$^{-1}$)
+ Dex Line 6.3
- Dex Line 6.3
days post germination
inRNAi*PTI1-8* (line 3.1)
B
+ Dex
- Dex
Root elongation rate (mm day$^{-1}$)
+ Dex Line 3.1
- Dex Line 3.1
days post germination
WT (Col-0)
C
+ Dex
- Dex
Root elongation rate (mm day$^{-1}$)
+ Dex Line Col-0
- Dex Line Col-0
days post germination

enhanced root elongation. Consistent with this interpretation, the primary roots of wild-type seedlings had similar lengths on both + Dex and – Dex plates (Figure 3.13C), showing that dexamethasone in itself had no influence on root elongation. The lengths of the primary roots were monitored over time to compare the kinetics of root elongation in inRNAi *PTI1-8* and WT seedlings. In the two inRNAi lines examined, the increased root lengths of Dex-treated seedlings derived from a transient increase in elongation rate, during day 2-3 after germination (Figure 3.13). Thereafter, relative root elongation rates were similar between + Dex and – Dex seedlings. These data show that, at least at these early stages, *PTI1-8* functions as a negative regulator of root elongation. There was no visually detectable change in aerial growth and development, with no apparent variation across lines in either leaf number or leaf sizes 7 days post germination (dpg).

Root elongation is determined by the cell flux through the transition and elongation zones, cellular rates of elongation and final cell lengths (Beemster and Baskin, 1998; Terpstra and Heidstra, 2009). As a first step to separate the role of these different factors, root anatomy was examined by confocal microscopy. A similar experimental set-up as described in the previous section was used where inRNAi *PTI1-8* seeds (lines 6.3 and 3.1) were plated on media with and without Dex, and roots were sampled on day 8 after germination.

All roots exhibited the classic cellular organization and anatomy of normal *Arabidopsis* roots (Figure 3.14), extensively documented in the literature (Petricka and Benfey, 2008; Perilli and Sabatini, 2010) (Figure 3.14). The root meristematic zone was, however, significantly longer in *PTI1-8* silenced seedlings (+ Dex plates)

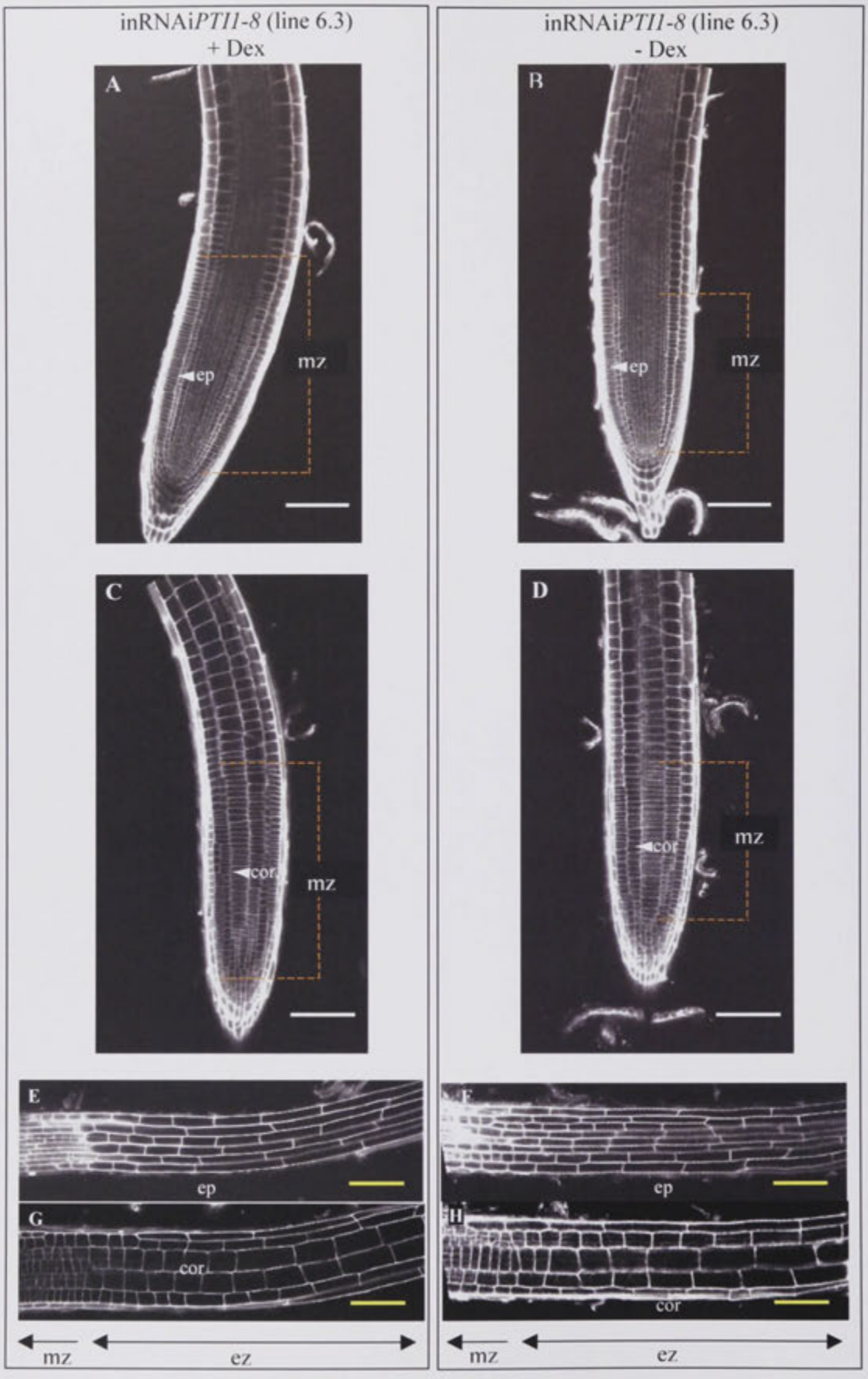
inRNAi*PTI1-8* (line 6.3)
+ Dex
inRNAi*PTI1-8* (line 6.3)
- Dex
A
B
C
D
ep
mz
cor
E
F
G
H
mz
ez

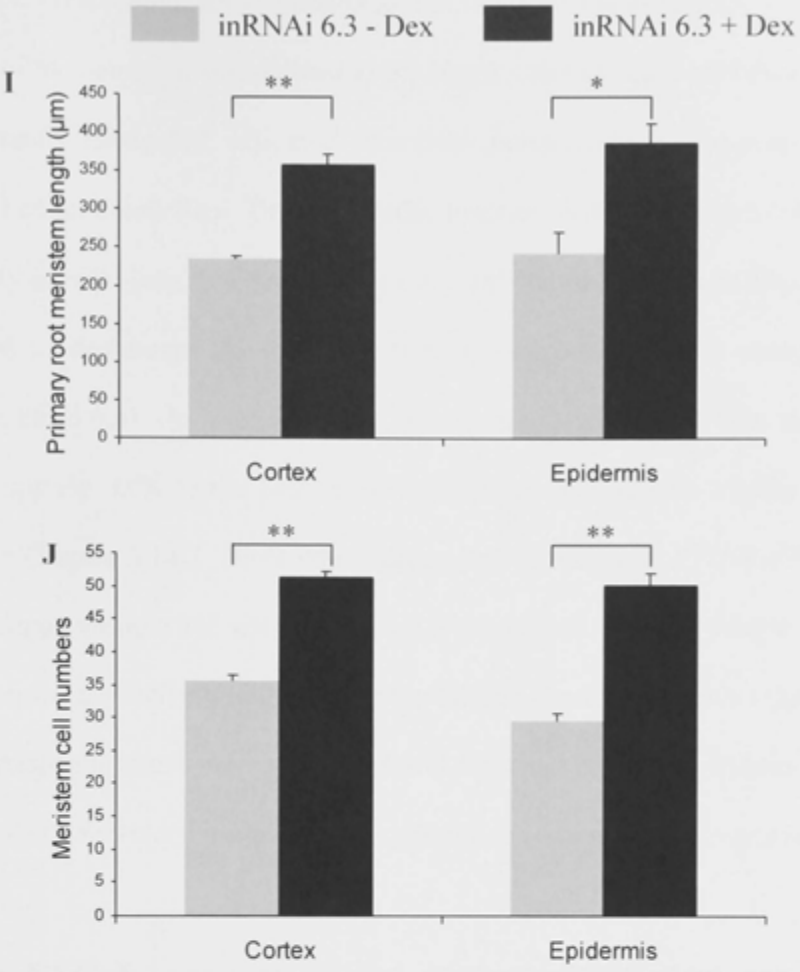


**Figure 3.14 (A-J): Root meristem size in *PTI1-8* silenced plants (+dex) compared to control plants (-dex).** Seedlings of inRNAi *PTI1-8* line, 6.3 were grown on vertical agar plates supplemented with Hoagland solution and 20 µM Dex (+) or no Dex (-).

A-D: Longitudinal optical sections of propidium iodide stained roots were captured on d8 after germination, allowing for measurements of meristematic zone (mz) lengths in the epidermal (ep) (A and B) and cortical (cor) layers (C and D) on + Dex and – Dex media (left and right panel, respectively).

E-H: Confocal images of epidermal (E and F) and cortical layers (G and H) in the elongation zone (EZ) of + dex inRNAi 6.3 and – dex inRNAi 6.3 seedlings.

I: Average length of primary root meristem in + dex inRNAi 6.3 and – dex inRNAi 6.3 seedlings. Error bars represent SE of the mean of four + Dex and four – Dex seedlings.

J: Average meristematic cell numbers in epidermal and cortical layer of the + dex inRNAi 6.3 and – dex inRNAi6.3 seedlings. * and ** indicates statistically significant (Student's t-test, * $p \leq 0.01$, ** $p \leq 0.0005$) (n = 4). White and yellow scale bars indicate 100 µm.

than in corresponding control plants grown on –Dex plates (Figure 3.14 A-D). The length of the meristem was defined as the length from the quiescent centre to the first significantly elongated cell and examined independently along epidermal and cortical cellular cell files. The plot profile function in ImageJ which measures pixel intensity over a given distance was used in combination with visual inspection which allowed to demarcate the boundary between meristematic and elongation zones (Appendix 3.6.4). In both cellular layers, meristem length was increased by approximately 35% in the Dex-induced seedlings compared to seedlings on –Dex medium (Figure 3.14I). These data indicate that silencing of *PTI1-8* affects the root meristem as a whole and not a specific cell type. Since the cells from the cortex and endodermis, collectively known as ground tissue, have a common origin known as the cortex-endodermis initial (Bennett and Scheres, 2010), the increased meristem size in *PTI1-8* silenced roots is likely to extend to the endodermal layer as well.

### 3.3.10 *PTI1-8* functions in the root meristem and regulates the number of proliferating cells

An extended meristematic zone may be the result of a higher number of proliferating cells or of an increased length of those cells, or of a concurrent increase in both of these parameters. To examine this, cortical and epidermal cell numbers within individual cell files were counted within the meristematic zone as defined above. The Dex-induced seedlings showed a 30% increase in cortical cell numbers and a 40% increase in epidermal cell numbers within the meristem compared to control seedlings (Figure 3.14J). These increases are similar in magnitude to those in total meristem size, implying that there was no significant change in the average length of meristematic cells. Direct measurements confirmed this (Table 3.3) (Student's t-test,

cortical layer p = 0.28; epidermal layer p = 0.46), indicating *PTI1-8* silencing had little effect on the volume at which meristematic cells divide, but rather affects the size of the stem cells population. Inspection of the cortical and epidermal layers in the transition and elongation zones distal to the meristem showed no detectable change in cell lengths either (Figure 3.14 E-H).

Table 3.3: Average cell length in the meristematic zone of *PTI1-8* silenced and control lines

| | Average cell length (μm) | |
|---|---|---|
| | Cortical layer | Epidermal layer |
| + Dex inRNAi6.3 | 6.99 ± 0.48 | 7.70 ± 0.99 |
| – Dex inRNAi6.3 | 6.65 ± 0.31 | 8.21 ± 1.03 |

Additional evidence of *PTI1-8* functioning in the root meristematic zone was obtained from GFP reporter studies. A translational fusion construct between the PTI1-8 protein sequence and the GFP reporter driven by the *PTI1-8* putative promoter sequence (1169 bp upstream of the start codon) was stably transformed into WT (Col-0) plants, and independent T1 transgenic lines were analysed for tissue-specific GFP fluorescence (Figure 3.15A). The fluorescence pattern of GFP was identical for all 4 independent lines, indicating it reflects correct *PTI1-8* promoter driven expression and had no positional artifacts. Seedlings harbouring the transgene showed a distinct fluorescence pattern in the root tip, compared to control seedlings with constitutive GFP expression (Figure 3.15B-E compared to 3.15F). The whole root meristem, from the quiescent centre to the elongation zone, showed strong GFP expression while there was no fluorescence beyond, contrary to control seedlings.

**Figure 3.15(A-F): genPTI1-8GFP reporter expression in meristematic zone 8 day old primary roots**

Schematic diagram of genPTI1-8GFP reporter construct based on pMDC vector (Curtis and Grossniklaus, 2003) (A). Four Independent T1 transgenic lines harbouring a translational fusion construct between *PTI1-8* and GFP driven by *PTI1-8* putative promoter (B-E). A line constitutively expressing 35S driven GFP was used as a control (F). In panels B-F, the frame on the left represents DIC photograph, the middle frame shows GFP fluorescence, and the right hand side frame is a composite image of bright field and fluorescence. Scale bars = 100 μm.

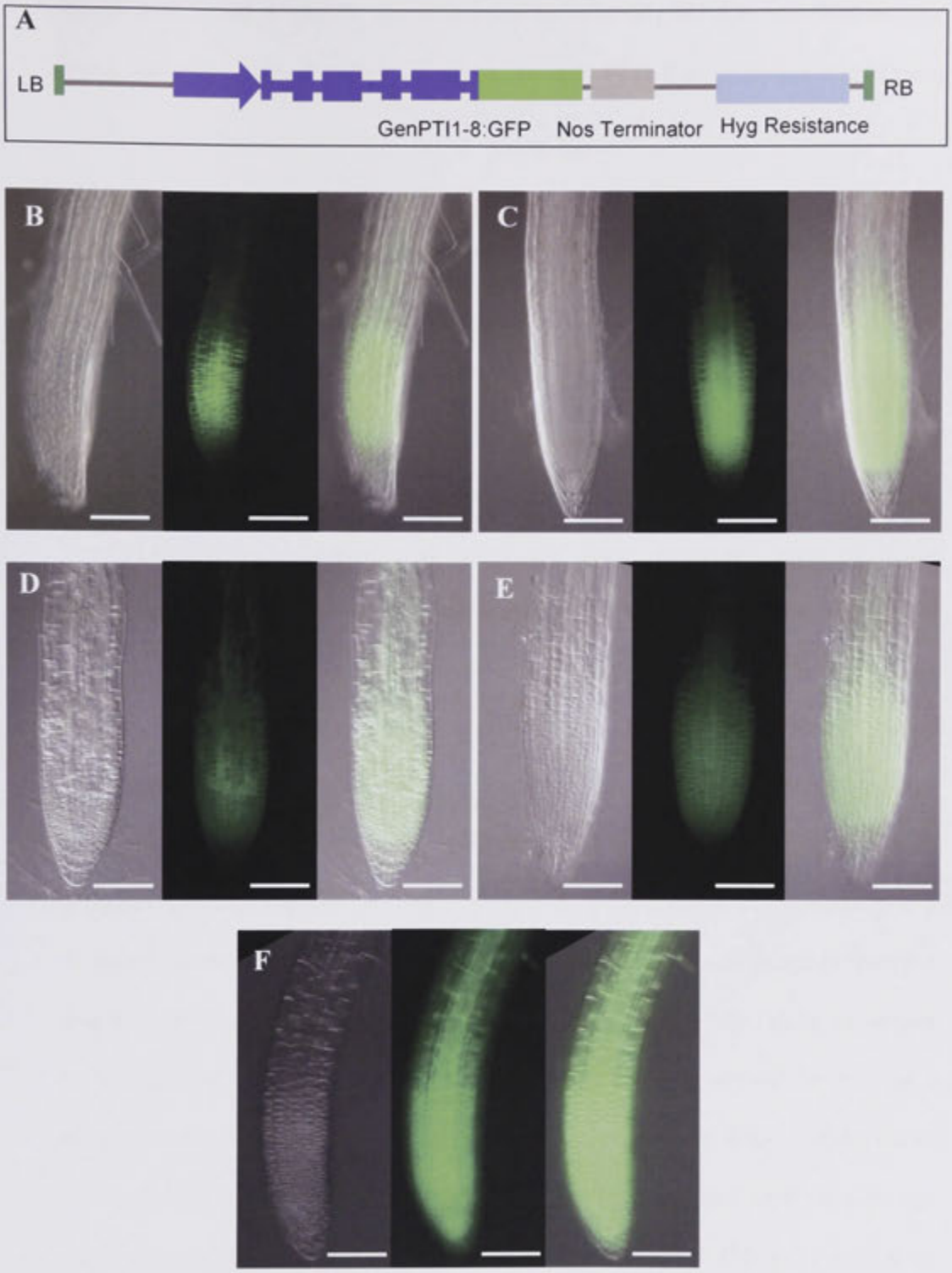
A
LB
RB
GenPTI1-8:GFP
Nos Terminator
Hyg Resistance
B
C
D
E
F

These data reveal a specific transcriptional activity of *PTI1-8* in the meristematic zone, and are consistent with the specific effect of *PTI1-8* on meristem size (Figure 3.14).

### 3.3.11 *PTI1-8* silencing induces earlier floral induction

At the seedling stage, the enhanced growth rate in the inRNAi lines appeared to be limited to the root; no difference in leaf number and size was apparent compared to wild-type. Intriguingly, however, analysis of endogenous *PTI1-8* transcripts levels (Chapter 2) as well as microarray data available on the BAR website (http://142.150.214.117/efp/cgi-bin/efpWeb.cgi) show relatively high transcript abundance in aerial parts of young and mature plants. To determine whether *PTI1-8* silencing may affect shoot development at later stages, the inRNAi lines and WT controls were grown in hydroponic Hoagland solution (0.3X) (Hoaglands and Arnon, 1950) supplemented with either Dex (20 μM) or a control DMSO solvent solution (0.02 %) (Appendix 3.6.5). No differences in growth rate or overall shoot morphology were observed between inRNAi *PTI1-8* lines and WT (Appendix 3.6.5). Strikingly however, by 30 dpg, floral induction had occurred in all plants of lines 6.3 and 3.1 and 68% of those representing a third inRNAi *PTI1-8* line (22.5), as evident by young floral buds at the centre of the rosettes. At that time none of the WT Col-0 plants growing alongside showed any floral buds and they only did so 7-8 days later (37 ± 2 dpg) (Figure 3.16). The number of rosette leaves per plant on d30 was approximately the same in silenced lines (17 ± 2) and WT (16 ± 3), indicating uniform leaf appearance rates across all genotypes. Similar data were obtained from an independent experiment where the inRNAi line 6.3 and WT were grown *in vitro* in large petri dishes (145 mm diameter, 17 mm deep) (Figure 3.17) containing agar

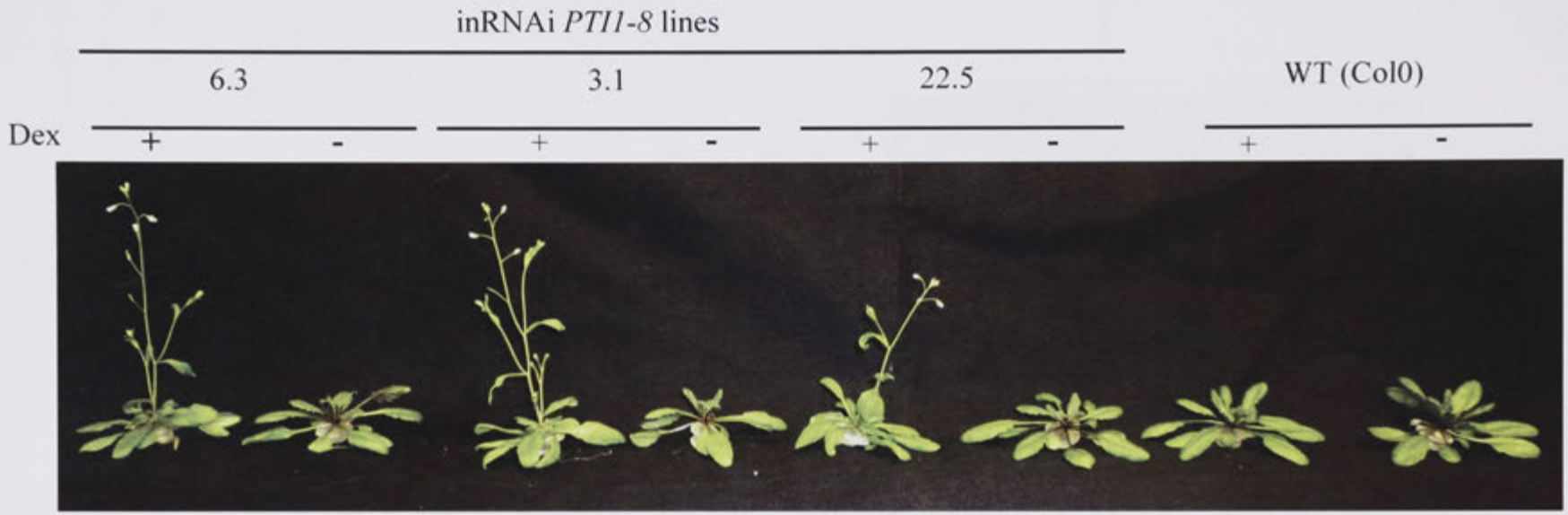


**Figure 3.16: 139.** WT (Col0) and 3 independent inRNAi *PTI1-8* lines (6.3, 3.1 and 22.5) were grown for 6 weeks under short-day conditions (10 hr photoperiod) in hydroponic solution supplemented with dexamethasone (20 μM) or with an equal volume of DMSO solvent only (0.02%). At 30 dpg, in the presence of dexmamethasone, all plants from lines 6.3 (n = 20) and 3.1 (n = 24) and 68% of plants in line 22.5 (n = 19) had started to bolt. In comparison at the same time, none of the WT (Col0) plants (n = 18) or transgenic RNAi lines growing in the absence of Dex (n = 23) had started bolting.

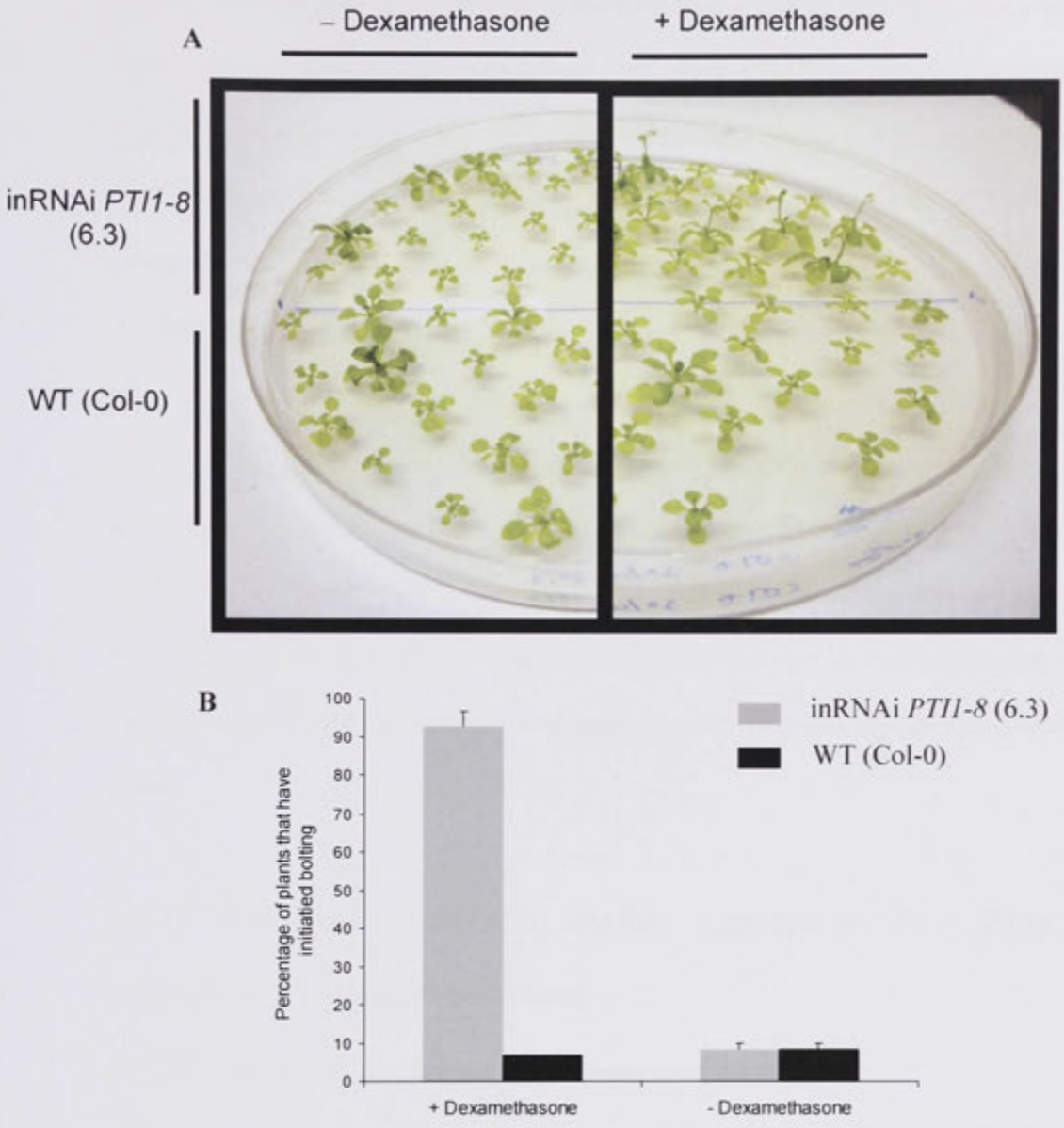


**Figure 3.17 (A,B): Early bolting phenotype of *PTI1-8* silenced plants**. inRNAi *PTI1-8* seeds (line 6.3) were germinated on Hoagland's media with (+) or without (-) 20 μM Dexamethasone. At day 25 post germination, a majority of inRNAi 6.3 plants growing in the presence of Dex clearly showed an extended primary bolt while very few plants of the corresponding control lines and untransformed wild-type had initiated bolting (A). Percentage of inRNAi6.3 and wild-type Col-0 plants growing in presence (+) or absence (-) of Dex that had a primary bolt was calculated (B). Error bars indicate SE of the 2 averages of two batches of 30 seedlings each.

media supplemented with Hoagland's solution, and no or 20 μM dexamethasone. At 25 dpg, over 90% of the Dex-treated inRNAi plants across two replicated plates clearly showed the emergence of a primary bolt (Figure 3.17). At the same time, less than 10% of wild-type plants and un-induced inRNAi plants had initiated bolting. The earlier floral induction and stem elongation seen in both greenhouse- and *in vitro* grown Dex-induced inRNAi lines suggest an involvement of *PTI1-8* in repressing the transition from vegetative to reproductive phase. In addition to autonomous genetic signals, a number of external environmental stimuli such as photoperiod, vernalization and abiotic stresses are also known to affect *Arabidopsis* flowering time (Sheldon *et al.*, 2008; Amasino, 2010). Future experiments using both genetic and physiological approaches and growth comparisons under different photoperiods and vernalization treatments are needed to elucidate the role of the *PTI1-8* gene in regulating phase transition and possibly internode elongation during the reproductive phase.

### 3.3.12 Transient expression studies demonstrate that PTI1-8 localises to the plasma membrane.

#### *3.3.12.1 In silico analysis of PTI1 protein structure*

The sequence of all PTI1-like proteins in *Arabidopsis* and other eudicot and monocot species is well conserved in the C-terminal kinase domain (Chapter 2 Figure 2.1, 2.3). The N-terminal region, however, contains variable segments that differ greatly in their amino acid sequence. Work carried out by Hermann *et al.*, (2006) showed that the N-terminal region of the maize ZmPTI1A contains sites of protein acylation, an important post-translational modification known to mediate membrane targeting (Resh, 1999). Through the use of GFP reporter constructs, the ZmPTI1A was shown

to localize to the plamsa membrane, and disruption of the conserved N-terminal sites abolished membrane targeting (Herrmann *et al.*, 2006).

To examine whether the *Arabidopsis* PTI1-like proteins shared similar membrane targeting sites the web-based tool TermiNator (http://www.isv.cnrsgif.fr/terminator3/index.html) was used to search the sequences of all 8 *Arabidopsis* PTI1 proteins for the presence of the two most common N-terminal post-translational lipid modifications associated with membrane attachment, palmitoylation and N-myristoylation (Resh, 1999). Among the 8 genes, only the PTI1-8 sequence showed the dual acylation signatures (Figure 3.18) suggesting that the protein may be membrane targeted. The palmitoylation and N-myristoylation sites specific to the *PTI1-8* protein suggest that the evolutionary path of the encoding gene may be quite distinct from that for the rest of the *Arabidopsis PTI1*-like genes, and may confer a unique non-redundant biological function.

### *3.3.12.2 Experimental evidence for PTI1-8 membrane targeting*

In order to experimentally determine the subcellular localisation of the PTI1-8 protein, GFP reporter fusion constructs (pMDC32 binary vector) (Curtis and Grossniklaus, 2003) were transiently expressed in *Nicotiana benthamiana* leaves, under the control of the constitutive 35S cauliflower mosaic virus promoter (see Materials and Methods, section 3.2.7.1).

The coding sequence of *PTI1-8* was amplified from Col-0 wild-type cDNA and translationally fused in-frame with the GFP protein to give rise to a single hybrid protein. To account for the possibility of the translational fusion resulting in incorrect

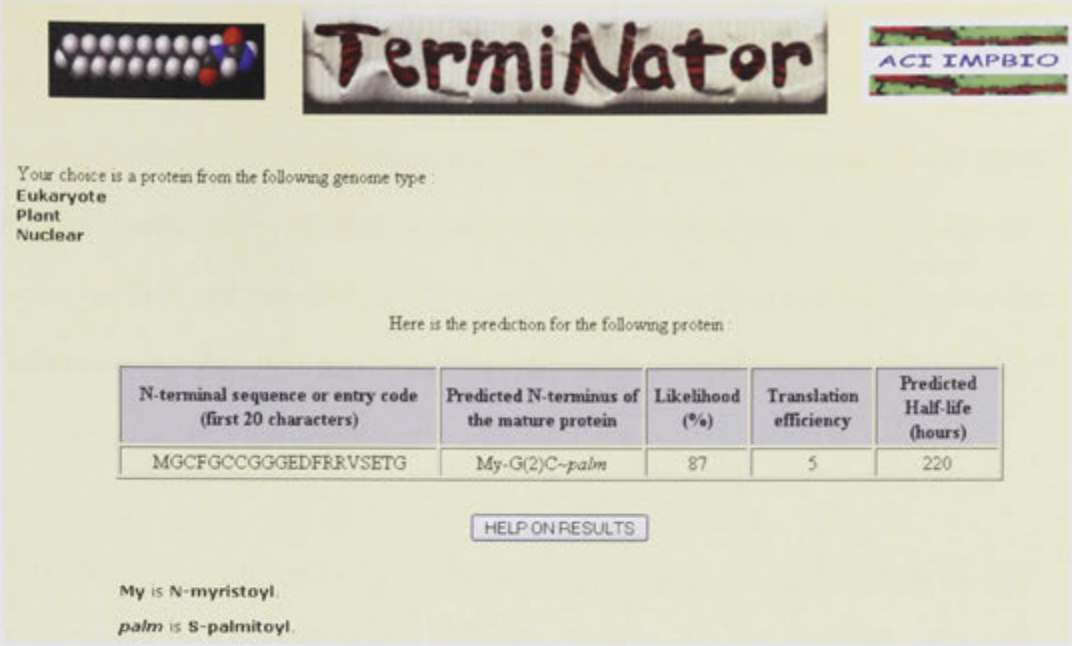


**Figure 3.18:** Screen capture of the result from the bioinformatics analysis of PTI1-8 protein sequence for conserved N-terminal sites for N myristoylation and S-palmitoylation, using the web-based tool TermiNator (http://www.isv.cnrs-gif.fr/terminator3/index.html)

folding of the hybrid protein, two separate constructs with GFP cloned either at N-terminal (GFP:PTI1-8) or C-terminal (PTI1-8:GFP) end of the *PTI1-8* sequence were made. A 35S:GFP construct expressing GFP constitutively was used as a positive control (Figure 3.19). All three constructs were introduced into the *Agrobacterium* strain GV3101 and transiently transformed into leaves of *Nicotiana benthamiana* via infiltration of the two halves of the leaf with 35S:GFP and 35S:PTI1-8GFP constructs, respectively (Appendix 3.6.6).

Two days after infiltration leaf sections were analysed for visualization of GFP fluorescence to ensure that the infiltration had been successful. No difference between sectors infiltrated with the PTI1-8GFP fusion construct and the control 35S:GFP construct was observed. Normal *Agrobacterium* associated chlorosis was seen in all infiltrated areas, regardless of the construct tested (Appendix 3.6.6).

Epifluorescence microscopy of leaf sections cut out of infiltrated leaf lamina showed that the 35S:PTI1-8GFP was only targeted to the cell margin (Figure 3.20, A1-A3) suggesting that the PTI1-8 protein localised to the plasma membrane. No fluorescence signal was detected in the nucleus. A very different pattern was observed for cells transformed with the control 35S:GFP construct where fluorescence was visible both at the cell periphery and in the nucleus (Figure 3.20, B1-B3), a pattern typical of constitutive GFP expression.

The above results were obtained with leaves infiltrated with the C-terminal fusion construct. Interestingly, no florescence was detected in leaves transformed with the

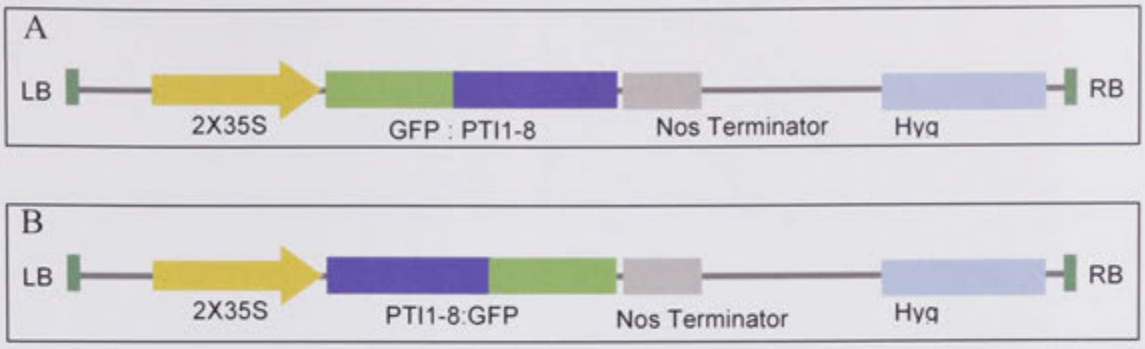


**Figure 3.19: Schematic diagram of reporter constructs for N- and C- terminal (A and B, respectively) fusions of PTI1-8 to GFP**. Both constructs were designed using Mark Curtis pMDC vectors (N-terminal fusion-pMDC44 and C-terminal fusion-pMDC84) (Curtis and Grossniklaus, 2003). *PTI1-8* cDNA was amplified and fused in frame with the GFP reporter gene. For the C-terminal fusion of *PTI1-8* to GFP, the stop codon of *PTI1-8* was removed to allow translational read-through of the protein.

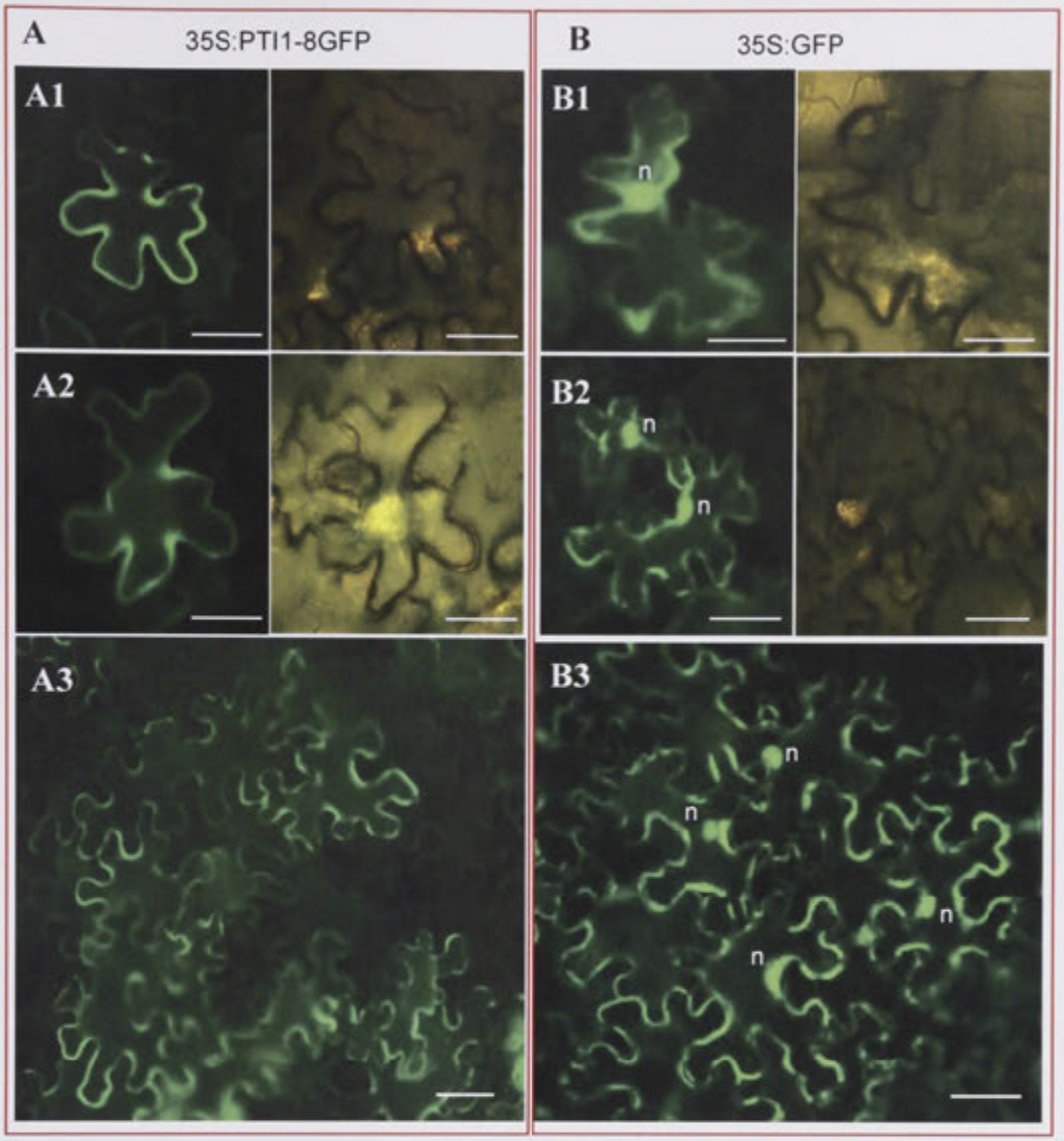


**Figure 3.20 (A and B): Subcellular localization of the PTI1-8GFP fusion protein in Tobacco epidermal cells**. The *PTI1-8* coding sequence fused to GFP (35S:PTI1-8GFP, pMDC84) under the control of the 35S promoter was transiently expressed in *Nicotiana benthamiana* using the Agroinfiltration technique and viewed using epifluorescence microscopy. Expression of 35:SPTI1-8GFP, showed fluorescence pattern mainly towards the cell periphery (A1-A2 high magnification [left panel-GFP fluorescence, right panel-Bright field], A3 low magnification) and no florescence in the nucleus, indicative of membrane localisation. The 35S:GFP showed fluorescence at the cell periphery as well as in the nucleus (n) (A1-A2 high magnification [left panel-GFP fluorescence, right panel-Bright field], A3 low magnification), which is characteristic fluorescence pattern for 35S driven GFP. Scale bar = 50 μm.

N-terminal 35S:GFPPTI1-8 construct (data not shown). The transformation was repeated a number of times, with similar results although sequencing confirmed that the coding sequence was in frame. The lack of GFP fluorescence with this N-terminal fusion construct therefore suggests that correct folding of the PTI1-8 protein may be dependent on post-translational modification requiring a free N-terminal end. This assumption gains support from the identification of the putative N-terminal acylation sites mentioned earlier, which are likely to be targeted for modification of the PTI1-8 protein. The complete absence of GFP fluorescence as opposed to mis-targeting suggests one of two possibilities: either the fusion to the N-terminal end led to improper folding of the GFP protein leading to the loss of fluorescence or a free N-terminus of the PTI1-8 protein is vital for its correct function without which the protein may be targeted for premature degradation.

To further demonstrate PTI1-8 association to the plasma membrane, *Nicotiana benthamiana* leaves were infiltrated with either the 35S:PTI1-8GFP or 35S:GFP constructs and 2 days later were treated with 0.8 M mannitol. Incubation with such high concentration of this osmoticum causes plasmolysis i.e. separation of the plasma membrane from the cell wall. As the membrane gets detached a fluorescently labelled plasma membrane will appear as a thin bright line, clearly separate from the cell wall (Takeda *et al.*, 2008; Sasaki *et al.*, 2010). This is what was observed in the plasmolysed cells expressing 35S:PTI1-8GFP, in both epidermal and mesophyll cells (Figure 3.21, A1-3). In comparison, in plasmolysed cells expressing 35S:GFP, fluorescence was very strong in the nucleus and in the cytoplasm surrounding chloroplasts (Figure 3.21, B1-3). This is especially evident from the fluorescence pattern observed in the mesophyll cells which contain a large number of chloroplasts

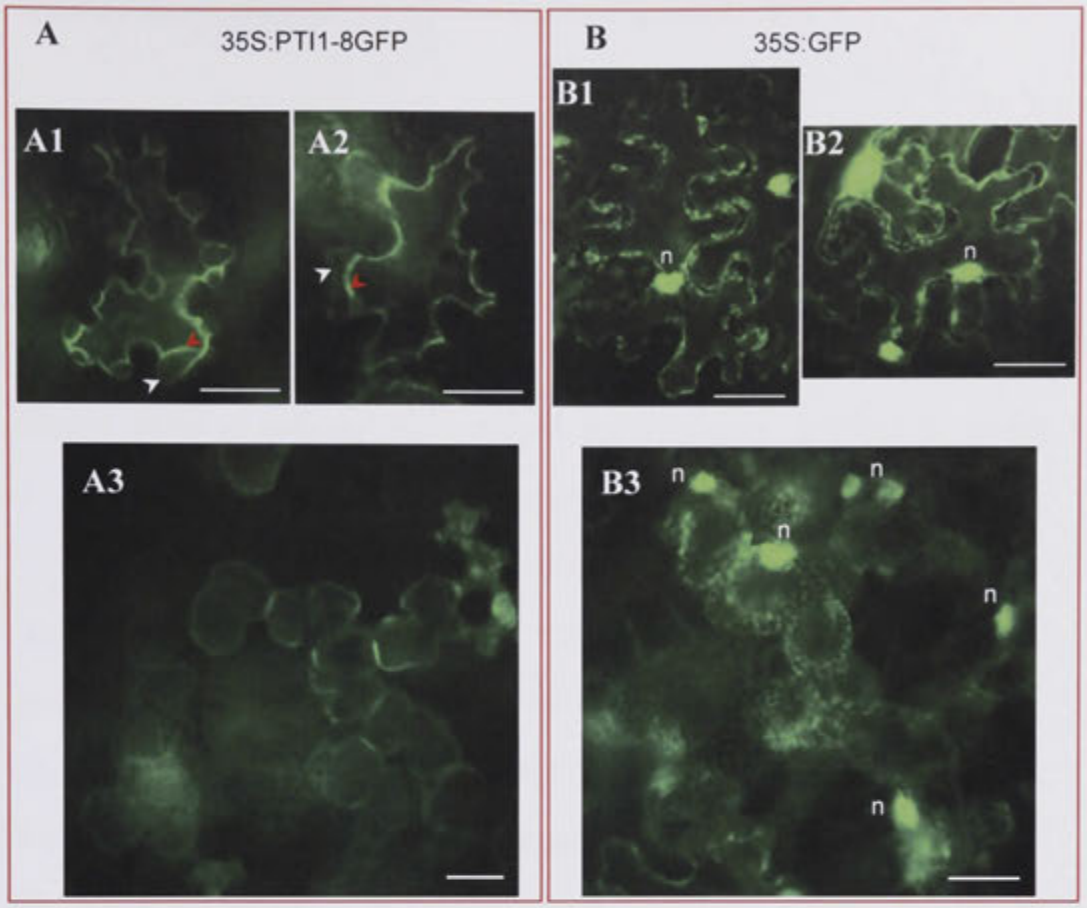


**Figure 3.21 (A, B): Plasmolysis of PTI1-8GFP expressing cells to demonstrate plasma membrane localisation.** Tobacco transiently expressing the 35S:PTI1-8GFP (A) and 35S:GFP (B) construct were plasmolysed using 0.8 M mannitol prior to viewing with an epifluorescent microscope. In the epidermal cells, 35S:PTI1-8GFP fluorescence was localised to the plasma membrane (red arrows) shown here as being detached from the cell wall (white arrows) as a result of mannitol-induced plasmolysis (A1-2). The 35S:GFP fluorescence is visible in the nucleus and cytosolic regions surrounding the chloroplasts (B1-2). In the mesophyll of control cells transformed with the 35S:GFP construct, fluorescence appeared as a reticulated pattern due to the large number of chloroplasts in these cells, in contrast to the smooth fluorescence pattern in cells expressing 35S:PTI1-8GFP. Scale bar = 50 μm.

making it appear as a diffuse reticulated pattern (Figure 3.21, B3).

As further confirmation of PTI1-8's subcellular localisation and to test for the possibility that the strong overexpression from the 35S promoter might cause mistargeting of the PTI1-8 protein, *Nicotiana benthamiana* leaves were agro-infiltrated with the PTI1-8GFP construct under the control of the native *PTI1-8* putative promoter sequence (the construct was previously described in section 3.3.10, Figure 3.15) (genPTI1-8GFP). Leaf cells transiently expressing this construct only showed a very faint GFP signal under epifluorescence microscopy, which probably reflects the weak activity of the *PTI1-8* promoter in *Nicotiana benthamiana* (data not shown). To overcome this, samples were observed by confocal microscopy that is more sensitive and allows for reliable detection of low fluorescence signals. Results were similar to those previously obtained with the 35S:PTI1-8GFP construct: the fluorescence signal clearly localised only to the cell plasma membrane (Figure 3.22).

Taken together, these results from GFP reporter studies suggest that the PTI1-8 protein is targeted to the plasma membrane and that this is most likely mediated by N-terminal myristoylation and/or palmitoylation.

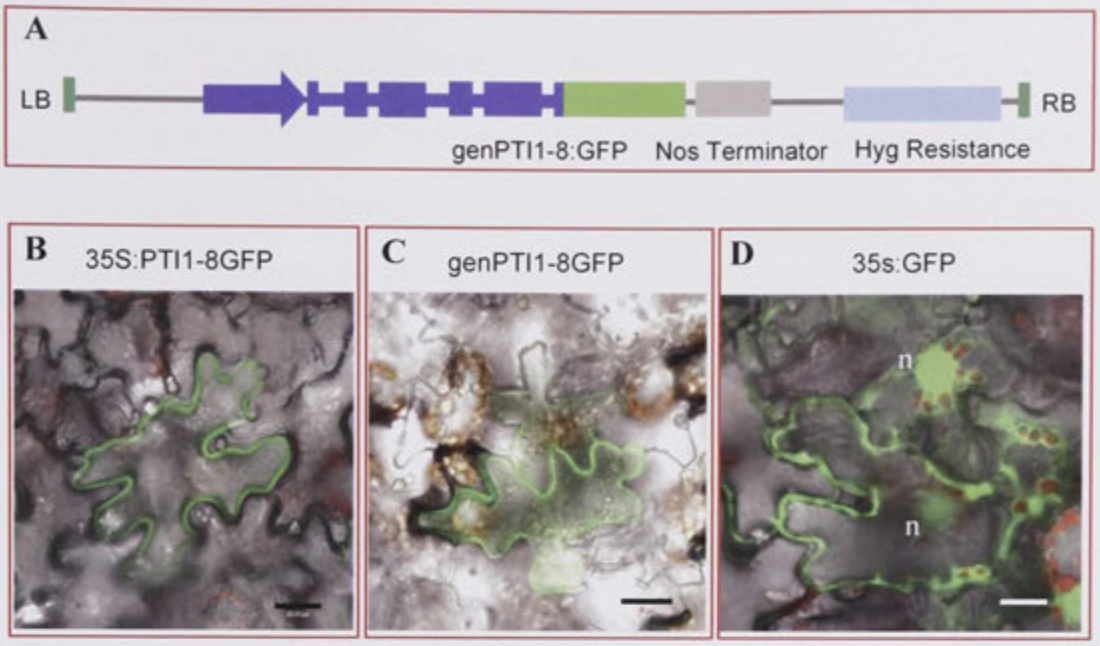


**Figure 3.22 Subcellular localisation of PTI1-8GFP under the control of 35S or PTI1-8 native promoter sequence**. Schematic diagram of the genPTI1-8GFP reporter construct (pMDC110 vector) (Curtis and Grossniklaus, 2003) (A). Tobacco leaves, transiently transformed with 35SPTI1-8:GFP (B), genPTI1-8GFP (C) and 35S:GFP (D) were viewed by confocal microscopy. The fluorescence patterns for PTI1-4GFP under the control of either 35S promoter (B) and *PTI1-8* native promoter (C) were similar, indicating plasma membrane targeting of the PTI1-8 protein. In contrast, 35S:GFP was expressed in the cytosolic region and nucleus (n, panel D). Scale bars = 20 μm.

## 3.4 Discussion

### 3.4.1 *PTI1-8* root developmental phenotype

Morphological analysis of lines with Dex-induced *PTI1-8* silencing revealed a significant increase in primary root length after 7 days of growth compared to control lines (Figure 3.13). As the germination rates on plates with and without Dex were similar, increased root length could be ascribed to a post-germinative enhancement of root elongation rate. Because the Dex-inducible system allows comparison of individual plants of the same genotype, the longer roots of seedlings exposed to Dex can be attributed to *PTI1-8* silencing. It remains to be seen, however, if *PTI1-8* exerts its function on root growth directly or indirectly. Indeed, measurements of the other *PTI1*-like gene transcripts in the *PTI1-8* silenced background revealed an increased expression of two isoforms, *PTI1-5* and *PTI1-6*. It is therefore possible that rather than acting directly, *PTI1-8* may be act by negatively regulating these two *PTI1* isoforms and that it is the slight overexpression of these two genes that may cause the elongated root phenotype observed in the inRNAi *PTI1-8* lines. Analysis of T-DNA knockout lines for *PTI1-5* and *PTI1-6* suggests that this is however unlikely, as they showed no difference in root growth (Figure 3.4). Consistent with this, a stably transformed 35S promoter driven over-expression line for *PTI1*-5 that was recently generated in the lab, also showed no discernable change in root length compared to wild-type (data not shown). This indicates that the root developmental phenotype seen in the inRNAi *PTI1-8* line is likely due to the silencing of *PTI1-8* itself, and points to a role of PTI1-8 protein in negatively regulating root elongation. Moreover, analysis of the kinetics of the elongation process revealed that its effect takes place early, between day 2 and day 3 after germination under the growth conditions used (Figure 3.13).

Microscopic analysis of the root growth zone provided further insights and showed that the meristem of *PTI1-8* silenced primary roots was significantly longer than that of roots of control plants (Figure 3.14). This increased length was proportional to an increase in cell numbers in both epidermis and cortex cell files while the final size of these cells was unaffected. Otherwise, there was no other discernable change in root anatomy between *PTI1-8* silenced and control lines. Taken together this suggests that *PTI1-8* activity role may help to regulate the total number of undifferentiated cells in the meristem. This can theoretically be achieved in two ways: *PTI1-8* could act to repress cell production in the meristem or alternatively to promote the onset of the cell expansion. Detailed kinematic analysis of root elongation will be used to determine the specific roles of *PTI1-8* in cell division and/or cell expansion. Interestingly, in transgenic *Arabidopsis* lines harbouring the GFP reporter gene fused to the *PTI1-8* genomic locus, fluorescence appeared to be localised mainly to the meristematic region of the root (Figure 3.15). This suggests that the effect of *PTI1-8* expression on cell production rates or/and expansion may be mediated by the activity of the PTI1-8 protein in the meristem itself rather than in the elongation zone.

### 3.4.2 *PTI1-8* in context with root hormone signalling pathways

A number of studies using reverse genetic analyses have identified loss-of-function or gain-of-function modifications of genes that affect root developement and meristem activity (Benfey *et al.*, 2010). Many of these genes have been implicated in hormone signalling or biosynthesis. The interactions of several hormones, such as auxin (Terpstra and Heidstra, 2009), cytokinin (Veit, 2006), gibberellin (Ubeda-Tomas *et al.*, 2009) and ethylene (Ortega-Martinez *et al.*, 2007) are known to affect

root elongation, meristem size and function. A notable feature is that most root developmental genes in the literature, are involved in pathways that positively regulate root elongation, as shown by the shorter root and meristem length of loss-of-function mutants (Iyer-Pascuzzi *et al.*, 2009; Benfey *et al.*, 2010). Therefore, the identification in this study, of a gene that functions as a negative regulator of root elongation is a very interesting finding.

In early stages of root development, the interaction of cytokinin and auxin is known to regulate the balance between cell differentiation and cell division, respectively, and in doing so determines final meristem size (Dello Ioio *et al.*, 2008). A number of cytokinin biosynthetic mutants have been identified that are characterised by an enlarged meristem and enhanced root elongation and, conversely, exogenous treatment with cytokinin results in reduced meristem size (Dello Ioio *et al.*, 2007) through a shift towards increased cell division and decreased cell differentiation. The phenotypic similarities between the inRNAi *PTI1-8* roots described in this study and roots of cytokinin deficient mutants such as *ahk3-3*, *arr1-4*, *arr12-2* (Dello Ioio *et al.*, 2007) suggest that *PTI1-8* could be involved in positively regulating the cytokinin pathway. Alternatively, it may be that *PTI1-8* is involved in repressing the gibberellin pathway, as it was recently discovered that gibberellin antagonises cytokinin mediated cell differentiation in the first few days post-germination (Moubayidin *et al.*, 2010). Thus, a transient increase in gibberellin levels in the inRNAi *PTI1-8* could also potentially disrupt the balance between cell division and differentiation. Consistent with this hypothesis the DELLA protein, RGA, a known repressor of the gibberellin signaling pathway (Silverstone *et al.*, 1998) (Silverstone *et al.*, 1998) shows an enlarged meristem phenotype similar to the inRNAi *PTI1-8*

lines and the cytokinin biosynthetic mutants (Moubayidin *et al.*, 2010).

A possible clue on which of these two possible pathways *PTI1-8* may be involved in comes from the pleiotropic early bolting phenotype observed in inRNAi *PTI1-8* lines (Figure 3.16). Although a preliminary observation, the early bolting phenotype seen in both greenhouse and *in vitro* grown Dex-induced RNAi lines suggests *PTI1-8* may be involved in repressing SAM transition from vegetative to reproductive phase. Gibberellin has been well documented in promoting early flowering in *Arabidopsis* which fits with *PTI1-8* acting as a repressor of the gibberellin pathway (Blazquez *et al.*, 1998; Mutasa-Gottgens and Hedden, 2009).

The proposed link of *PTI1-8* with GA, or cytokinin, signalling has to be taken as a hypothesis to be rigorously tested in future work. The possibility of *PTI1-8*'s involvement in other independent pathways cannot be ruled out. For example, accumulating evidence in the last few years suggests ROS as important signaling molecules in root development (Pitzschke *et al.*, 2006; Swanson and Gilroy, 2010). Notably, a recent study has identified that a gradient of ROS species in the root tip controls transition from cell proliferation to cell differentiation (Tsukagoshi *et al.*, 2010). The bHLH transcription factor, *UPB1* was shown to regulate this ROS gradient and it is noteworthy that the *upb1* mutant and the inRNAi *PTI1-8* lines studied here have very similar phenotypes: longer roots and increased meristem length. The possibility of *PTI1-8* acting on root elongation via control on ROS gains even more support from the fact that four *PTI1*-like genes (*PTI1-1*, *PTI1-2*, *PTI1-3* and *PTI1-4*) have been shown to interact with the ROS-inducible OXI1 kinase (Anthony *et al.*, 2006; Forzani *et al.*, 2011) thus posing the intriguing question of whether PTI1-8 also interacts with OXI1. Interestingly, previous studies have shown

*OXI1* expression is localised in the root apical meristem (Anthony *et al.*, 2004; Forzani *et al.*, 2011) and *OXI1* transcript levels were found to be very abundant in actively dividing cells (Anthony *et al.*, 2004). This provides additional circumstantial evidence that *PTI1-8* and *OXI1* may be involved in overlapping pathways. Interaction between between these proteins is currently being tested in the lab, however, as the PTI1-8 protein is likely to be membrane targeted, the split ubiquitin yeast two hybrid system (Johnsson and Varshavsky, 1994) is being employed as it allows the study of membrane protein interactions. Future genetic and physiological experiments will test these hypotheses and will make use of well established root growth assays to study hormone and ROS sensitivity as well as mutants affected in hormone and ROS signalling/metabolism.

### 3.4.3 Concluding remarks

The 5 single T-DNA knockout mutants and 2 double mutants corresponding to the other *PTI1* isoforms did not reveal any obvious difference in root elongation (Figure 3.4) or aerial phenotype. It is therefore intriguing that *PTI1-8* silencing confers a root developmental phenotype suggesting that among the 8 PTI1 isoforms, *PTI1-8* function does not completely overlap with the remaining *PTI1* genes. Results from the *in silico* promoter analysis and endogenous transcript measurements suggested diverse endogenous expression patterns for the 8 *PTI1* genes could be one explanation for diversification of the family (Chapter 2, Section 2.3.7). Another evolutionary strategy for diversification is to alter the subcellular targeting within the cell for individual *PTI1* isoforms (Sappl *et al.*, 2004). For instance, protein localisation of the highly conserved Calcium-Dependent Protein Kinase (CDPK) family members in two separate studies in *Arabidopsis* and wheat showed variable

subcellular targeting thus providing a mechanistic basis to explain CDPK isoform-specific function (Dammann *et al.*, 2003; Li *et al.*, 2008). Indeed, the work carried out to isolate the maize *ZmPTI1* genes showed that only one out of four isoforms was plasma membrane targeted and conferred a developmental pollen-specific phenotype (Herrmann *et al.*, 2006). In the present study, *in silico* analysis of the variable N-terminal region of 8 *Arabidopsis PTI1* amino acid sequences revealed PTI1-8 as the only isoform to contain the conserved signal motifs for both N-myristoylation and S-palmitolyation which are essential for membrane association (Resh, 1999) (3.18). Analysis of GFP fusion constructs showed that the PTI1-8 protein was targeted specifically to the plasma membrane (Figure 3.20-22). Although the possibility of membrane targeting for the seven other *Arabidopsis* PTI1 isoforms cannot be discounted, the palmitoylation and N-myristoylation sites specific to the PTI1-8 protein suggest that this isoform may have more distinct functions from other family members, which may provide one explanation for the unique non-redundant root phenotype. Future experiments that focus on site-directed mutagenesis of the N-terminal conserved amino acids would give further insights into the role of acylation in PTI1-8 membrane targeting.

## 3.5 Reference


**Alonso JM, Stepanova AN, Leisse TJ, Kim CJ, Chen H, Shinn P, Stevenson DK, Zimmerman J, Barajas P, Cheuk R, Gadrinab C, Heller C, Jeske A, Koesema E, Meyers CC, Parker H, Prednis L, Ansari Y, Choy N, Deen H, Geralt M, Hazari N, Hom E, Karnes M, Mulholland C, Ndubaku R, Schmidt I, Guzman P, Aguilar-Henonin L, Schmid M, Weigel D, Carter DE, Marchand T, Risseeuw E, Brogden D, Zeko A, Crosby WL, Berry CC, Ecker JR** (2003) Genome-wide insertional mutagenesis of *Arabidopsis* thaliana. Science **301:** 653-657

**Amasino R** (2010) Seasonal and developmental timing of flowering. Plant J **61:** 1001-1013

**Anthony RG, Henriques R, Helfer A, Meszaros T, Rios G, Testerink C, Munnik T, Deak M, Koncz C, Bogre L** (2004) A protein kinase target of a PDK1 signalling pathway is involved in root hair growth in *Arabidopsis*. Embo Journal **23:** 572-581

**Anthony RG, Khan S, Costa J, Pais MS, Bogre L** (2006) The *Arabidopsis* protein kinase PTI1-2 is activated by convergent phosphatidic acid and oxidative stress signaling pathways downstream of PDK1 and OXI1. J Biol Chem **281**: 37536-3746

**Beemster GT, Baskin TI** (1998) Analysis of cell division and elongation underlying the developmental acceleration of root growth in *Arabidopsis* thaliana. Plant Physiol **116:** 1515-1526

**Benfey PN, Bennett M, Schiefelbein J** (2010) Getting to the root of plant biology: impact of the *Arabidopsis* genome sequence on root research. Plant J **61:** 992-1000

**Bennett T, Scheres B** (2010) Root development-two meristems for the price of one? Curr Top Dev Biol **91:** 67-102

**Blazquez MA, Green R, Nilsson O, Sussman MR, Weigel D** (1998) Gibberellins promote flowering of *Arabidopsis* by activating the LEAFY promoter. Plant Cell **10:** 791-800

**Briggs GC, Osmont KS, Shindo C, Sibout R, Hardtke CS** (2006) Unequal genetic redundancies in *Arabidopsis*--a neglected phenomenon? Trends Plant Sci **11:** 492-498

**Clough SJ, Bent AF** (1998) Floral dip: a simplified method for Agrobacterium-mediated transformation of *Arabidopsis* thaliana. Plant J **16:** 735-743

**Craft J, Samalova M, Baroux C, Townley H, Martinez A, Jepson I, Tsiantis M, Moore I** (2005) New pOp/LhG4 vectors for stringent glucocorticoid-dependent transgene expression in *Arabidopsis*. Plant J **41:** 899-918

**Curtis MD, Grossniklaus U** (2003) A gateway cloning vector set for high-throughput functional analysis of genes *in planta*. Plant Physiol **133:** 462-469

**Dammann C, Ichida A, Hong B, Romanowsky SM, Hrabak EM, Harmon AC, Pickard BG, Harper JF** (2003) Subcellular targeting of nine calcium-dependent protein kinase isoforms from *Arabidopsis*. Plant Physiol **132:** 1840-1848

**Davis AM, Hall A, Millar AJ, Darrah C, Davis SJ** (2009) Protocol: Streamlined sub-protocols for floral-dip transformation and selection of transformants in *Arabidopsis* thaliana. Plant Meth **5:** 3

**Dello Ioio R, Linhares FS, Scacchi E, Casamitjana-Martinez E, Heidstra R, Costantino P, Sabatini S** (2007) Cytokinins determine *Arabidopsis* root-meristem size by controlling cell differentiation. Curr Biol **17:** 678-682

**Dello Ioio R, Nakamura K, Moubayidin L, Perilli S, Taniguchi M, Morita MT, Aoyama T, Costantino P, Sabatini S** (2008) A genetic framework for the control of cell division and differentiation in the root meristem. Science **322:** 1380-1384

**Forzani C, Carreri A, de la Fuente van Bentem S, Lecourieux D, Lecourieux F, Hirt H** (2011) The *Arabidopsis* protein kinase PTI1-4 is a common target of the oxidative signal-inducible1 (OXI1) and MAP kinases. Febs J **278**: 1126-1136

**Helliwell C, Waterhouse P** (2003) Constructs and methods for high-throughput gene silencing in plants. Methods **30:** 289-295

**Herrmann MM, Pinto S, Kluth J, Wienand U, Lorbiecke R** (2006) The PTI1-like kinase ZmPti1a from maize (Zea mays L.) co-localizes with callose at the plasma membrane of pollen and facilitates a competitive advantage to the male gametophyte. BMC Plant Biol **6:** 22

**Hoaglands DR, Arnon DA** (1950) The Water Culture Method of Growing Plants Without Soil. California Agricultural Experiment Station Bulletin: 1-39

**Iyer-Pascuzzi A, Simpson J, Herrera-Estrella L, Benfey PN** (2009) Functional genomics of root growth and development in *Arabidopsis*. Curr Opin Plant Biol **12:** 165-171

**Johnsson N, Varshavsky A** (1994) Split ubiquitin as a sensor of protein interactions *in vivo*. Proc Natl Acad Sci U S A **91:** 10340-10344

**Li AL, Zhu YF, Tan XM, Wang X, Wei B, Guo HZ, Zhang ZL, Chen XB, Zhao GY, Kong XY, Jia JZ, Mao L** (2008) Evolutionary and functional study of the CDPK gene family in wheat (Triticum aestivum L.). Plant Mol Biol **66:** 429-443

**Moore I, Samalova M, Kurup S** (2006) Transactivated and chemically inducible gene expression in plants. Plant J **45:** 651-683

**Moubayidin L, Perilli S, Dello Ioio R, Di Mambro R, Costantino P, Sabatini S** (2010) The rate of cell differentiation controls the *Arabidopsis* root meristem growth phase. Curr Biol **20:** 1138-1143

**Mutasa-Gottgens E, Hedden P** (2009) Gibberellin as a factor in floral regulatory networks. J Exp Bot **60:** 1979-1989

**Naito Y, Yamada T, Matsumiya T, Ui-Tei K, Saigo K, Morishita S** (2005) dsCheck: highly sensitive off-target search software for double-stranded RNA-mediated RNA interference. Nucleic Acids Res **33:** W589-591

**O'Malley RC, Ecker JR** (2010) Linking genotype to phenotype using the *Arabidopsis* unimutant collection. Plant J **61:** 928-940

**Ortega-Martinez O, Pernas M, Carol RJ, Dolan L** (2007) Ethylene modulates stem cell division in the *Arabidopsis* thaliana root. Science **317:** 507-510

**Perilli S, Sabatini S** (2010) Analysis of root meristem size development. Methods Mol Biol **655:** 177-187

**Petricka JJ, Benfey PN** (2008) Root layers: complex regulation of developmental patterning. Curr Opin Genet Dev **18**: 354-361

**Pitzschke A, Forzani C, Hirt H** (2006) Reactive oxygen species signaling in plants. Antioxid Redox Signal **8:** 1757-1764

**Prigge MJ, Otsuga D, Alonso JM, Ecker JR, Drews GN, Clark SE** (2005) Class III homeodomain-leucine zipper gene family members have overlapping,

antagonistic, and distinct roles in *Arabidopsis* development. Plant Cell **17:** 61-76

**Reddy GV, Meyerowitz EM** (2005) Stem-cell homeostasis and growth dynamics can be uncoupled in the *Arabidopsis* shoot apex. Science **310:** 663-667

**Resh MD** (1999) Fatty acylation of proteins: new insights into membrane targeting of myristoylated and palmitoylated proteins. Biochim Biophys Acta **1451:** 1-16

**Samson F, Brunaud V, Balzergue S, Dubreucq B, Lepiniec L, Pelletier G, Caboche M, Lecharny A** (2002) FLAGdb/FST: a database of mapped flanking insertion sites (FSTs) of *Arabidopsis* thaliana T-DNA transformants. Nucleic Acids Res **30:** 94-97

**Sappl PG, Heazlewood JL, Millar AH** (2004) Untangling multi-gene families in plants by integrating proteomics into functional genomics. Phytochemistry **65:** 1517-1530

**Sasaki T, Mori IC, Furuichi T, Munemasa S, Toyooka K, Matsuoka K, Murata Y, Yamamoto Y** (2010) Closing plant stomata requires a homolog of an aluminum-activated malate transporter. Plant Cell Physiol **51:** 354-365

**Sessions A, Burke E, Presting G, Aux G, McElver J, Patton D, Dietrich B, Ho P, Bacwaden J, Ko C, Clarke JD, Cotton D, Bullis D, Snell J, Miguel T, Hutchison D, Kimmerly B, Mitzel T, Katagiri F, Glazebrook J, Law M, Goff SA** (2002) A high-throughput *Arabidopsis* reverse genetics system. Plant Cell **14:** 2985-2994

**Sheldon CC, Hills MJ, Lister C, Dean C, Dennis ES, Peacock WJ** (2008) Resetting of FLOWERING LOCUS C expression after epigenetic repression by vernalization. Proc Natl Acad Sci U S A **105:** 2214-2219

**Silverstone AL, Ciampaglio CN, Sun T** (1998) The *Arabidopsis* RGA gene encodes a transcriptional regulator repressing the gibberellin signal transduction pathway. Plant Cell **10:** 155-169

**Swanson S, Gilroy S** (2010) ROS in plant development. Physiol Plant **138:** 384-392

**Takahashi A, Agrawal GK, Yamazaki M, Onosato K, Miyao A, Kawasaki T, Shimamoto K, Hirochika H** (2007) Rice Pti1a negatively regulates RAR1-dependent defense responses. Plant Cell **19:** 2940-2951

**Takeda S, Gapper C, Kaya H, Bell E, Kuchitsu K, Dolan L** (2008) Local positive feedback regulation determines cell shape in root hair cells. Science **319:** 1241-1244

**Terpstra I, Heidstra R** (2009) Stem cells: The root of all cells. Semin Cell Dev Biol **20:** 1089-1096

**To JP, Haberer G, Ferreira FJ, Deruere J, Mason MG, Schaller GE, Alonso JM, Ecker JR, Kieber JJ** (2004) Type-A *Arabidopsis* response regulators are partially redundant negative regulators of cytokinin signaling. Plant Cell **16:** 658-671

**Tsukagoshi H, Busch W, Benfey PN** (2010) Transcriptional regulation of ROS controls transition from proliferation to differentiation in the root. Cell **143:** 606-616

**Ubeda-Tomas S, Federici F, Casimiro I, Beemster GT, Bhalerao R, Swarup R, Doerner P, Haseloff J, Bennett MJ** (2009) Gibberellin signaling in the endodermis controls *Arabidopsis* root meristem size. Curr Biol **19:** 1194-1199

**van Dijken AJ, Schluepmann H, Smeekens SC** (2004) *Arabidopsis* trehalose-6-phosphate synthase 1 is essential for normal vegetative growth and transition to flowering. Plant Physiol **135:** 969-977

**Veit B** (2006) Stem cell signalling networks in plants. Plant Mol Biol **60:** 793-810

**Wielopolska A, Townley H, Moore I, Waterhouse P, Helliwell C** (2005) A high-throughput inducible RNAi vector for plants. Plant Biotechnol J **3:** 583-590

**Xu P, Zhang Y, Kang L, Roossinck MJ, Mysore KS** (2006) Computational estimation and experimental verification of off-target silencing during posttranscriptional gene silencing in plants. Plant Physiol **142:** 429-440

**Zhou J, Loh YT, Bressen RA, Martin GB** (1995) The tomato gene Pti1 Encodes a serine/threonine kinase that is phophorylated by Pto and is invloved in hypersensitive response. Cell **83:** 925-935

**Zou HW, Wu ZY, Yang Q, Zhang XH, Cao MQ, Jia WS, Huang CL, Xiao X** (2006) Gene expression analyses of ZmPti1, encoding a maize Pti-like kinase, suggest a role in stress signaling. Plant Science **171:** 99-105

## 3.6 Appendix

SUMMARY OF QUERY

Number of sequences submitted = 1

siRNA length = 20 nt

The 5' end of antisense strand must be A or U

The first 7 bases of antisense strand (5' - 3') have at least 5 A or U bases

The 5' end of sense strand must be G or C

Percentage GC content: 30% to 70%

Mismatch allowed = 0

Target dataset = Arabidopsis version 12.1 release on 10/8/2004

- Hit summary
- Hit details
- Predicted efficient siRNAs

Top • Hit details • Predicted efficient siRNAs

**Hit Summary**

Query: query_seq. Select IDs for analysis of their functional domains and associated GO terms

| Target ID | Functional Annotation |
|---|---|
| ☐TC252972 | GB\|BAB02745.1\|11994558\|AB022216 serine/threonine protein kinase-like protein (Arabidopsis thaliana;) , complete |

**Appendix 3.6.1.** Screen capture of results obtained using the web based siRNA tool (http://bioinfo2.noble.org/RNAiScan.htm) (Xu *et al.*, 2006) that scans for potential 20 bp off-target silencing sequences using the *PTI1-8* RNAi 267 bp silencing fragment. The result shows a single hit in the Arabidopsis database, TC252972, corresponding to the target *PTI1-8* gene (Genbank accession: BAB02745.1) and therefore high specificity of the chosen RNAi fragment.

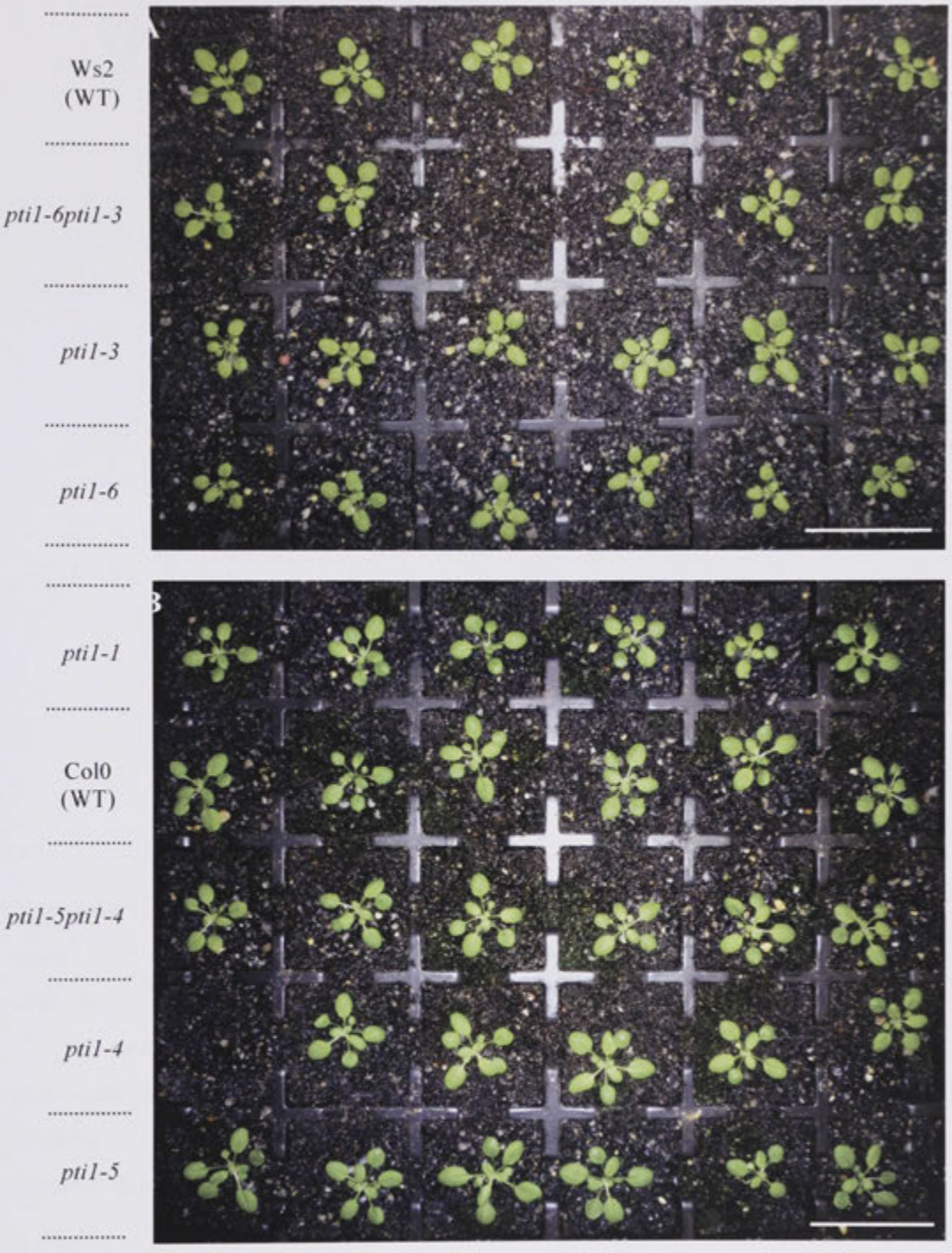


**Appendix Figure 3.6.2:** Soil grown 21 day-old *pti1* mutants and corresponding WT (Col-0, Ws2). Scale bar = 5cm

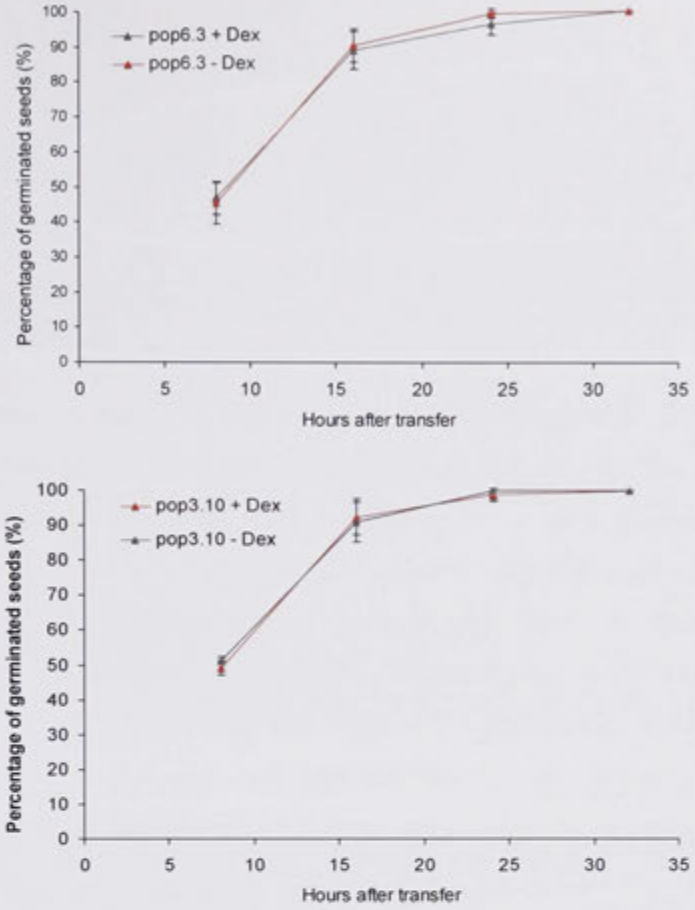


**Appendix 3.6.3: Germination assay for two independent inRNAi *PTI1-8* lines.** Seeds were stratified at 4 $^{0}$C in the dark for 3 days and then transferred to growth cabinets (SD 10 hour day, 14 hour night, temperature 21$^{0}$C, light intensity 120 µE $m^{-2}$ $s^{-1}$). For each line, approximately 60 seeds were plated in triplicate and the number of germinated seeds was counted at 8 hour intervals. Germination was defined here as the breaking of the seed coat with a visible radicle protrusion. Error bars represent SE of the mean for three replicate plates

**Appendix 3.6.4: Estimation of meristem length of primary roots using ImageJ.**

The plot profile function measures pixel intensity over a given distance or in this case along a given layer of cells and can be used to identify cell wall boundaries (peaks). The plot obtained can thus be used to differentiate the meristem zone based on closely packed peaks (red box) and elongation zone where the peaks are more spread out reflecting cells that rapidly elongating (blue box). Shown above are plot profiles of a representative inRNAi line 6.3 primary root growing in – dex (A) and in + dex (B) illustrating the difference in meristem size. Scale bars indicate 100 µm.

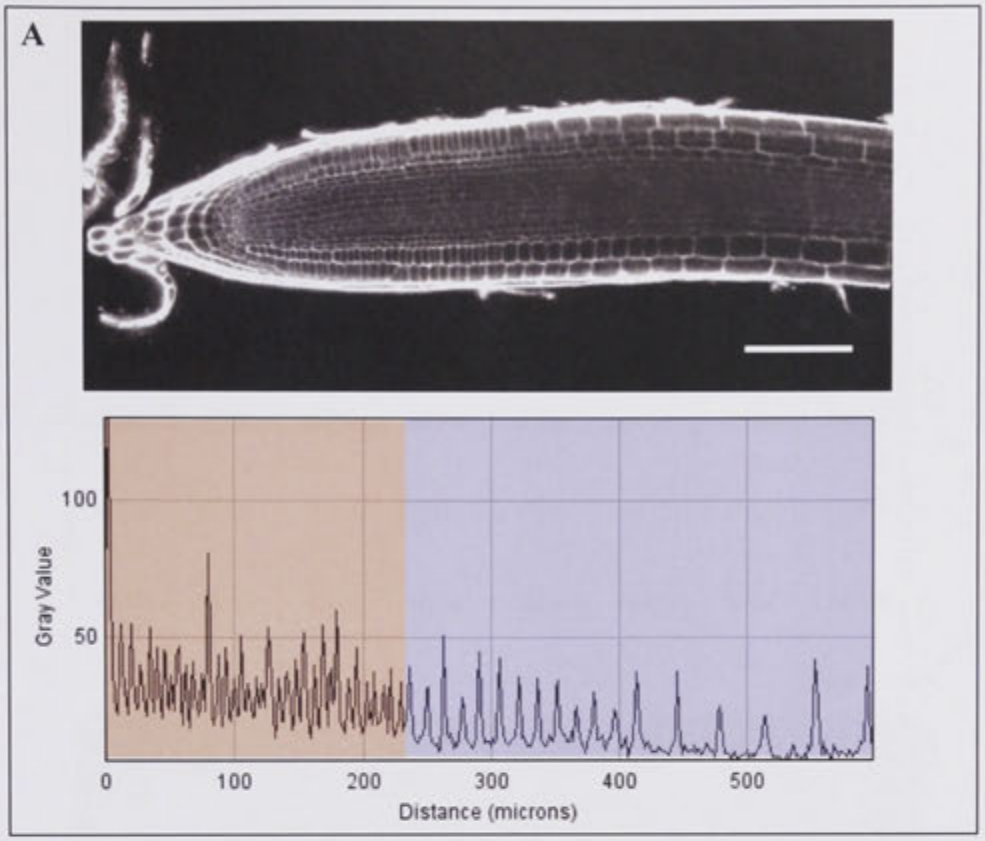
A
100
50
Gray Value
0
100
200
300
400
500
Distance (microns)

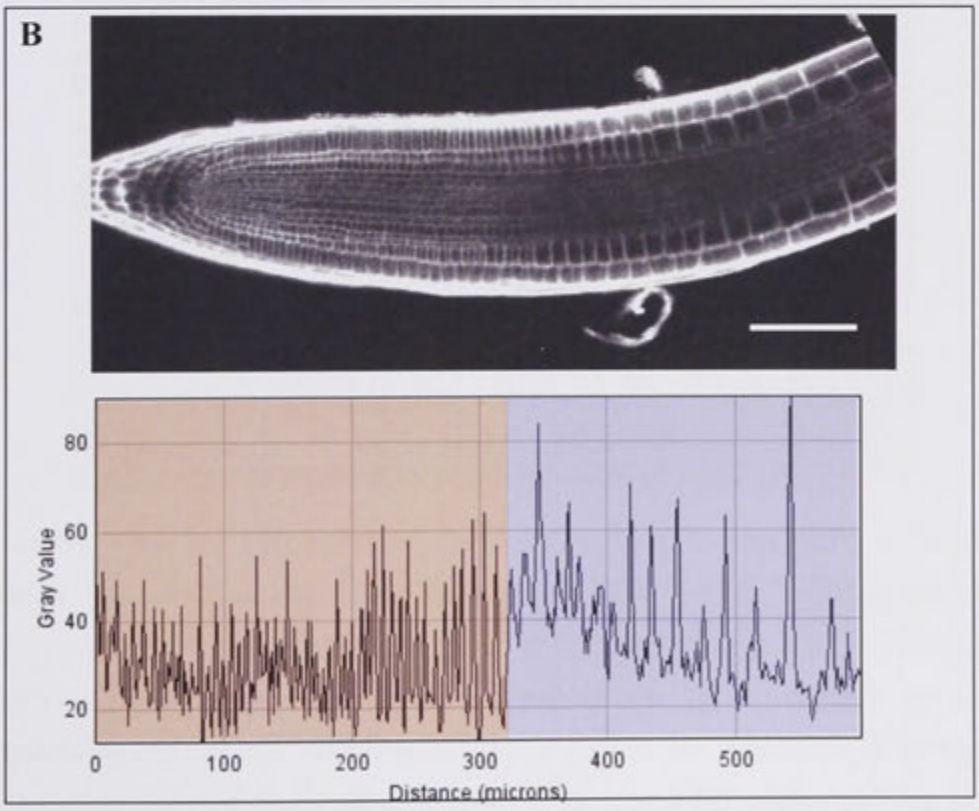
B
80
60
40
20
Gray Value
0
100
200
300
400
500
Distance (microns)

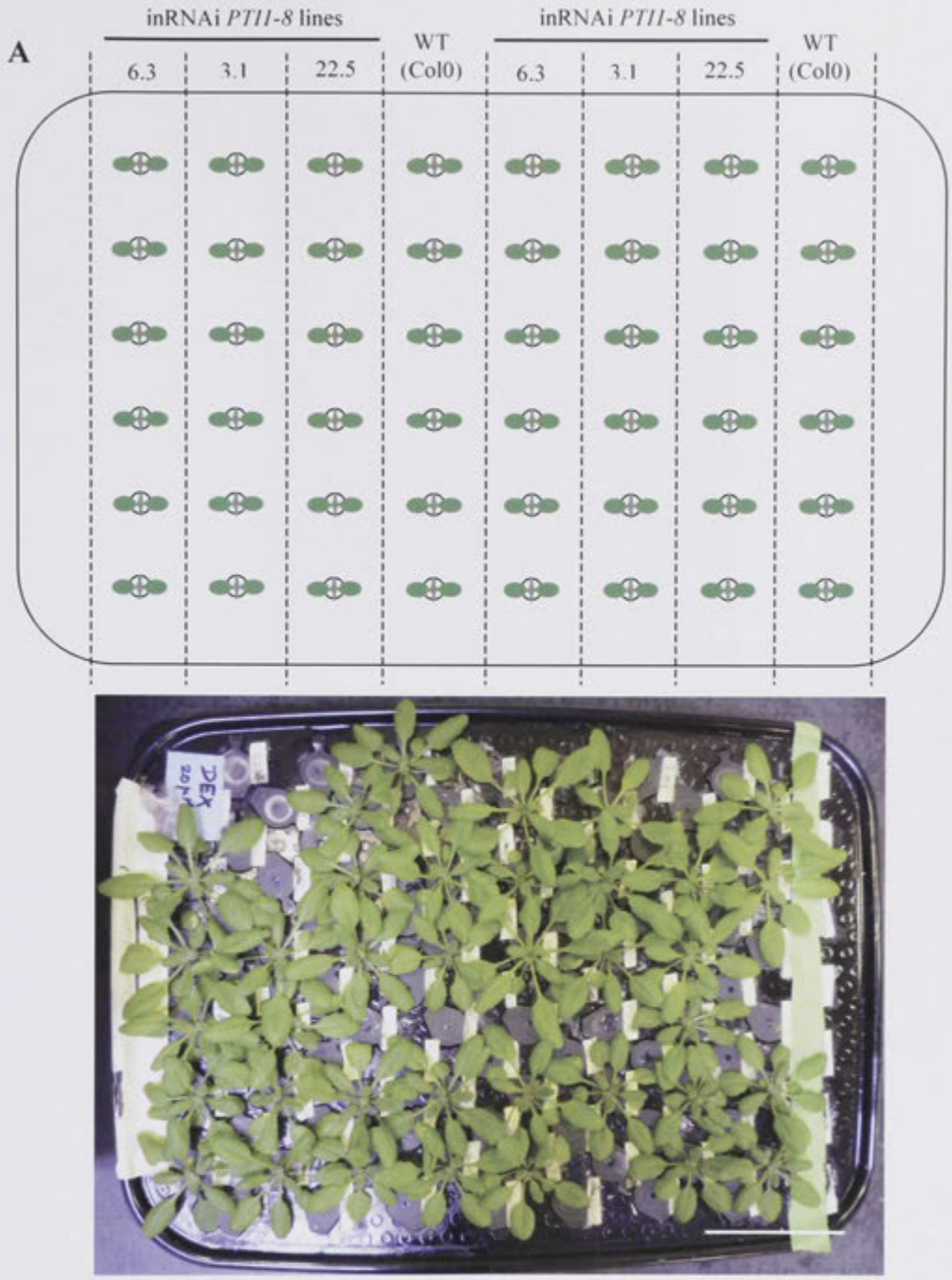


**Appendix 3.6.5: in RNAi *PTI1-8* lines grown in 1/3 Hoagland's hydroponic medium.** Cartoon illustrating the arrangement of 3 inRNAi *PTI1-8* silencing lines (6.3, 3.1 and 22.5) and WT (Col0) growing in a hydroponic setup (A). Representative hydroponic box with 4 week old Col0 (WT) and inRNAi *PTI1-8* seedlings, n = 3 Dex treated boxes and (n = 1 DMSO treated box-not shown). No discernable differences in shoot growth were observed between inRNAi lines and WT plants growing in the presence of 20 μM dexamethasone (B). Three scale bar = 5 cm.

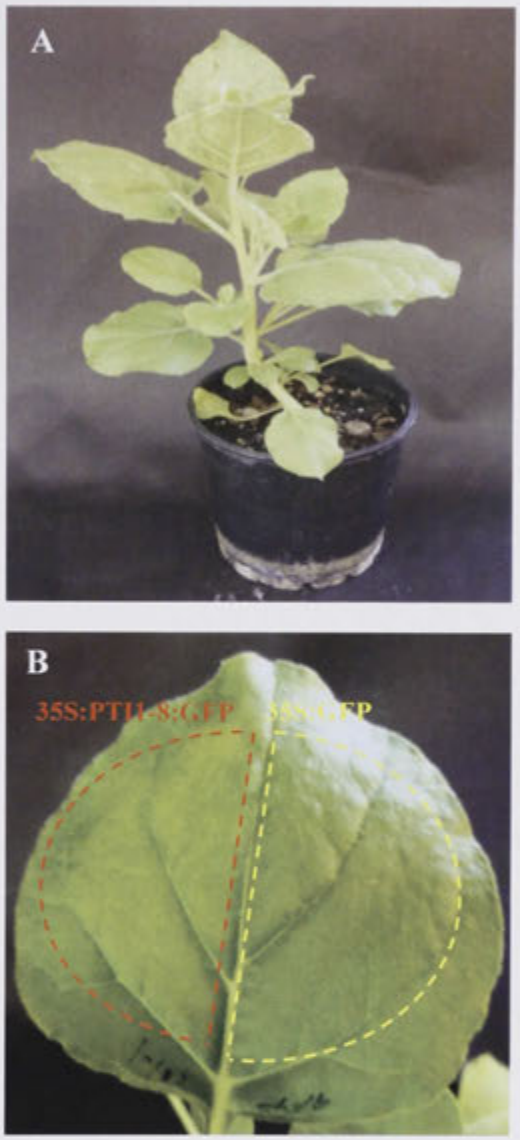


**Appendix 3.6.6.** *Agrobacterium* mediated infiltration of 35S:PTI1-8GFP and 35S:GFP overexpression constructs in *Nicotiana benthamiana* (A). A single infiltrated leaf of *N. benthamiana.* The two constructs were infiltrated on either side of the mid vien.

| Primer Name | Target | Sequence 5' → 3' | Purpose | Upper (U) /Lower (L) |
|---|---|---|---|---|
| prPti4f | At3g17410 PTI1-8 | GGATCCAAGTCAAAAGATAGATACTCGC | promoter PTI1-8 GFP fusion | U |
| prPti4r | At3g17410 PTI1-8 | GCGGCCGCATACGGGTTCCTGT | promoter PTI1-8 GFP fusion | L |
| Pti4 SALK5'UTRf | At3g17410 PTI1-8 | CTCGACGAAAGTTTCTAATTATAGGGTT | T-DNA screening SALK 13971 | U |
| Pti4 SALK5'UTRr | At3g17410 PTI1-8 | CGAAAACTTCAAGGTGGTTGTTG | T-DNA screening SALK 13971 | L |
| 35SPti4nostop-r | At3g17410 PTI1-8 | AAGCTTATACGGGTTCCTGTG | PTI1-8 C-terminal GFP fusion | L |
| Pti4SALK_LB_f | At3g17410 PTI1-8 | TGTGCTCGGAACCTTTGGCTA | T-DNA screening SALK 094451 | U |
| Pti4SALK_RB_r | At3g17410 PTI1-8 | CAATGATTTCTATAGATGCAAAGAGGTG | T-DNA screening SALK 094451 | L |
| At3g17410_RNAi_for | At3g17410 PTI1-8 | GGATCCGAAGAGTTTCGTGTGAGA | Amplifies RNAi fragment (Constitutive and Inducible constructs | U |
| At3g17410_RNAi_rev | At3g17410 PTI1-8 | GAATTCTATGAACCCTCACCAATCAAG | Amplifies RNAi fragment (Constitutive and Inducible constructs | L |
| Pti4CDSpETfor | At3g17410 PTI1-8 | GGATCCATGGGCTGCTTTGG | PTI1-8 N-terminal GFP fusion | U |
| Pti4CDSpETrev | At3g17410 PTI1-8 | AAGCTTTCAATACGGGTTCCTGTG | PTI1-8 N-terminal GFP fusion | L |
| Pti0-RTfor | At3g62220 PTI1-5 | TGCCTGGAGCTAATGATTATGGAGGTC | Semi-quant RT-PCR SALK T-DNA 020728 | U |
| AtPTOi_L | At3g62220 PTI1-5 | CAGGCTTTGCTCCCTTCACACCTT | Semi-quant RT-PCR SALK T-DNA 020728 | L |
| ACT2-2 | At3g18780 ACT2 | GCT CGT AGT CAA CAG CAA CAA | Loading control for Semi-quant RT-PCR | U |
| ACT2-1 | At3g18780 ACT2 | GCC ATC CAA GCT GTT CTC TC | Loading control for Semi-quant RT-PCR | L |

| Primer Name | Target | Sequence | Purpose | Upper/Lower |
|---|---|---|---|---|
| Pti2-RTrev | At2g47060 PTI1-4 | TGCCTGGAGCTAATGATTATGGAGGTC | Semi-quant RT-PCR SALK T-DNA 0643275 | L |
| AtPTi2_U | At2g47060 PTI1-4 | GCTTTGGGTGTTGTGGGGAGGAT | Semi-quant RT-PCR SALK T-DNA 0643275 | U |
| Pti5-RTrev | At1g06700 PTI1-1 | ATGTCATGCAACGATCCCATTGTT | Semi-quant RT-PCR SALK T-DNA 086563C | L |
| AtPti5_U | At1g06700 PTI1-1 | AATAGAAGACTCAAATGAAGAGCAACAACTGA | Semi-quant RT-PCR SALK T-DNA 086563C | U |
| Pti1-RTrev | At2G43230 PTI1-6 | CAATGACATTGCGGGGACATCAA | Semi-quant RT-PCR FLAG T-DNA 325B10 | L |
| AtPTi1_U | At2g43230 PTI1-6 | TCGTCTCTCTGGTTTATTGCTCGTTGAT | Semi-quant RT-PCR FLAG T-DNA 325B10 | U |
| Pti6-RTrev | At3g59350 PTI1-3 | CGATAGATTAAAATCAGCGATCTTGGCTT | Semi-quant RT-PCR FLAG T-DNA 543G06 | L |
| AtPti6_U | At3g59350 PTI1-3 | TGAAAATGAACACCTCAGAAGCCCTAA | Semi-quant RT-PCR FLAG T-DNA 543G06 | U |
| RP15 | At3g62220 Pti1-5 | CGCGCTTTACGAGTTTGGG | T-DNA screening SALK line N520728 | U |
| LP15 | At3g62220 Pti1-5 | GCTGCTCCAACAGCAATCTTCAC | T-DNA screening SALK line N520728 | L |
| RP7b | At2g47060 PTI1-4 | GCACAGAAGGGTCCTCCAGTTG | T-DNA screening SALK line N564325 | U |

| Primer Name | Target | Sequence | Purpose | Upper/Lower |
|---|---|---|---|---|
| Pti1FLAG_RB_f | At2g43230 PTI1-6 | TCACCTCCTTTCGTCTCTGCCTCTCATTTG | T-DNA screening FLAG T-DNA 325B10 | U |
| Pti1FLAG_LB_r | At2g43230 PTI1-6 | CAACCACCTACGCATCTTCCCTCTCTTGC | T-DNA screening FLAG T-DNA 325B10 | L |
| Pti5Wisc-rev | At1g06700 PTI1-1 | CCCTTCCTACCTGTAATCGCACAATA | T-DNA screening SALK T-DNA 086563C | L |
| Pti5Wisc-for | At1g06700 PTI1-1 | GCAAAACATGAGGTTAAGAAGGAAGC | T-DNA screening SALK T-DNA 086563C | U |
| Pti6FLAG_RB_f | At3g59350 PTI1-3 | TTGAAAGATGGAAAGGCTGTCGCGGT | T-DNA screening FLAG T-DNA 543G06 | U |
| Pti6FLAG_LB_r | At3g59350 PTI1-3 | TGCTCCTTGGACTCCTTTCCTCCCGTGTAA | T-DNA screening FLAG T-DNA 543G06 | L |
| LBb55 | SALK LB | GACCGCTTGCTGCAACTCTC | T-DNA border primers | - |
| RBb1 | SALK LB | GTATGTGCTTAGCTCATTAAACTCCAG | T-DNA border primers | - |
| FLAG_LB4 | Versailles T-DNA LB | CGTGTGCCAGGTGCCCACGGAATAGT | T-DNA border primers | - |
| FLAG_RB4 | Versailles T-DNA RB | TCACGGGTTGGGGTTTCTACAGGAC | T-DNA border primers | - |
| AtPTOi_L | At3g62220 PTI1-5 | CAGGCTTTGCTCCCTTCACACCTT | qRT-PCR | L |
| AtPTOi_U | At3g62220 PTI1-5 | ATGGGAATTCGAGGATACTTGTCTTTGAGT | qRT-PCR | U |
| AtPTi1_L | At2g43230 PTI1-6 | AGATCGTCTACAGCTCTCGGTTTATCCAA | qRT-PCR | L |
| AtPTi1_U | At2g43230 PTI1-6 | TCGTCTCTCTGGTTTATTGCTCGTTGAT | qRT-PCR | U |
| AtPTi2_U | At2g47060 PTI1-4 | GCTTTGGGTGTTGTGGGGAGGAT | qRT-PCR | U |
| AtPTi2_L | At2g47060 PTI1-4 | GTGCAGTTTCAGAGGCTTGGTGGT | qRT-PCR | L |

| Primer Name | Target | Sequence | Purpose | Upper/Lower |
|---|---|---|---|---|
| AtPTi3_U | At2g30740 PTI1-2 | AATGAAGAGGTGCATTTGAAAAGTCCAT | qRT-PCR | U |
| AtPTi3_L | At2g30740 PTI1-2 | CTCATCCACAGACAAGGGAGGAACTTC | qRT-PCR | L |
| AtPti5_U | At1g06700 PTI1-1 | AATAGAAGACTCAAATGAAGAGCAACAACTGA | qRT-PCR | U |
| AtPti5_L | At1g06700 PTI1-1 | ACAGGTGCTGGTTTTGAATTCTTATGATTT | qRT-PCR | L |
| AtPti6_U | At3g59350 PTI1-3 | TGAAAATGAACACCTCAGAAGCCCTAA | qRT-PCR | U |
| AtPti6_L | At3g59350 PTI1-3 | GCAGGCACATCAATAGATGGAGGCT | qRT-PCR | L |
| AtPti4newfor | At3g17410 PTI1-8 | GACGGGGACGTTGAGCACAAAGA | qRT-PCR | U |
| AtPti4newrev | At3g17410 PTI1-8 | AATTTAGGGGTTGCCCATGTCACGA | qRT-PCR | L |
| Pti7F | At1g48210 PTI1-7 | GAGGATTTTCGCAACGCTACTGACAC | qRT-PCR | U |
| Pti7R | At1g48210 PTI1-7 | ACTGGAATGGCTGGTACAGAAATAGGC | qRT-PCR | L |
| AtAPTnew-for | At1g27450 APT1 | GGTGAGCGTGCTATTATTATTGATGACCT | qRT-PCR (Internal Reference) | U |
| AtAPTnew-rev | At1g27450 APT1 | CTAGTTTCTCCTTTCCCTTAAGCTCTGGTA | qRT-PCR(Internal Reference) | R |
| PDF2_qPCR_for | At1g13320 PDF2 | TAACGTGGCCAAAATGATGC | qRT-PCR | U |
| PDF2_qPCR_rev | At1g13320 PDF2 | GTTCTCCACAACCGCTTGGT | qRT-PCR | L |

**Appendix 3.6.7: Real-time , T-DNA screening, RT and cloning primers used in Chapter 3**

# Chapter 4

## Functional analysis of *pti1* mutants in response to biotic stress

# Chapter 4

## 4.1 Introduction

The interaction between a plant and a pathogen is a complex dynamic process that reflects the evolutionary struggle between the host and the invader. To prevent the colonisation of the host tissue by the invading pathogen, the plant's defence can be divided into two distinct phases. The first phase or the primary line of defence is the extracellular recognition of highly conserved elicitors, known as pathogen associated molecular patterns (PAMPs), by transmembrane pattern recognition receptors (PRRs) (Jones and Dangl, 2006). Recognition of the pathogen at this stage leads to the induction of basal defences known as PAMP-triggered immunity (PTI). The second phase of plant immunity takes place within the cell and is referred to as the effector-triggered immunity (ETI). Here, plant resistance (R) genes that encode nucleotide binding-leucine rich repeats (NB-LRR) proteins recognize products of pathogen avirulence genes (avr), known as effectors, leading to hypersensitive cell death response (HR) at the site of infection (Jones and Dangl, 2006). The observation of his interaction (either direct or indirect) between the plant R- and pathogen Avr-proteins, led to the development of the "gene-for-gene" model which has now been experimentally validated in numerous plant species (Preston, 2001; Nomura et al., 2005; Dodds and Rathjen, 2010).

In tomato, the bacterial speck disease is caused by the hemi-biotrophic pathogen, *Pseudomonas syringae* pathovar *tomato* DC3000 strain which carries the avirulence genes avrPTO and avrPTOB. Resistance to *P. syringae* pathogenic bacterium is conferred by the molecular complex made of the NBLRR protein, SlPRF, and the

serine threonine kinase SlPTO (Salmeron et al., 1996; Pedley and Martin, 2003). The SlPRF/SlPTO complex recognizes the products of the avirulence genes *AvrPTO* and *AvrPTOB* and triggers downstream defence signals that result in a cell death-mediated hypersensitive response (HR) (Mucyn et al., 2006). Despite numerous genetic screens, however, it is still unclear precisely how resistance (R) -protein mediated recognition of pathogens leads to downstream activation of HR. Candidates for downstream partners of the tomato SlPTO were identified using a yeast two hybrid assay and include the protein kinase SlPTI1 which belongs to the PTI1 family and the transcription factors SlPTI4, SlPTI5 and SlPTI6 (Zhou et al., 1995; Zhou et al., 1997). SlPTI1 was shown to be capable of autophosphoprylation and is also phosphorylated by SlPTO *in vitro*. Additionally, tobacco plants overexpressing SlPTI1 show accelerated HR in leaves when challenged with the *P. syringae* effector protein AvrPTO, indicating a functional role of SlPTI1 in SlPTO-mediated disease resistance pathway (Zhou et al., 1995). Since the identification of the tomato SlPTI1 by Zhou *et al.* (1995), orthologs have been identified in soybean, rice, maize and *Arabidopsis* indicating that the PTI1 genes represent an ancient family conserved among diverse plant species (Staswick, 2000; Anthony et al., 2006; Herrmann et al., 2006; Takahashi et al., 2007; Forzani et al., 2011). Moreover, PTI1 orthologs in rice, maize and soybean have been shown to be involved in pathogen signalling (Staswick, 2000; Herrmann et al., 2006; Takahashi et al., 2007), consistent with the early studies in tomato.

The aim of this chapter is to examine the involvement of the *Arabidopsis PTI1* genes in defence signalling. The *P. syringae* pathovar *tomato* (*Pst*) DC3000 is known to be an aggressive pathogen in *Arabidopsis* (Preston, 2001; Katagiri et al., 2002) and

therefore constitutes a powerful tool for mutant screens on disease resistance to hemi-biotrophic pathogens. The pathogen was used to challenge several of the *Arabidopsis pti1* mutants described in the previous chapter and selected on the basis of the phylogenetic study presented in Chapter 2 (Section 2.3.5). Two independent techniques were used for quantifying the growth of the bacteria within infected leaves. Gene expression analysis and an *in vitro* protein-protein interaction assay were used for an initial investigation of PTI1 signalling pathways.

## 4.2 Materials and Methods

### 4.2.1 Plant material and growth conditions

The *Arabidopsis thaliana* accession (ecotype Columbia) Col-0 was used as wild-type in the experiments described in this chapter. The confirmed T-DNA knockout mutants *pti1-5* (SALK 020728), *pti1-4* (SALK 065325) and the derived double mutant *pti1- 5pti1-4* described previously in chapter 3 (3.3.1) were used in the pathogen challenge experiments. The *PTI1-5* and *PTI1-4* genes were chosen for these experiments based on the phylogenetic tree discussed earlier (Chapter 2, Figure 2.5), where they were positioned in close proximity to PTI1 isoforms OsPTI1A, SlPTI1 and ZmPTI1B. These genes have been previously shown to be directly of indirectly involved in pathogen response (Zhou et al., 1995; Herrmann et al., 2006; Takahashi et al., 2007). To test the sensitivity of the *pti1* mutants to the virulent strain of *Pseudomonas syringae* DC3000, the DNA biomass and the CFU assay were employed for quantifying bacterial growth following infection in two independent experiments (Figure 4.1). The plant growth conditions were optimised for each experiment separately. The growth condition for the CFU assays are identical to that previously described in Chapter 2, materials and methods, section - 2.2.1.3.

#### *4.2.1.1 Plant growth conditions for DNA biomass assay*

The DNA biomass experiment was undertaken at Dr. Peer Schenk's laboratory at the University of Queensland (Australia). Seeds for WT Col-0 and *pti1* mutants were sown at high density on the surface of UC (University of California) soil mix in punnet cell trays and stratified at $4^0$ C in the dark for three days. The trays were then

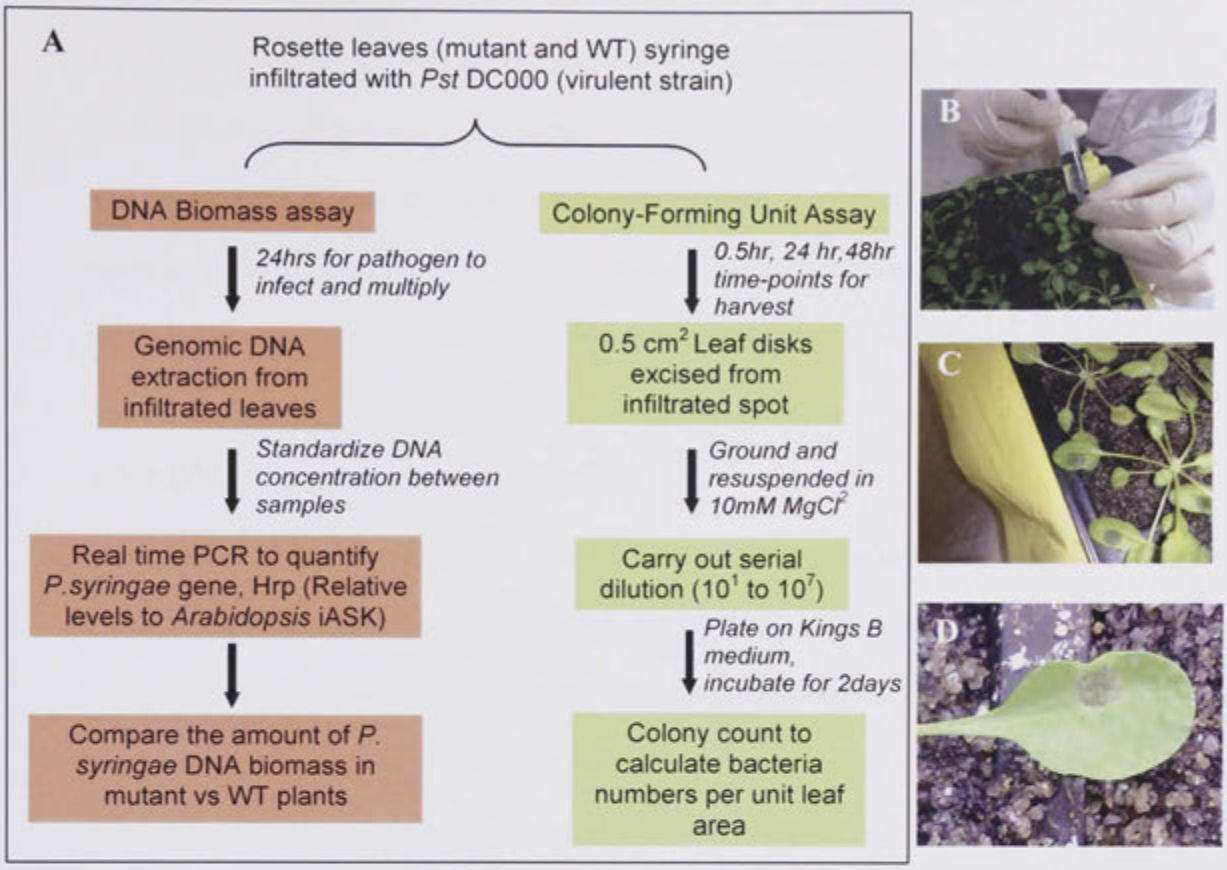


**Figure 4.1 (A-D): *Pseudomonas syringae* DC3000 (*Pst* DC3000) virulent strain infiltration and *in planta* quantification**

Flowchart describing the steps involved in the DNA biomass and CFU assays for *Pst* DC3000 bacterial enumeration (A). *Pst* DC3000 ($OD_{600}$=0.05) was syringe infiltrated on the abaxial side of 5 week old rosette leaves which appear water soaked (B,C). Disease symptoms such as chlorosis were apparent 2-3 days post inoculation at the site of infiltration (D).

transferred to growth cabinets under short day conditions (8hr day length). Eighteen days after sowing, seedlings were transplanted to separate punnet cell trays at a density of 4 plants per cell and returned to the growth cabinet. Environmental conditions were as described in Chapter 2, materials and methods section 2.2.1.3. The plants were then acclimated for ~2 weeks, before inocluation of *Pst* DC3000 bacteria (inoculum density, $OD_{600}$ – 0.05) Leaf inoculation procedure is as previously described in Chapter 2, materials and methods section 2.2.2.1.2.

### 4.2.2 DNA biomass assay

The assay which measures increase of bacteria in *Arabidopsis* infected leaf tissues is based on relative quantification of the *Pst* DC3000 bacterial and plant DNA by means of real-time quantitative PCR. The DNA biomass assay has been shown to be highly sensitive and can also discriminate between genotypes that show subtle differences in pathogen growth (Winton et al., 2002; Brouwer et al., 2003; Gachon and Saindrenan, 2004). The primers that target the *Pseudomonas* DNA, specifically amplify a region within the *HRPZ* (Hypersensitive reaction pathogenicity Z) (Yuan and He, 1996) gene that belong to the type III secreted proteins located in a pathogenicity island, which encodes a cluster of *HRP* related genes in the genome (Alfano et al., 2000). The *HRPZ* gene is also known to be a good reporter gene for the *Pseudomonas* diagnostic assay as it is pathovar-specific and is found to be common for all *Pseudomonas syringae* pv. *tomato* isolates (Alfano et al., 2000). The primers used for amplifying plant DNA targeted the *Arabidopsis* Shaggy-kinase-like 11 gene (i*ASK11*, At5g26751) and has previously been employed to quantitatively monitor the growth of the fungi *Alternaria brassicicola* and *Botrytis cinerea* (Gachon and Saindrenan, 2004).

For each genotype, a total of 120 plants were grown and used in 3 biological replicates (n=20 plants) for inoculation with *Pst* DC3000 and mock inoculum (10 mM $MgCl_2$). Four week old WT (Col-0) and *pti1* mutant plants were challenged with the *Pst* DC3000 bacteria using the infiltration technique described previously. Two rosette leaves per plant were infiltrated with *Pst* DC3000 with an inoculum of optical density ($OD_{600}$) 0.05 or a mock solution (10 mM $MgCl_2$). The infiltration was carried out 1 hour after subjective dawn. Immediately following infiltration, the plant trays were covered with a vented plexiglass lid to maintain high relative humidity around the plants until harvest. 24 hours post-infection, infiltrated leaves were cut at the base of the lamina with a scalpel and DNA was extracted using CTAB procedure described previously (Chapter 3, Materials and Methods, 3.2.6.7). DNA concentration ($A_{260}$) and quality ($A_{260}/A_{280}$ ratio) was measured using the NanoDrop® ND-1000 Spectrophotometer. Sequencing of the PCR product confirmed the efficiency of the primers to specifically amplify a portion of the *P. syringae HRPZ* gene (Data not shown).

Relative quantification of *Pst* DNA using HRPZ primers and *Arabidopsis* DNA using iASK11 primers were carried out using the ABI PRISM® 7900HT Sequence Detection System (Applied Biosystems) according to the manufacturers instructions. Each reaction contained: 2.5 µL of DNA template (1:40 dilution), 2.5 µL of forward and reverse primer mix (1.2 µM each), and 5 µL Sybr Green PCR Master Mix (FastStart Universal SYBR® Green, Roche). *HRPZ* transcript abundance for WT and mutant was expressed relative to that of the *iASK11* gene to correct for differences in template loading.

### 4.2.3 CFU growth assay

The CFU assay for *Pst* DC3000 is a technique for measuring bacterial multiplication in the host tissue at regular intervals following infection. For a virulent pathogen such as the *Pst* DC3000 strain used in these experiments, previous studies have demonstrated colonization in host tissue occurs over several days and the number of bacteria increases more than 10,000 fold over this period. In order to test the sensitivity of the *pti1* mutants to *Pst* DC3000, the *in planta* quantification of the bacteria was carried out 1 and 2 days after infection. These sampling points were also chosen based on previous results obtained in the DNA biomass assay for which differential growth of the bacteria in the *pti1-5* mutant compare to WT was observed 1 day after infection.

Infiltrated leaves from WT and *pti1* mutant plants were sampled for bacterial CFU quantification 24 and 48 hours after inoculation with *Pst* DC3000. To establish *in planta* bacterial levels immediately following infiltration, leaves of all genotypes were also harvested 1 hour after inoculation. At the two time points, six leaves from six independent plants were harvested and divided into 3 biological replicates of 2 leaves each. The leaves were detached just above the petiole and washed in 70% ethanol for 1 minute. This step was skipped for the 1 hour time point as, so close to inoculation, the bacteria would still be present on the surface of the blade. Following ethanol wash, the leaves were blotted dry and rinsed in sterile MilliQ water for 1 minute. Using a 0.25 $cm^2$ borer, leaf discs were excised from the bacterial infiltrated portion of the leaf. At each time-point, three samples of 2 discs each were assayed for measurement of *in planta* bacterial growth. The leaf discs were placed in 1.5 mL microcentrifuge tubes with 100 µL of sterile MilliQ water, and ground using plastic

micropestlesTM (Eppendorf) until no intact tissue was still visible. The pestle was washed with 900 µL sterile water, and the rinsing water was collected in the original tube together with the ground tissue sample. The resulting 1 mL tissue samples were then vortexed and mixed thoroughly, and serially diluted 1:10. 10 µL of each serial dilution was then plated as a single spot on King's B medium (King et al., 1954) (Kanamycin 50 µg/mL) in large square plates, and allowed to dry onto the surface. The plates were then incubated at $28^0$ C for 2 days, after which colony-forming units were counted for each of the 10 µL spots. Only spots that contained readily countable colonies (between 10 and 70 colonies) were used for enumerating bacterial colony numbers. *Pst* DC3000 growth within the host was expressed as log (colony forming units/ unit leaf area).

### 4.2.4 Gene expression analysis

As a first step to investigate the *pti1-5* enhanced resistance to *Pst* DC3000 (see Results section, below), qRT-PCR measurements of transcript abundance of defence marker genes and putative signalling partners were done in separate experiment (independent from the previous DNA biomass and CFU experiments). WT (Col-0) and *pti1-5* mutant plants were grown for 5 weeks in a growth chamber and 2-3 rosette leaves per plant were inoculated with *Pst* DC3000 bacteria as previously described (2.2.2.1.2). was carried out 2 hours after subjective dawn and leaves from *Pst* DC3000 infiltrated- and mock treated-leaves (10mM $MgCl_2$) were harvested 4, 24 and 48 hours after inoculation. At each time point, for both mock- and pathogen-treated plants, 3 biological replicates corresponding to pools of 8 to 10 infiltrated rosette leaves were harvested by cutting them just above the petiole, and snap-frozen in liquid nitrogen. The leaves of each replicate sample were ground separately into a

fine powder using a mortar and pestle chilled with liquid nitrogen. Total RNA was isolated from approximately 40 mg of frozen tissue using the SV Total RNA isolation kit (Promega) according to the protocol provided by the manufacturer. Two micrograms of total RNA was used for first strand cDNA synthesis and subsequent transcript measurements were performed using ABI PRISM® 7900HT Sequence Detection System (Applied Biosystems) according to the manufacturer's instructions. Details on cDNA synthesis, Primer design and qRT-PCR set-up are as previously described in Chapter 2, Materials and methods. Two internal reference genes, *PDF2* (At1g13320) and *APT1* (At1g27450) were used for normalizing gene expression. qRT-PCR results are presented as fold change normalised to the expression of internal reference gene ($2^{-\Delta Ct}$, reference gene = 1) and to expression in mock treatments [$2^{-\Delta\Delta Ct}$, $\Delta\Delta Ct$ = Ct (sample) – Ct (reference sample), reference sample = 1] (Pfaffl, 2001). All primers used in this Chapter are given in Appendix 4.6.1.

### 4.2.5 Yeast-two-hybrid assay

In order to assess the physical interaction between OXI1 and PTI1-5, the yeast-twohybrid method was chosen. The full length cDNA of *OXI1* and *PTI1-5* was amplified by PCR from cDNA derived from Col-0 seedlings. *PTI1-5* coding sequence was cloned in frame with the GAL4 DNA-binding domain of the vector pGBKT7 (Clontech) using *Eco*RI and *Bam*H1 sites. *OXI1* coding sequence was cloned in frame with the GAL4 activation domain of the vector pGADT7 (Clontech) using *Nde*I and *Sal*1 sites. Control vectors were also included in the experiment. pGADT7:SV40/pGBKT7:p53 and pGADT7:SV40/pGBKT7:lam supplied by in the MatchmakerTM GAL4 Two-hybrid kit (Clontech) were used as the positive and

negative controls, respectively. Additional negative controls included pGBKT7:PT1-5/pGADT7 empty vector and pGADT7:OXI1/pGBKT7 empty vector. The preparation of competent cells and co-transformations into the yeast strain AH109 were performed by LiCl method as described in the MatchmakerTM GAL4 Two-hybrid user manual (Clontech PT3247-1). The transformants grown on appropriate drop out media to monitor transformation efficiency (-Leu, -Trp) as well as the activation of the reporters HIS3 and/or ADE2 for protein-protein interactions (-Leu, -Trp, -His and/or -Leu, -Trp, -His, -Ade).

## 4.3 Results

### 4.3.1 Choice of *Arabidopsis pti1* mutants for pathogen challenge experiments

The strategy adopted in this chapter was to initially analyse loss of function mutants in the *PTI1* genes most closely related to characterised *PT1* homologs involved in disease resistance in tomato, rice and maize. The phylogenetic tree constructed in Chapter 2 (Figure 2.5) showed that the *Arabidopsis* genes *PTI1-5*, *PTI1-4*, *PTI1-8* and *PTI1-7* cluster within the same major branch as the *SlPTI1* (tomato), *OsPTI1A* (rice) and *ZmPTI1B* (maize) genes. Unfortunately, due to the unavailability of confirmed T-DNA insertion knockout lines for the *PTI1-8* and *PTI1-7* genes at the time this present study was conducted, only the *pti1-5* and *pti1-4* single mutant and the double mutant *pti1- 5pti1-4* were included in the pathogen challenge experiments presented here.

### 4.3.2 *pti1-5* single and *pti1-5pti1-4* double mutants have enhanced resistance to the bacterial pathogen *Pst* DC3000

Single insertion mutants *pti1-5*, *pti1-4* and derived double mutant *pti1-5pti1-5* along with WT (Col-0) control were challenged with the virulent strain of *P. syringae* pv. *tomato* DC3000 (*Pst* DC3000) using the standard syringe infiltration technique (Katagiri et al., 2002) (Details are described in Materials and Methods section). In order to estimate the growth of the bacterium *in planta*, the DNA biomass assay was carried out which involves comparison of the amounts of DNA from the pathogen (*Pst* DC3000) (Hypersensitive reaction pathogenicity Z, *HRPZ* gene) and the host (*Arabidopsis* leaves) (*Arabidopsis* Shaggy-kinase-like 11 gene, *IASK11*). The first

signs of chlorosis were apparent 2-3 days post inoculation (dpi) in both WT and mutant plants (Figure 4.2 A), followed by tissue collapse within 7 days. Chlorosis was mostly confined to the infiltrated spot indicating that the bacterial inoculate concentration was fairly even among leaves tested. DNA biomass assays revealed a 50% lower biomass of *Pst* DC3000 DNA in the infiltrated leaves of *pti1-5* relative WT plants (Figure 4.2 B), indicating that a loss of *PTI1-5* function restricts the growth of the virulent *Pst* DC3000 population either directly or indirectly. In the *pti1-4* mutant, however, *Pst* DC3000 DNA biomass did not significantly differ from that in WT and the double mutant *pti1- 5pti1-4* showed a similar decrease in bacterial biomass to that measured in the single *pti1-5* mutant. These results indicate that the compromised growth of the bacteria observed in the double mutant is related to the *PTI1-5* loss of function and independent of the *PTI1-4* mutation.

### 4.3.3 The *pti1-5* loss-of-function leads to impaired growth of virulent *Pst* DC3000 pathogen *in planta*

To confirm results obtained in the previous screen, the same pathogen challenge was repeated as described above in a second experiment where the more traditional Colony- Forming Unit (CFU) assay was employed to quantify pathogen growth. This technique is based on direct bacterial colony counts from punched leaf discs that have been ground, suspended in a buffer and plated in serial dilutions on Kings B medium (King et al., 1954). (Katagiri et al., 2002) (see Material and Methods for a flow chart describing the steps involved in this technique).

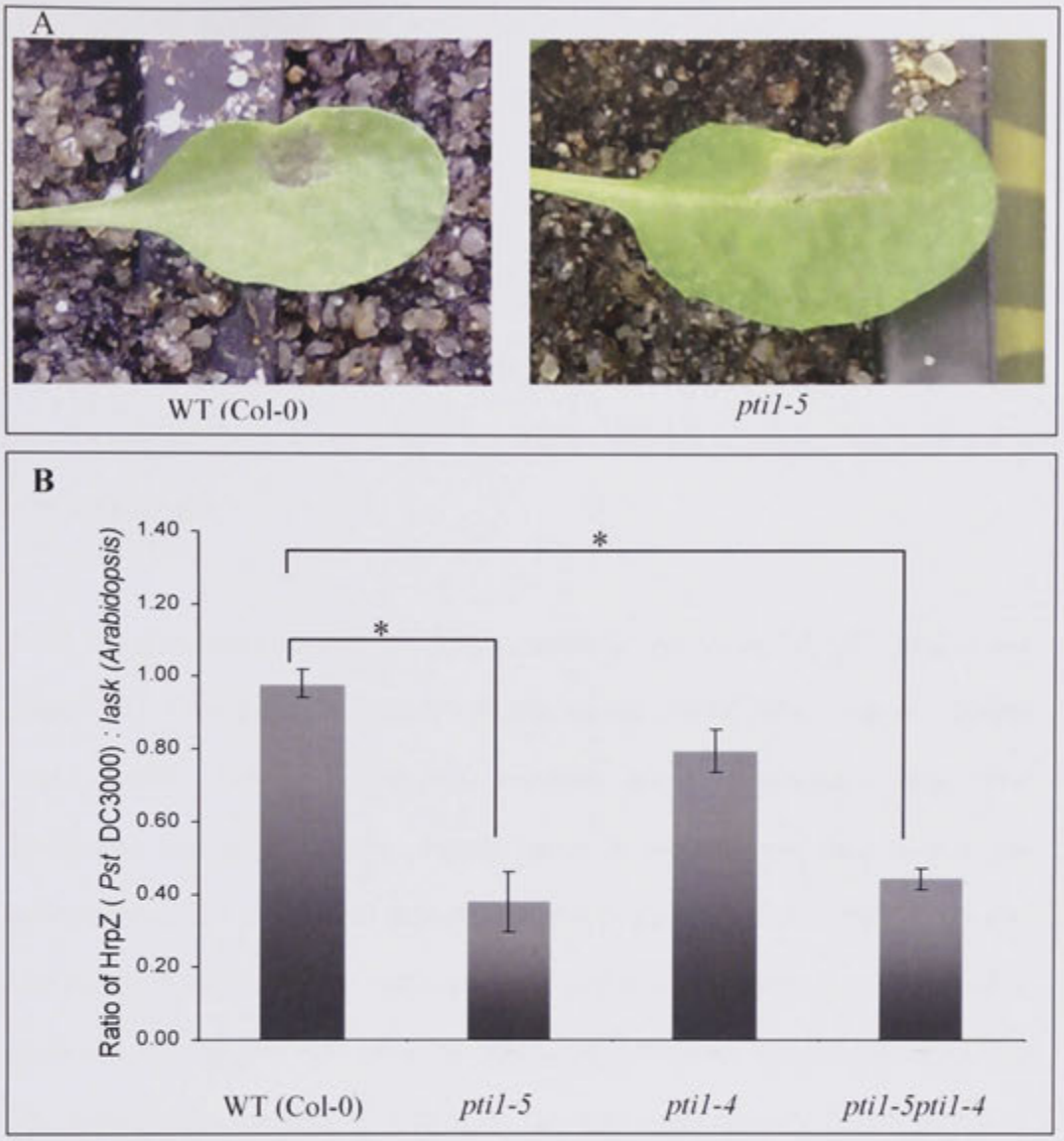


**Figure 4.2 (A,B): *pti1-5* and *pti1-5pti1-4* confer enhanced resistance to *Pseudomonas syringae* pv. *tomato* (*Pst*) strain DC3000**. Disease symptoms in the infiltrated region were visible 1 days post infection (A). Bacterial populations were measured 24 hours post infection using the DNA biomass assay (B). The graph shows relative DNA levels of *Pst* DC3000 *HRPZ* gene normalised to Arabidopsis *IASK11* gene. The error bars indicate ± SE of the mean of 3 biological replicates comprising 40 *Pst* DC3000 infiltrated rosette leaves. * denotes significantly different values between mutant and WT (Col-0) (Students t-test, *: $P \leq 0.002$).

A preliminary experiment was conducted to calibrate the method, using only WT (Col-0) plants. Rosette leaves from 5 week old Col-0 plants were challenged with the *Pst* DC3000 strain through infiltration as described, and bacterial growth was quantified at three time points, d0, d1 and d3. As expected *Pst* DC3000 growth was exponential with respect to time over this period, resulting in a straight line when plotted on a logarithmic scale (Figure 4.3, $r^2$= 0.975). This is the typical growth curve expected from a compatible interaction between a susceptible host and a virulent pathogen.

Next, the genotypes used in the first experiment (*pti1-5*, *pti1-4*, *pti1-5pti1-4* and control WT, Col-0) were infiltrated with the virulent *Pst* DC3000 strain or a 10mM $MgCl_2$ mock solution. The average bacterial density measured 1 hour after inoculation was fairly uniform among leaves of all lines and calculated to be approximately 2.5 x 103 CFU per unit leaf area (Figure 4.4). Forty-eight hours post inoculation, bacterial growth was clearly reduced in *pti1-5* and *pti1-5pti1-4* mutants relative to WT (Figure 4.5) while no significant differences were observed 24 hpi. The reduction in bacterial growth at 48 hpi was approximately 2 fold, which is consistent with the decrease in *Pst* DC3000 DNA biomass observed at 24 hpi in the first experiment. The lack of correlation between the two assays may represent higher sensitivity of the Real-time PCR technique to detect small differences in *Pst* growth as compared to colony counts for the CFU assay. As with the first experiment, growth of *Pst* DC3000 on *pti1-4* mutant leaves were observed to be similar to that in WT, although colony counts at both time points studied were highly variable between biological replicates (Figure 4.5).

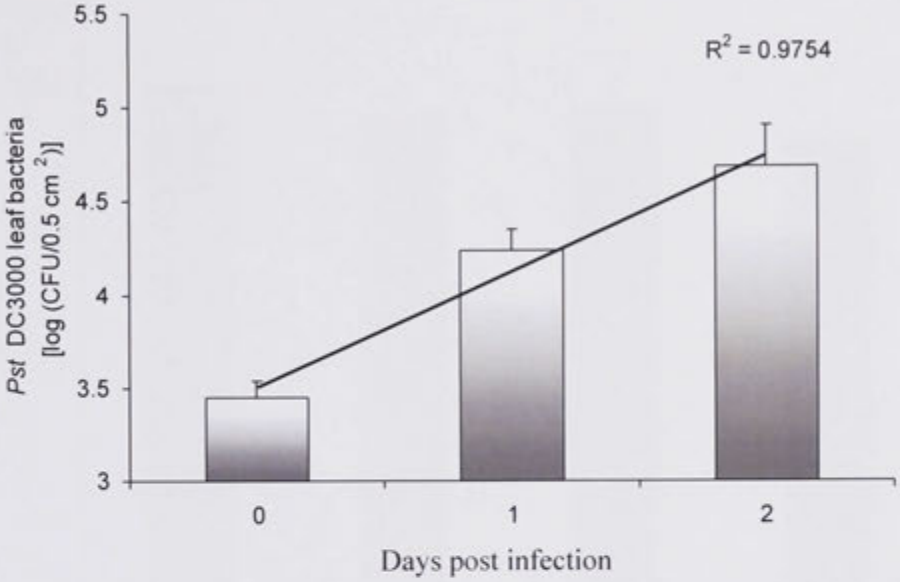


**Figure 4.3: Multiplication of virulent *Pseudomonas syringae* pv. *tomato* strain DC3000 in WT (Col-0) plants**. Rosette leaves of 5 week old Col-0 plants were infiltrated with virulent *Pst* DC3000 bacteria. Leaves were sampled at day 0, 1 and 2 and *in planta* bacterial populations were determined by Colony Forming Unit (CFU) assay. Growth of the virulent strain of *Pst* DC3000 is plotted on a log scale. Error bars indicate + SE of the mean of 3 replicate samples.

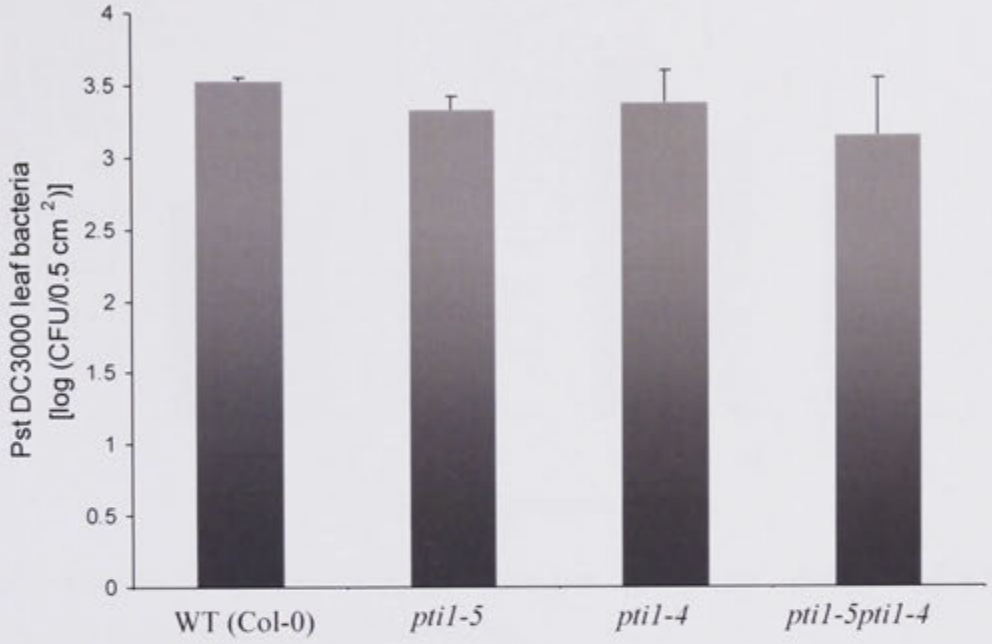


**Figure 4.2: *Pst* DC3000 bacterial numbers for WT and *pti1* mutant lines 1 hour after inoculation as determined by the CFU assay**. Error bars indicate SE of the mean of 3 biological replicates for each genotype.

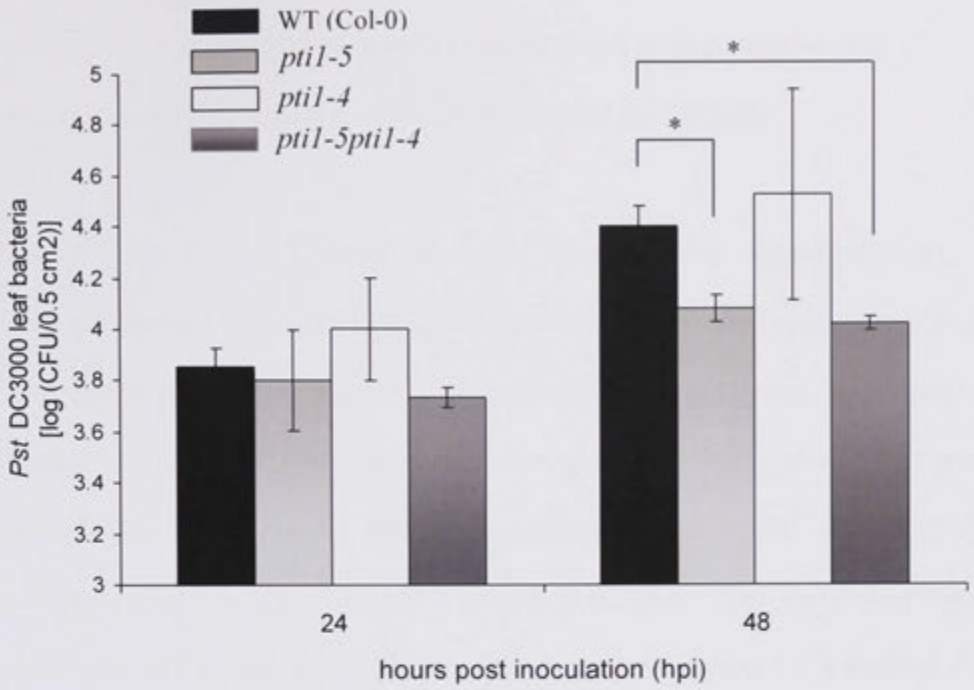


**Figure 4.5: Bacterial growth after 48 hours post inoculation with *Pst* DC3000 is reduced in the *pti1-5* and *pti1-5pti1-4* leaves.**

Bacterial populations were measured 24 and 48 hours post infection (hpi) using the CFU biomass assay and is plotted on a log scale. The error bars indicate ± SE of the mean of 3 biological replicates. * denotes significantly different values in mutant compared to WT (Col-0) (Students t-test, *: $P \leq 0.05$).

Taken together, the results from these two independent pathogen challenge experiments and quantification methods of bacterial growth suggest that *PTI1-5* functions as a negative regulator of basal resistance to *Pst* DC3000.

Infiltrated leaves from WT, single mutant *pti1-5* and double mutant *pti1-5 pti1-4* were also analysed 4 days after infection to examine whether the impaired growth of *Pst* DC3000 in the mutant correlated with reduced disease symptoms. There was no difference among lines in the severity of lesions caused by the bacteria, as assessed visually (Figure 4.6), suggesting that between d2 and d4, *Pst* DC3000 was somehow able to compensate for an initial lag in growth in the *pti1-5* and *pti1-5pti1-4* lines. Alternatively, WT plants may have been able to partially restrict the growth of *Pst* DC3000 between d2 and d4.

### 4.3.4 Enhanced expression of defence genes in the *pti1-5* mutant after *Pst* DC3000 infection

An important feature of plant-pathogen interactions is the involvement of hormone signalling pathways. Phytohormones that have been identified to play key roles in regulating activation of plant defences include salicylic acid (SA), jasmonic acid (JA) and ethylene (ET) (Spoel and Dong, 2008; Bari and Jones, 2009). Genes relating to SA, JA and ET have been used extensively as markers of stress responses in the host plants (Schenk et al., 2000; Spoel and Dong, 2008).

As an initial step towards understanding the enhanced resistance of the *pti1-5* mutant, the expression levels of *PR1* (SA induced), *PR4* (ET induced) and *PDF1.2* (JA/ET induced) genes were monitored following *Pst* DC3000 challenge. After


**Figure 4.6: Representative leaves for WT (Col-0) and *pti1* mutants showing *Pst* DC3000 induced necrosis**. Leaves of 5 week old plants were syringe infiltrated with *Pst* DC3000 bacteria on either side of the mid-vein. Photos of detached leaves were taken 4 days after inoculation. Scale bar = 1cm

infiltration with the *Pst* DC3000, infected leaves from mutant and WT plants were harvested at 4, 24 and 48 hpi for RNA isolation to compare expression kinetics of the defence marker genes. Following infection, an increase in *PR1* and *PR4* expression was observed in both WT and *pti1-5*. The inductions levels were initially similar in the WT and mutant (4 and 24h time points), by 48 hpi significantly higher levels of *PR1* and *PR4* was detected in the pti1-5 mutant (Figure 4.7) In contrast, *PDF1.2* expression was down-regulated. The down-regulation appeared greater in the mutant but due to the variation of expression values for this gene, this was not statistically significant (Figure 4.7). The antagonistic suppression of JA signalling and downstream responsive genes such as *PDF1.2* by SA induction has been well documented in plant-biotrophic interactions (Beckers and Spoel, 2006).

In summary, infiltration of *Pst* DC3000 caused an induction of *PR*-like genes and repression of *PDF1.2* in both WT and mutant leaves. These responses, were however, enhanced in *pti1-5* and correlates well with increased basal resistance to *Pst* DC3000 infection compared with the WT.

### 4.3.5 Evidence of direct protein-protein interaction between the PTI1-5 and OXI1

The *Arabidopsis* oxidative stress inducible AGC kinase, OXI1 has been shown to interact with four *Arabidopsis* PTI1 isoforms; PTI1-1, PTI1-2, PTI1-3 and very recently PTI1-4 (Anthony et al., 2006; Forzani et al., 2011). OXI1 kinase has also been demonstrated to be required for resistance against virulent and avirulent strains of *Pseudomonas syringae* (Petersen et al., 2009). In light of the involvement of *PTI1-5* in the response to *P. syringae* described above, these hinted to the possibility OXI1

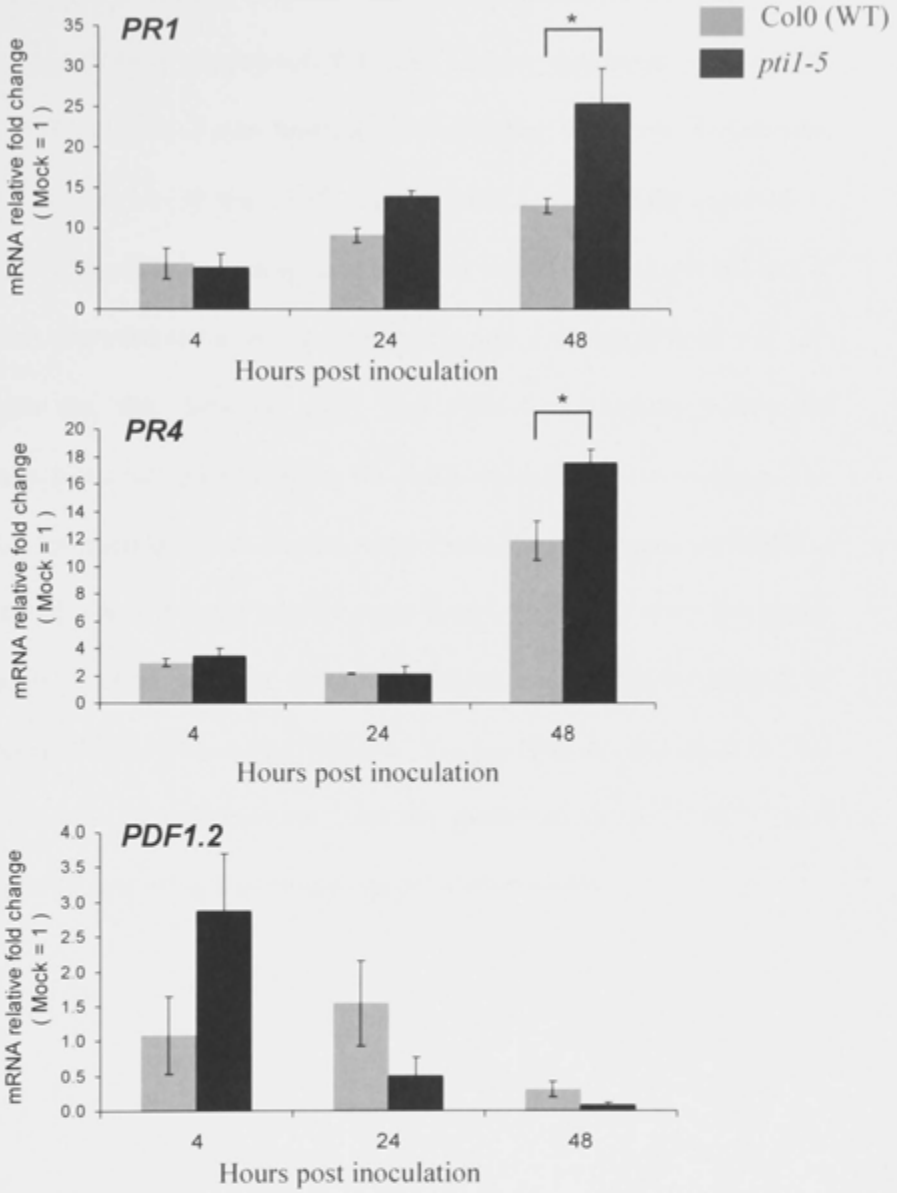


**Figure 4.7: qRT-PCR expression analysis of defense marker genes in *pti1-5* mutant and WT (Col-0) plants inoculated with *Pst* DC3000**. Transcript abundance in infected leaves is expressed relative to expression in control leaves after normalization to the expression of reference genes *APT1* and *PDF2*. Error bars indicate ± SE of the mean of 3 biological replicates. Each replicate corresponds to a pool of 8-10 rosette leaves. * indicates statistical significance between *pti1-5* mutant and WT (Student's t-test $p \leq 0.05$).

may interact with the PTI1-5 isoform as well. As a preliminary step, *OXI1* expression was analysed in the *pti1-5* mutant background. These results show *OXI1* transcripts were significantly up-regulated in the mutant compared to the WT, suggesting that *OXI1* and *PTI1-5* may function in overlapping pathways (Figure 4.8). Interestingly, the expression of the MAP kinase, *MPK3*, previously reported to function in the OXI1 signalling pathway as an indirect downstream target (Rentel et al., 2004), was also observed to be up-regulated in the *pti1-5* mutant (Figure 4.8). To further investigate the link between *OXI1* and *PTI1-5*, I recently tested the interaction between these two proteins using the yeast-two-hybrid *in vitro* assay. The full-length cDNA for each of these kinases were cloned into the yeast-two-hybrid vectors and co-transformed into the AH109 yeast strain. The result from this assay clearly shows an interaction between these two kinases as detected by growth of yeast colonies on media plates lacking Histidine, the positive reporter used for the interaction (Figure 4.9). Experiments are currently underway to test if OXI1 and PTI1-5 also interact *in vivo* using a co-immunoprecipitation assay.

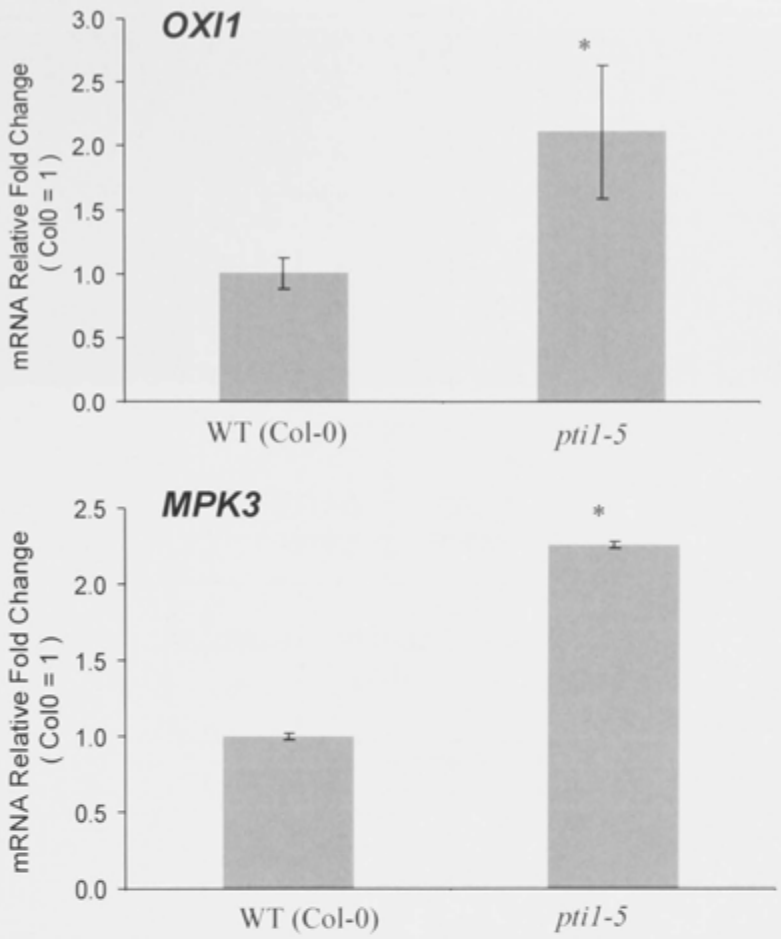


**Figure 4.8: qRT-PCR expression analysis of *OXI* and *MPK3* in the *pti1-5* mutant compared to WT (Col0).** mRNA levels were normalized to the level of invariant reference genes *APT1* and *PDF2*. Error bars indicate ± SE of the mean of 3 biological replicates. Each replicate is a pool of approx 8 rosette leaves. * indicates statistical significance of the difference between *pti1-5* mutant and WT (Student's t-test $p \leq 0.05$).

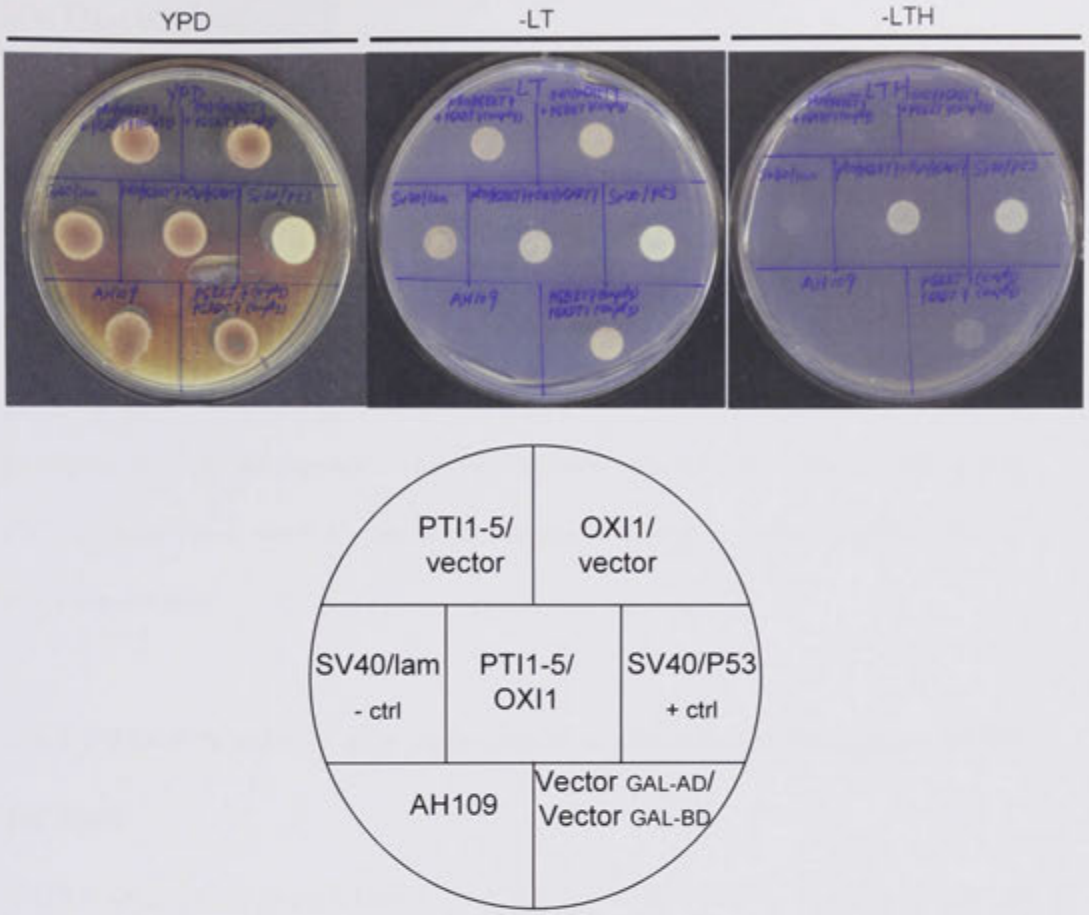


**Figure 4.9: Positive *in vitro* protein interaction between OXI1 and PTI1-5.** Yeast-two hybrid assay in which *PTI1-5* cDNA fused to the *GAL4* DNA-binding domain (pGBKT7) and *OXI1* cDNA fused to the *GAL4* activation domain (pGADT7). *PTI1-5* and *OXI1* combined with corresponding empty vectors were included in the assay as negative controls. Additional positive (SV40/ p53) and negative (SV40/:lam) controls were obtained from the Clontech Matchmaker™ GAL4 yeast-two-hybrid kit. AH109 is the background yeast strain used in the assay. The left side panel shows growth of yeast on YPD medium which allows growth of all yeast colonies. The centre panel shows the growth of yeast colony on the control SD (synthetically defined) drop-out plate, lacking leucine (L) and tryptophan (T) (-LT). Right side panel shows the growth of the yeast colony on SD, drop-out plate lacking -LT and the Histidine (HIS3) reporter (-LTH). The positive interaction for OXI1 and PTI1-5 was also confirmed using the Adenine (ADE2) reporter on quadruple selection plate (-LTHA) (Data not shown).

## 4.4 Discussion

In the *PTI1* phylogenetic analysis conducted in Chapter 2, the three pathogen-related *PTI1* genes from tomato (*SlPTI1*) (Zhou et al., 1995), rice (*OsPTI1A*) (Takahashi et al., 2007) and maize (*ZmPti1B*) (Herrmann et al., 2006) clustered together on the same major branch of the phylogenetic tree (Figure 2.5), suggesting an evolutionary basis for their conserved function in plant defence response. Based on their relative proximity to these three genes on the phylogenetic tree, two *Arabidopsis PTI1* genes, *PTI1-5* and *PTI1-4*, were chosen to investigate a potential orthologous function in disease resistance.

### 4.4.1 *PTI1-5* functions as a suppressor of plant basal resistance to *Pst* DC3000

T-DNA single mutants *pti1-5* and *pti1-4* and the derived double mutant *pti1-5pti1-4* were assayed for their sensitivity to the virulent bacterial pathogen *Pseudomonas syringae* pv. *tomato* (*Pst*) DC3000. The results from two independent *in planta* bacterial quantification assays clearly demonstrate that the *pti1-5* and *pti1-5pti1-4* mutant plants have enhanced basal resistance against *Pst* DC3000 (Figure 4.2, 4.5). No difference in bacterial growth was observed for the *pti1-4* mutant leaves compared with WT, suggesting that the enhanced resistance observed in the double mutant was most likely due to the mutation in the *PTI1-5* locus alone. The similar bacterial growth in the *pti1-4* mutant compared with WT is in agreement with results of a recent study where this mutant was also assayed for sensitivity to virulent *Pst* DC3000 (Forzani et al., 2011).

Defence responses against *Pst* DC3000 are thought to be mediated by SA-, JA- and ET-dependent signalling pathways (Glazebrook, 2005). Both negative and positive crosstalk between these phytohormones exists in plants in response to pathogen infection (Schenk et al., 2000; Spoel and Dong, 2008). The enhanced disease resistance phenotype of the *pti1-5* mutant is also shown to correlate with increased gene expression of *PR1* and *PR4*, two defence-related genes commonly used as markers for SA and ET induction, respectively (De Vos et al., 2005) (Figure 4.7). In contrast, the expression of the JA-responsive *PDF1.2* in the same samples was slightly lower in the mutant compared with WT, possibly reflecting an increased SA-mediated repression of *PDF1.2* (Spoel and Dong, 2008). Thus, if the *pti1-5* mutant accumulates higher levels of SA, as indicated by the elevated *PR1* transcript level, this could in turn; result in stronger inhibition of the JA-responsive *PDF1.2* expression. This implies that *PTI1-5* could function as a suppressor of the SA signalling pathway. Further experiments will test this by directly measuring SA and JA levels in the *pti1-5* mutant before and after infection with *P. syringae*.

Interestingly, lowered *Pst* DC3000 bacterial counts in *pti1-5* plants and up-regulated expression of defence marker genes did not manifest itself as reduced disease symptoms (Figure 4.6). This may suggest that the increased basal resistance observed in *pti1-5* mutant is transient, with the pathogen somehow being able to gradually compensate for its initial lag in growth. Future studies using lower inoculum densities to give more time for the pathogen to grow within the host tissue may reveal differences in disease symptoms. Additionally, hypo-virulent strains of *Pst* DC3000 could also be employed that may enhance the ability to detect differences in the plant immune response between *pti1-5* mutant and WT. Trypan

blue staining to monitor early cell death would be useful to visualize the onset of differences in susceptibility to pathogen between mutant and WT leaves.

Given the *pti1-5* phenotype observed here, it is intriguing that WT plants challenged with the same pathogen did not show any differential expression of *PTI1-5* transcripts (Chapter 2, Fig 2.13A). A simple explanation could be that if a change in *PTI1-5* expression was transient, it may not have been detected at the time-points chosen for the expression analysis (4 hrs, 24 hrs and 48 hrs). It is also possible that there may be no correlation between *PTI1-5* transcriptional regulation and protein function in response to *P. syringae* infection. Since *PTI1-5* encodes a putative kinase, the function of the protein in negatively regulating immune responses may be mediated posttranscriptionally by its phosphorylation status, requiring no change in the steady-state levels of the mRNA transcript and protein.

### 4.4.2 Comparison with *PTI1* pathogen related genes in other species

The enhanced disease resistance phenotype of the mutant suggests that *PTI1-5* functions as a negative regulator of basal resistance against *Pst* DC3000. This is in contrast to the tomato *SlPTI1* which, when overexpressed in tobacco, induced an enhanced HR response, indicating it was a positive regulator of defence signalling (Zhou et al., 1995). Similar to the *pti1-5* phenotype observed in this study, the rice loss-of-function mutant *Osptil1a* was also shown to negatively regulate basal resistance to a compatible race of the rice blast fungus, *Magnaporthea grisea* (Takahashi et al., 2007), suggesting functional homology between the two genes. Consistent with this idea, the PTI1 phylogenetic tree (Figure 2.5) shows the *PTI1-5* is the closest *Arabidopsis PTI1*-like isoform to the *OsPTI1A* gene. Complementation

of the *pti1-5* mutant with rice *OsPTI1A* would be an approach to provide direct evidence of function homology between these genes. Interestingly, complementation of the *Osptila* mutant with the *SlPTI1* tomato cDNA led to a suppression of the *Osptila* disease resistance phenotype (Takahashi et al., 2007), a surprising result given the apparently opposite effects of the two genes in pathogen signalling. The authors suggest that although the SlPTI1 and OsPTI1A proteins are likely to share the same function at the molecular level, the endogenous HR signaling pathways in which these proteins operate may have evolved differently in rice and tomato. This may also be the case for the *Arabidopsis* PTI1-5 and SlPTI1 proteins.

The *Osptila* rice mutant was characterised by spontaneous lesions on leaves triggered by the inappropriate activation of the HR pathway (Takahashi et al., 2007). The *Arabidopsis pti1-5* mutant identified here, on the other hand, did not show any similar growth defects and was indistinguishable from wild-type. Given the high sequence homology within the *Arabidopsis PTI1* multi-gene family (Chapter 2, Figure 2.3), it is possible however, that *PTI1-5* may have partially overlapping functions with the other PTI1 isoforms. In anticipation for this, the double mutant *pti1-5pti1-4* was generated based on the clustering of the two genes in the *PTI1* phylogenetic tree and *in silico* predictions that they represent segmentally duplicated paralogs. There was no evidence for an additive effect of the two mutations in the response to *Pst* DC3000 infection, with the double mutant behaving essentially as *pti1-5* (Figure 4.3, 4.5). Future experiments including a wider range of double mutants as well as higher order mutants, will provide insights into the level of specificity and redundancy within the family with respect to disease resistance pathways.

### 4.4.3 Signalling pathway for PTI1-5

In its enhanced basal resistance to *P.syringae* phenotype the *Arabidopsis pti1-5* mutant is similar to the rice OsPti1a mutant which shows increased resistance to the rice blast fungus (Takahashi et al., 2007). The two proteins may thus represent kinases with orthologous function. Consistent with this, is the recent evidence that the rice OXI1-like kinase (OsOXI1) interacts with and phosphorylates Osptila (Matsui et al., 2010). Both rice and *Arabidopsis* OXI1-like kinases have been demonstrated to play a positive regulatory role in disease resistance and are activated by ROS stimuli (Petersen et al., 2009; Matsui et al., 2010). Using the yeast-two-hybrid assay, I was able to show a positive interaction between OXI1 and PTI1-5 proteins. Taken together, these various lines of evidence strongly suggest that the OXI1-PTI1 pathway for disease resistance may be conserved in both species.

Matsui *et al* (2010) proposed a model to account for the involvement of OsOXI1 and OsPti1a kinases in defence signalling in rice (Figure 5.4). They hypothesized that ROS accumulation following pathogen infection activates the OsOXI1 kinase, which in turn phosphorylates OsPTIa. The phosphorylation of OsPTIa suppresses its negative regulatory function on downstream defence responses. The model therefore suggests suppression of defence responses is mediated by a dephosphorylated state of OsPti1a protein. Consistent with this theory, mutant Osptila proteins deficient in autophosphorylation activity were still able to complement the enhanced disease resistance phenotype of the Osptila mutant. However, site directed mutagenesis of the threonine 233 (T233) of OsPti1a, which is a major target for OsOXI1 mediated phosphorylation, led to an opposite enhanced susceptibility to the bacterial pathogen *Xanthomonas oryzae* pv. *oryzae* (*Xoo*) (Matsui et al., 2010).

Based on the OXI1 positive and PTI1-5 negative regulatory roles in *Arabidopsis* defence signalling and the preliminary evidence for a direct interaction of the two proteins (Chapter 4), it is reasonable to propose that a similar mechanism as proposed by Matsui *et al* (2010) for rice, may be conserved in *Arabidopsis*. Thus, phosphorylation of PTI1-5 kinase by OXI1 could suppress its negative regulatory function thereby activating downstream ROS responses (Figure 4.10). This hypothesis can be tested by carrying out similar site directed mutagenesis experiments as undertaken for the rice OsPTI1A study (Matsui et al., 2010). Furthermore, the mitogen activated protein kinase, MPK3, which has been proposed to be an indirect target of OXI1 (Rentel et al., 2004), was also differentially expressed in the *pti1-5* mutant background indicating that the signal might transduce via the MAPK cascade. Based on these preliminary results, experiments are currently underway testing PTI1-5 direct interaction with OXI1 and MPK3 as well generating double mutants for epistatic analysis.

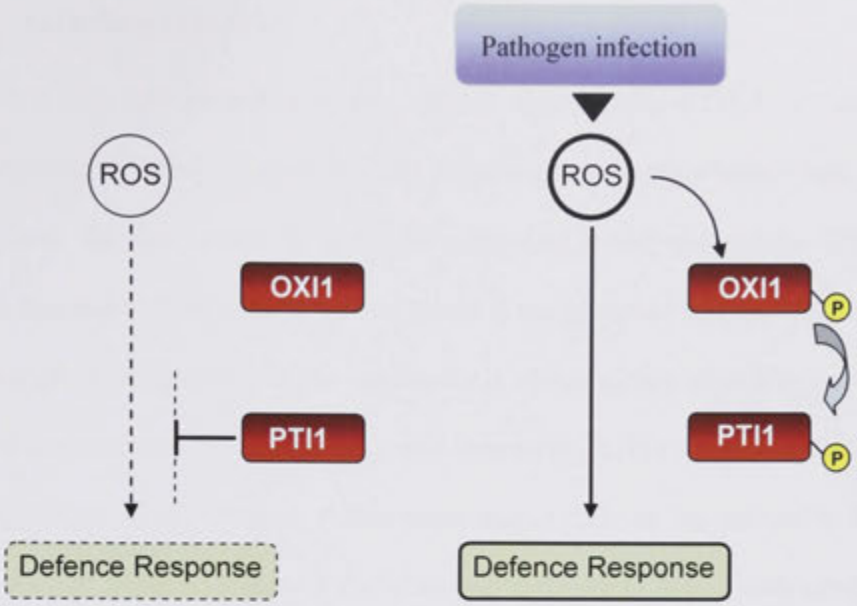


**Figure 4.10: Hypothetical model proposed by Matsui et al (2010) to explain how OsOXI1 controls defence signalling in rice through phosphorylation of OsPTI1A.** OsPTI1A functions in suppressing ROS dependent defence responses. Increased ROS production triggered by pathogen infection leads to phosphorylation of OXI1 which in turn relieves OsPti1a negative regulatory function on downstream defence response.

### 4.4.4 Concluding remarks

In summary, the data presented in this chapter suggests that PTI1-5 functions to negatively regulate basal resistance against *Pseudomonas syringae* which indicates a possible role for the protein in pathogen-associated molecular pattern (PAMP) triggered immunity. It remains to be elucidated if the proposed role for PTI1-5 as a suppressor of ROS signalling is also applicable in other defence signalling pathways such as those mediated by effector triggered immunity (ETI) or against other kinds of pathogen such as necrotrophs. Future experiments that test the sensitivity of the *pti1-5* mutant to avirulent strains of *Pseudomonas syringae* or fungal pathogens such as *fusarium oxysporum* or *Botrytis cinerea* would provide insights into the PTI1-5 signalling pathway. The demonstrated role of *PTI1-5* in plant disease resistance and *PTI1-8* in root development (Chapter 3) indicates functional specificity within the *Arabidopsis PTI1* family and suggests individual isoforms have evolved to signal diverse upstream cues to downstream adaptive responses.

## 4.5 Reference


**Alfano JR, Charkowski AO, Deng WL, Badel JL, Petnicki-Ocwieja T, van Dijk K, Collmer A** (2000) The Pseudomonas syringae Hrp pathogenicity island has a tripartite mosaic structure composed of a cluster of type III secretion genes bounded by exchangeable effector and conserved effector loci that contribute to parasitic fitness and pathogenicity in plants. Proc Natl Acad Sci U S A **97:** 4856-4861

**Anthony RG, Khan S, Costa J, Pais MS, Bogre L** (2006) The *Arabidopsis* protein kinase PTI1-2 is activated by convergent phosphatidic acid and oxidative stress signaling pathways downstream of PDK1 and OXI1. J Biol Chem **281**: 37536-3746

**Bari R, Jones JD** (2009) Role of plant hormones in plant defence responses. Plant Mol Biol **69:** 473-488

**Beckers GJ, Spoel SH** (2006) Fine-Tuning Plant Defence Signalling: Salicylate versus Jasmonate. Plant Biol (Stuttg) **8:** 1-10

**Brouwer M, Lievens B, Van Hemelrijck W, Van den Ackerveken G, Cammue BP, Thomma BP** (2003) Quantification of disease progression of several microbial pathogens on *Arabidopsis* thaliana using real-time fluorescence PCR. FEMS Microbiol Lett **228:** 241-248

**De Vos M, Van Oosten VR, Van Poecke RM, Van Pelt JA, Pozo MJ, Mueller MJ, Buchala AJ, Metraux JP, Van Loon LC, Dicke M, Pieterse CM** (2005) Signal signature and transcriptome changes of *Arabidopsis* during pathogen and insect attack. Mol Plant Microbe Interact **18:** 923-937

**Dodds PN, Rathjen JP** (2010) Plant immunity: towards an integrated view of plant-pathogen interactions. Nat Rev Genet **11:** 539-548

**Eulgem T, Somssich IE** (2007) Networks of WRKY transcription factors in defense signaling. Curr Opin Plant Biol **10:** 366-371

**Forzani C, Carreri A, de la Fuente van Bentem S, Lecourieux D, Lecourieux F, Hirt H** (2011) The *Arabidopsis* protein kinase PTI1-4 is a common target of the oxidative signal-inducible1 (OXI1) and MAP kinases. Febs J **278**: 1126-1136

**Gachon C, Saindrenan P** (2004) Real-time PCR monitoring of fungal development in *Arabidopsis* thaliana infected by Alternaria brassicicola and Botrytis cinerea. Plant Physiol Biochem **42:** 367-371

**Glazebrook J** (2005) Contrasting mechanisms of defense against biotrophic and necrotrophic pathogens. Annu Rev Phytopathol **43:** 205-227

**Herrmann MM, Pinto S, Kluth J, Wienand U, Lorbiecke R** (2006) The PTI1-like kinase ZmPti1a from maize (Zea mays L.) co-localizes with callose at the plasma membrane of pollen and facilitates a competitive advantage to the male gametophyte. BMC Plant Biol **6:** 22

**Jones JD, Dangl JL** (2006) The plant immune system. Nature **444:** 323-329

**Katagiri F, Thilmony R, He SY** (2002) The *Arabidopsis* Thaliana-Pseudomonas Syringae Interaction. *In* The *Arabidopsis* Book, Vol1,p doi: 10.1199/tab.0039

**King EO, Ward MK, Raney DE** (1954) Two simple media for the demonstration of pyocyanin and fluorescin. J Lab Clin Med **44:** 301-307

**Matsui H, Yamazaki M, Kishi-Kaboshi M, Takahashi A, Hirochika H** (2010) AGC kinase OsOxi1 positively regulates basal resistance through suppression of OsPti1a-mediated negative regulation. Plant Cell Physiol **51:** 1731-1744

**Mucyn TS, Clemente A, Andriotis VME, Balmuth AL, Oldroyd GED, Staskawicz BJ, Rathjen JP** (2006) The tomato NBARC-LRR protein Prf interacts with Pto kinase in vivo to regulate specific plant immunity. Plant Cell **18:** 2792-2806

**Nomura K, Melotto M, He SY** (2005) Suppression of host defense in compatible plant-Pseudomonas syringae interactions. Curr Opin Plant Biol **8:** 361-368

**Pedley KF, Martin GB** (2003) Molecular basis of Pto-mediated resistance to bacterial speck disease in tomato. Annu Rev Phytopathol **41:** 215-243

**Petersen LN, Ingle RA, Knight MR, Denby KJ** (2009) OXI1 protein kinase is required for plant immunity against Pseudomonas syringae in *Arabidopsis*. J Exp Bot **60:** 3727-3735

**Pfaffl MW** (2001) A new mathematical model for relative quantification in real-time RT-PCR. Nucleic Acids Res **29:** e45

**Preston G** (2001) Pseudomonas syringae pv. tomato: the right pathogen, of the right plant, at the right time. Mol Plant Pathol **1:** 263-275

**Rentel MC, Lecourieux D, Ouaked F, Usher SL, Petersen L, Okamoto H, Knight H, Peck SC, Grierson CS, Hirt H, Knight MR** (2004) OXI1 kinase is necessary for oxidative burst-mediated signalling in *Arabidopsis*. Nature **427:** 858-861

**Rushton PJ, Somssich IE, Ringler P, Shen QJ** (2010) WRKY transcription factors. Trends Plant Sci **15:** 247-258

**Salmeron JM, Oldroyd GE, Rommens CM, Scofield SR, Kim HS, Lavelle DT, Dahlbeck D, Staskawicz BJ** (1996) Tomato Prf is a member of the leucine-rich repeat class of plant disease resistance genes and lies embedded within the Pto kinase gene cluster. Cell **86:** 123-133

**Schenk PM, Kazan K, Wilson I, Anderson JP, Richmond T, Somerville SC, Manners JM** (2000) Coordinated plant defense responses in *Arabidopsis* revealed by microarray analysis. Proc Natl Acad Sci U S A **97:** 11655-11660

**Spoel SH, Dong XN** (2008) Making sense of hormone crosstalk during plant immune responses. Cell Host & Microbe **3:** 348-351

**Staswick P** (2000) Two expressed soybean genes with high sequence identity to tomato Pti1 kinase lack autophosphorylation activity. Arch Biochem Biophys **383:** 233-237

**Takahashi A, Agrawal GK, Yamazaki M, Onosato K, Miyao A, Kawasaki T, Shimamoto K, Hirochika H** (2007) Rice Pti1a negatively regulates RAR1-dependent defense responses. Plant Cell **19:** 2940-2951

**Winton LM, Stone JK, Watrud LS, Hansen EM** (2002) Simultaneous one-tube quantification of host and pathogen DNA with real-time polymerase chain reaction. Phytopathol **92:** 112-116

**Yuan J, He SY** (1996) The Pseudomonas syringae Hrp regulation and secretion system controls the production and secretion of multiple extracellular proteins. J Bacteriol **178:** 6399-6402

**Zhou J, Loh YT, Bressen RA, Martin GB** (1995) The tomato gene Pti1 Encodes a serine/threonine kinase that is phophorylated by Pto and is invloved in hypersensitive response. Cell **83:** 925-935

**Zhou J, Tang X, Martin GB** (1997) The Pto kinase conferring resistance to tomato bacterial speck disease interacts with proteins that bind a cis-element of pathogenesis-related genes. The EMBO Journal **16:** 3207-3218.

| Primer Name | Target | Sequence 5' → 3' | Purpose | Upper (U) /Lower (L) |
|---|---|---|---|---|
| pti0 y2h_sense | At3g62220 PTI1-5 | CATATGATGAGCTGTTTTGGCTGTTGC | Y2H cloning | L |
| pti0 y2h_anti | At3g62220 PTI1-5 | 5'GGATCCCTAAGGTGCTCCTTCTCCTG3' | Y2H cloning | U |
| oxi1 y2h_sense | At3g25250 OXI1 | AGGAATTCATGCTAGAGGGAGATGAGAA | Y2H cloning | L |
| oxi1 y2h_anti | At3g25250 OXI1 | TGGGATCCTTAAAATACCAAAAAATTGTT | Y2H cloning | U |
| AtAPTnew-for | At1g27450 APT1 | GGTGAGCGTGCTATTATTATTGATGACCT | qRT-PCR (Internal Reference) | U |
| AtAPTnew-rev | At1g27450 APT1 | CTAGTTTCTCCTTTCCCTTAAGCTCTGGTA | qRT-PCR (Internal Reference) | R |
| AtPTIa | At3g62220 PTI1-5 | ATGAGCTGTTTTGGCTGTTG | Y2H cloning | U |
| AtPTIb | At3g62220 PTI1-5 | AAGGTGCTCCTTCTCCTGC | Y2H cloning | L |
| AtPti5_U | At1g06700 PTI1-1 | AATAGAAGACTCAAATGAAGAGCAACAACTGA | qRT-PCR | U |
| AtPti5_L | At1g06700 PTI1-1 | ACAGGTGCTGGTTTTGAATTCTTATGATTT | qRT-PCR | L |
| AtPti6_U | At3g59350 PTI1-3 | TGAAAATGAACACCTCAGAAGCCCTAA | qRT-PCR | U |
| AtPti6_L | At3g59350 PTI1-3 | GCAGGCACATCAATAGATGGAGGCT | qRT-PCR | L |
| AtPti4newfor | At3g17410 PTI1-8 | GACGGGGACGTTGAGCACAAAGA | qRT-PCR | U |
| AtPti4newrev | At3g17410 PTI1-8 | AATTTAGGGGTTGCCCATGTCACGA | qRT-PCR | L |
| Pti7F | At1g48210 PTI1-7 | GAGGATTTTCGCAACGCTACTGACAC | qRT-PCR | U |
| Pti7R | At1g48210 PTI1-7 | ACTGGAATGGCTGGTACAGAAATAGGC | qRT-PCR | L |
| AtAPTnew-for | At1g27450 APT1 | GGTGAGCGTGCTATTATTATTGATGACCT | qRT-PCR (Internal Reference) | U |
| AtAPTnew-rev | At1g27450 APT1 | CTAGTTTCTCCTTTCCCTTAAGCTCTGGTA | qRT-PCR(Internal Reference) | R |

| Primer Name | Target | Sequence | Purpose | Upper/Lower |
|---|---|---|---|---|
| PDF2_qPCR_for | At1g13320 PDF2 | TAACGTGGCCAAAATGATGC | qRT-PCR | U |
| PDF2_qPCR_rev | At1g13320 PDF2 | GTTCTCCACAACCGCTTGGT | qRT-PCR | L |
| PR1-for | At2g14610 PR1 | GCAGCCTATGCTCGGAGCTAC | qRT-PCR | U |
| PR1-rev | At2g14610 PR1 | GCCAGACAAGTCACCGCTACC | qRT-PCR | L |
| PR1-rev | At2g14610 PR1 | GCCAGACAAGTCACCGCTACC | qRT-PCR | L |
| PDF1.2-for | At5g44420 PDF1.2 | TTGCTGCTTTCGACGCA | qRT-PCR | U |
| PDF1.2-rev | At5g44420 PDF1.2 | TGTCCCACTTGGCTTCTCG | qRT-PCR | L |
| SP/MAPK3 cDNA/1082-1181 | At3g45640 MPK3 | CACTGTTGAACAAGCTCTGAATCACC | qRT-PCR | U |
| ASP/MAPK3 cDNA/1082-1181 | At3g45640 MPK3 | CTCATCCAGAGGCTGTTGTTCGA | qRT-PCR | L |
| newOXI1-f | At3g25250 OXI1 | ATGCGATCGATTATTGTCCGGGA | qRT-PCR | U |
| newOXI1-r | At3g25250 OXI1 | CTCCGCCGCGTAAAATCTGATAATCT | qRT-PCR | L |

**Appendix 4.6.1 : Real-time and Yeast-two hybrid cloning primers**

# Chapter 5

## Conclusions and future directions

# Chapter 5: Conclusion and future directions

## 5.1 ROS, a common theme in *Arabidopsis* PTI1 signalling pathway?

Previously identified PTI1-like kinases in monocots and dicots have been implicated in signalling pathways relating to plant defence (SlPTI1, OsPTI1A) (Zhou *et al.*, 1995; Takahashi *et al.*, 2007), abiotic stress (ZmPTI1C) (Zou *et al.*, 2006) and pollen development (ZmPTI1A) (Herrmann *et al.*, 2006). This diverse range of functions is at first sight intriguing given the high level of sequence conservation among *PTI1* genes both inter- and intra- species (Zhou *et al.*, 1995; Tian *et al.*, 2004; Herrmann *et al.*, 2006; Takahashi *et al.*, 2007). The impetus for carrying out this project was to gain insights into the degree of functional specialisation and redundancy among *PTI1* isoforms and possible mechanisms by which these isoforms could integrate diverse signals. To achieve this, a comparative genomics study of the *Arabidopsis PTI1* multi-gene family was undertaken, making use of the extensive genetic resources and tools available in this species for molecular and reverse genetics approaches to examine the function of individual family members.

In Chapter 2, gene expression analysis demonstrated that several members of the family are differentially regulated at the transcriptional level during plant development and in response to both biotic and abiotic stresses. This suggested divergence in expression of individual isoforms as a possible evolutionary strategy for the expansion and retention of *PTI1* genes in *Arabidopsis*. The two next chapters provide evidence of functional specificity within the family, with two PTI1 genes, *PTI1-8* and *PTI1-5*, shown to regulate root elongation and pathogen response,

respectively. The involvement of *PTI1-5* and *PTI1-8* isoforms in these two seemingly disparate processes raises an interesting question: Have the two kinases evolved to function in pathways that are completely independent of each other or are there shared molecular components between the pathways they operate in? Results from this thesis and the literature lead to favour the latter hypothesis and propose the AGC VIII kinase, OXI1, as a convergence point. *Arabidopsis OXI1* kinase has previously been shown to be required for immunity against *P. syringe* (Petersen *et al.*, 2009) and is also specifically expressed in the fast dividing cells of the root apical meristem, much like *PTI1-8* (Anthony *et al.*, 2004). Previous studies have also demonstrated that OXI1 physically interacts with and phosphorylates 4 other *PTI1*-like isoforms: PTI1-1, PTI1-2, PTI1-3 - (Anthony et al., 2006); and very recently PTI1-4 - (Forzani et al., 2011), however, no physiological role has been assigned to these isoforms. In the course of writing this thesis, I tested direct interaction between the OXI1 protein and another PTI1 isoform, PTI1-5, in a yeast two hybrid (Y2H) assay (Fields and Song, 1989). The results clearly show an interaction between the two proteins, and experiments are currently underway to confirm the interaction *in vivo* using co-immunoprecipitation assays.

OXI1 kinase is rapidly activated by ROS or treatments that increase ROS production (*Pseudomonas syrinage*, *Peronospora parasitica*) and has therefore been postulated to be an upstream responder that transmits the signals via a phosphorylation cascade (Rentel *et al.*, 2004). Supporting this claim, the *oxi1* knockout mutation confers a stunted root hair phenotype (Anthony *et al.*, 2004; Rentel *et al.*, 2004) similar to that caused by defective ROS signalling (Foreman *et al.*, 2003). The identification of OXI1 as a partner of multiple PTI1 isoforms suggests a general model where *PTI1*

genes would function in *OXI1*-mediated ROS signalling pathways triggered by a range of common stimuli (Figure 5.1). Consistent with this hypothesis, an increasing body of evidence points to ROS as important signalling molecules in plants, able to modulate stress-induced responses (Torres, 2010; Suzuki *et al.*, 2011) and development (Swanson and Gilroy, 2010; Van Norman *et al.*, 2011). In context with the specific *pti1* mutant phenotypes observed in this study, ROS is known to play a vital role in both pathogen signalling (Rentel *et al.*, 2004; Torres, 2010) and root meristem maintenance (Tsukagoshi *et al.*, 2010). The diverse and complex roles played by ROS require a high degree of signal selectivity and specificity that is thought to be determined by the chemical identity of the particular reactive oxygen species produced, the sub-cellular site of its production, and downstream kinase cascades (Apel and Hirt, 2004; Pitzschke *et al.*, 2009). The different PTI1 isoforms could potentially represent another avenue through which specificity of ROS signalling is achieved. ROS generation could trigger a signalling cascade in which different PTI1 isoforms, depending on developmental- or stress-related cues, are recruited into the OXI1 signalling pathway leading to downstream adaptive changes (Figure 5.1). The active recruitment of a specific PTI1 isoform into the OXI1 cascade is likely to be mediated by other protein co-factors or anchoring proteins in much the same way as scaffolding proteins are known to mediate specificity for the MAPK cascades (Bardwell *et al.*, 2001). Identifying these protein cofactors through techniques like yeast two hybrid screening (Fields and Song, 1989) will be central to understanding how specificity is maintained. Signal integrity could also be maintained through specific intracellular locations of the different PTI1 isoforms. For example, in the current study, PTI1-8 is shown to be plasma membrane localised. The plasma membrane is also a key site for ROS producing enzymes

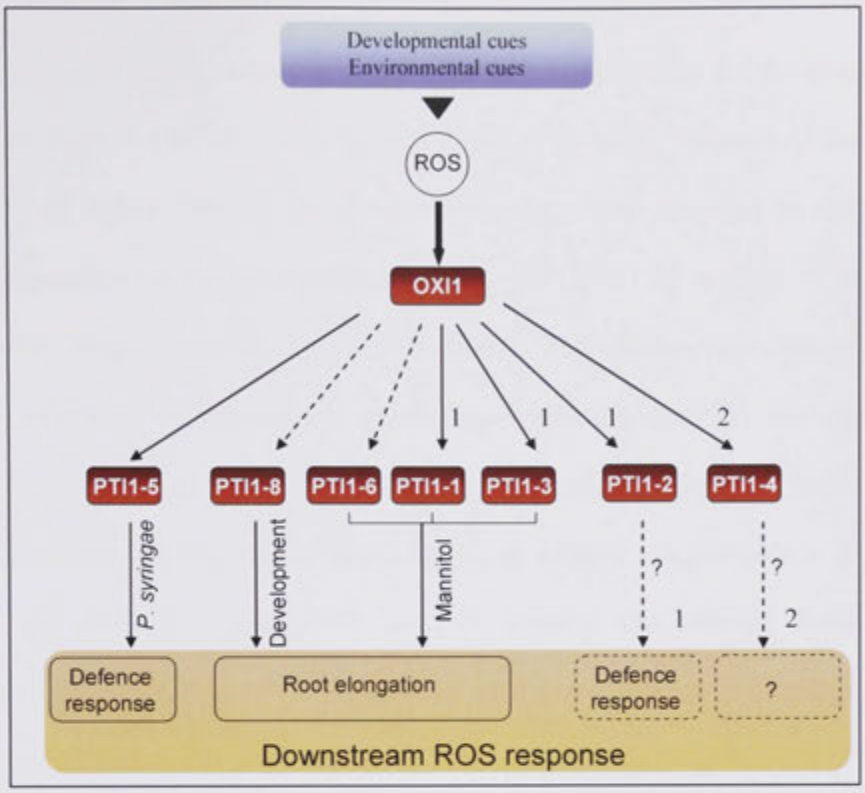


**Figure 5.1: Working model for *Arabidopsis* PTI1 signal transduction through upstream OXI.** In response to developmental or stress related cues, increased ROS production activates OXI1, which represents a point of signal divergence. Depending on the initial cue, OXI1 interacts with and phosphorylates specific PTI1 isoforms, which ultimately leads to various downstream ROS dependent adaptive responses, such as altered root development or plant immunity. Solid lines represent established links and dashed lines represent putative links. Arrows labelled with digit 1 or 2, describe demonstrated or putative interactions or downstream responses in other studies: 1. Anthony et al. (2006), 2. Forzani *et al.* (2011).

NADPH-oxidases which influence the levels of cytosolic and cell-wall associated ROS species and play an important role in regulating plant stress and developmental programs (Foreman *et al.*, 2003; Torres, 2010). The OXI1 kinase has also been shown to be highly dynamic in its cellular localisation as observed in root hairs, where depending on the developmental stage, GFP-OX11 is targeted to different subcellular compartments (Anthony *et al.*, 2004). The cellular versatility of OXI1 may be important in determining interactions with different PTI1 isoforms in a specific physiological context. Techniques such as Bimolecular fluorescence complementation (BiFC) should prove useful to address this possibility (Bracha-Drori *et al.*, 2004). By tagging OXI1 and PTI1 proteins with different fluorescence molecules, the interaction and co-localisation of the two proteins to specific cellular compartments can be visually assessed.

Preliminary results from a recent experiment aimed at examining the effects of *PTI1* loss of function on root development under abiotic stress indicate that other *PTI1* isoforms than *PTI1-8* and *PTI1-5* are likely to be involved in ROS dependent responses. Four *pti1* mutants, *pti1-1*, *pti1-3*, *pti1-6* and the double mutant *pti1-3pti1-6* showed reduced sensitivity of root elongation to mannitol compared to the WT control (Figure 5.2 A, B). Mannitol is frequently used as an osmoticum to decrease the osmotic and water potentials of the growing media; however, it also permeates cells and is known to cause metabolic changes resulting in non-osmotic related effects. A well-known characteristic of mannitol is its ability to actively scavenge ROS species (Smirnoff and Cumbes, 1989; Seckin *et al.*, 2009). In fact a number of fungal pathogens synthesize mannitol upon infection as a strategy to suppress ROS-mediated plant defences (Jennings *et al.*, 1998; Voegele *et al.*, 2005). Therefore, the

**Figure 5.2: Primary root length in *pti1* loss of function mutants after 5 days of growth on mannitol (A,B) and PEG (C) supplemented media relative to that in WT**. Roots of *pti1-1* mutant (Col-0 background ,A) and *pti1-3*, *pti1-6* and *pti1-3pt1-6* mutants (Ws2 background, B) were less sensitive to mannitol than WT roots (means +/- SD, n=3). PEG (MW-8000) treatment caused a similar reduction of root length in *pti1-1* mutant and Col-0 background seedlings (C), over a range of external osmotic pressures matching that of caused by addition of mannitol to the growth medium (-0.5 to -1.3 MPa). * and ** indicate statistically significant differences between mutant and corresponding WT at a given mannitol or PEG concentration (Student's t-test, ** $p \leq 0.01$; * $p \leq 0.05$). Seeds were germinated on control plates ([mannitol or PEG]=0), and transferred to fresh plates on day 5, including for controls There was no significant difference in root length between WT and mutants at the time of transfer, so that the significant differences measured 5 days later cannot be ascribed to differences in germination rates or root elongation pre-treatment (Appendix 5.5.1).

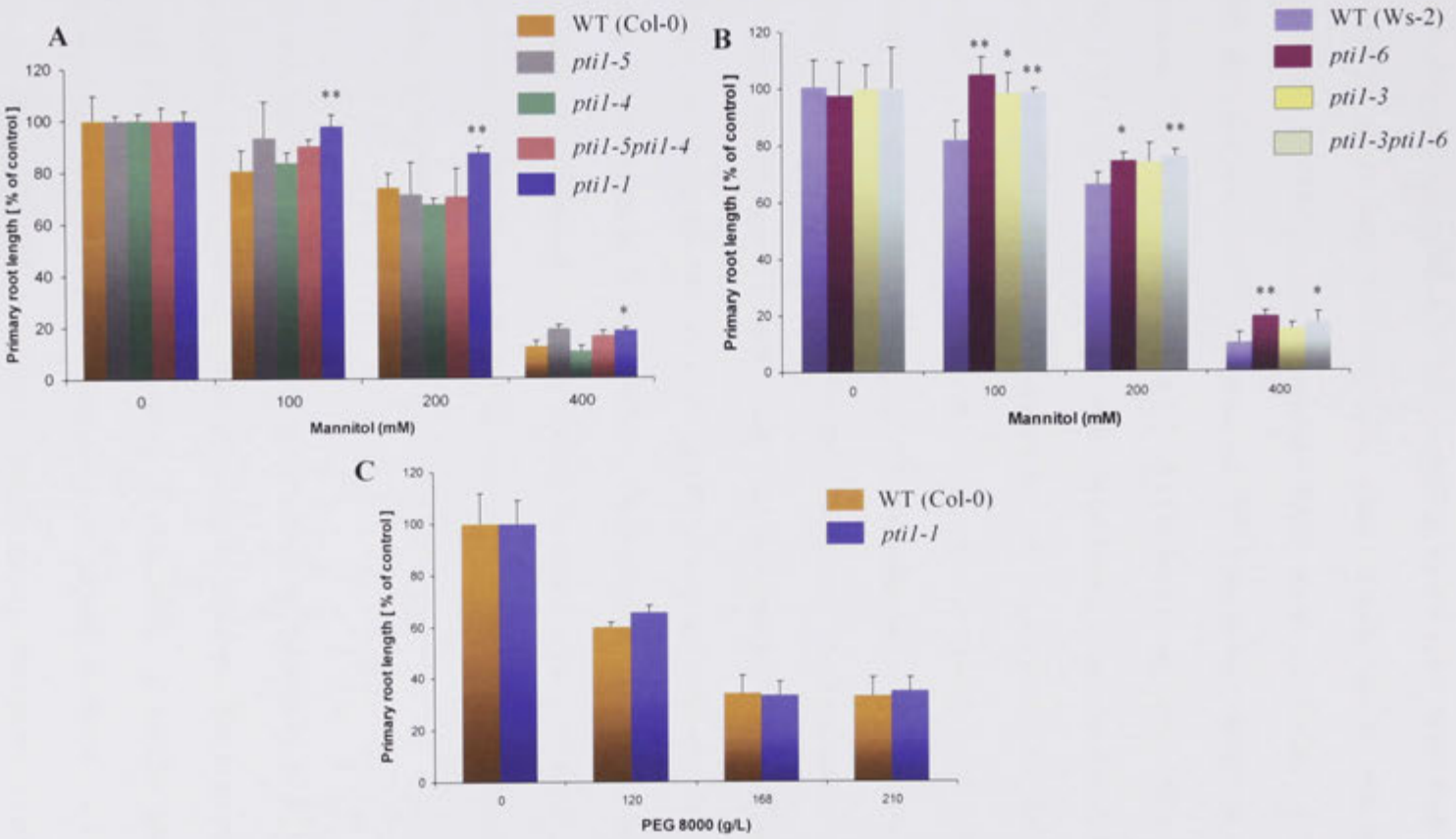
A
WT (Col-0)
pti1-5
pti1-4
pti1-5pti1-4
pti1-1
Primary root length [ % of control ]
Mannitol (mM)
B
WT (Ws-2)
pti1-6
pti1-3
pti1-3pti1-6
Primary root length [ % of control ]
Mannitol (mM)
C
WT (Col-0)
pti1-1
Primary root length [ % of control ]
PEG 8000 (g/L)

negative regulatory effect of *PTI1-1*, *PTI1-3* and *PTI1-6* on root elongation could stem from the suppression of ROS signalling by mannitol rather than from osmotic stress *per se*. In support of this claim, when the *pti1-1* mutant was assayed for its sensitivity to PEG (molecular weight = 8000), another commonly used osmoticum that does not permeate the cell wall, no difference in root elongation was observed compared to WT control (Figure 5.2 C) (Verslues et al., 2006). Also noteworthy is that PTI1-1 and PTI1-3 have previously been shown to interact with OX11 (Anthony *et al.* 2006), strengthening the possibility that these kinases are involved in ROS signalling. Future experiments that employ other commonly used ROS scavengers such as ascorbic acid (Luwe *et al.*, 1993; Monshausen *et al.*, 2007) will be used to directly assess the *pti1* mutants for altered response. These should include additional mutants and transgenic lines for other PTI1 isoforms such as *PTI1-8* and *PTI1-5*. A study carried out by Anthony *et al.* (2006) already indicates that this latter isoform may be involved in ROS signalling. Overexpression of *PTI1-2* in *Arabidopsis* protoplasts indeed led to a considerably increased activity of the ROS dependent promoter, *GST6* (Chen et al., 1996), even in the absence of exogenously added ROS inducing signalling, H202.

In spite of the many links with ROS signalling, the possibility of *PTI1* genes being involved in other signalling pathways cannot be ruled out. For example, in the same study as mentioned above (Anthony *et al.*, 2006), the authors position PTI1-2 downstream of OXI1 for ROS signalling and provide evidence that lipid signalling also converges on PTI1-2 and OXI1 cascade through the upstream kinase, PDK1. In addition, in Chapter 3, an alternate hypothesis involving gibberellin and/or cytokinin hormone signalling pathways was also discussed as a possible explanation for the

*pti1-8* accelerated root elongation phenotype. Further in-depth phenotypic, biochemical and molecular characterisation of the individual pti1 mutants is necessary to establish whether these genes function in converging or independent pathways.

## 5.2 The negative regulatory role of the *Arabidopsis* PTI1 kinases in stress and developmental related responses

The rice *OsPTI1A* has been proposed to play a negative regulatory role in plant defence signalling. Matsui *et al.*, (2010) proposed a model in which they hypothesized an unphosphorylated OsPTI1A to function in suppressing downstream ROS responses and that this inhibition was removed through phosphorylation by OsOXI1. Experimental evidence presented by Matsui *et al.*, (2010) supporting this hypothesis and similarity with the *PTI1-5* signalling pathway was discussed earlier in Chapter 4 (4.4.3). In addition to the role of *PTI1-5* in suppressing plant defence responses, phenotypes such as constitutively enhanced root elongation (PTI1-8) and reduced sensitivity of root elongation to mannitol (*PTI1-1*, *PTI1-3* and *PTI1-6*) also show that the causative genes have a negative regulatory function in their corresponding pathways. This raises the intriguing possibility that OXI1 signalling through the different PTI1 isoforms as hypothesized earlier could also be mediated in a similar fashion (Figure 5.3). If this is true, then the *pti1* mutant phenotypes observed in this study could be a result of inappropriate activation of downstream ROS responses. Future experiments that specifically test OXI1's ability to phosphorylate the different PTI1 isoforms are needed to provide a clearer picture of the signalling pathway. This can be combined with a genetic approach by generating

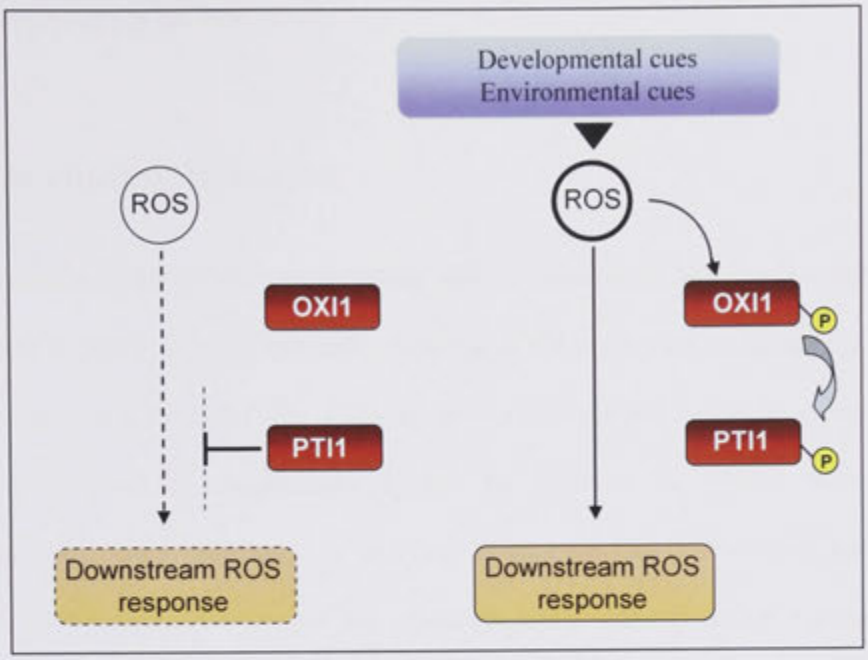


**Figure 5.3: Putative model to explain the negative regulatory function of *Arabidopsis PTI1* isoforms.** The un-phosphorylated PTI1 kinase functions in suppressing downstream ROS responses. Specific development- or stress related cues cause increased ROS production leading to activation of OXI1 which subsequently phosphorylates PTI1. Phosphorylation of PTI1 releases its negative regulatory function thereby activating downstream ROS response. Figure adapted from Matsui *et al.* (2010).

double mutant lines of *oxi1* and the different *pti1* mutants to study epistatic interaction between the two genes.

## 5.3 Concluding Remarks

The overarching aim of the current study was to characterise the *Arabidopsis PTI1* genes and in doing so boost our understanding of the molecular processes related to this family. Like many of the PTI1 kinases characterised in other species, the different isoforms in *Arabidopsis* appear to function in diverse stress and development related processes. A unifying theme for the *PTI1*-related functions appears to be the activation of the upstream OXI1 kinase which represents a convergence point for ROS signalling. The expansion of the *Arabidopsis PTI1* family may thus represent an evolutionary strategy to increase the genetic robustness of ROS signalling and in doing so permit a finer control of ROS dependent responses.

## 5.4 Reference


**Anthony RG, Henriques R, Helfer A, Meszaros T, Rios G, Testerink C, Munnik T, Deak M, Koncz C, Bogre L** (2004) A protein kinase target of a PDK1 signalling pathway is involved in root hair growth in Arabidopsis. Embo J **23:** 572-581

**Anthony RG, Khan S, Costa J, Pais MS, Bogre L** (2006) The Arabidopsis protein kinase PTI1-2 is activated by convergent phosphatidic acid and oxidative stress signaling pathways downstream of PDK1 and OXI1. J Biol Chem **281**: 37536-3746

**Apel K, Hirt H** (2004) Reactive oxygen species: Metabolism, oxidative stress, and signal transduction. Annual Review of Plant Biology **55:** 373-399

**Bardwell AJ, Flatauer LJ, Matsukuma K, Thorner J, Bardwell L** (2001) A conserved docking site in MEKs mediates high-affinity binding to MAP kinases and cooperates with a scaffold protein to enhance signal transmission. J Biol Chem **276:** 10374-10386

**Bracha-Drori K, Shichrur K, Katz A, Oliva M, Angelovici R, Yalovsky S, Ohad N** (2004) Detection of protein-protein interactions in plants using bimolecular fluorescence complementation. Plant J **40:** 419-427

**Chen WQ, Chao G, Singh KB** (1996) The promoter of a H2O2-inducible, Arabidopsis glutathione S-transferase gene contains closely linked OBF- and OBP1-binding sites. Plant J **10:** 955-966

**Fields S, Song O** (1989) A novel genetic system to detect protein-protein interactions. Nature **340:** 245-246

**Foreman J, Demidchik V, Bothwell JH, Mylona P, Miedema H, Torres MA, Linstead P, Costa S, Brownlee C, Jones JD, Davies JM, Dolan L** (2003) Reactive oxygen species produced by NADPH oxidase regulate plant cell growth. Nature **422:** 442-446

**Forzani C, Carreri A, de la Fuente van Bentem S, Lecourieux D, Lecourieux F, Hirt H** (2011) The Arabidopsis protein kinase PTI1-4 is a common target of the oxidative signal-inducible1 (OXI1) and MAP kinases. Febs J **278**: 1126-1136

**Herrmann MM, Pinto S, Kluth J, Wienand U, Lorbiecke R** (2006) The PTI1-like kinase ZmPti1a from maize (Zea mays L.) co-localizes with callose at the plasma membrane of pollen and facilitates a competitive advantage to the male gametophyte. BMC Plant Biol **6:** 22

**Jennings DB, Ehrenshaft M, Pharr DM, Williamson JD** (1998) Roles for mannitol and mannitol dehydrogenase in active oxygen-mediated plant defense. Proc Natl Acad Sci U S A **95:** 15129-15133

**Luwe M, Takahama U, Heber U** (1993) Role of Ascorbate in Detoxifying Ozone in the Apoplast of Spinach (Spinacia oleracea L.) Leaves. Plant Physiol **101:** 969-976

**Monshausen GB, Bibikova TN, Messerli MA, Shi C, Gilroy S** (2007) Oscillations in extracellular pH and reactive oxygen species modulate tip growth of Arabidopsis root hairs. Proc Natl Acad Sci U S A **104:** 20996-21001

**Petersen LN, Ingle RA, Knight MR, Denby KJ** (2009) OXI1 protein kinase is required for plant immunity against Pseudomonas syringae in Arabidopsis. J Exp Bot **60:** 3727-3735

**Pitzschke A, Djamei A, Bitton F, Hirt H** (2009) A major role of the MEKK1-MKK1/2-MPK4 pathway in ROS signalling. Mol Plant **2:** 120-137

**Rentel MC, Lecourieux D, Ouaked F, Usher SL, Petersen L, Okamoto H, Knight H, Peck SC, Grierson CS, Hirt H, Knight MR** (2004) OXI1 kinase is necessary for oxidative burst-mediated signalling in Arabidopsis. Nature **427:** 858-861

**Seckin B, Sekmen AH, Turkan I** (2009) An Enhancing Effect of Exogenous Mannitol on the Antioxidant Enzyme Activities in Roots of Wheat Under Salt Stress. J Plant Growth Regul **28:** 12-20

**Smirnoff N, Cumbes QJ** (1989) Hydroxyl Radical Scavenging Activity of Compatible Solutes. Phytochem **28:** 1057-1060

**Suzuki N, Koussevitzky S, Mittler R, Miller G** (2011) ROS and redox signaling in the response of plants to abiotic stress. Plant Cell Environ. Early view June 2011 DOI: 10.1111/j.1365-3040.2011.02336.x

**Swanson S, Gilroy S** (2010) ROS in plant development. Physiol Plant **138:** 384-392

**Takahashi A, Agrawal GK, Yamazaki M, Onosato K, Miyao A, Kawasaki T, Shimamoto K, Hirochika H** (2007) Rice Pti1a negatively regulates RAR1-dependent defense responses. Plant Cell **19:** 2940-2951

**Tian AG, Luo GZ, Wang YJ, Zhang JS, Gai JY, Chen SY** (2004) Isolation and characterization of a Pti1 homologue from soybean. J Exp Bot **55:** 535-537

**Torres MA** (2010) ROS in biotic interactions. Physiol Plant **138:** 414-429

**Tsukagoshi H, Busch W, Benfey PN** (2010) Transcriptional regulation of ROS controls transition from proliferation to differentiation in the root. Cell **143:** 606-616

**Van Norman JM, Breakfield NW, Benfey PN** (2011) Intercellular Communication during Plant Development. Plant Cell **23:** 855-864

**Verslues PE, Agarwal M, Katiyar-Agarwal S, Zhu JH, Zhu JK** (2006) Methods and concepts in quantifying resistance to drought, salt and freezing, abiotic stresses that affect plant water status. Plant J **45:** 523-539

**Voegele RT, Hahn M, Lohaus G, Link T, Heiser I, Mendgen K** (2005) Possible roles for mannitol and mannitol dehydrogenase in the biotrophic plant pathogen Uromyces fabae. Plant Physiol **137:** 190-198

**Zhou J, Loh YT, Bressen RA, Martin GB** (1995) The tomato gene Pti1 Encodes a serine/threonine kinase that is phophorylated by Pto and is invloved in hypersensitive response. Cell **83:** 925-935

**Zou HW, Wu ZY, Yang Q, Zhang XH, Cao MQ, Jia WS, Huang CL, Xiao X** (2006) Gene expression analyses of ZmPti1, encoding a maize Pti-like kinase, suggest a role in stress signaling. Plant Sci **171:** 99-105

**Appendix 5.5.1**

Root elongation which is known to be quite sensitive to water and osmotic stress was monitored over a 5d period following treatment on young seedlings germinated under optimal conditions. Briefly, seeds for the different lines were plated on standard Hoagland's media (Hoaglands and Arnon, 1950) and grown for 4 days on vertically oriented plates. Seedlings were then carefully transferred to non supplemented plates plates or plates supplemented with different concentrations of mannitol (100, 20, 400 mM) or PEG8000 (120, 168, 210 Mm g/L). The concentrations of PEG and mannitol in the growing media were adjusted to cause a similar decrease in water potential (in the range (-0.5 to -1.3 MPa). As PEG prevents agar polymerization, it was infused into the growing medium as described in Verslues *et al.*, (2006).

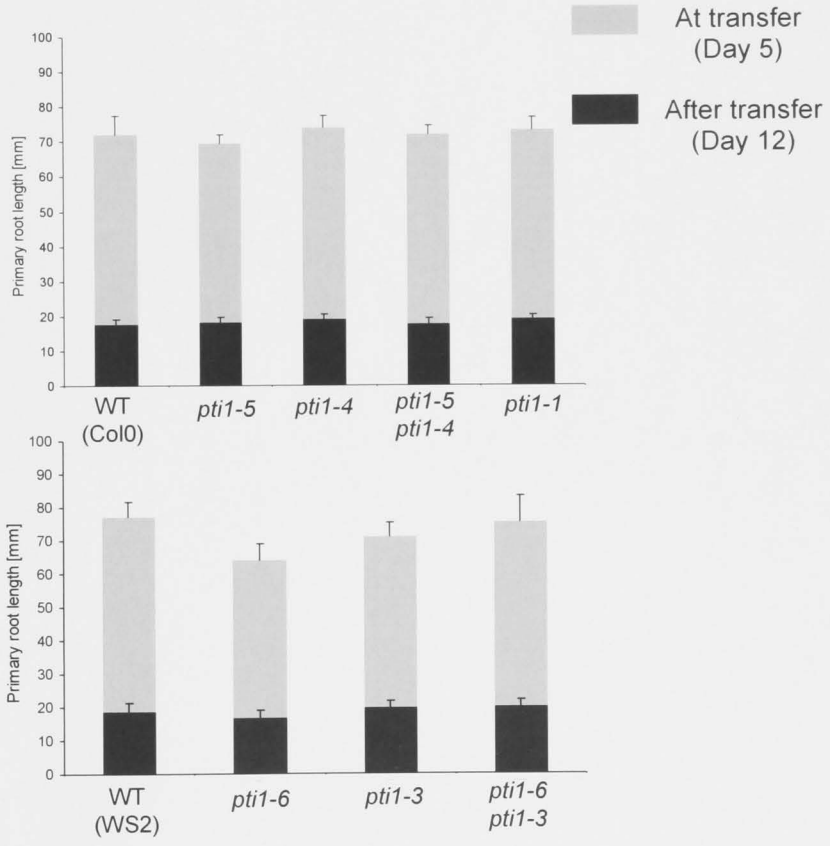


**Mannitol and PEG Root elongation Bioassay**

Primary root lengths of *pti1* mutants in the (A) Col0 and (B) Ws2 background ecotypes on unsupplemented media plates. Root length was measured at two stages of seedling growth: 5 days (At transfer) and 12 days (After transfer) on un-supplemented Hoaglands media plates. (mean +/- SD, n=12).